Muscle fuel uptake

a result of hormone and substrate interaction affecting regional blood flow

By

Lucy Henrietta Clerk, BSc(Hons)

Submitted in fulfillment of the requirements for the degree of Doctor of Philosophy

Division of Biochemistry
University of Tasmania
December 2001

TABLE OF CONTENTS

ACKNOWLEDGEMENTS

First and foremost I would like to thank my supervisor Professor Michael Clark for his continuing support and encouragement throughout my Ph.D. I am very appreciative for the assistance given for the attendance of scientific conferences.

Secondly I am very much indebted to Maree Smith who has helped me endlessly with experimental assistance, in particular for chapters 3 and 4. In addition, I am grateful for the help from Cate Wheatley for chapter 5.

I would also like to thank Drs Steve Rattigan and Stephen Richards for their astute advise on experimental and theoretical matters. Dr Stephen Richards offered invaluable assistance in the experiments for chapter 5.

I am also very appreciative for the help of Geoffrey Appleby for expert technical assistance during the entirety of my Ph.D.

One of the most important aspects of my Ph.D. was the friendships that I gained with a number of members from the Biochemistry Department and the Animal House, in particular Michelle Wallis, Nathan Parry, Carla Di Maria, Maree Smith, Michelle Vincent, John Newman, Eloise Bradley, Zhang Lei, Cate Wheatley, Joanne Youd, Sara Jackson, William Walker, Julie Harris, Murray Plaister, Donna Cummins and Katy O'May. I am grateful to these people for making my time at Biochemistry very enjoyable.

I would also like to thank Campbell Charles Simpson for his help and encouragement throughout my Ph.D.

Finally, to my family (in particular Isabel, James and Robert Clerk and Laird Taylor) to whom this thesis is dedicated.

STATEMENT

The work in this thesis has been undertaken exclusively for the use of a Ph.D. in the area of Biochemistry, and has not been used for any other higher degree or graduate diploma in any university. All written and experimental work is my own, except that which has been referenced accordingly.

Lucy Henrietta Clerk

AUTHORITY OF ACCESS

This thesis may be available for loan and limited copying in accordance with the Copyright Act 1968.

Lucy Henrietta Clerk

ABBREVIATIONS

ACh	acetylcholine
SACS	S-acyl cysteine sulfoxide
ACRP	adipocyte related protein
AT	adipose tissue
ATP	adenine triphosphate
AII	angiotensin
AIB	α-aminoisobutyric acid
AMPK	AMP-activated protein kinase
ANOVA	analysis of variance
r	arteriole diameter
apoCII	apolipoprotein CII
BP	blood pressure
BSA	bovine serum albumin
BK	bradykinin
BCAA	branched chain amino acid
CCh	carbamyl choline
CO	cholesteryl oleate
CT	connective tissue
cGMP	cyclic guanosine monophosphate
CLE	chylomicron lipid emulsion
2-DG	2-deoxyglucose
D.Wt.	dry weight
eNOS	endothelial nitric oxide synthase
EDL	extensor digitorum longus
FABP	fatty acid binding protein
FAT	fatty acid translocase
FATP	fatty acid transport protein
FBF	femoral blood flow
Q	flow

FFA	free fatty acid (unesterified)
G.White	gastrocnemius white
G.Red	gastrocnemius red
GIR	glucose infusion rate
R'g	glucose uptake
HR	heart rate
HIRS	heat-inactivated rat serum
HEPES	N-[2-Hydroxyethyl]piperazine-N'[2-ethanesulfonic acid]
iNOS	inducible nitric oxide synthase
Ins	insulin
IMGU	insulin-mediated glucose uptake
IRS-1	insulin receptor substrate 1
Lip	lipid/heparin
LPL	lipoprotein lipase
meth AIB	methyl- aminoisobutyric acid
3-MH	3-methyl histidine
α-met 5-HT	α-methyl serotonin
1-MU	1-methyl urate
1-MX	1-methyl xanthine
nNOS	neuronal nitric oxide synthase
NO	nitric oxide
NOS	nitric oxide synthase
L-NAME	N(omega)-nitro-L-arginine methyl ester
NIDDM	non insulin dependent diabetes mellitus
NE	norepinephrine
$\dot{V}O_2$	oxygen consumption
PP	perfusion pressure
PAT	perimysial adipose tissue
PI3-Kinase	phosphatidyl inositol-3 kinase
P	pressure
PKB/Akt	protein kinase B

PKCθ	protein kinase C θ
RBC	red blood cells
R	resistance
RU	resistance units
5-HT	serotonin
SM	skeletal muscle
SE	standard error
BH4	tetrahydrobiopterin
TG	triglyceride
TO	triolein
TNFα	tumor necrosis factor α
vaso	vasopressin
VR	vascular resistance
VpO_2	venous partial oxygen pressure
VLDL	very low density lipoprotein
W.Wt.	wet weight

PREFACE

Some of the data presented in this thesis has been published or presented at scientific meetings and has been listed below.

LIST OF PUBLICATIONS DIERECTLY ARISING FROM THIS THESIS

Clerk LH, Smith ME, Rattigan S and Clark, MG. Increased chylomicron triglyceride hydrolysis by connective tissue flow in perfused rat hindlimb: implications for lipid storage. *J. Lipid Res.* 2000 41: 329-335.

Clark MG, Rattigan S, **Clerk LH**, Vincent MA, Clark ADH, Youd JM, and Newman JMB. Nutritive and non-nutritive blood flow: rest and exercise. *Acta Physiol. Scand.* 2000 Apr; 168(4):519-530.

Clark MG, **Clerk LH**, Newman JMB and Rattigan S. Interaction between metabolism and flow in tendon and muscle. *Scand. J. Med. Sci. Sports.* 2000, 10:338-345.

Clerk LH, Rattigan S and Clark, MG. Lipid Infusion Impairs Physiologic Insulin-Mediated Capillary Recruitment and Muscle Glucose Uptake *in vivo. Diabetes.* 2001, *in press.*

Clerk LH, Smith ME, Rattigan S and Clark, MG. Decreased insulin-mediated free fatty acid and glucose uptake when non-nutritive flow predominates in perfused rat hindlimb: implications for hyperlipidemia and hyperglycemia in hypertension. S*ubmitted in 2001 for publication.*

OTHER PUBLICATIONS

Smith GD, de Chazal NM, Tozer G and **Clerk LH**. Temperature stress and oxygen inhibition in a *Nostoc* cyanobacteium. *Aust. J. Plant Physiol.* 1998, 25: 365-370.

POSTERS AT SCIENTIFIC MEETINGS

Australian Society for the Study of Obesity (ASSO). Gold Coast, Australia. Accepted for presentation in October 1998.
Clerk LH, Smith ME, Rattigan S and Clark, MG.
Circulating Triglyceride and Muscle.

European Association for the Study of Diabetes (EASD). Jerusalem, Israel. Accepted for presentation in September 2000.
Clerk LH, Smith ME, Rattigan S and Clark, MG.
Haemodynamic insulin resistance increases fatty acid uptake by connective tissue adipocytes in red muscles.

ABSTRACT

Substantial evidence now exists for two distinct vascular circuits within skeletal muscle. The nutritive capillary circuit directly nourishes skeletal myocytes, whereas another slightly larger set of non-nutritive vessels is probably interspersed within connective tissue of the septa and tendons. The fluctuation of flow between these two circuits allows sensitive control of nutrient delivery, which is often independent of changes in total flow. These innate flow patterns can be manipulated *in vitro* by the infusion of vasoactive agents into the perfused rat hindlimb. Certain vasoconstrictors (including serotonin) increase connective tissue flow at the expense of muscle capillary flow, denying access of glucose and insulin to the myocytes and inducing acute insulin resistance. *In vivo*, insulin itself causes increased flow to the muscle capillaries, and this insulin-mediated capillary recruitment is often blocked in insulin resistant states.

This thesis primarily investigates the uptake of blood-borne metabolites during serotonin infusion in the perfused rat hindlimb, including glucose, fatty acids (FFA, both albumin-bound and derived from chylomicron-triglyceride) and amino acids. In addition, the effect of elevated plasma FFA on the action of insulin to recruit capillaries was investigated in the euglycaemic, hyperinsulinaemic clamp *in vivo,* from the metabolism of 1-methyl xanthine.

When the ratio of non-nutritive to nutritive flow was increased in the perfused rat hindlimb, the insulin-mediated uptake of glucose, Na-palmitate (albumin-bound) and α-aminoisobutyric acid were reduced. Unlike the other fuels tested, with high non-nutritive flow the uptake of FFA from chylomicron-triglyceride hydrolysis was increased. It was therefore reasoned that non-nutritive flow was accessing a population of adipocytes within the muscle connective tissue, most likely in the perimysium. This perimysial adipose tissue is responsible for muscle 'marbling'.

In the experiments determining the effect of FFA on insulin-mediated glucose uptake *in vivo*, FFA inhibited both insulin-mediated capillary recruitment and glucose uptake, thus elevated FFA *in vivo* were able to induce a state of insulin resistance, likely to be partly mediated by reduced capillary recruitment or nutritive flow. Accordingly, elevated FFA prevent perfusion of the nutritive capillaries to some degree, resulting in predominantly non-nutritive flow. This likely results in the reduced access and uptake of insulin, glucose, amino acids and albumin-bound fatty acids by myocytes, contributing to their buildup in the plasma. However, increased flow through the non-nutritive vessels of the muscle connective tissue, increased the exposure of lipoproteins to lipolytic enzymes. Thus, non-nutritive flow probably nourishes connective tissue adipocytes and increases the potential for fat accretion within the muscle.

The results within this thesis offer important insights into nutrient access in skeletal muscle, in particular with elevated FFA *in vivo*. A reduction in nutritive flow, caused by elevated plasma FFA, is likely to reduce the uptake of glucose, amino acids and FFA into the myocytes, however increase fat deposition in the muscle connective tissue. This

may contribute to the reduction in oxidative capacity, and accelerated 'marbling' and insulin resistance of human muscle.

CHAPTER 1

1 Introduction

1.1 Skeletal muscle fuel metabolism and the whole body: a perspective

Skeletal muscle (SM) makes up approximately 38% of the entire human body mass and therefore largely influences whole body substrate uptake and utilization (127). Lipid and carbohydrate are the predominant fuels for SM metabolism, however the carbon chains from amino acid catabolism may contribute up to 15% of the muscle energy during exercise (273). In addition, SM utilizes 25% of the whole body oxygen consumption during rest, which can exceed 90% during intense exercise (reviewed in (90)).

1.1.1 Vasoconstrictors affecting fatty acid, amino acid and glucose uptake

1.1.1.1 Skeletal muscle lipid uptake

In vivo, FFA oxidized by SM are obtained from a number of sources. These include albumin-bound fatty acids, circulating lipoproteins or cytoplasmic deposits within the cell. More recently the presence of adipocytes interlaced between muscle fibres has been suggested as an alternative source, however their importance remains to be determined (283).

TG may be transported to peripheral tissues as micellar lipoproteins (including very low-density lipoproteins (VLDL) and chylomicrons). VLDL are mainly released from the liver during fasting, and are thus assembled from endogenous TG. Post-prandial delivery of FFA occurs via chylomicrons assembled in the enterocytes (reviewed in (109)). FFA are released from the core of the lipoprotein by the enzyme lipoprotein lipase (LPL), situated in the capillary lumen (55) (68) (272).

During a period of elevated lipid requirements, FFA are mobilized from adipose tissue (AT) stores (interfibirillar or elsewhere). Albumin acts as a blood-borne carrier for the FFA. Due to their lipophilic nature, albumin-bound FFA and FFA derived from lipoprotein hydrolysis are firstly adsorbed onto the luminal surface of the capillary endothelial cell. A number of mechanisms have been postulated for FFA crossing the endothelium. FFA traverse the endothelium either unbound, bound to albumin, or bound to a fatty acid transport protein (283). Fatty acids may also pass between endothelial cells bound to albumin, however it has been reported that the albumin molecule is probably too big to pass through these clefts (reviewed in (283)). One postulated method for FFA to traverse the endothelial cell is the 'flip-flop' of un-ionized FFA. In this model FFA rapidly 'flip' from the luminal to the abluminal plasmamembrane (104) (103). However, whether FFA cross the endothelial cell (in particular through the cytoplasm) either unaided or via facilitated transport is a contentious issue. SM uptake of FFA from the blood has been reported to be a function of FFA concentration by some authors (67), however others have reported the uptake to be saturable (278) (279). Saturable uptake implies a carrier-mediated mechanism for transport into myocytes. Over ten putative membrane fatty acid transporters have been described, and the most important include fatty acid binding protein (FABP), fatty acid transport protein ($FATP_{PM}$) and fatty acid translocase (FAT) (reviewed in (104) (31)). The β-pleated sheets of all these transporters are thought to form a tertiary structure resembling two halves of a clam-shell that shield the hydrophobic FFA from the cytoplasm. FFA are then adsorbed from the outer leaflet of the endothelial cell and cross the interstitial space on an albumin carrier (reviewed in (283)). A similar transport mechanism to the endothelium is thought to occur across the sarcolemma and the membranes of other parenchymal tissues. Once adsorbed from this membrane, the FFA are thought to be bound by a cytoplasmic FABP which is the intracellular equivalent of albumin. This reduces the unbound FFA concentration, increasing the gradient from the extracellular FFA, and thus facilitating uptake.

Approximately 90% of the FFA entering the resting myocyte are esterified into lipid droplets located adjacent to the mitochondria (272) (157). Thus, the myocyte has a ready reserve of FFA available for β-oxidation within the mitochondria. The glycerol

moiety for TG synthesis is thought to be from glucose-derived dihydroxyacetone phosphate, which forms glycerol-3-phosphate (207). This has recently been challenged by Guo and Jensen (101) who demonstrated that the minute amounts of glycerol kinase (the enzyme that phosphorylates glycerol into glycerol-3-phosphate) in rat and human SM are likely to substantially contribute to trigylceride synthesis (and therefore whole body glycerol uptake). Alternatively, glycerol-3-phosphate may be provided from lactate (297). However the most widely accepted hypothesis is that glycogen supplies dihydroxyacetone phosphate that is then converted to glycerol-3-phosphate (207). Alternatively fatty acids may be oxidized in the mitochondria (very-long chain fatty acids are first shortened, and often oxidized in the peroxisomes (reviewed in (283)) or used to synthesize phospholipids and other cell components (e.g. prostaglandins).

1.1.1.2 Skeletal muscle carbohydrate uptake

The hydrophilic property of glucose impedes transport across the plasma membrane, therefore facilitated transport is mandatory. By 1992 five SM glucose transporters (members of the GLUT family) of approximately 45kDa were identified (reviewed in (13)). Since then more have been discovered, including GLUT9 in leukocytes and brain; however this transporter appears to be absent from SM (36). In SM, sarcolemmal GLUT1 transports glucose during the basal state while glucose uptake simulated by insulin is facilitated by GLUT4 (reviewed in (308)). Insulin binding to the α-subunit of the insulin receptor stimulates tyrosine kinase activity of the β-subunit (reviewed in (237) and (114)). This causes rapid phosphorylation and activation of insulin-receptor substrate-1 (IRS-1) (115). Wortmannin has been shown to inhibit insulin-stimulated glucose uptake (189), suggesting phosphatidyl inositol 3 kinase (PI3-Kinase) is also involved in one of the intracellular insulin signaling pathways. Insulin-receptor substrate-1 (IRS-1) may thus stimulate PI3-Kinase, which then may activate protein kinase B (PKB/Akt). PKB/Akt acts to transport GLUT4 from an intracellular pool to the membrane. The steps involved in the signaling pathway between PKB and GLUT4 translocation, as yet, remain unidentified, however much research has been done into the mechanism for GLUT4 translocation to the membrane. SNAP 23, Vamp 2

and syntaxin 4 form a complex in SM known as SNARE (soluble N-ethylmaleimide-sensitive factor attachment protein receptor) that is required for vesicle-membrane fusion. Other ancillary proteins that may be involved have been identified, including Munc18c, synip, VAP 33 and rab 4 (reviewed in (79) and (114)). While GLUT4 is considered to be the major glucose transporter that is activated by insulin, GLUT8 has recently also been identified to be insulin sensitive (36).

The body has only a limited capacity for carbohydrate storage and is therefore readily converted to fat. Once inside the cell glucose is irreversibly phosphorylated by SM hexokinase to glucose-6-phosphate, which is then able to undergo glycolysis or glycogen synthesis. Insulin attenuates glycogen synthase kinase-3, therefore activating glycogen synthase (190).

1.1.1.3 Skeletal muscle amino acid uptake

Many of the amino acids are comparatively bulky and are hydrophilic, therefore also require facilitated transport. A number of SM amino acid transporters have been identified, and they vary in their sensitivity to insulin and their dependence on sodium (292). These transporters contain a cluster of membrane spanning regions that form a hydrophilic channel across the membrane, through which the amino acids can pass. Amino acids may be carried by multiple transporters, but selectivity is usually determined by the side chain. The A, L, N^M and ASC systems are dominant in SM. System A is a uniporter that carries the amino acids alanine, serine, glutamine, methionine or glycine ((43), reviewed in (29) (42) (292)). System L carries the large, neutral amino acids valine, leucine, isoleucine, methionine, phenylalanine, tyrosine or tryptophan (reviewed in (292)). System N^M transports glutamine, asparagine or histidine, while the major substrates for the ASC transporters are alanine, serine or cysteine (2) (42). Insulin greatly affects systems A and N^M ((165) (29) reviewed in (56)), and the effects of insulin and exercise are additive (309).

After entering the myocyte amino acids may be transaminated before entering the tricarboxcylic acid cycle for oxidation (reviewed in (273) (90)). In particular, valine and isoleucine are able to form the TCA intermediate succinyl-CoA, however leucine

and isoleucine can form acetyl CoA which can enter the TCA cycle (reviewed in (90)). While most essential amino acids undergo metabolism in the liver, the periphery (including SM and AT) is the major site of degradation of the branched chain amino acids (BCAA, valine, leucine and isoleucine). They may also be used for the synthesis of cell components, including enzymes and transporters, and often activate mRNA translation and gene expression. Amino acids are not stored as polymers in the body, however the largest pool of protein found in the body is in the myocyte. 66% of SM amino acids are components of the myofibrillar proteins actin and myosin (reviewed in (90)). Myofibrillar protein breakdown can be measured by detecting 3-methyl histidine (3-MH) release from muscle.

1.1.2 Nutrient uptake is affected by delivery (blood flow)

The delivery of nutrients to SM via the bloodstream is not only dependent on substrate concentration and flow rate, but is also largely influenced by the location of blood flow in SM. While it would appear likely that fuel uptake closely correlates with muscle total flow, we have shown that the uptake of nutrients is more closely associated with capillary flow than total flow to the muscle (209). Vasoactive agents such as insulin therefore may act to recruit capillaries without necessarily affecting total flow. For this to occur, flow must be drawn from another area within the muscle. There is now substantial evidence that two parallel circuits exist in the SM, and flow to each can be intimately regulated by the addition of certain vasoactive substances (reviewed in (46) (48)). Blood flow may therefore increase in one area (e.g. capillaries) at the expense of the other (possibly muscle septa and tendons). The uptake of glucose, amino acids and fatty acid (both albumin bound and free-fatty acid (FFA) derived from chylomicron-triglyceride (TG)) therefore will depend on the extent of capillary perfusion. An imbalance between capillary recruitment and de-recruitment will affect nutrient uptake and storage and may therefore predispose to certain metabolic syndromes, including diabetes. Both vasoactive agents and fuels themselves may affect glucose uptake by muscle. While flow may influence substrate uptake, uptake may also has some effect on total flow (in particular a reduction in capillary recruitment with insulin in diabetes), however this remains to be determined. Clearly the two factors, uptake and both total

and capillary flow, cannot be separated, and both factors are crucial in understanding the haemodynamic actions of insulin and mechanisms of insulin resistance.

1.1.2.1 Insulin acts to increase blood flow to muscle

While insulin stimulates glucose, fatty acid and amino acid transport and metabolism, it is now widely accepted that insulin also produces significant complementary increases in blood flow (reviewed in (15)). This additional vasodilatory action of insulin is thought to be largely nitric oxide (NO) dependent (260) (37) (231). NO is formed from the enzyme nitric oxide synthase (NOS) during the conversion of L-arginine to L-citrulline (reviewed in (17)). This reaction requires oxygen and NADPH as cofactors and is stimulated by a rise in cytoplasmic Ca^{2+} levels. Insulin acts on PKB/Akt in the endothelial cell via a PI3-Kinase activated pathway, which is postulated to phosphorylate and activate PKB/Akt and then NOS (62). Insulin also promotes the association of calmodulin with NOS to disrupt the suppressive effect of calveolin on the enzyme's activity (250). NO diffuses to the vascular smooth muscle cells and stimulates cyclic guanosine monophosphate (cGMP) production and subsequent vasodilatation. NOS is found throughout the vasculature and myocytes of SM (250) and NO may thus be generated in the myocytes, endothelial cell or smooth muscle.

Insulin has a haemodynamic action to increase capillary flow independently of changes to total flow

Dissociation between total flow and skeletal muscle metabolism

Insulin is believed to have a haemodynamic action in SM to increase total flow to the muscle and subsequently increase glucose uptake (148) (16) (4). Despite this well documented action, not all studies have shown increases in total flow with insulin (136) (200). Some researchers have shown increases in insulin-mediated glucose uptake (IMGU) with increased total flow (16) (83), but others have not (240) (177) (244) (124) (186). Pitkanen *et al.* (201) also infused the endothelium-dependent vasodilator sodium nitroprusside, and found increases in total leg flow and flow dispersion, but decreased

glucose extraction in resting muscle of healthy men. Moreover the increases in glucose uptake often precedes increases in total flow (83) (148). Similarly, oxygen consumption was unrelated to forearm blood flow *in vivo* (83). The uptake of glucose and oxygen by *in vivo* SM preparations therefore appear to be unrelated to total flow.

Metabolism is associated with capillary flow - evidence for capillary recruitment

Dissociation of the effects of insulin on glucose uptake and flow have also been shown in our laboratory *in vivo*. While total flow showed no clear relationship to IMGU, it was clearly proportional to capillary flow when determined by the conversion of the exogenous substrate 1-methyl xanthine (1-MX) to 1-methyl urate (1-MU), by the capillary-endothelial enzyme xanthine oxidase (209). Despite similar increases in total flow with both insulin and epinephrine, only insulin increased capillary flow (1-MX metabolism, (209)). In addition, collaborators of our laboratory in the U.S.A have reported no increase in total flow with 3 mU/mg/kg insulin, although an increase in capillary flow was evident (as determined by the distribution of albumin microbubbles) within 30 minutes of insulin infusion (287). Moreover, N(omega)-nitro-L-arginine methyl ester (L-NAME, an inhibitor of NOS) partially prevented insulin-stimulation of 1-MX conversion (289). Therefore insulin acts to recruit capillaries independently of changes in total flow, and this process is partly mediated by NO.

Definition of capillary recruitment

Capillary recruitment is the opening of previously quiescent capillaries for increased filtration. Recruitment is therefore an additional mechanism to distension (increase in capillary lumen volume) for increasing capillary perfusion. Distension is controlled by the vasodilatation of smooth muscle high in the vascular tree coordinating flow to all capillaries, therefore increasing total flow to all distal capillaries (reviewed in (172)). Recruitment may only affect certain subsets of capillaries by accessing the preceding terminal arteriole, thereby reducing the area between perfused capillaries and maximizing the area of substrate diffusion (reviewed in (248) (172)). Arteriolar

resistance will therefore exert primary control over the exposed capillary surface area for the exchange of nutrients.

Skeletal muscle resistance vessels

SM generates substantial whole body arterial blood pressure due to a large resistance to increases in cardiac output. Flow through SM resistance vessels is demonstrated by the equation:

$$Q = P/R$$

Where: Q is the flow, P the pressure and R the resistance. Moreover, the resistance is related to the arteriole diameter by the equation:

$$R = 1/r^4$$

Where: R is the vascular resistance and r is the arteriole diameter. Therefore, a small increase in the radius will produce a large decrease in vascular resistance, resulting in large increases in vessel flow.

Classification of resistance vessels in the skeletal muscle microcirculation

Precapillary arterioles can be classified according to their proximity to the feed arteriole. The arteriole directly downstream from the feed artery is usually designated as the 1st order arteriole (1A, approximately 100 μm) (248). All subsequent arterioles are classified in increasing order. The next apparent diameter reduction down the vascular tree represents the beginning of the 2nd order arteriole (2A). A transverse arteriole is usually a 3rd order arteriole, and, depending on the classification system used, the more distal 4th and 5th order arterioles (<15μm) directly precede the capillary modules (capillaries arising from a common arteriole). The 3rd to 5th order arterioles (≤40 μm) are thought to be responsible for capillary recruitment, therefore recruitment occurs in multiple capillary modules (172). A similar classification method is used for the venular vessels, where the post-capillary venules are designated 4 or 5V. 1st order venules (1V) are those leaving the muscle and often lie adjacent to the 1st order arterioles.

Vasoactive agents

The capillary endothelial surface area and hydrostatic pressure are of primary importance in determining capillary filtration, and these factors are largely influenced by the arterial and venular tone. Capillary filtration of the SM microcirculation can be manipulated by the use of vasoactive agents. Agents that constrict or dilate resistance vessels may alter both resistance and the distribution of blood flow within the SM.

Topically applied serotonin (5-HT) to the microvasculature of the rat cremaster muscle elicits dose-dependent changes in vessel tone (298). Concentrations ranging from 10^{-8} to 10^{-4} M causes substantial dilation of 4th order arterioles (classified in this case as the arterioles just preceding the capillaries), while at 10^{-4} M, constriction of the 1st order arterioles occurred (298).

Despite the arterial vessels being classical 'resistance vessels', changes in venous resistance may also exert control over capillary hydrostatic pressure. It is now evident that circulating vasopressin, angiotensin (AII) and catecholamines have constrictor effects on venules. The former two however produce only minor venular constriction compared to the arterioles. Norepinephrine (NE, 0.1 μM) increased arterial pressure and decreased venular pressure by a similar extent despite constriction in A1-A4 and V3-V1 (9). No change in constriction of the V4 may be due to only minute amounts of smooth muscle in these vessels. NE had greater constrictor effects on more distal arterioles. As already stated insulin may increase arteriole diameter through the release of NO (260) (37) (231) (307). In addition, prostaglandins stimulated by AII, bradykinin (24) and insulin (310) (284) also have vasodilatory effects. Infusion of either a NOS inhibitor, or an inhibitor of prostaglandin synthesis, prevented insulin-mediated reductions in forearm vascular resistance, suggesting the co-release of both with insulin (284). Prostaglandin release from the perfused rat hindlimb, had no effect on glucose uptake, however the dilatory effect of prostaglandins may be absent in this preparation, as it appears to be with insulin (310). It is therefore generally thought that vasodilators increase capillary filtration and vasoconstrictors decrease capillary filtration, however our laboratory has identified vasoconstrictors that are able to both increase and decrease substrate uptake by the perfused rat hindlimb (as discussed later in this chapter).

It is widely thought that the arterioles determine the extent of capillary perfusion, however for this mechanism to occur, arterioles must predetermine which capillary modules are to be perfused before the blood reaches the capillaries themselves (an unlikely phenomenon). In addition, adjacent fibres from different motor units (the group of muscle fibres innervated by a single motor neurone) can be supplied by a common capillary therefore dilation of the preceding arteriole would potentially supply unworking muscle fibres (reviewed in (172)). Moreover, the smaller order arterioles (larger, generally 1st and 2nd order) lie adjacent to the corresponding venules, allowing diffusion of muscle-derived substances into the arteriole. However, as discussed above it is the more distal arterioles that are responsible for capillary recruitment.

The primary controlling unit of capillary recruitment has recently been suggested to be the capillaries themselves (248) (172). One recently suggested hypothesis is that substances released from metabolically active muscle act locally to hyperpolarize adjacent endothelial cells. The endothelial cell may then transmit this membrane potential along the endothelial walls via gap junctions (membrane low resistance areas) to preceding resistance vessels (reviewed in (241) (248) (249)). Maximal perfusion of highly active muscle then occurs via signal transmission from the small arterioles (regulating capillary perfusion) to feed arteries external to the muscle (reviewed in (248)).

The direct application of NE, acetylcholine (ACh) and bradykinin (BK) to capillary endothelial cells of the rat extensor digitorum longus (EDL), constricted (with NE) or dilated (with ACh and BK) upstream arterioles (168). Super-perfusion experiments that were designed to omit the diffusion of released substances to the arterioles, led the authors to conclude that a dilatory signal was electronically conducted from the capillary to the arteriole via the endothelial cells. Therefore, a muscarinic receptor antagonist applied to the arteriole did not prevent vasodilatation after ACh administration to the capillary. Similarly K^+ caused depolarization of the endothelial cell membrane (reviewed in (172)). Substances released from the muscle fibres may cause local vasodilatation of post-capillary venules and subsequent vasodilatation in proximal arterioles.

It is also possible that capillary filtration is controlled by vasodilatation of the post-capillary venule by insulin. Endothelial NOS (eNOS) is distributed throughout the SM vasculature, including the venular vessels (250). A shear-stress related increase in NO release has been detected in the venules of SM with increased flow rates (142). A signal may then be transmitted up the vascular tree to the resistance vessels. Moreover, reduced oxygen tension and pH in the venule, with contraction, may stimulate RBC to release ATP. Direct application of ATP to venules results in dilation of upstream arterioles (52), and increases in venular ATP concentration cause dilation of adjacent arterioles (105). Moreover, the diffusion of oxygen via arterioles to adjacent tissue has been reported (70). Although capillary hydrostatic pressure is maximal with increased arteriole diameter and decreased venular diameter, it would seem logical that dilation in both would occur to allow removal of the extra flow and muscle metabolites.

As discussed above, capillary flow may be influenced by both the arteriole and venular network, and these changes are not always dependent on total blood flow. It therefore follows that fuel partitioning and uptake in SM will not always follow total flow. Anomalies in SM substrate uptake and blood flow have been well documented. The differences have been attributed to SM flow heterogeneity (46) (48).

Skeletal muscle capillaries

In 1923 August Krogh observed that a large number of capillaries in resting SM in frogs and guinea pigs contained either no RBC, or contained RBC that were stationary (147). Either electrical stimulation or massaging of the muscle resulted in substantial capillary recruitment. This phenomenon had already been noted after the application of heavy metals (reviewed in (147)). Krogh's model for oxygen exchange, however, described the capillaries of SM to be of homogenous distribution, so that all areas received oxygen from the nearest capillary (146). Despite this, it is widely recognized that the vessels in most muscles have a more random anatomical spacing. Goldman and Popel (86) have recently published complex computational models for certain capillary arrangements in SM and found that maximal tissue oxygen occurs in tortuous capillaries with concomitant cross-connections to other capillaries. Therefore,

due to the tortuosity of capillaries in shortened SM, Krogh's model may not be applicable (203).

1.1.3 History of anomalies of substrate delivery in skeletal muscle

1.1.3.1 Isolated, incubated muscle preparations

Insulin has been shown to increase 3-O-methylglucose uptake in the incubated soleus, however this was a smaller increment than obtained in hindlimb perfusion experiments (despite having a larger basal glucose uptake) (138). Although the creatine phosphate levels are comparable to fresh muscle, it is likely that in the soleus, the inner core may be anoxic, resulting in a higher basal glucose uptake, that is not apparent in muscles with less mitochondria (for example in the extensor digitorum longus (EDL)). The above effects are independent of the muscle vasculature, regulating flow patterns, and are often vastly different from *in situ* and *in vivo* preparations. During *in vivo* muscle preparations SM oxygen and nutrient supply is regulated by haematocrit, haemoglobin oxygen saturation, nutrient concentration and vascular delivery (reviewed in (116)).

1.1.3.2 A dual skeletal muscle microcirculation

In 1977 Grubb and Snarr (100) reported that IMGU was not further increased after a critical flow rate in perfused rat hindlimb. They suggested that the excess flow was escaping into another set of vessels that were "too thick" for optimal exchange. Individuals that were prone to psychological "nervous attacks" were noticed to have higher venous oxygen saturation than "less excitable" subjects (113). Similarly, infusion of NE to simulate this effect, resulted in increased flow however no change in calculated oxygen consumption (113). The bisphasic response of adrenaline on SM oxygen uptake was demonstrated in 1931 by von Euler (291) in the perfused hindleg of dogs. Adrenaline was found to both decrease and increase oxygen consumption (VO_2) at concentrations of $10^{-8.5}$ and $10^{-9} - 10^{-10}$ M respectively.

A key paper in presenting the anomalies of blood flow and oxygen uptake was reported by Pappenheimer (192), where a reduction in blood flow during intravenous administration of adrenaline to the isolated perfused dog hindlimb, increased VO_2. Alternatively, in the isolated perfused dog gastrocnemius, increased flow caused by electrical stimulation of the associated tibial nerve, reduced the arterial/venous oxygen extraction. The transient increase in VO_2 noted after stimulation contributed to the complicated recovery period and suggested these vasoconstrictor nerves have different localities and responses. These experiments also suggested that vasoconstrictor nerves may allow alterations in innate flow patterns within SM to allow perfusion of different areas (with different endothelial surface areas), depending on muscle requirements. Importantly, these observations did not correlate with changes in total blood flow to the muscle; from this he proposed that a dual vascular system existed within SM (192).

Alternative metabolic effects in a muscle with constant total flow, led Renkin to propose two metabolically and spatially distinct areas of the vasculature within SM (219). It appeared that certain vasomodulators were acting to increase capillary perfusion, while different doses or different vasoactive substances increased flow to the "escape" vessels that bypassed the capillary network.

Failure to produce convincing evidence for the existence of true arteriovenous anastamoses in SM (199) (257) (106) (11) led to the search for other possible anatomical candidates to encompass the "escape" circulation. Barlow *et al.* (12) recorded an increase in the clearance of ^{24}Na injected into the muscle bed during simultaneous infusion of intravenous epinephrine. The opposite response occurred with epinephrine infusion when the ^{24}Na was injected into muscle septa and tendons. Lindbom and Arfors (156) noted that feeding arterioles of the tenuissimus muscle often supplied both muscle capillaries and vessels of the neighboring connective tissue (CT). This view was supported by Grant and Wright (95). Using intravital microscopy, Borgstrom *et al.* (32) showed that the rabbit tenuissimus muscle contained capillaries and adjacent CT that were supplied by the same feed arterioles.

Our laboratory has produced mounting evidence to infer two distinct regions of SM blood flow (46) (48). The effects produced by the addition of certain vasoconstrictors cannot be explained simply by increases in oxygen consumption, due to

the energy used by smooth muscle (the proposed "hot pipes" theory). While this may contribute to some of the energy consumed during vasoconstriction, certain vasoconstrictors cause a decrease in SM oxygen consumption (211). In addition, the effects of vasoconstrictors on metabolism are absent in incubated muscle systems (211), implicating the importance of substances delivered via the vascular route. Moreover, these metabolic effects are not seen during concomitant infusion of a vasodilator, implying vascular effects of these agents. Changes in vascular permeability, and thus conditions for metabolic exchange, were ruled out, as the vasoconstrictor, 5-HT, that decreases oxygen uptake in the perfused rat hindlimb, is known to increase vascular permeability (reviewed in (167)). Taking these results into consideration, the most likely explanation for the two responses is the existence of two distinct, parallel pathways in SM in which blood can flow that are linked by a common transverse arteriole. One consists of the muscle capillaries and the other of a different set of vessels probably located in the muscle septa and tendons (181).

Nutritive flow

The pathway offering the greatest potential for nutrient exchange and therefore having the highest metabolic capacity (i.e. oxygen consumption), is paralleled by increases in the uptake of glucose, and the efflux of purines, pyrimidines and lactate (46). This occurs with no increase in total blood flow to the muscle. This vascular route has been termed nutritive due to the positive effect on metabolic rate, and is thought to consist of capillaries directly nourishing myocytes. Therefore, increasing access to this area is analogous to the capillary recruitment seen with insulin. The capillaries run parallel to the muscle fibres and are in close contact for nutrient exchange. Whether the increase in flow is the stimulus for increased metabolism, or visa versa, remains to be determined. Isolated SM was found to undertake a transient overcompensation in oxygen consumption after a period of oxygen deprivation. This oxygen payback was determined to be around 70% of the total oxygen lost during anoxia (76) (230) and suggested that oxygen can influence its own uptake. Therefore an increase in oxygen delivery (and that of other substrates) may increase its own metabolism. Another

possibility is that a shear stress-related paracrine signal, caused by the increased flow, is responsible for the increased metabolism (reviewed in (46)). It is important to note that increased metabolism by resting muscle (when exposed to appropriate vasoconstrictors) is always associated with increased perfusion pressure. As eluded to earlier, insulin does not affect pressure or oxygen uptake by the perfused hindlimb; this may be significant.

Manipulating the degree of capillary recruitment allows almost instantaneous alterations of exchange efficiency. Until now, insulin has been discussed as a major effector of capillary recruitment, however other vasoactive substances are able to manipulate the micovasculature for maximal perfusion. These have been termed Type A vasoconstrictors and include low frequency sympathetic nerve stimulation (102), α1-adrenergic agonists (including NE (≤0.1μM) (180)), AII (53), vasopressin (53) and low doses of various vanilloids (98).

The infusion of type A vasoconstrictors into the perfused rat hindlimb causes substantial red blood cell (RBC) washout (180), indicative of the recruitment of nutritive capillaries that are not perfused at rest. Vascular corrosion casting revealed higher flow dispersion throughout the hindlimb after infusion of the Type A vasoconstrictors, despite no increase in cast weight. Moreover, these vasoconstrictors increased the amount of fluorescent dextran that could be trapped in these capillaries after removal of the constriction (180). Nutritive flow in SM is currently determined using a variety of techniques including laser doppler flowmetry (45) (44), the conversion of 1-MX by the capillary endothelial enzyme xanthine oxidase (209) and following the intravascular pathway of albumin microbubbles (287).

Vasoconstrictors (Type A) thought to increases the perfusion of this area, probably act by impeding perfusion of a second area (termed non-nutritive). Flow can then only pass through the capillaries. Maximal perfusion of this nutritive area is thought to occur during stages of increased metabolic requirement, for example during exercise.

It is of interest to determine whether capillary recruitment with the Type A vasoconstrictors acts via similar mechanisms to insulin-mediated capillary recruitment (as discussed earlier). Diversion of flow to the capillary network (after the addition of a Type A vasoconstrictor) and an associated pressure increase, appears to stimulate

metabolism (oxygen and glucose uptake, lactate output etc.). Increased metabolism may therefore produce a signal molecule that is released from the myocyte, which may then cause vasodilatation (along with that from shear-stress) to further promote access to this pathway. In preparations such as the perfused rat hindlimb however, the vasculature is already fully dilated, so no complementary dilatory effect of the Type A vasoconstrictors would be seen. Type A vasoconstrictors may also cause some constriction of the post-capillary venules, increasing capillary hydrostatic pressure and thus facilitating exchange. These two factors thus suggest that increased uptake is from increased delivery, which can be manipulated via vasoactive agents through either constriction or dilation).

Non-nutritive flow

Blood diverted to the non-nutritive shunt vessels accesses an area within the SM with poor potential for nutrient exchange. Vasoconstrictors accessing this area are termed Type B and include 5-HT (211), high doses of NE (2.5μM (180)), and high doses of vanilloids (98). A significant reduction in oxygen consumption with no decrease in total flow is observed in perfused hindlimb muscles, that is not apparent in incubated muscle systems (211).

Less than half of the blood flowing into SM is thought to access this area in resting muscle (108). These non-nutritive vessels are located within individual muscles, as fluorescent microspheres remain trapped in dissected muscle after selective perfusion of non-nutritive sites. In addition, there appears to be a reduction in surface muscle flow as recorded by a decrease in the external laser doppler signal with 5-HT (measuring non-vectorial movement of RBC). Whether this is due to a decrease in flow dispersion or whether the non-nutritive vessels are not on the muscle surface remains unresolved. Using internal probes, non-nutritive sites can be detected within the muscle, but are not as frequent as nutritive sites (45). Other researchers suggest that these vessels are on the edge of muscles (311) and our laboratory has made convincing measurements of non-nutritive flow in muscle tendons (181). The tendon vasculature is connected to vessels present in the muscle perimysium (CT surrounding the fibre bundles). This CT may

therefore house the non-nutritive vessels. If so, the tendon may reflect non-nutritive flow changes on a smaller scale.

Studies using microsphere entrapment have shown that the non-nutritive vessels are slightly larger than the true muscle capillaries, and are thus produce less resistance to flow (288). As discussed earlier, 5-HT constricts larger arterioles or possibly even feed arteries, therefore it is likely that during 5-HT infusion the flow passes down the pathway of least resistance (the non-nutritive vessels). High doses of NE similarly constrict larger arterioles and/or feed arteries. This too would attenuate capillary flow, thus redirecting blood through non-nutritive vessels.

Non-nutritive flow and insulin resistance

5-HT infusion decreased IMGU in the perfused rat hindlimb (211) and decreased conversion of the exogenous substrate 1-MX to 1-MU (209). In addition, an analogue of 5-HT (α-methyl 5-HT) caused insulin resistance *in vivo* with diminished metabolism of 1-MX due to insulin (210). Non-nutritive flow therefore produces an acute state of muscle insulin resistance, probably by denying access of glucose and insulin to the capillaries. During long stages of physical inactivity and enhanced non-nutritive flow, changes in gene expression may lead to detrimental glucose tolerance and ultimately contribute to insulin-resistance (reviewed in (47)). Reports on SM blood flow with insulin resistance have been conflicting. It has been reported that NIDDM patients have a lower basal leg blood flow that remains unstimulated with insulin (149). Others have found no change (258). While there is no clear association between total flow and insulin resistance, it is likely that insulin resistance is associated with decreased capillary flow.

1.1.4 Mechanisms of fuel metabolism and insulin resistance

Insulin resistance may be loosely defined as a diminished insulin response (reviewed in (34)), resulting in decreased IMGU by SM, which is largely due to attenuated translocation of GLUT4 to the plasma membrane (reviewed in (237)). It is

likely that capillary flow (and thus glucose and insulin delivery) is reduced in Type 2 diabetes, and an imbalance of fatty acid and glucose may also largely determine SM insulin sensitivity.

1.1.4.1 Substrate competition

Infusion of fatty acids *in vivo* causes many of the alterations seen with insulin resistance (including hyperinsulinaemia, hypertriglyceridaemia and hypertension) and may therefore be a major contributing factor to the pathophysiology of obesity and diabetes (239). These diseases represent a defect in the uptake and release of substrates by most tissues, in particular AT, SM and liver. AT resistance to insulin results in uncontrolled lipolysis and a large release of FFA into the blood. Released FFA may have adverse affects on SM insulin sensitivity and glucose uptake. Since SM accounts for the majority of insulin-mediated glucose uptake by the body, investigation into the defective mechanisms in this tissue are of fundamental importance.

The Randle Cycle

Mechanisms for the reduction in glucose uptake/phosphorylation and glycogen synthesis with insulin resistance are not well understood; FFA have largely been implicated as a mediator. Elevated FFA appear to be linked to the reduction in oxidative and non-oxidative glucose disposal in SM. In 1963 Randle (206) proposed the Glucose/Fatty Acid Cycle as a mechanism for increased fatty acid oxidation inhibiting glucose uptake/oxidation, and this has been demonstrated in both rats and humans (128) (300) (135) (176) (224) (220). Under the Randle hypothesis, a buildup of cellular glucose 6-phosphate occurs from elevated mitochondrial ratios of acetylCoA/CoA and NADH/NAD+ (from increased FFA uptake and oxidation) that regulate pyruvate dehydrogenase by pyruvate dehydrogenase kinase. The additional buildup of cytoplasmic citrate (an allosteric regulator of phosphofructokinase) augments this effect. Elevated glucose-6-phosphate levels will inhibit hexokinase and ultimately reduce

insulin-mediated glucose uptake. Subsequent pyruvate build-up may also increase lactate formation, a substrate for gluconeogenesis, thus contributing to hyperglycaemia.

Lack of evidence for the Randle cycle in human SM

While the Randle Cycle has gained considerable acceptance, it could not be demonstrated in the perfused rat hindquarter with oleate or palmitate using supraphysiological insulin concentrations (232). In addition, in pmi28 myotubes palmitate but not mysitic or stearic acid decreased IMGU (266). There appears to be even less evidence for its existence in humans. Despite Boden *et al.* (27) demonstrating an increase in the ratio of mitochondrial acetylCoA/CoA with elevated FFA, no increase in muscle citrate or glucose-6-phosphate was observed (226) (27). Moreover, FFA have been shown to inhibit pyruvate dehydrogenase but only modestly inhibited glucose oxidation (135). SM hexokinase activity was not different between lean humans and those with NIDDM (134). In addition, effects on glucose disposal are dependent on FFA concentration (26). Importantly, elevated FFA are not always reported in patient with NIDDM, and therefore may not be causative (202).

Type-II diabetics have a large intracellular pool of TG in SM (73) (92) (110) which may cause increased rates of lipid oxidation (a key component of the Randle cycle). Ellis *et al.* (69) have published data suggesting that the intracellular accumulation of long chain acylCoA is as important as the blood-borne FFA (27) (227) in determining muscle insulin-sensitivity, which appears to be negatively correlated to the intramyocellular store (reviewed in (111)) and to the activation of glycogen synthase by insulin (197). This is despite the fact that larger intramyocellular pools also occur in athletes (who are highly insulin sensitive). This apparent paradox may be explained by the differing morphology and location of the intracellular pools, which are larger and more closely associated with the mitochondria in athletes (reviewed in (111)).

While increased fat oxidation may cause some decrease in glucose disposal, an initial defect in glucose oxidation (as suggested by Randle) may not be the cause. Reports on glucose-6-phosphate levels in muscle after the infusion of TG emulsions such as Intralipid® have been conflicting (227) (27). It appears that the onset of glucose

uptake is time dependent. Boden *et al.* (27) reported an initial decrease in glycolysis was compensated for by an increase in glycogen synthesis, causing no net change in glucose uptake. After approximately 2 hours of Intralipid® infusion, glycogen synthesis was also attenuated causing a reduction in muscle glucose uptake. In contrast, Roden *et al.* (227) however, saw an initial reduction in glucose transport/phosphorylation due to elevated FFA followed by reduced glycolysis and glycogen synthesis.

Alterations in dietary FFA may modify membrane phospholipid content. Membrane phospholipids are indicative of insulin sensitivity and may alter insulin binding, and the extent of saturation of membranes lipids is also correlated to the amount of lipid stores within the myocyte (reviewed in (111)). Alternatively FFA may act indirectly to inhibit muscle glucose disposal (i.e. effects on other tissues), for example, alter insulin-secretion (41) and hepatic glucose and TG production.

The Reverse Randle Cycle

Despite Randle's proposition that enhanced FFA oxidation decreases that of glucose, it has been shown that SM glucose oxidation is actually higher in Type 2 diabetics than people with normal insulin tolerance under fasting hyperglycaemia (reviewed in (133)). Once glucose has entered the myocyte there appears to be no reduction in glucose disposal with insulin resistance, suggesting that it is the transport that is limiting its utilization (227).

The 'Reverse Randle cycle' was proposed in a study utilizing the hyperglycaemic, hyperinsulinaemic clamp in the human forearm (253). These researchers found that a decrease in glucose-6-phosphate impaired glucose oxidation, however if glucose uptake was maintained during a period of elevated FFA, FFA oxidation was inhibited, despite no reduction in glucose oxidation. This is in direct opposition to the Randle cycle and suggests this cycle may be peculiar to rat heart and diaphragm.

Failure to reproduce this cycle in the perfused rat hindlimb, led Reimer *et al.* (217) to suggest that increased glucose degradation to glycerol-3-phosphate increases the potential for FFA esterification to form TG (instead of undergoing oxidation).

Moreover, glycerol-3-phosophate acyl transferase is stimulated by insulin (170), however with insulin resistance it would be expected that reduced stimulation of this enzyme would reduce the potential for FFA to deposit as intracellular TG. However, insulin resistance is associated with increased SM TG deposits (73) (92) (110). SM LPL is also reduced in type-2 diabetes (202), and is thus not likely to be contributing to the increased SM TG.

Increased levels of malonylCoA increasing long chain acyl CoA with insulin resistance

Increased glucose oxidation leads to the build-up of long chain acyl CoA, which may be the cause of insulin resistance. SM acetyl CoA carboxylase is regulated by phosphorylation or cytosolic citrate. A combination of insulin and glucose (and high fructose) have been shown to activate acetylCoA carboxylase β, therefore increasing malonylCoA formation (65) (238). The phosphorylation and inactivation of acetylCoA carboxylase by AMP-activated protein kinase (AMPK) reduces FFA synthesis. In addition, malonyl CoA perturbs the passage of long chain fatty acylCoA's into the mitochondria via allosteric inhibition of carnitine palmitoyl transferase 1 (reviewed in (234) (107)). AMPK also phosphorylates and subsequently inhibits hormone sensitive lipase, preventing FFA release. Therefore AMPK increases FFA oxidation, but inhibits FFA synthesis (preventing energy-requiring processes). AMPK also phosphorylates glycogen synthase, resulting in increased glucose oxidation and decreased fatty acid oxidation (reviewed in (107)).

By a similar mechanism it has been proposed that SM hexokinase IV (glucokinase) is inhibited by long chain Acyl CoA via the hexosamine-phosphate pathway (275). The resulting decrease in glucose-6-phosphate, causes a build up of cellular glucose which has adverse affects on GLUT4 translocation (attenuating glucose uptake and utilization) (134). It has recently been reported that there is a colocalization of acylCoA synthetase-1 and GLUT4 in adipocytes suggesting direct influence of one over the other (256).

Reduced lipid oxidation may contribute to intracellular accumulation of long chain acylCoA's increasing diacylglycerol and activating protein kinase C (in particular ε and θ isoforms) therefore inhibiting IRS-1 and insulin receptor activation (97). These mechanisms are outlined in the diagram below (Fig. 1).

Amino acids may also alter the metabolism and storage of glucose. Leucine inactivates glycogen synthase kinase-3, therefore increasing glycogen storage (196). Glutamine also stimulates glycogen synthesis in addition to attenuating the rate of SM protein synthesis and breakdown (reviewed in (221)).

1.1.5 Summary

Many possible mechanisms may therefore be causal of insulin resistance. Most are controlled by substrate competition and availability and are likely to be greatly influenced by the existence of two vascular networks operating in parallel within SM. Altering the extent of capillary recruitment or capillary de-recruitment may provide some link between the inability of insulin to recruit capillaries and insulin resistance.

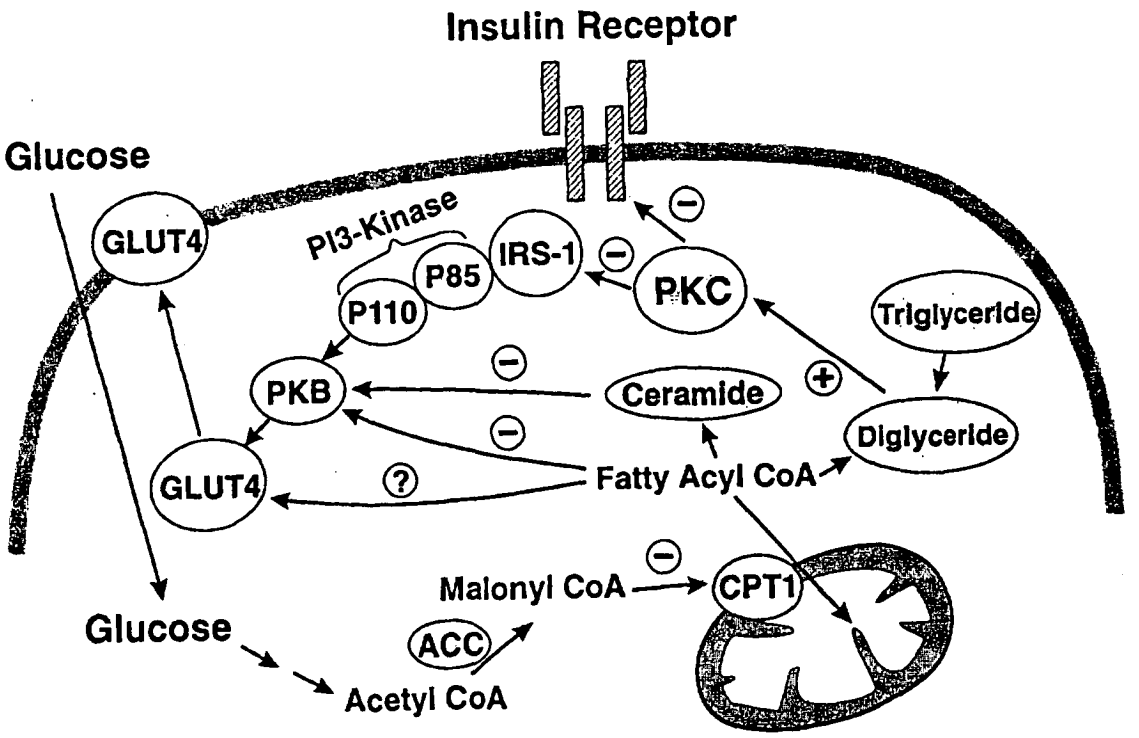

Figure 1. Possible mechanisms for substrate-induced insulin resistance (133).

1.2 Substrate affecting skeletal muscle blood flow

While insulin may affect nutrient uptake by increasing muscle total flow, we believe that uptake is more closely correlated with capillary flow. The previous section discussed the potential biochemical mechanisms for SM capillary recruitment with insulin. Possible controlling mechanisms are shown here in Fig. 2. Two main ideas have been proposed. The first is that insulin may act directly on the muscle, endothelial cell, SM or vascular smooth muscle to produce NO. In fact, NOS is located throughout the myocytes and SM vasculature (250). Another possibility is that increased metabolism in the myocytes (from insulin infusion) results in the production of metabolites that cause the release of NO. The metabolites (e.g. adenosine, K^+, CO_2 etc) might act locally to hyperpolarize the capillary endothelial cell, which is then transmitted to the preceding

arterioles (as discussed in the first section of this chapter). Alternatively, released metabolites may act on more remote locations in the SM vasculature by diffusion, to either act directly on the smooth muscle or the endothelial cell, resulting in NO production. Whether the vasodilatory effect of insulin is due to direct effects on the endothelium (i.e. due to insulin signaling in the endothelial cell) or due to metabolic effects in the myocytes, will be difficult to determine. One approach will be to utilize substances that inhibit metabolism in muscle cells, and then subsequently determine if the vasodilatation with insulin is retained.

1.2.1.1 Insulin signaling and elevated fatty acids

In insulin resistance we believe that the ability of insulin to recruit capillaries is either reduced or absent. It is likely that abnormal levels of glucose, fatty acids and possibly amino acids play some role in contributing to this endothelial dysfunction. Any point in the pathways postulated in Fig. 2, may be disrupted by abnormal substrate levels, which may affect insulin sensitivity.

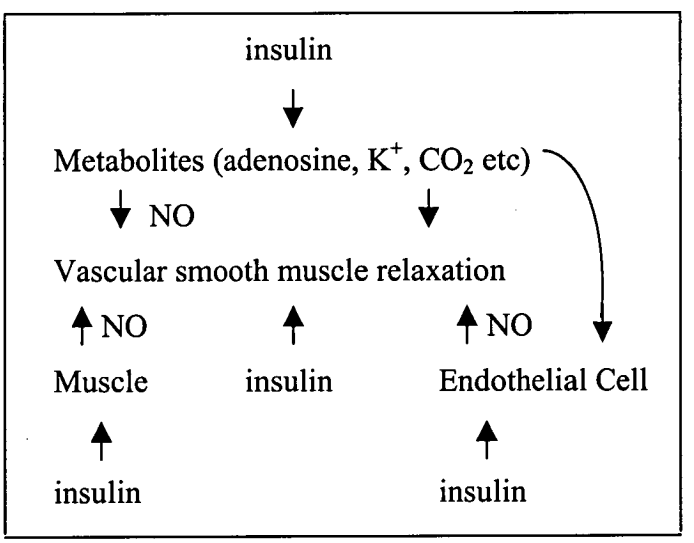

Figure 2. Possible mechanisms for insulin-induced capillary recruitment

Glucose, amino acids and fatty acids have some effects on muscle total flow. Glucose itself has been shown to increase leg blood flow (49) but fructose has not (290). Lundholm *et al.* (159) infused an amino acid cocktail into the human leg which produced positive effects on glucose uptake, lactate efflux, leg blood flow and oxygen consumption. In contrast, FFA are usually reported to have adverse affects on muscle blood flow, in particular, FFA have been reported to effect nitric oxide-induced vasodilatation by insulin (261). As a result total flow is reduced. However FFA may also have important effects on capillary flow. By using an *in vivo* assay to measure exogenous 1-MX metabolism by xanthine oxidase (an enzyme located in muscle capillary endothelial cells) we can determine the effects of abnormal substrate levels on the extent of capillary perfusion. It is therefore of interest to determine if elevated FFA interfere with insulin-mediated capillary recruitment.

Insulin has been linked to the stimulation of eNOS via activation of PKB/Akt (62), probably in both muscle and endothelial cells. In addition, as described in the first section, NOS is distributed throughout the vasculature (including the endothelial cells lining capillaries, arterioles and venules, and also in the vascular smooth muscle and the myocytes themselves (250)). Insulin can therefore activate NOS and stimulate NO production in any of these tissues.

FFA have been found to attenuate endothelial dependent dilation but not endothelial independent vasodilatation, suggesting direct effects of the FFA on the endothelial cell (262) (155). Disruption of PI3-Kinase affects PKB/Akt situated downstream from IRS-1 (the primary substrate for the insulin receptor) which directly phosphorylates NOS (62). Therefore, FFA and FFA derivatives (e.g. ceramide) are able to influence endothelium dependent vasodilatation and possibly capillary recruitment. Palmitic acid also decreased insulin stimulated phosphorylation of the insulin receptor, IRS-1 and PKB/Akt (266). Moreover, FFA have been shown to enhance the activity of PKC θ, which subsequently inhibits insulin signaling, in particular IRS-1 associated PI3-Kinase (97).

Another possibility is that FFA are able to interfere with the NO release or insulin signaling in the vascular smooth muscle. Insulin has been shown to increase ^{3}H 2-DG uptake by perfused aortic vascular smooth muscle cells of lean Zucker rats, which was inhibited in the obese Zucker despite significant amounts of GLUT4 in this tissue (10). While these results suggest that vascular smooth muscle is an insulin-sensitive tissue, there is little evidence to infer that the vascular smooth muscle associated with SM is also.

Knockout mice for the endothelial cell insulin receptor have been shown to have no deficiency in SM glucose uptake/disposal (285). From this it is reasoned that the muscle is the key factor regulating insulin sensitivity. These experiments, however, may have been more convincing if an insulin clamp was used, instead of a glucose tolerance test, to determine insulin sensitivity. The vascular responsiveness to insulin in these mice remains to be determined. However, Huang *et al.* (118) found in eNOS knockout mice that some dilation was maintained with ACh, due to the release of an unknown endothelial derived hyperpolarizing factor. Insulin may therefore stimulate a signal in SM (possibly from increased metabolism, e.g. adenosine, K^{+}, CO_2 etc) that acts locally on capillary endothelial cells. By a mechanism discussed earlier the metabolites may hyperpolarize the endothelial cell and this is conducted to the arteriole for the production of NO. NO may then diffuse to the underlying smooth muscle for vasodilatation, and capillary recruitment. Alternatively the metabolite may diffuse throughout the muscle to ultimately reach the endothelial cell of the preceding terminal arteriole and produce NO or NO may diffuse from venules adjacent to arterioles. Due to the presence of NOS in the myocytes (250) it is also possible that metabolites released from glucose oxidation may act locally to produces NO in the myocyte.

As suggested earlier, one metabolite that may be upregulated as a result of glucose metabolism, is adenosine. Dela and Stallknecht (61) saw no increase in the interstitial concentration of adenosine with insulin (as measured by microdialysis). Abbink-Zandbergen *et al.* (1), however, showed that addition of the adenosine receptor antagonist theophylline, to an insulin clamp in humans, prevented the insulin-induced increases in total blood flow. Therefore insulin may release adenosine in a similar manner to exercise or hypoxia (163). During hypoxia it is thought that the release of

adenosine from the SM may directly affect smooth muscle or endothelial cells. Alternatively adenosine may act on receptors on the SM to release K^+ for subsequent vasodilatation (either directly or indirectly (163)).

It is therefore an appealing hypothesis that metabolites released from SM may cause vasodilatation ('metabolic coupling'). However against this fact, fructose infusion with concomitant increases in carbohydrate oxidation did not increase blood flow in humans (290).

A proposed mechanism for the reduction in glucose uptake with FFA has been shown (reviewed in (194)) where FFA inhibit PI3-Kinase and IRS-1 phosphorylation. The inhibition of PI3-Kinase by FFA does not appear to be confined to the endothelial cell. The inhibition of muscle PI3-Kinase will also affect muscle metabolism, and appear to develop at the same time (i.e. after 2 hours in humans). Therefore the effects on the myocyte and endothelium cannot be separated. Moreover, while FFA are known to attenuate endothelial dependent vasodilatation, they have also been shown to reduce endothelial independent vasodilatation (160).

1.3 Summary of literature and research aims

Two vascular networks exist in SM. One is likely to consist of the muscle capillaries, and the other, the associated CT (septa and tendons). Insulin may therefore recruit capillaries by drawing flow from the CT, resulting in no change in total flow to the muscle. Certain vasoconstrictor agents have also been shown to alter the distribution of flow between the two compartments, without changing total flow. Most current studies to date report on the effects of increased metabolites on total blood flow, but as it now appears apparent that the perfusion of certain subsets of capillaries is more important, this effect needs to be determined. Conversely, the elevated FFA associated with insulin resistance may contribute to the inability of insulin to recruit capillaries (therefore denying access of glucose and insulin to the muscle). Clearly the effects of

substrate metabolism and blood flow can not be separated as each exert control over the other.

Research aims:

1. To determine how vasoactive agents affect the uptake of blood-borne metabolites (glucose, amino acids and fatty acids (both albumin bound and fatty acids derived from chylomicron-TG)) in SM.

   This will be approached by using vasoconstrictors in the perfused rat hindlimb to determine the uptake of radiolabeled substrate.

2. To determine whether elevated FFA interfere with insulin-mediated glucose uptake and capillary recruitment?

   This will involve the use of the euglycaemic hyperinsulinaemic clamp to determine the effects of elevated FFA on muscle [^{3}H] 2-deoxyglucose uptake and insulin mediated capillary recruitment (1-MX metabolism).

CHAPTER 2

2 General Methods

2.1 Introduction

To assess the uptake of blood-borne metabolites by SM, the perfused rat hindlimb was used in chapters 3, 4 and 5. The surgery and general perfusion protocol is described below. Any deviations or other details from this method are outlined in individual chapters. The experiments assessing blood flow in the rat *in vivo* (Chapter 6) are outlined in the "methods section" of that chapter.

2.2 Perfused rat hindlimb

2.2.1 Animals

Male hooded Wistar rats were cared for according to the Australian Code of Practice for the Care and Use of Animals for Scientific Purposes (1990 Australian Government Publishing Service, Canberra). Rats were housed in the local animal house and kept on a 12 hour light/dark cycle maintained at 22°C. All animals were allowed free access to water and a standard laboratory chow (Gibson's, Hobart) of 21.4% protein, 4.6% lipid, 68% carbohydrate and 6% crude fiber with added vitamins and minerals.

2.2.2 Krebs buffer

Krebs Henseleit buffer consisted of

118 mM NaCl

4.74 mM KCl

1.19 mM KH_2PO_4

1.18 mM $MgSO_4$

25 mM $NaHCO_3$

5.0 mM (Chapter 5) or 8.3 mM glucose (Chapters 3 and 4).

2.2.3 Perfusion buffer

The perfusion buffer used in chapters 3, 4 and 5 are outlined in the individual chapters and consisted of Krebs buffer containing either 6% Ficoll® (Chapters 3 and 4) or a combination of bovine serum albumin (BSA) and bovine RBC (Chapter 5). After gassing the buffer for >30 min with either carbogen (95% O_2: 5% CO_2) (Chapters 3 and 4) or a mixture of 95% air: 5% CO_2 (Chapter 5), $CaCl_2$ was added to a final concentration of 2.54 mM. All buffers were filtered through a 0.45 μm filter before use. Individual recipes for each perfusion type are outlined in the methods section of each results chapter.

2.2.4 Surgery for perfusion of the rat hindlimb

An intraperitoneal injection of pentobarbitone sodium was given to anaesthetise rats (5-6 mg $100g^{-1}$ body weight) before the surgical procedure. Surgery was performed essentially as described previously (233) (53), with minor changes outlined below. Ligatures were placed around various blood vessels to isolate the left hindlimb for perfusion (shown in Fig. 1).

After loss of sensory perception, a string ligature was tightly tied around the left tarsus and the base of the tail to prevent perfusion of the left foot and tail. The abdominal skin was cut to gain access to the underlying midline of the body wall. An incision was made along the midline and extended up from the pubic symphis to the xyphoid process covering the sternum. Both the left and right epigastric vessels were ligated with cotton and a small section of the body wall between the two ligatures (upper and lower) was removed from either side. A ligature was tied around the left skin vessel (adjacent to the left femoral vein and artery). The testes were tied and removed, and the

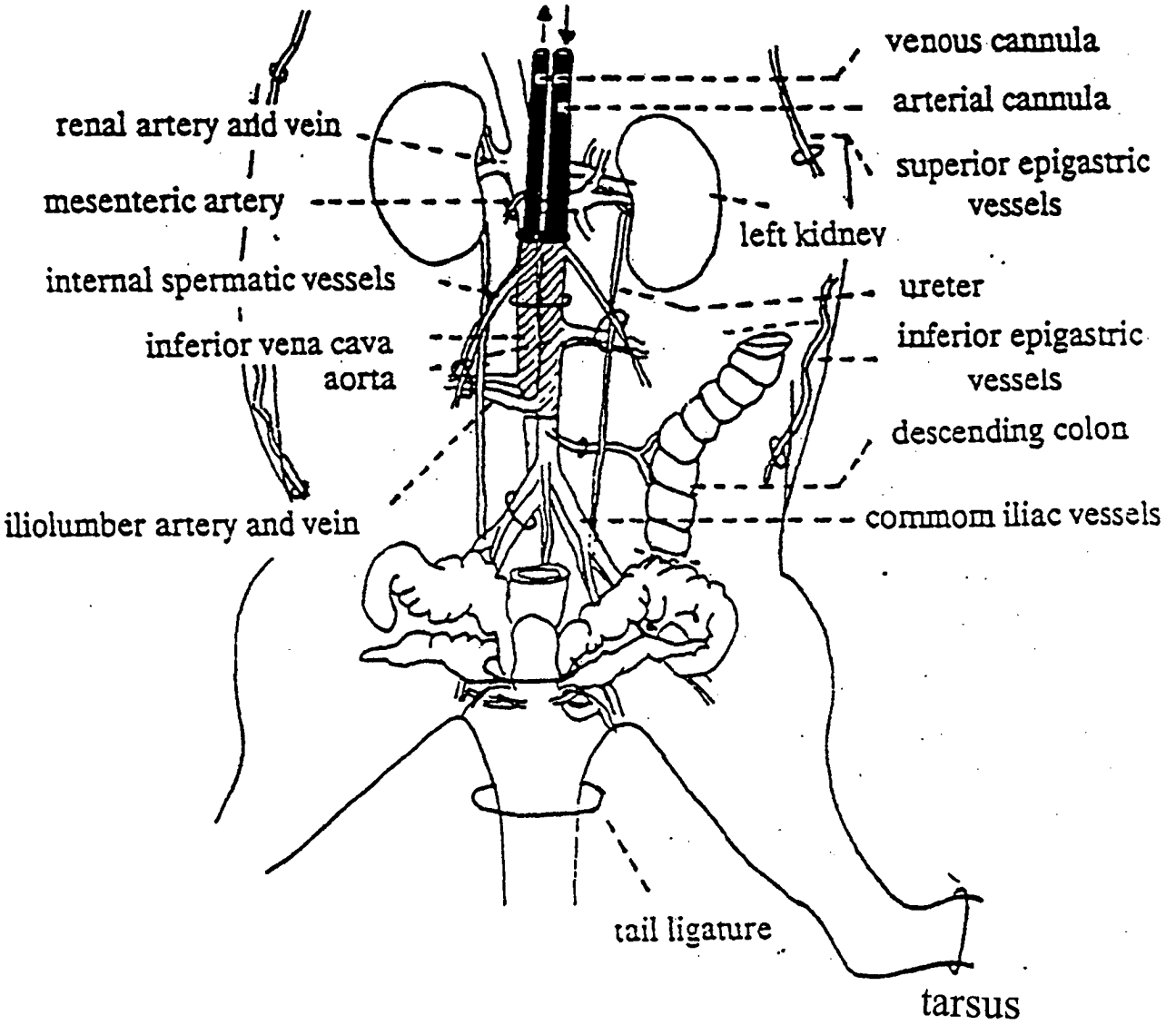

Figure 1 Surgery for the perfused rat hindlimb

Diagrammatic representation of blood vessel ligation and cannulation. Modified from Ross (229) and Greene (96).

bladder and seminal vesicles were tied together and the seminal vesicles were removed. Two ties were placed around the lower descending colon at a distance of approximately 5 mm and a cut was made between the two ties. A third tie was placed around the duodenum and the superior mesenteric vessel, just proceeding the stomach, and the gastrointestinal tract was subsequently removed in its entirety. A single ligature was placed around the left iliolumbar, ureter and the internal spermatic vessels. An identical ligation was performed on the same vessels of the right side. In all experiments only the left hindlimb was perfused, therefore flow to the contralateral limb was prevented by ligating the right common iliac vessel.

The inferior vena cava was separated from the descending aorta, and two silk ties were placed under each at the level of the renal and iliolumbar vessels. In some experiments, heparin was subsequently injected (200 IU) into the vena cava above the renal vessel. A one-minute delay was allowed, to ensure adequate circulation of the heparin before commencement of the surgery. The vena-cava tie, adjacent to the renal vessel, was secured and an 18 Gauge Terumo Surflow cannula (with needle) was inserted into the vein. The needle was removed to allow blood flow and the cannula secured with the lower tie. The same procedure was followed for cannulation of the aorta, however this was achieved using a 20 Gauge Terumo Surflow cannula attached to a 1 ml syringe containing 0.9% saline. Insertion of this cannula was facilitated by the use of a small needle threader. The entire surgical procedure did not exceed 30 minutes.

The rat was immediately placed on a water-pad heated to 37°C, and tubing was attached to the aorta cannula for delivery of the perfusion buffer. The hindlimb was not without flow for more than two minutes. A tube was attached to the venous cannula to allow collection of the venous effluent in a waste bucket, or for re-circulation into the buffer reservoir (see chapters 3, 4 and 5 for exact method). The rat was then killed with a lethal dose of nembutal by intracardiac injection. A string ligature was tied around the rat belly at the level of the L4 vertebra to impede extraneous flow.

2.2.5 Perfusion apparatus

Most experiments were conducted in a non-recirculating manner (as shown in Fig. 2) unless otherwise indicated. The perfusion equipment was encased in a perspex cabinet heated to 37°C. The apparatus shown in Fig. 2 is detailed below.

Perfusion buffer (described in each results chapters 3, 4 and 5) was aspirated from the buffer reservoir via a Cole-Parmer Masterflex® pump at a constant flow (of either 4 or 8 ml/min). The buffer was initially pumped into a small bubble trap within a water-jacketed heat exchange coil maintained at 37°C. The buffer then passed through silastic tubing (Dow Corning) surrounded by a carbogen-gassed lung (95% O_2 / 5% CO_2), unless indicated otherwise. Finally, the buffer was pumped into a small bubble trap proximal to the rat (containing an infusion port (for delivery of infused substances) and a side-arm attached to a pressure gauge to monitor the arterial perfusion pressure (PP) throughout the experiment). The buffer then entered the arterial cannula for perfusion of the left hindlimb. The venous effluent passed through a 0.5 ml Clark-type electrode to measure hindlimb oxygen consumption ($\dot{V}O_2$) and for venous sampling, before entering the waste container. The PP and $\dot{V}O_2$ was continually monitored via a WinDaq data acquisition system on a computer adjacent to the cabinet.

2.2.6 Vasoactive agents

During the perfusion vasoactive agents were either added as a bolus to the reservoir, or infused into the port proximal to the hindlimb via an LKB Microperpex® Peristaltic pump. The dose of agent used is detailed in each chapter.

2.2.7 Perfusion Protocols

The perfusion protocols used in Chapters 3, 4 and 5 are shown below. The concentrations of all infusions are outlined in the individual chapters.

Protocol A

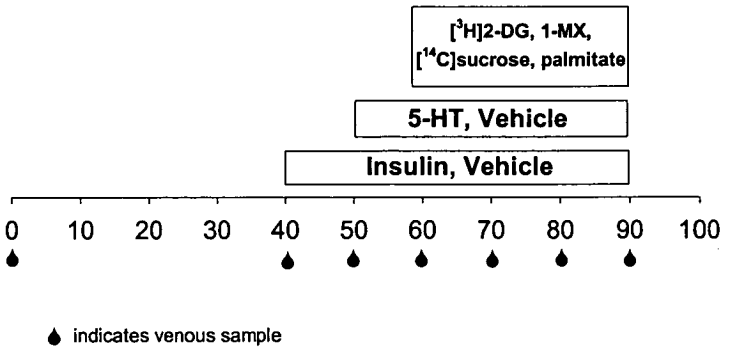

Protocol B

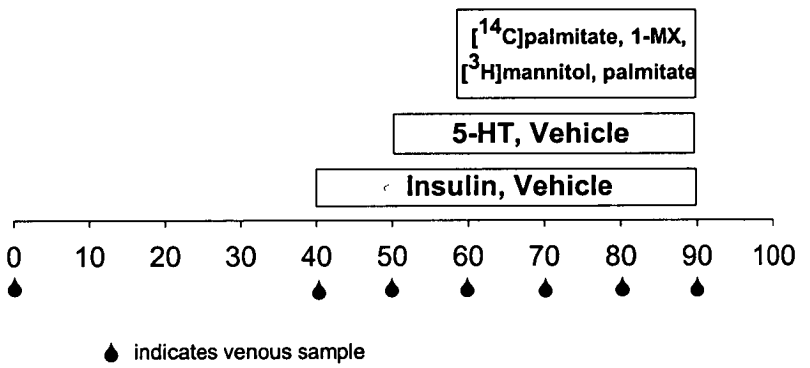

Protocol C

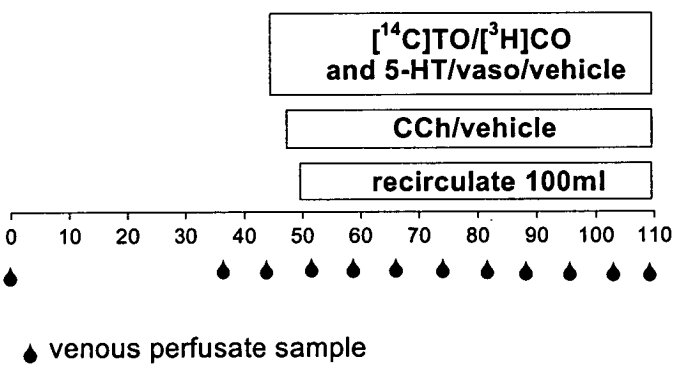

Protocol D

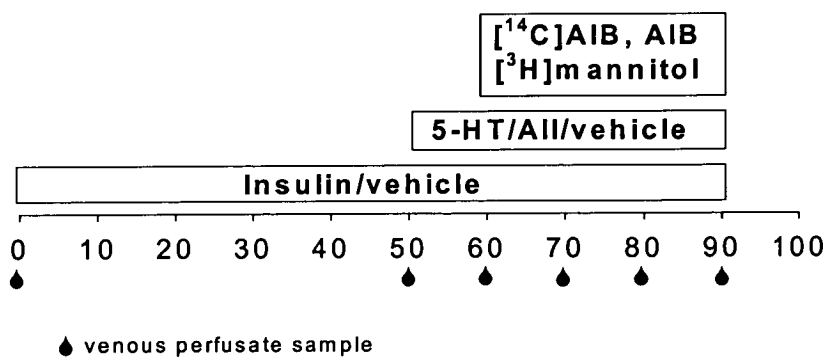

2.2.7.1 Protocol A - Chapter 3

The uptake of the non-metabolizable substrate [^{3}H] 2-DG into the non-recirculating perfused rat hindlimb was determined under the conditions described above. Time 0 is the beginning of hindlimb perfusion, and all other additions are indicated in the boxes. The following perfusion types were conducted:

1. controls (vehicle)
2. insulin (Ins, 75 nM)
3. serotonin (5-HT) + Ins (3 μM and 75 nM respectively).

After 30 min of 2-DG infusion the radioactivity in the hindlimb muscles was determined.

2.2.7.2 Protocol B - Chapter 3

The uptake of [^{14}C] palmitic acid into the non-recirculating perfused rat hindlimb was determined as described in the protocol above. Time 0 is the beginning of hindlimb perfusion, and all other additions are indicated in the boxes. The following perfusion types were conducted:

1. controls (no additions)
2. Ins (75 nM)
3. 5-HT (3 μM)
4. 5-HT + Ins (3 μM and 75 nM respectively).

After 30 min of [^{14}C] palmitic acid infusion the radioactivity in the hindlimb muscles was determined.

2.2.7.3 Protocol C - Chapter 4

To determine the effects of 5-HT and vasopressin (vaso) on chylomicron TG hydrolysis, the following re-circulating perfusion types were conducted:

1. controls (no additions)
2. 5-HT (0.5-1 μM)
3. 5-HT + carbamyl choline (0.5-1 μM and 100 μM CCh respectively)
4. vaso (0.5 nM)

5-HT and vasopressin were added as bolus doses to the reservoir of some perfusions. In some experiments the vasodilator CCh was infused to reverse the effects of 5-HT on PP and $\dot{V}O_2$. CCh infusion commenced before the buffer was recirculated. After discarding the first 30 ml of perfusate (of the 130 ml perfusion medium containing CLE) the remaining 100 ml was recirculated through the hindlimb for 1 hour.

2.2.7.4 Protocol D - Chapter 5

To assess the uptake of the amino acid analogue α amino isobutyric acid (AIB), the following perfusion types were conducted:

1. Controls (no additions)
2. Ins (18 mU/ml)
3. AII (50 nM)
4. AII + Ins (50 nM and 18 mU/ml respectively)
5. 5-HT (1 μM)
6. 5-HT + Ins (1 μM and 18 mU/ml respectively)

The hindlimbs were perfused according to the protocol shown above (protocol D). After a 40 min equilibration period, 50 mM AIB was infused with 400 Ci [^{14}C] AIB and 40 Ci [^{3}H] mannitol for 30 min at a dilution of 1/100 (final concentration 0.5 mM AIB). Perfusions assessing the uptake with insulin used 18 mU/ml of Ins added as a bolus to the perfusion buffer. In some perfusions, either 1 μM 5-HT or 50 nM AII were infused 5 min prior to AIB infusion. AIB was infused for the remainder of the experiment (30 min).

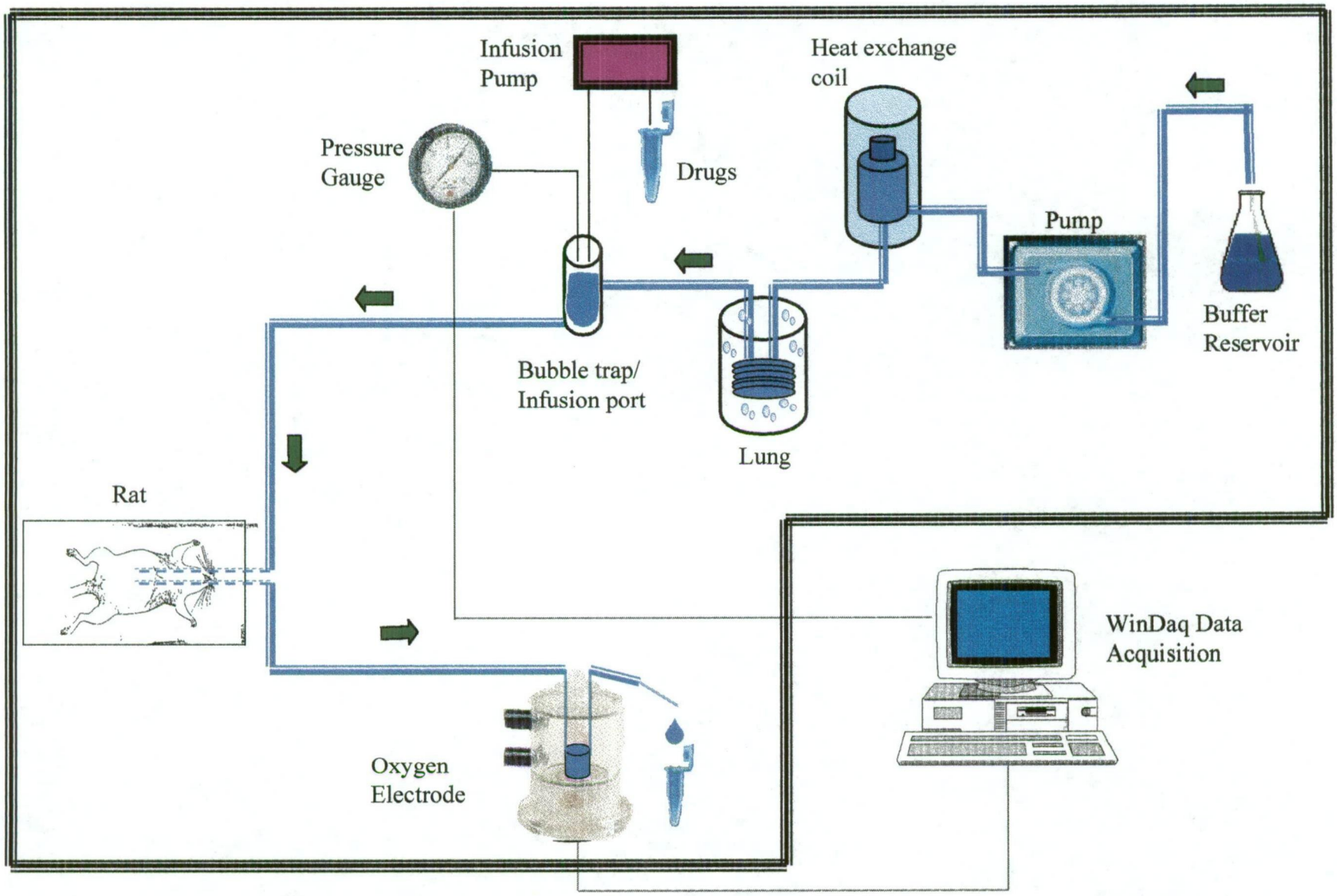

Figure 2. Apparatus for the non-recirculating constant flow, pump-perfused rat hindlimb

2.2.8 Calculation of oxygen consumption (VO_2)

Muscle oxygen consumption was calculated using the Fick Principle:

$$VO_2 = \frac{\beta \times (P_aO_2 - P_vO_2) \times (flow/1000) \times 60}{\text{Muscle weight (g)}}$$

*Where β = calculated from the Bunsen coefficient

α = the volume (ml) of oxygen dissolved per ml of plasma at 0°C and 760 mmHg. α is 0.0214 in plasma at 37°C.

$\beta = \alpha / (22.4 \times 760)$

= 0.0214 ml/L / (22.4 mM x 760mmHg)

= 1.257 μmol/L/mmHg

*Where P_aO_2 = arterial PO_2 using the calibrations from the oxygen electrode for the arterial, air and oxygen and using their known PO_2.

$$P_aO_2 = \frac{\text{cal Ar} - \text{cal Air}}{\text{Cal } 100\%O_2 \text{ cal Air}} \times (PO_2 \text{ at } 100\% - PO_2 \text{ in Air}) + PO_2 \text{ in Air}$$

Where: *cal Ar* = electrode arterial calibration

cal Air = electrode air calibration

cal 100%O_2 = electrode oxygen calibration

PO_2 at 100% = 760 mm Hg – 47 mmHg (H_2O vapour pressure at 37°C, due to the use of a wet oxygen electrode).

= 713 mmHg

PO_2 in Air = 154 mmHg

*Where P_vO_2 = venous PO_2 calculated the same as the P_aO_2 however the value for cal Ar was replaced by the value for the venous effluent.

*Where *flow* = perfusion flow rate in ml/min, which is defined in chapters 3, 4 and 5.

*Where *muscle weight* = total perfused muscle mass, which has been previously been determined to be $1/12^{th}$ of the body weight (for a single perfused hindlimb (223)).

2.3 Measurement of plasma glucose and lactate

Venous samples were immediately spun in an Eppendorf centrifuge and the plasma eluted into another vial. Venous and arterial (from the buffer reservoir) samples were analysed for glucose and lactate using a YSI 2300 STAT Plus Glucose Analyser.

2.4 Radioactivity uptake into muscle

After all hindlimb perfusions the soleus, plantaris, extensor digitorum longus (EDL), gastrocnemius red (G.Red), gastrocnemius white (G.White), and the anterior tibialis were removed. Individual muscles were weighed and then freeze-dried overnight to obtain dry weight. Muscles were re-hydrated in 1 ml of distilled H_2O and dissolved in 1 ml of ®Soluene (tissue solubiliser; Packard). Muscles were digested for a few days in a 40°C water bath before addition of 100 µl of acetic acid and 16 ml of Amersham Biodegradable Counting Scintillant. Dissolved muscle samples were counted for radioactivity using a dual label program (to detect [^{14}C] and [^{3}H]).

As used in Protocol A, muscles were counted for [^{3}H] 2-DG and [^{14}C] sucrose, and in Protocol B for [^{14}C]palmitic acid and [^{3}H]mannitol in Chapter 3. In chapter 4, muscles were counted for [^{14}C]oleic acid and [^{3}H] CO (Protocol C). In chapter 5, muscles were counted for [^{14}C] AIB and [^{3}H] mannitol (Protocol D).

2.5 Perfusate radioactivity

In all perfusions, venous samples were taken at regular intervals and a known amount was added to Amersham Biodegradable Counting Scintillant for determination of perfusate radioactivity (using the program described above). As used in Protocol A, perfusate samples were counted for [^{3}H] 2-DG and [^{14}C] sucrose, and in Protocol B for [^{14}C]palmitic acid and [^{3}H]mannitol in Chapter 3. In chapter 4, samples were counted for [^{14}C]oleic acid and [^{3}H] CO (Protocol C). In chapter 5, samples were counted for [^{14}C] AIB and [^{3}H] mannitol (Protocol D).

2.6 1-MX metabolism

The metabolism of the exogenous substrate 1-MX by the capillary endothelial enzyme xanthine oxidase was determined in chapters 3 and 6. Precipitation of the samples with perchloric acid is outlined in those chapters. Samples were then loaded onto a C-18 reverse phase high performance liquid chromatography column. The 1-MX disappearance was calculated from arterio-venous plasma 1-MX difference and multiplied by femoral blood flow. More specific details are given in the individual chapters.

2.7 Statistics

All tests were performed using the SigmaStat^{TM} statistical program (Jandel Software Corp.). In order to ascertain differences between treatments, the statistical significance of differences between groups of data was assessed by one or two way analysis of variance (ANOVA) for sets of experiments containing multiple groups. For experiments comparing only one experimental group to the controls, student's t-tests were used. Significant differences were recognized at $P<0.05$. One, two or three symbols were used to show significance of $P<0.05$, $P\leq0.01$ and $P\leq0.001$ respectively. In

the perfusion chapters (Chapters 3, 4 and 5) the symbols used to show significance were: '*' (to show significance from controls), '#' (to show significance from 5-HT), '^' (to show significance from 5-HT+CCh), '+' (significant from insulin infusion), '&' (to show significance from AII infusion) and '$' (to show significance from AII and insulin infusion). In the *in vivo* experiments (Chapter 6) the symbols used were '*' (to show significance from Ins treated group) and '†' (to show significance from Lip + Ins treated group).

CHAPTER 3

3 Hormonal effects on FFA uptake by the constant flow perfused rat hindlimb

3.1 Introduction

We have previously reported that the vasoconstrictor, 5-HT is able to reduce capillary (nutritive) flow in SM perfused with a BSA/Krebs buffer. This was determined by measuring the metabolism of infused 1-MX, a substrate for the capillary endothelial enzyme, xanthine oxidase (211). Reduced capillary flow was associated with decreased muscle oxygen consumption and marked insulin-resistance with regard to insulin-mediated glucose uptake, both in individual muscles and across the entire hindlimb (211). We have proposed that this is due to decreased access of insulin and glucose to the myocytes, and may contribute to hyperinsulinaemia and hyperglycaemia respectively.

Other researchers have shown that elevated plasma FFA levels are also associated with insulin resistance. This may be a consequence of either reduced FFA uptake by limb tissues or elevated FFA release from AT. Increased FFA uptake and oxidation have generally been considered as the primary cause of reduced insulin-mediated glucose uptake by muscle (206), but the exact mechanism for insulin resistance via substrate competition is unresolved. Recently, the SM of insulin resistant humans has been shown to have a reduced capacity to oxidise FFA (132).

The perfused rat hindlimb is a widely accepted model for determining the effect of substrate uptake by SM, and is preferable over cultured myocytes and incubated muscle preparations, as the vasculature remains intact. Thus, vasoactive substances can be delivered through the vessels, as occurs *in vivo*. Using fluorescent microspheres to monitor blood flow distribution we have shown that as a percentage of total flow, the

isolated hindlimb is primarily comprised of SM, with bone, skin and fat contributing only minimally (208). The perfused rat hindlimb gives comparable rates of oxygen consumption to SM *in vivo* (164) (233) and perfusing the hindlimb with a Krebs Henseleit buffer and bovine serum albumin (BSA) produces acceptable levels of glucose uptake (164). Red blood cell (RBC) may also be added (304) to emulate blood *in vivo*. Additionally, we have shown that oxygen uptake is correlated with muscle or nutritive capillary flow (304) (208) and is thus commonly used as a surrogate indicator of capillary flow. While the rat hindlimb is commonly perfused with bovine serum albumin (BSA)/Krebs, it was found that FFA liberated from hydolyzed circulating TG preferentially bound the BSA rather than being taken up by the myocytes (Chapter 4). Trapping fatty acids generated from hydrolysis in the vasculature may be advantageous, due to removal of the components of uptake and oxidation. Alternatively, Ficoll® may be used to measure the uptake of FFA from isolated or artificial lipid solutions.

Whereas lipid is hydrophobic, glucose is highly water-soluble and is therefore readily transported in the blood stream. As a result, glucose uptake can be easily measured in the perfused rat hindlimb and *in vivo*. Glucose substrates that are both metabolized and not-metabolized have been used. [^{3}H] glucose is often used as a measure of whole body glucose disposal. Constant infusion of [^{3}H] glucose into the rat *in vivo*, and arterial sampling to monitor the specific activity, gives a measure of hepatic glucose release and whole body disposal. This substrate is however disadvantageous as it is both taken up and released by muscles, thus no real measure of muscle uptake can be made. [^{14}C] glucose is also used, but is readily metabolized and measurements of metabolism must also be made. Fluorescent glucose analogues are also used (186) (150). We have commonly used [^{3}H] 2-deoxyglucose (2-DG) both in the perfused rat hindlimb (211) and *in vivo* (305). This substrate is taken up by myocytes and immediately converted to [^{3}H] 2-deoxyglucose- 6-phosphate, with no further metabolism. [^{3}H] 2-deoxyglucose- 6-phosphate can then be separated from [^{3}H] 2-DG to give a measure of glucose content in the myocytes and in the extracellular space (vessels and interstitial space) respectively.

The present study aimed to examine the effect of low nutritive flow mediated by 5-HT infusion in the Ficoll®-perfused rat hindlimb, on fatty acid and glucose uptake.

Due to the addition of extracellular [^{14}C] or [^{3}H] markers to all experiments, the uptake of [^{3}H]2-deoxyglucoe (2-DG) and [^{14}C] palmitic acid were determined in separate perfusions. To minimize variability, both perfusion buffers contained 8.3 mM glucose and 1.2 mM palmitic acid. As a consequence we were unable to determine whether the FFA had any effect on glucose uptake. Rather, focus was on assessing whether low nutritive flow, with expected haemodynamic insulin resistance, had any effect on the uptake of [^{14}C] palmitic acid.

3.2 Materials and Methods

3.2.1 [^{14}C] palmitic acid solution

Palmitic acid (369.2 mg), 1.4 ml 1 M NaOH, 28 ml of distilled H_2O and 80 μCi [^{14}C] palmitic acid (Amersham) were heated at 75-90°C for 20 min until saponified. The solution was then cooled to 50-60°C prior to the addition of Krebs-Ringer bicarbonate buffer (90.6 ml) containing 6% (wt/vol) BSA. Finally, the mixture was passed through a 1.2 μm filter and stored at –20°C until used.

3.2.2 Unlabeled palmitic acid solution

Unlabeled Na-palmitate (albumin-bound) was prepared by the same protocol as the [^{14}C] palmitic acid solution, with the omission of the [^{14}C] palmitic acid.

3.2.3 Mannitol solution

To monitor perfusate in the interstitial and vascular space of the perfused muscle, a solution containing 65 mM mannitol and 40 μCi [^{3}H] mannitol (NEN) was prepared.

3.2.4 [^{3}H] 2-Deoxyglucose solution

A solution of 90 μCi [^{3}H] 2-deoxyglucose (2-DG, Amersham), 2 mM sucrose and 50 μCi [^{14}C] Sucrose (Amersham) was prepared. [^{14}C] Sucrose was used in these perfusions instead of [^{3}H] mannitol in order to correct for volume in the extracellular space when infusion [^{3}H]2-DG.

3.2.5 Hindlimb Perfusions

General protocol

The left hindlimbs of 140-160 g rats were perfused in a non-recirculating mode with 6% (wt/vol) ®Ficoll (Amersham Pharmacia Biotech.) containing Krebs-Henseleit buffer (section 2.2.2 of the Methods chapter) and 1.27 mM $CaCl_2$ at 8 ml/min. The buffer was continually gassed via a sialastic tube oxygenator with carbogen (95% O_2 : 5% CO_2), and the temperature was maintained at 37°C in a heat-exchanger coil. The rat and apparatus were in a temperature-controlled cabinet at 37°C. All other details are described in section 2.2 of the Methods chapter of this thesis.

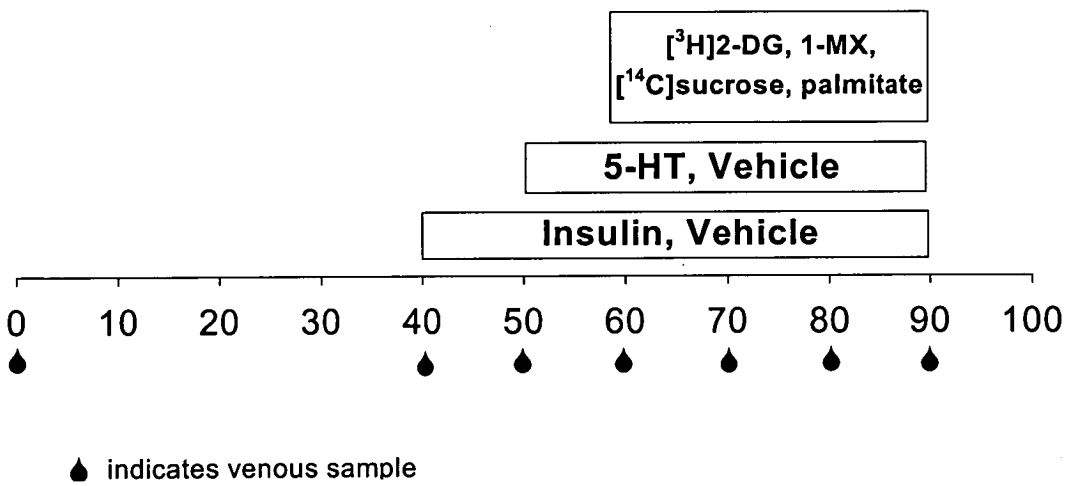

Figure 1. Perfusion protocol for [^{3}H] 2-DG uptake

Perfusion protocol for [^{3}H] 2-DG uptake

The uptake of the non-metabolizable substrate [^{3}H] 2-DG into the perfused rat hindlimb was determined under the conditions described above (Fig. 1). Time 0 is the beginning of hindlimb perfusion, and all other additions are indicated in the boxes. The following perfusion types were conducted:

1. controls (vehicle)
2. insulin (Ins, 75 nM, Humulin®, Aza Research Pty Ltd)
3. 5-HT + Ins (3 μM and 75 nM respectively).

After completion of the surgical procedure (described in section 2.2.4 of the Methods chapter), the rat hindlimb was perfused for 40 min with 6% ®Ficoll/Krebs buffer (sections 2.2.2 and 2.2.3 of the Methods chapter). Following this equilibration period, Ins (if used) was infused for the entirety of the experiment. The infusion of 5-HT (if used) was commenced at 50 min and continued for the entirety of the experiment. The effect of 5-HT infusion alone was not determined as this vasoconstrictor has previously been shown to have no effect on basal [^{3}H]2-Deoxyglucose uptake (211). At 60 min, the buffer reservoir was changed and the rat hindlimb then perfused (while maintaining the infusion of Ins and 5-HT or vehicle with medium) containing the following constituents:

-26 ml unlabeled palmitic acid solution (described in section 3.2.2, 1.2 mM final)
-1.3 ml [^{3}H] 2-Deoxyglucose solution (described in section 3.2.4)
-232.7 ml gassed 6% ®Ficoll/Krebs buffer
-0.65 ml 10 mM 1-MX.

The hindlimb was perfused with this mixture for 30 min (time 0 to 30 min in Figure 1) and venous samples of 1.5 ml were taken every 10 min. The total perfusion time was 90 min.

Perfusion protocol for [^{14}C] palmitic acid uptake

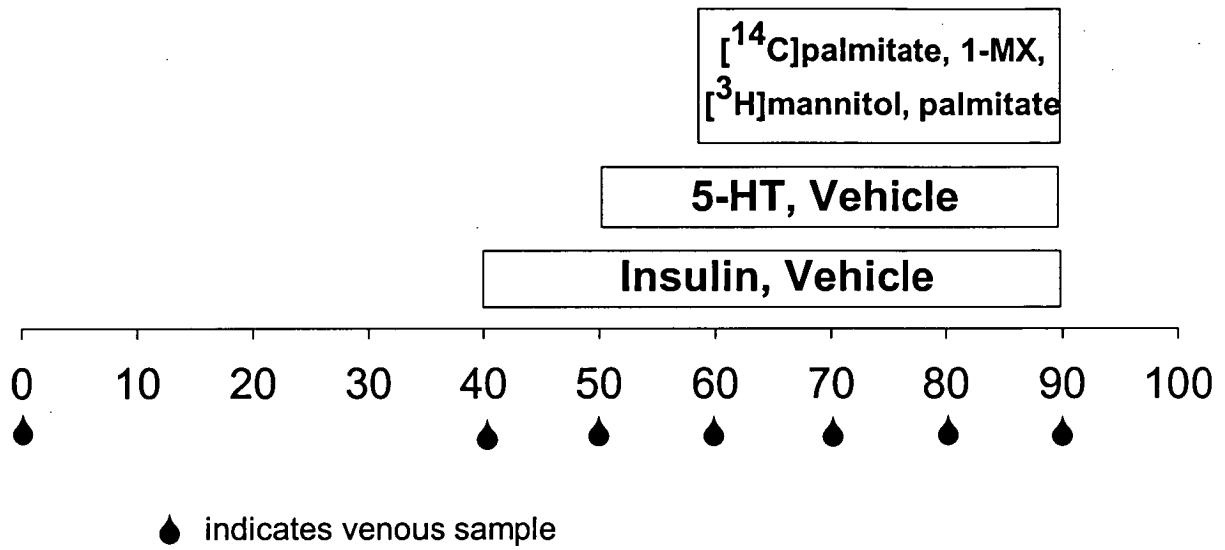

Figure 2. Perfusion protocol for [^{14}C] palmitic acid uptake

The uptake of [^{14}C] palmitic acid into the perfused rat hindlimb was determined as described in the protocol above (Fig. 2). Time 0 is the beginning of hindlimb perfusion, and all other additions are indicated in the boxes. The following perfusion types were conducted:

1. controls (no additions)
2. Ins (75 nM, Humulin®, Aza Research Pty Ltd)
3. 5-HT (3 μM)
4. 5-HT + Ins (3 μM and 75 nM respectively).

After completion of the surgical procedure (described in section 2.2.4 of the Methods chapter), the rat hindlimb was perfused for 40 min with 6% ®Ficoll/Krebs buffer. Following this equilibration period, Ins (if used) was infused for the entirety of the experiment. The infusion of 5-HT (if used) was commenced at 50 min and continued

for the entirety of the experiment. At 60 min the buffer was changed and the rat hindlimb then perfused with medium containing the following constituents, while maintaining the infusion of ins and 5-HT or vehicle:

-26 ml [^{14}C] palmitic acid solution (described in section 3.2.1, 1.2 mM final)
-2 ml mannitol solution (described in section 3.2.3)
-232 ml gassed 6% ®Ficoll/Krebs buffer
-0.65 ml 10 mM 1-MX.

The hindlimb was perfused with this mixture for 30 min (time 0 to 30 min in Figure 2) and venous samples of 1.5 ml were taken every 10 min. The total perfusion time was 90 min.

3.2.6 Perfusate glucose and lactate determination

The concentrations of glucose and lactate in each venous perfusate sample were determined as described in section 2.3 of the Methods chapter.

3.2.7 Perfusate radioactivity measurements

Perfusate samples containing radioactivity were immediately centrifuged to remove RBC. Samples (200 µl) were then added to 6 ml Amersham Biodegradable Counting Scintillant and counted using a dual label counting system (for the detection of [^{3}H] and [^{14}C]) as described in Chapter 2 section 2.5

3.2.8 Muscle radioactivity uptake

After perfusion, the soleus, plantaris, EDL, G.Red, G.White and tibialis of the left hindlimb were removed. The muscles were digested and analysed as described in the Methods chapter, section 2.4 of this thesis.

3.2.9 Calculation of muscle extracellular space

In all perfusions either [^{14}C] sucrose or [^{3}H] mannitol was infused to determine the muscle extracellular space. The extracellular space (ml.g^{-1}) was calculated from the amount of radioactivity in each muscle (dpm.g^{-1}) and the specific activity of the infused solution (dpm.ml^{-1}).

3.2.10 Determination of 1-MX conversion

Perfusate samples of 100 µl were de-proteinised with 25 µl 2 M perchloric acid, centrifuged, and an aliquot of 40 µl injected onto a reverse-phase HPLC column. Values obtained from the HPLC were used to calculate the disappearance of 1-MX. Full details are given in Chapter 2 section 2.6.

3.2.11 Statistical Analysis

Statistically significant differences for oxygen uptake ($\dot{V}O_2$) and perfusion pressure (PP) between groups over the 30 min perfusion period were assessed using two-way, repeated-measures analysis of variance (ANOVA). All other tests were conducted using one-way ANOVA.

P values less than 0.05 were considered to be significant. One, two or three symbols were used to denote *P* values of <0.05, ≤ 0.01 and ≤ 0.001 respectively. The symbols used were '*' (to show significance from control perfusions), '+' (significant from Ins infusion), and '#' (significant from 5-HT infusion).

3.3 Results

Only the uptake of [^{14}C] palmitic acid and [^{3}H] 2-DG were determined in separate experiments. The other measurements ($\dot{V}O_2$, PP, 1-MX metabolism, glucose uptake, lactate efflux, wet weight to dry weight ratios of the muscles, and the muscle extracellular space) were pooled and shown in Figures 3, 4, 5, 8 and 9.

Figure 3 shows the time course for the effects of 3 μM 5-HT, 75 nM Ins, and 5-HT + Ins on $\dot{V}O_2$ (panel A) and PP (panel B). Maximal stimulation with 5-HT (with or without Ins) occurred at the beginning of perfusion with the palmitic acid perfusion medium (0 min on graph). 5-HT (without Ins) decreased $\dot{V}O_2$ from 22.0 ± 0.5 to 9.7 ± 0.8 μmol/g/h during maximum stimulation (P<0.001) when compared to control perfusions (Fig. 3, panel A). This was accompanied by increased PP from 41.6 ± 1.3 to 167.7 ± 13 mmHg (Fig. 3, panel B, P<0.001). Using a combination of 5-HT and Ins, $\dot{V}O_2$ and PP were also significantly different when compared with control perfusions (from 22.0 ± 0.5 to 9.6 ± 0.6 μmol/g/h (P<0.001) and from 41.6 ± 1.3 to 180.7 ± 7.8 mmHg (P<0.001) respectively). Overall, the addition of 5-HT with or without Ins significantly reduced oxygen consumption by the perfused rat hindlimb. Since in this system $\dot{V}O_2$ is a surrogate indicator of nutritive capillary flow, capillary flow was deemed to be reduced with 5-HT infusion.

The metabolism of 1-MX, by the capillary enzyme xanthine oxidase, is a further indicator of capillary perfusion. The metabolism of 1-MX was also reduced when comparing 5-HT to control perfusions (from 5.8 ± 0.4 to 4.5 ± 0.4 nmol/min/g (P=0.024), Fig. 4). Furthermore, 1-MX metabolism was reduced with the co-infusion of 5-HT and Ins, in comparison to the infusion of Ins alone (from 5.9 ± 0.5 to 3.8 ± 0.4 nmol/min/g (P=0.004)).

While we have established a reduction in capillary flow with 5-HT infusion in these experiments, insulin resistance was also tested. The total glucose uptake and lactate efflux by the entire perfused mass was determined from arterio-venous differences (Figure 5, panels A and B respectively). Glucose uptake across the total perfused mass was stimulated by approximately 3-fold (from 12.2 ± 0.7 to 29.2 ± 1.7 μmol/g/h (P<0.001)). 5-HT reduced the insulin-mediated glucose uptake across the entire hindlimb (from 29.2 ± 1.7 to 23.1 ± 1.8 μmol/g/h (P=0.005)). Lactate efflux (panel B) significantly increased with Ins infusion (from 37.7 ± 1.4 to 48.9 ± 4.1 μmol/g/h (P=0.01)) when compared to control perfusions.

A set of experiments using the non-metabolizable glucose tracer, 2-DG were conducted to confirm a state of ins-resistance with 5-HT in the individual hindlimb muscles. Ins significantly increased 2-DG uptake in all hindlimb muscles tested (Fig. 6,

panel A). This increase was greater than 6-fold (from 13.6 ± 1.4 to 82.1 ± 4.6 μmol/g/h (P<0.001)) when averaging the uptake into all muscles (Fig. 6, panel B). The addition of 5-HT to Ins perfusions however decreased 2-DG uptake in all muscles, in particular in the EDL and tibialis. Averaging the hindlimb muscles, panel B shows the addition of 5-HT reduced hindleg insulin-mediated glucose uptake from to 82.1 ± 4.6 to 41.6 ± 6.7 μmol/g/h (P<0.001).

Panel A of Figure 7 shows the uptake of [^{14}C] palmitic acid by the hindlimb muscles. While the infusion of Ins tended to increase the uptake of [^{14}C] palmitic acid, this was not significant. The infusion of 5-HT significantly reduced the uptake of [^{14}C] palmitic acid in the EDL and the tibialis. When insulin was co-infused with 5-HT, there was also a significant reduction in fatty acid uptake by the muscles with predominantly white fibres (EDL, G.white and tibialis). 5-HT decreased insulin-mediated [^{14}C] palmitic acid uptake from 38.3 ± 2.6 to 11.2 ± 4.0 μmol/g/h in the EDL (P<0.001), 14.6 ± 2.2 to 6.0 ± 1.7 μmol/g/h in the G.White (P=0.036) and 33.6 ± 0.6 to 10.2 ± 3.7 μmol/g/h in the tibialis (P<0.001). When averaging the uptake across the selected muscles (Fig. 7, panel B), the co-infusion of 5-HT and Ins significantly reduced the uptake compared to insulin infusion alone (from 26.9 ± 2.3 to 13.4 ± 2.7 μmol/g/h (P=0.02)).

The extracellular space (radioactivity in the blood vessels and interstitial space) of the hindlimb muscles was determined using either [^{14}C] sucrose or [^{3}H] mannitol as extracellular markers. Negligible difference was recorded between all groups within each muscle sampled (Fig. 8). Wet weight to dry weight ratio of the muscles was increased in some muscles during 5-HT infusion, however was mostly unaltered between experimental types (Fig. 9).

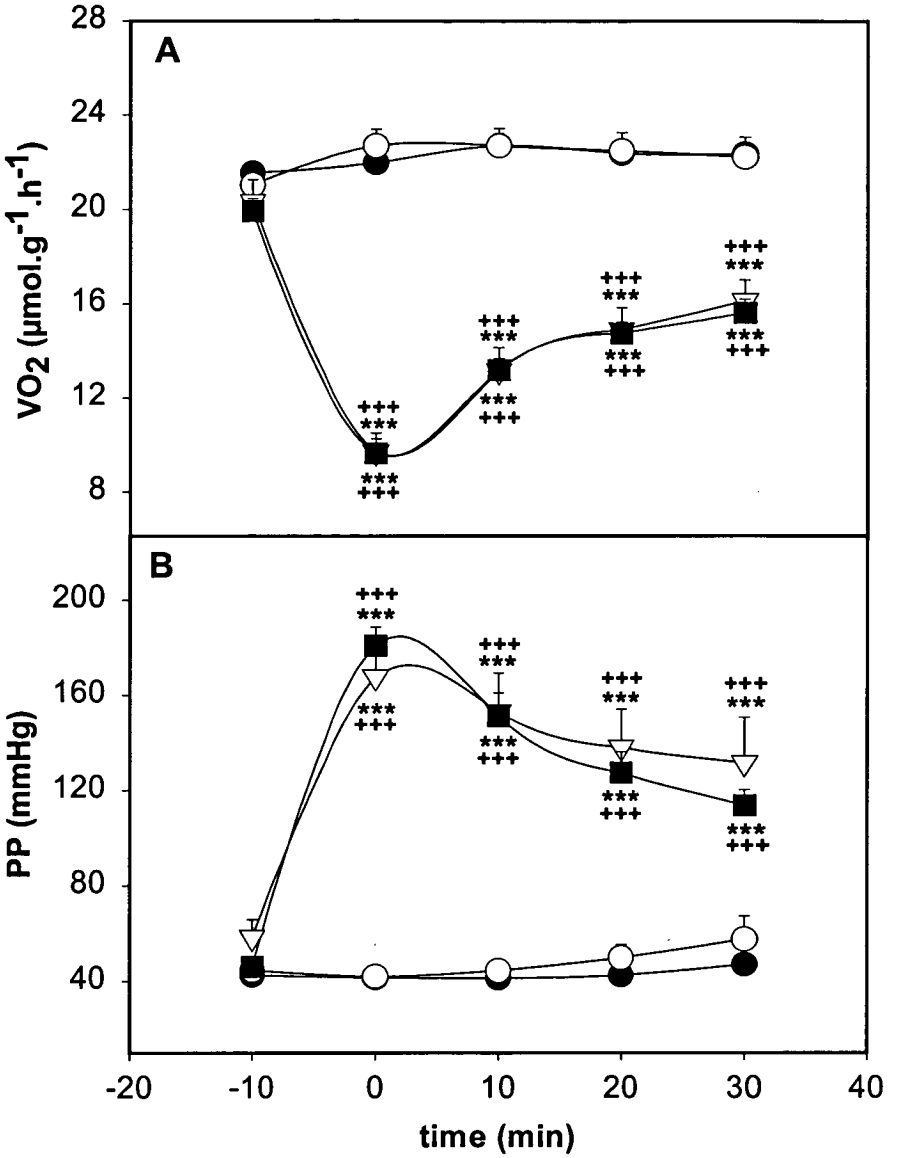

Figure 3. Hindlimb oxygen consumption ($\dot{V}O_2$, panel A) and perfusion pressure (PP, panel B) in the constant flow, Ficoll® perfused rat hindlimb. Perfusions were control (●), 75 nM Ins (○, from -20 min), 3 μM 5-HT (■, from –10 min), or the infusion of both Ins and 5-HT (▽). Rat hindlimbs were perfused with [^{3}H] 2-DG solution or [^{14}C] palmitic acid buffer (from 0 min to 30 min). Values are means ± SE (n=10-11) and given in gram wet weight. Significance symbols are denoted by '*' (from control) and '+' (from Ins), where two or three symbols represents $P \leq 0.01$ and $P \leq 0.001$ respectively.

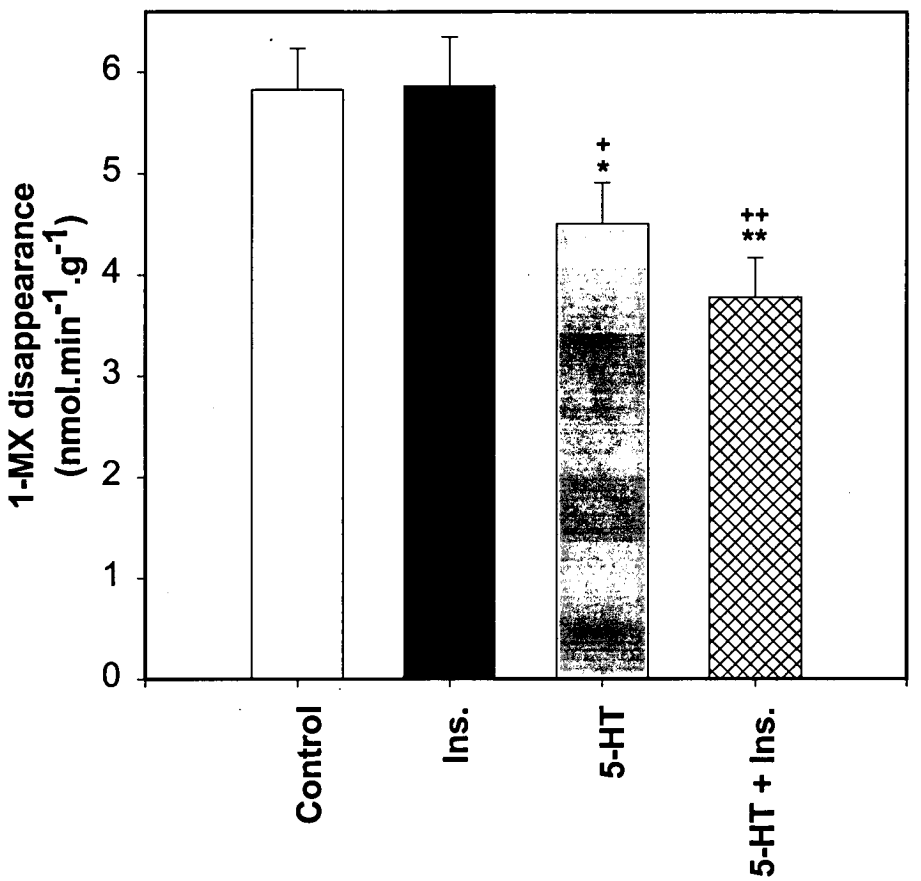

Figure 4. Hindlimb 1-MX metabolism (a surrogate indicator of capillary/nutritive flow) in the constant flow, Ficoll® perfused rat hindlimb perfused with either [^{14}C] palmitic acid or [^{3}H] 2-DG. Perfusions were control (white bar), 75 nM Ins (black bar), 3 μM 5-HT (grey bar) or 5-HT + Ins (cross-hatched bar). Values are means ± SE (n=10-11) and given in gram wet weight. Significance symbols are denoted by '*' (from control) and '+' (from Ins), where one or two symbols represents $P<0.05$ and $P\leq0.01$ respectively.

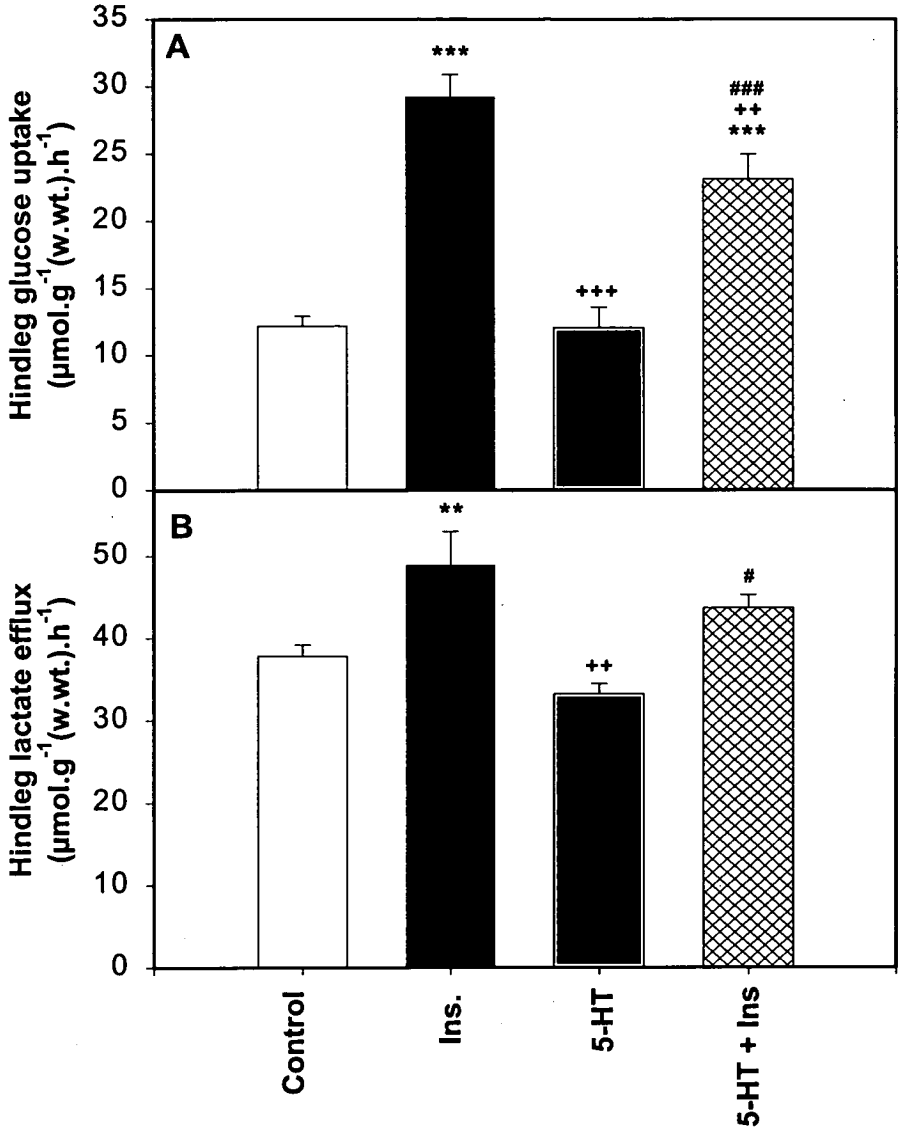

Figure 5. Hindleg glucose uptake (panel A) and lactate efflux (panel B) during constant flow, Ficoll® perfusion with either [^{14}C] palmitic acid or [^{3}H] 2-DG. Perfusions were control (white bar), 75 nM Ins (black bar), 3 µM 5-HT (grey bar) or 5-HT + Ins (cross-hatched bar). Values are means ± SE (n=10-11) and given in gram wet weight. Significance symbols are as described in the methods section of this chapter. Significance symbols are denoted by '*' (from control), '+' (from Ins) and '#' (from 5-HT), where one, two or three symbols represents $P<0.05$, $P\leq0.01$ and $P\leq0.001$ respectively.

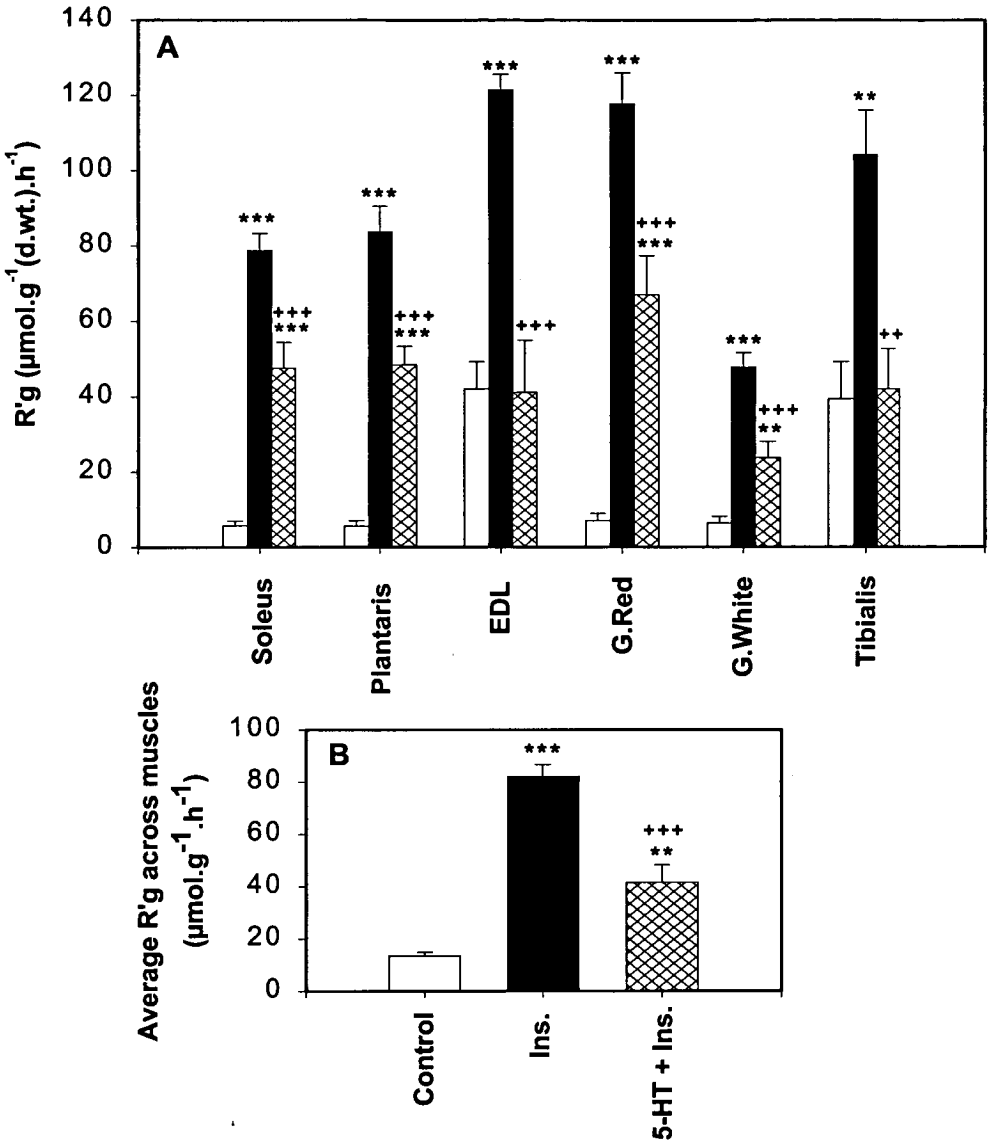

Figure 6. The uptake of [^{3}H] 2-DG (R'g) by the rat hindlimb perfused with Ficoll®/Krebs buffer containing 8.3 mM glucose and 1.2 mM palmitic acid. Perfusions were conducted with no extra additions (white bars), with the infusion of 12.5 mU/ml Ins (black bars) and with a co-infusion of 3 µM 5-HT and 75 nM Ins (hatched bars). The effects of individual hindlimb muscles are shown in panel A and the average effect across all muscle samples is shown in panel B. Values are means ± SE (n=5-6) and given in gram dry weight. Significance symbols are denoted by '*' (from control) and '+' (from Ins), where two or three symbols represents $P \leq 0.01$ and $P \leq 0.001$ respectively.

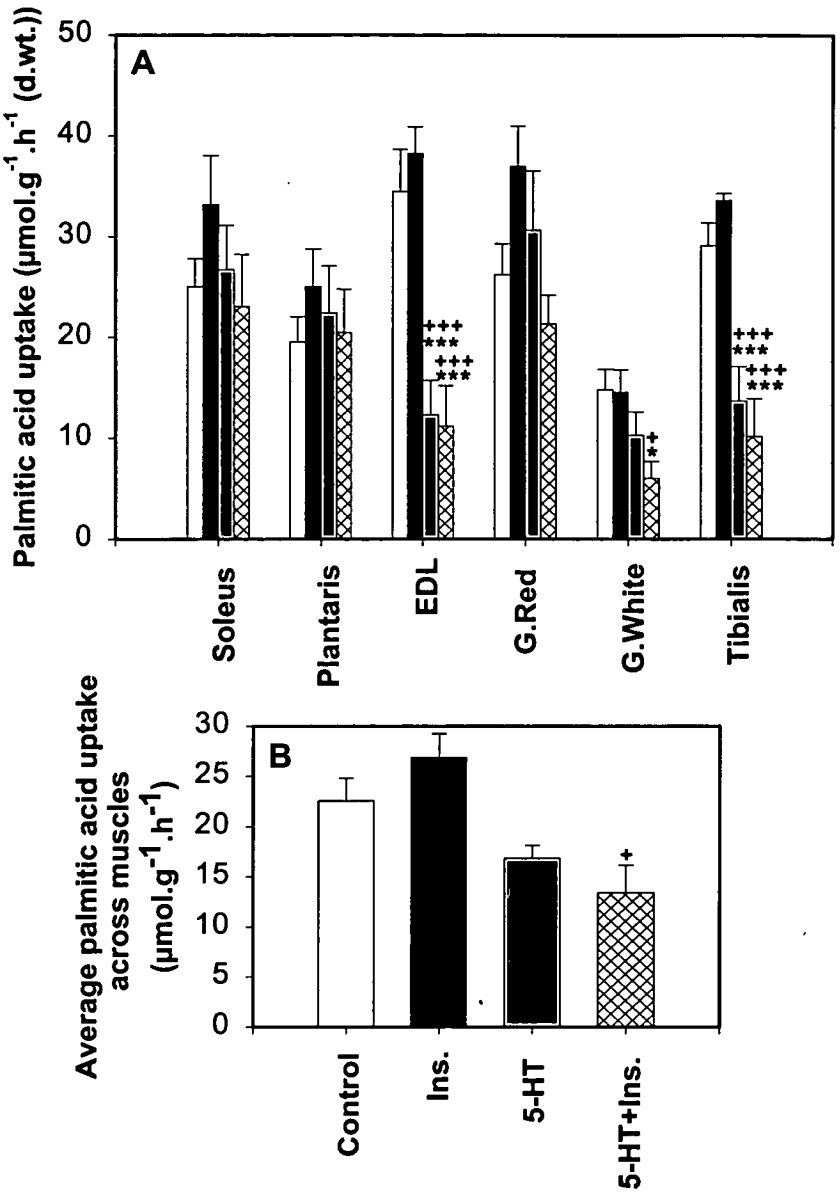

Figure 7. The uptake of [^{14}C] palmitic acid by the rat hindlimb perfused with Ficoll®/Krebs buffer containing 8.3 mM glucose and 1.2 mM palmitic acid. Perfusions were conducted with no extra additions (white bars), 75 nM Ins (black bars), 3 µM 5-HT (grey bars) and 3 µM 5-HT + 75 nM Ins (hatched bars). The effects of individual hindlimb muscles are shown in panel A and the average effect across all muscle samples is shown in panel B. Values are means ± SE (n=5-6) and given in gram dry weight. Significance symbols are denoted by '*' (from control) and '+' (from Ins), where one or three symbols represents $P<0.05$ and $P\leq0.001$ respectively

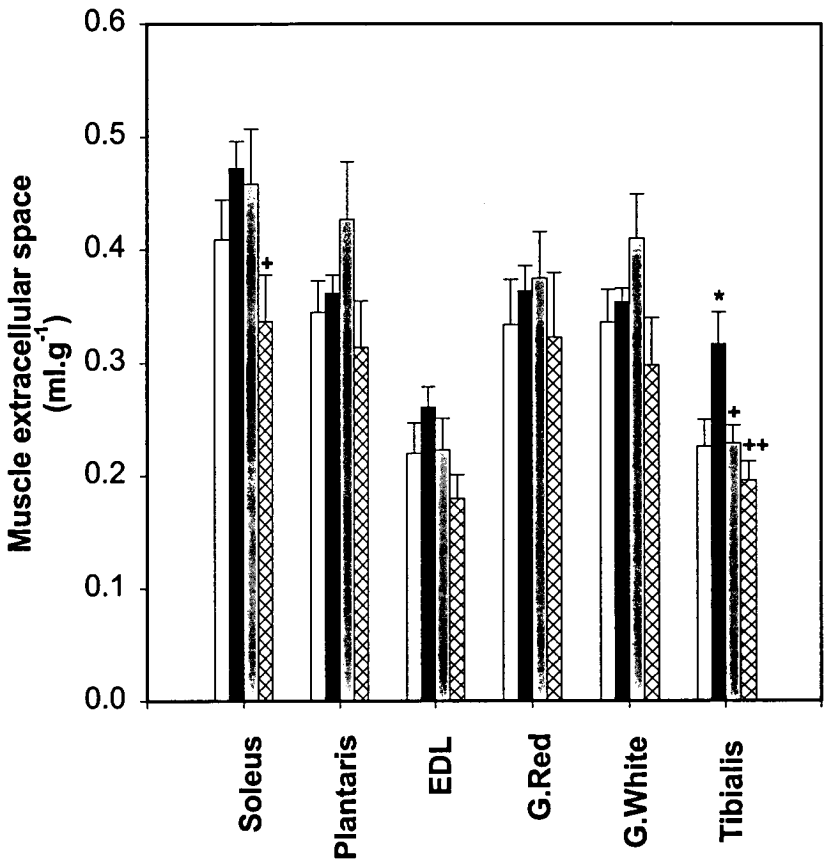

Figure 8. Muscle extracellular space (comprising the vascular volume and interstitial space) of selected muscles of the rat hindlimb perfused with Ficoll®/Krebs buffer containing either [^{3}H] 2-DG or [^{14}C] palmitic acid. Perfusions were: control (white bars), 175 nM Ins (black bars), 3 μM 5-HT (grey bars) or 5-HT + Ins (hatched bars). Values are means ± SE (n=10-11) and given as grams wet weight. Significance symbols are denoted by '*' (from control) and '+' (from Ins), where one or two symbols represents $P<0.05$ and $P\leq0.01$ respectively

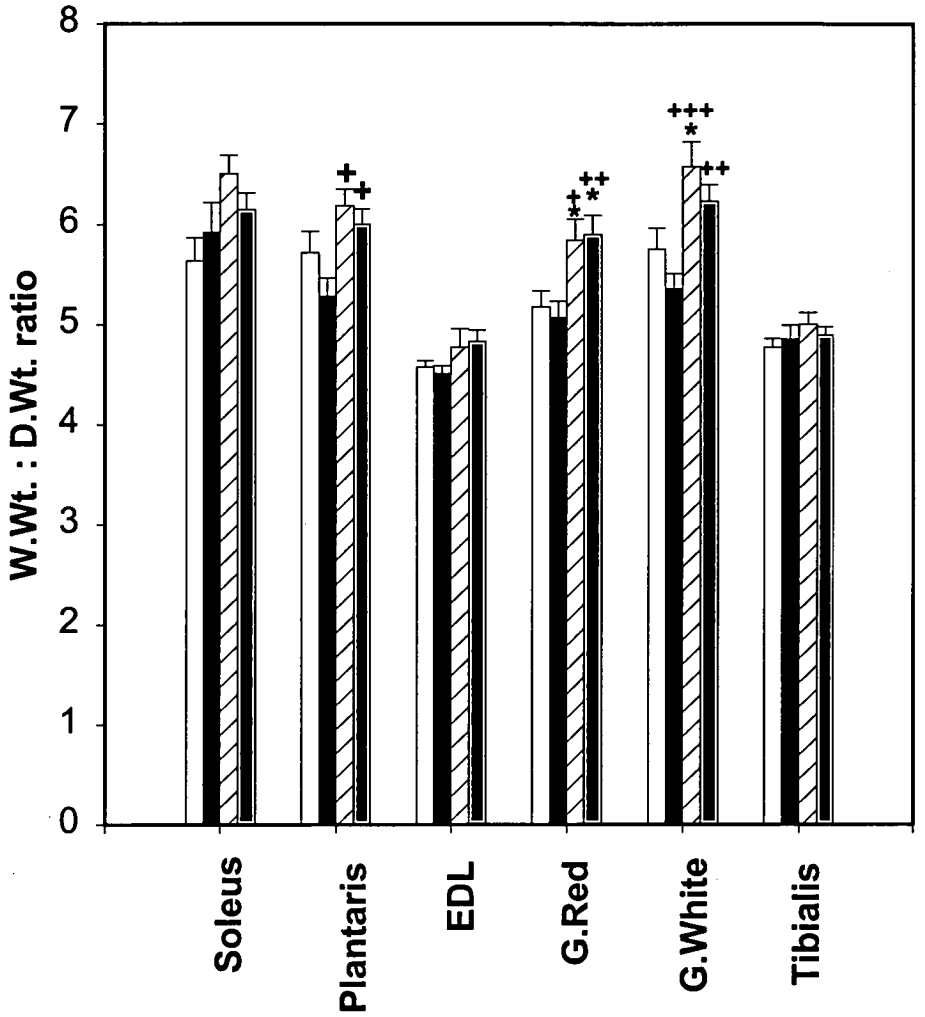

Figure 9. Muscle wet weight (W.Wt.) to dry weight (D.Wt.) ratios for the rat hindlimb perfused with Ficoll®/Krebs buffer containing either [^{3}H] 2-DG or [^{14}C] palmitic acid. Perfusions were: control (white bars), 75 nM Ins (black bars), 3 μM 5-HT (grey bars) or 5-HT + Ins (hatched bars). Values are means ± SE (n=10-11). Significance symbols are denoted by '*' (from control) and '+' (from Ins), where one, two or three symbols represents $P<0.05$, $P\leq0.01$ and $P\leq0.001$ respectively.

The weights of all muscles were compared before and after drying to determine if oedema was present. Hindlimb perfusions at 37°C using a Krebs buffer containing BSA instead of Ficoll® usually yield a wet weight to dry weight ratio of approximately 5 (unpublished results). These perfusions averaged approximately 5.5, which was indicative of marginally higher levels of oedema (Fig. 9). The infusion of 5-HT significantly increased the oedema in the plantaris and the red and white gastrocnemius muscles.

3.4 Discussion

The main finding from this chapter was the reduced muscle FFA uptake across the entire hindlimb when non-nutritive flow predominated. This corresponded with insulin-mediated glucose uptake also being impaired. When individual muscles were analysed separately this effect was only significant in those with predominantly white muscle fibres (EDL, tibialis and G.White). These results imply that fuel-partitioning responds differently in individual muscles and caution must be taken when measuring total uptake or release of metabolites from or into the perfusate.

The population of adipocytes interlacing the perimysium and individual fibres must also be considered when dissecting whole muscles. The results from Chapter 4 of this thesis imply that intermuscular AT actively contributes to muscle lipolytic activity. Those experiments measured the uptake of chylomicron TG into hindlimb muscles with predominantly non-nutritive flow (reduced capillary flow). Unlike the albumin-bound FFA, the uptake of FFA derived from chylomicron-TG is dependent on the exposure and activity of LPL. We found more hydrolytic activity (probably due to increased exposure to LPL) with 5-HT infusion in the red muscles. Due to the reduction in metabolism and increased hydrolytic activity, it was reasoned that non-nutritive flow increased TG access to adipocytes in the muscle CT, in particular the perimysial adipose tissue (which we have given the acronym 'PAT').

Uptake of albumin-bound FFA is however not dependent on LPL activity and is likely to be more dependent on endothelial surface area and FFA transporters (278) (279). Therefore FFA uptake was expected to decrease with reduced capillary perfusion

(5-HT infusion). While this appears (from Fig. 7) to be apparent in only the muscles with predominantly white fibres, it is likely to have occurred also in the red muscles. The uptake into the myocytes of the red muscle is, however, probably masked by FFA extraction into PAT. This may also explain why the insulin-mediated uptake of 2-DG is not reduced to the same extent with 5-HT in the red muscles (as insulin may stimulate glucose uptake into PAT as a precursor for TG synthesis).

Reduced muscle uptake of FFA during haemodynamic insulin resistance implies that TG deposits within the myocyte will be also reduced. Classically, it is thought that elevated plasma FFA during insulin resistance are re-assembled into lipoproteins in the liver for metabolism in the periphery, leading to increased SM TG. As expected, a correlation between insulin resistance and muscle TG levels (94) (144) (195) (197) and increased lipid oxidation (99) have been recorded.

Despite reports of increased intramyocellular TG with insulin resistance, there are many emerging papers showing that FFA uptake is decreased with impaired glucose tolerance (281) and women with visceral obesity (51). In addition, reduced lipid oxidation has been recorded in subjects with NIDDM (132) and visceral obesity (51). The findings reported in this chapter are thus in agreement with those reported by Turpeinen *et al.* (281), showing that the uptake of FFA is reduced when insulin-mediated glucose uptake is impaired. Therefore intracellular accumulation of TG may be a result of reduced lipid oxidation, rather than increased fatty acid uptake. Obese Zucker rats have been shown to have higher ratios of SM FFA uptake and glycerol release than their lean counterparts (280). It is possible that in those experiments, that the FFA uptake was into the PAT. Large PAT deposits may also explain why these obese rats have very high levels of glycerol release.

The presence of FFA in these perfusions may have had some influence on 2-DG uptake into the muscles. Others have shown that FFA have no effect on basal glucose uptake (122) (176), but reduce insulin-mediated glucose uptake by SM. Insulin (1 mU/ml) has been shown to increase FFA uptake by the perfused rat hindlimb (217). Despite this effect, no reduction in glucose uptake was seen, therefore indicating the absence of the Randle cycle in resting perfused SM. In addition, Ikeda *et al.* (122) used 1 mU/ml insulin in the perfused rat hindlimb and found no reduction in glucose uptake

with a combination of 1 mM oleic acid and 0.5 mM palmitic acid (122). However at 0.5 and 0.1 mU/ml insulin glucose uptake was decreased with the same FFA addition, with a concomitant decrease in insulin clearance. At the very high insulin concentration used in these experiments (75 nM/12.5 mU/ml) glucose uptake was most likely unaltered by the presence of 1.2 mM palmitic acid. In addition, the rates of 2-DG uptake in this chapter are comparable to those reported by Rattigan *et al.* (211).

While FFA and insulin appear to influence glucose uptake, glucose and insulin may also influence FFA uptake. Although insulin tended to increase FFA uptake into most muscles, this was not significant. Ohashi *et al.* (188) evaluated the effects of different concentrations of glucose and insulin on FFA uptake by the perfused rat hindquarter. With high plasma glucose, FFA uptake was increased with low insulin concentrations, however at higher insulin concentrations (5 mU/ml) the uptake was reduced. At 12.5 mU/ml insulin used in these experiments there was no significant change in FFA uptake.

Capillary perfusion was determined by the activity of the capillary endothelial enzyme, xanthine oxidase, to convert the infused 1-MX. All perfusions contained FFA, which are shown to reduce insulin-mediated capillary recruitment *in vivo* in Chapter 6 of this thesis. In these perfusions there was no increase in capillary flow with insulin infusion and 1.2 mM palmitic acid. Without FFA in the perfusion buffer, we have previously shown that insulin was also unable to increase access to xanthine oxidase in perfusion. This is in contrast to *in vivo* experiments where insulin increases capillary flow independently of changes in total flow to the muscle (as discussed in the Introduction chapter of this thesis) and re-enforces the view that the perfused hindlimb is fully dilated in the basal state. As such, insulin is unable to further increase capillary perfusion as indicated by 1-MX metabolism (Fig. 4).

In summary, the predominantly non-nutritive flow pattern induced in these experiments by the vasoconstrictor 5-HT resulted in significant reduction in FFA and insulin-mediated glucose uptake across the entire hindlimb. While these experiments determined the acute effects of non-nutritive flow on FFA and insulin-mediated glucose uptake, long term non-nutritive flow may result in a down-regulation of fatty acid

transporters in muscle, and ultimately contribute to significant chronic elevations in plasma FFA.

CHAPTER 4

4 Effects of CT or non-nutritive flow on chylomicron TG hydrolysis by the constant flow perfused rat hindlimb.

4.1 Introduction

Chapter 3 showed the effects of predominantly non-nutritive flow on the uptake of albumin-bound FFA. While this is dependent on the capillary surface area, the uptake of FFA from circulating TG requires initial hydrolysis, and is therefore dependent on the distribution of lipolytic enzymes (in particular LPL). LPL is attached to the vascular endothelium by proteoglycans, which allow protrusion of the enzyme into the vascular lumen. Here it acts to hydrolyze TG from circulating TG-rich lipoproteins (chylomicrons and very-low density lipoproteins) into FFA and glycerol. The resulting FFA are taken up by tissues capable of lipid oxidation (e.g. muscle) or storage (e.g. AT, muscle) (55) (68).

The hydrolysis of TG to FFA and glycerol has been found to be proportional to the active amount of LPL in the vasculature (157) (272) and ultimately may depend on whether circulating TG has access to the active form of LPL or other hydrolytic enzymes. The uptake of circulating TG is highest in slow twitch red fibres, medium in fast twitch red and least in fast twitch white (272) (161). In SM, an important determinant of muscle metabolism is the supply of substrate to the myocytes and is therefore controlled by the proportioning of flow between two distinct vascular circuits (48) (180). The first is termed nutritive and describes flow predominantly to the muscle cells. Blood flowing through the second circuit, termed non-nutritive, almost certainly passes through vessels of the CT associated with the muscle (181). Flow through this route results in the physical isolation of nutrients and hormones (including oxygen, glucose, TG and insulin) from the myocytes (46). As a result there is limited opportunity for muscle nutrient uptake. Since TG hydrolysis is dependent upon its exposure to

hydrolytic enzymes, it follows that the total hydrolysis of TG entering the muscle will be greater when the predominance of flow is through the circuit in which the majority of the hydrolytic activity is distributed. To date there have been no studies describing the location of SM TG hydrolytic activity including LPL, and its relative distribution in muscle nutritive capillaries or in CT vessels (non-nutritive for muscle) (181).

It is now believed that nutritive circulation is through capillaries in close contact with the muscle fibres, and, as a result, the clearance of ions and oxygen is accelerated. When flow is largely through the non-nutritive pathway, the flow is thought to pass through muscle CT; in this state the clearance of ions and oxygen is decreased. Vasoconstrictor action to constrict vessels leading to CT vessels (Type A vasoconstrictors) under conditions of constant total flow will therefore re-divert flow into the muscle capillaries (nutritive) and consequently increase metabolism. Alternatively, vasoconstrictors impeding flow to muscle capillaries (Type B) will increase CT (non-nutritive) flow.

To measure TG hydrolysis in the perfused rat hindlimb, lipoprotein emulsions can be synthesized using a mixture of radiolabeled and cold TG, cholesterol esters, and phospholipids and apoproteins for forming a shell around the hydrophobic TG (215). Alternatively, chylomicrons can be synthesized endogenously. Chylomicrons can be extracted from the lymph of rats fed radiolabeled palmitate and corn oil (161), however this method often results in very low yields of labeled TG, and is technically more difficult than preparing artificial emulsions.

Thus, the present study addresses the issue of whether vasoconstrictors (including 5-HT (Type B) and vasopressin (Type A)) that specifically alter the proportion of non-nutritive and nutritive flow in the constant flow perfused rat hindlimb (46) (48), alter the rate of hydrolysis of circulating TG.

4.2 Materials and Methods

4.2.1 TG emulsion

Chylomicron lipid emulsion (CLE) was prepared essentially as described by Redgrave and Callow (214) and each ml contained 7.5 mg triolein, 0.33 mg cholesteryl

oleate, 0.22 mg cholesteryl acetate, 2.6 mg phosphatidyl choline, 10 μmol N-[2-Hydroxyethyl]piperazine-N'[2-ethanesulfonic acid] (HEPES, pH 7.4), 150 μmol NaCl and 0.25 ml heat-inactivated rat serum (HIRS) as a source of apolipoproteinCII (apoCII, acts as a cofactor for LPL). CLE contained either 1.25 μCi [^{3}H]-cholesteryl oleate (CO, [cholesteryl-1,2,6,7-3H(N)]-cholesteryl oleate, Amersham) or 0.42 μCi [^{14}C]-triolein (TO, [carboxyl-^{14}C]-triolein, Amersham) and hydrolysis/uptake of each measured separately. The mixture was sonicated at an output frequency of 23 KHz, for two rounds of 1 min each. All emulsions were used on the day of preparation (using fresh HIRS).

4.2.2 Heat-inactivated rat serum (HIRS)

Donor animals were anaesthetized and blood collected by an intracardiac puncture. Blood was slowly withdrawn using a 21-gauge butterfly needle attached to a 1 ml syringe containing 0.1 ml citrate. The syringe was changed several times during one collection. This procedure reduced the amount of suction and therefore the amount of platelet activation. Serum collected in this way was devoid of any platelet-derived 5-HT. Serum platelets were eliminated by clotting with thrombin (30 μl/ml). The remaining serum was heated at 56°C for 30 min to inactivate endogenous lipases (18).

4.2.3 Hindlimb perfusions

Hindlimb surgery was essentially as described in section 2.2.4 of the Methods chapter. Heparin was not used as an anticoagulant, as this has the potential to displace LPL from the vascular endothelium and distribute it throughout the perfusate. The left hindlimb of the rat was perfused in a recirculating mode at 37 °C with 100 ml of perfusion medium comprising Krebs Henseleit buffer (described in the Methods chapter, section 2.2.2) containing 6 % (wt/vol) Ficoll® (Pharmacia Biotech) (unless indicated otherwise) with 8.3 mM glucose and 1.27 mM $CaCl_2$. The buffer was continuously gassed with 95 % O_2:5 % CO_2 via a silastic tube oxygenator while maintained at 37°C in a heat exchanger coil. Constant flow perfusions were conducted at 8 ml/min; constant

pressure perfusions at 85 mmHg. After a 40 min equilibration period the buffer reservoir was changed to one containing 125 ml of the 6% Ficoll® and 5 ml of CLE.

4.2.4 Modulation of CT flow

5-HT is one of a number of vasoconstrictors previously shown to increase non-nutritive or CT flow at the expense of muscle nutritive flow in the constant flow perfused rat hindlimb (46) (48). Although other members of this group such as high dose NE, high frequency sympathetic nerve stimulation and high dose vanilloids give similar results in terms of increasing non-nutritive flow. 5-HT is the least complicated (produces a mono-component dose-response curve (63)) and was the model vasoconstrictor of choice. Thus, as shown in Fig. 1, 5-HT (Sigma) was added as a bolus into the buffer reservoir of the appropriate perfusions to give a final concentration of 0.5-1 μM (to achieve a peak perfusion pressure of approximately 100 mmHg above basal). After discarding the first 30 ml of perfusate (of the 130 ml perfusion medium containing CLE) the remaining 100 ml was recirculated through the hindlimb for 1 hour. Samples (2.5 ml) were withdrawn from the venous line every 15 min.

In some experiments the vasodilator CCh was infused at a final concentration of 100 μM to reverse the effects of 5-HT on PP and $\dot{V}O_2$. CCh infusion commenced before the buffer was recirculated. This was designed to allow the PP and $\dot{V}O_2$ to return to near-basal states before TG recirculation and prevent perfusion under predominantly non-nutritive conditions. Infusion was continued for a further 12.5 min after recirculation.

The type A vasoconstrictor vasopressin was added as a bolus dose (0.5 nM) to the reservoir of some perfusions to investigate the effects of increased $\dot{V}O_2$ and PP on chylomicron TG hydrolysis.

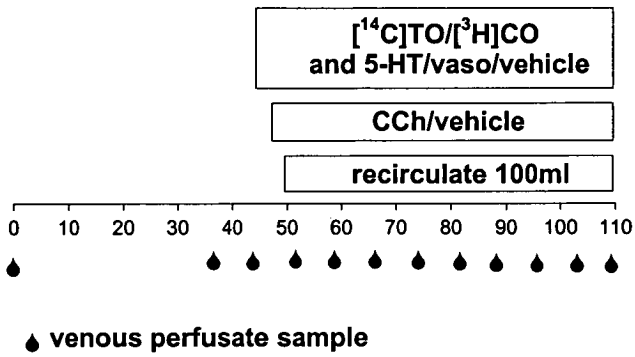

Figure 1: Perfusion protocol for measuring chylomicron triglyceride hydrolysis by the perfused rat hindlimb

4.2.5 TG hydrolysis

Perfusate samples (1 ml) from perfusions using [^{14}C]-TO were added to 4 ml methanol:chloroform 2:1 in 10 ml glass tubes with screw caps. The tubes were vortexed (3 x 30 s) and maintained at room temperature (22 °C) before centrifuging at 2500 ×g for 10 min. The entire lower layer was removed with a glass pipette into a 5 ml test tube and evaporated to dryness in a water bath at 40 °C under a stream of nitrogen. The residue was reconstituted into 100 µl of the chloroform:methanol mixture and 15 µl was immediately applied to a Merck silica gel 60 F_{254} aluminium sheet (Merck). Standards (10 µl of 10 mg/ml) of TO, CO, and oleic acid were also applied as spots. The plates were run using a mixture of n-heptane:diethyl ether:glacial acetic acid (80:20:1). Plates were visualized in an iodine tank and TO and oleic acid spots were scraped into separate plastic tubes and counted with 4 ml of Amersham Biodegradable Counting Scintillant. Recovery of counts after thin layer chromatography was periodically checked by comparing the total radioactivity scraped from one lane of the silica plate (a lane was

designated for each perfusate sample) with the known amount of radioactivity of the corresponding perfusate sample before solvent extraction. The recovery was between 90 and 110 percent.

4.2.6 Muscle radioactivity uptake

After perfusion, the soleus, plantaris, G.White and G.Red, tibialis and EDL muscles of the perfused hindlimb were removed. Within the context of this study it is important to note that interfibrillar CT adipocytes are contained within each muscle. Excised muscles were counted for radioactivity using the method described in section 2.4 of the Methods chapter.

4.2.7 Statistical analysis

The statistical significance of differences between groups of data was assessed by one or two way analysis of variance (ANOVA) for sets of perfusions containing multiple groups. For perfusions comparing only one group to the controls student's t-tests were used. Significant differences were recognized at $P<0.05$. One, two or three symbols were used to show significance of $P<0.05$, $P\leq0.01$ and $P\leq0.001$ respectively. Symbols used were '*', '#' and '^' to show significance from controls, 5-HT and 5-HT+CCh respectively.

4.3 Results

The Clearance of chylomicron TG by perfused muscle has not previously been studied and it was therefore necessary to conduct a number of preliminary experiments to determine an optimal procedure. The commonly used albumin-containing perfusion medium was not entirely satisfactory as FFA released by LPL were subsequently bound by the albumin and little was taken up by the hindlimb. A second difficulty encountered was the high contamination of serum albumin by lipases. Thus lipase substrates such as *p*-nitrophenyl palmitate were rapidly hydrolysed (data not shown) causing basal rates of

hydrolysis to be largely attributable to these contaminants when using albumin-containing perfusion medium. Accordingly, we chose to use Ficoll®-containing perfusion medium. With this medium there was no hydrolysis due to the perfusion medium alone and the uptake of released FFA occurred so that muscle-specific uptake could be compared at the completion of each perfusion.

Figure 2 shows the time course for the effects of 0.5-1 μmol 5-HT, 0.5-1 μM 5-HT with 100 μM CCh or 0.5 nM vasopressin on changes in $\dot{V}O_2$ and PP in the constant flow, Ficoll® perfused rat hindlimb. Changes in $\dot{V}O_2$ and PP both reached a maximum at 15 min which then declined as the vasoconstrictors were metabolised by the hindlimb during the recirculating perfusion. However, changes in $\dot{V}O_2$ and PP were significantly different ($P<0.05$) from controls at all time points for 5-HT and vasopressin. The addition of CCh blocked the pressor and oxygen effects by 5-HT. Mean values for muscle [^{14}C]-FFA uptake (60 min), oxygen uptake (15 min) and perfusion pressure (15 min) are shown in Table 1. $\dot{V}O_2$ was inhibited by approximately 38.9% and muscle [^{14}C]-FFA uptake increased by approximately 227.2 % by 5-HT (Table 1). The increase in TG hydrolysis and the decrease in oxygen uptake due to 5-HT were each significant (P <0.05 and $P<0.001$ respectively). FFA found in the perfusate of 5-HT perfusions were also significantly higher than the controls ($P<0.05$). These high hydrolytic rates were reversed when 5-HT effects were blocked by CCh and thereby supporting the view that the effects were indicative of flow redistribution, and not due to 5-HT receptor-mediated effects on muscle cells.

Addition of vasopressin to the buffer reservoir produced no significant decline in chylomicron TG hydrolysis (Table 1), despite an increase in $\dot{V}O_2$ (Table 1). However, the perfusate FFA with vasopressin were significantly higher than those for the control perfusions (Table 1).

Constant pressure perfusions were also conducted. These confirmed the high hydrolytic rates with 5-HT (Table 2). Since these perfusions deliberately used BSA rather than Ficoll®, FFA released from TO became bound to the BSA and allowed measurement of its appearance in perfusate samples. Corrections due to endocytosis were not necessary, however basal rates of TO hydrolysis in control perfusions may

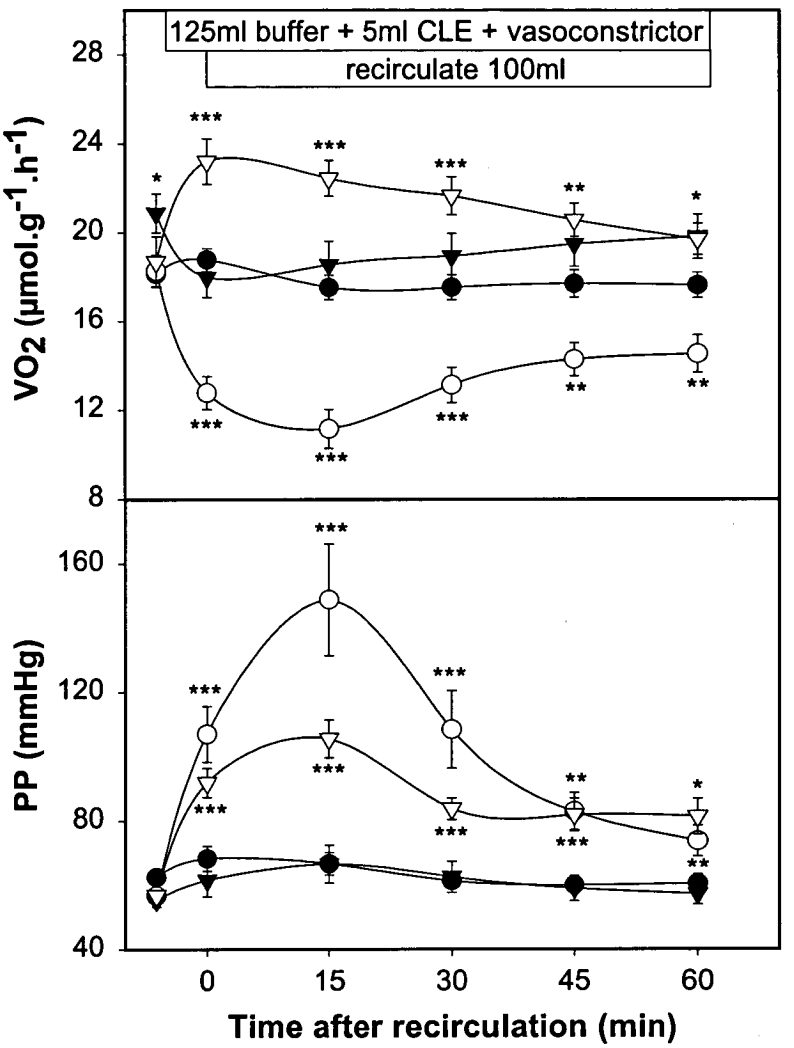

Figure 2. Time course for the effects of 5-HT, 5-HT with CCh and vasopressin on oxygen consumption ($\dot{V}O_2$) and perfusion pressure (PP) in the constant flow Ficoll®-perfused rat hindlimb. All perfusions were conducted at constant flow (8 ml/min) using a recirculating mode (total buffer volume = 100 ml). Basal values are at t = –6.25 min. Additions at -6.25 min were vehicle (●), 0.5-1 µM 5-HT (○), 0.5-1 µM 5-HT + 100µM CCh (▼) or 0.5 nM vasopressin (▽). Values are means ± SE. **,P<0.01; ***,P<0.001 for treatment versus vehicle (n=10-12). Due to the differences among most groups, values were only compared to control perfusions.

Constant Flow Ficoll® Perfusions

	Control	5-HT	5-HT+CCh	vasopressin
TG hydrolysis (nmolFFA.h^{-1}.g^{-1})	184 ± 28	602 ± 132**	231 ± 24$^{\#}$	255 ± 68$^{\#\#}$
$\dot{V}O_2$ (μmol.g^{-1}.h^{-1})	16.7 ± 0.6	10.2 ± 1***	19.2 ± 2.1$^{\#\#\#}$	21.3 ± 0.9*$^{\#\#\#}$
PP (mmHg)	70.6 ± 5	170 ± 27***	62.4 ± 7$^{\#\#\#}$	99.0 ± 8$^{\#\#}$
Muscle FFA (nmol.g^{-1}.h^{-1})	161 ± 25	508 ± 133*	200 ± 6.3$^{\#}$	169 ± 55$^{\#}$
Perfusate FFA (nmol.g^{-1}.h^{-1})	23.5 ± 12	93.1 ± 15*	30.7 ± 19	86.3 ± 22*

Table 1. Effect of 5-HT, 5-HT + CCh, and vasopressin on TO hydrolysis, $\dot{V}O_2$ and PP by the perfused rat hindlimb at constant flow.

The TO substrate was a chylomicron-lipid emulsion (214). Perfusions were constant flow, recirculating and set at 8 ml/min. TO and oleic acid radioactivity analyses were conducted on perfusate samples taken at intervals of 15 min throughout perfusions of 60 min duration (Fig. 2). Average rates of FFA formation (perfusate FFA) over 60 min were measured by thin layer chromatography. Muscle [^{14}C]-oleic acid uptake into the hindlimb were at 60 min. Values for maximal changes in $\dot{V}O_2$ and PP were taken 15 min after recirculation. Values are means ± SE (n=5-7). One symbol, $P<0.05$; two symbols, $P\leq0.01$; three symbols, $P\leq0.001$. Symbols are '*' and '#' to show significance from control and 5-HT perfusions respectively.

have been affected by contamination of the serum albumin by lipases (as confirmed by the high activity of serum albumin perfusate to hydrolyse *p*-nitrophenyl palmitate). As with the Ficoll® perfusions, TO hydrolysis was however also increased with 5-HT in these constant pressure perfusions (Table 2). Increases in TO hydrolysis were not a result of 5-HT activating the enzyme (Table 3).

The uptake of [^{14}C]-FFA and [^{3}H]-CO into hindlimb muscles after one hour of chylomicron recirculation is shown in Figure 3. Panel A illustrates that perfusing the hindlimb with 5-HT increased the uptake of [^{14}C]-FFA into certain muscles. The increased uptake was significant in the soleus, plantaris and G.Red muscles. The percentage uptake of [^{3}H]-CO into hindlimb muscles from Ficoll® perfusions is shown in Figure 3, panel B. After TG hydrolysis the chylomicron retains the CO, and therefore the uptake of [^{3}H]-CO into muscles may be due to either endocytosis of the chylomicron or chylomicron remnant. Even if the reported CO uptake was of the nascent chylomicron, the uptake of [^{14}C]-FFA into the muscles of the 5-HT perfusions were still considerably greater than that recorded for endocytosis. Therefore the [^{14}C]-FFA found in the muscles are likely to be attributable to TG hydrolysis. Alternatively CO uptake exceeded that of TO in the vasopressin perfusions. This is suggestive of uptake of the chylomicron remnant. If this were the case then the FFA formed from TG in the chylomicron must remain in the perfusate. In fact, the perfusate FFA levels with vasopressin are significantly higher than the control value (Table 1).

Figure 4 is a plot of the percentage content of slow oxidative fibres against the uptake of [^{14}C]-FFA in a hindlimb preconstricted with 5-HT for each muscle. [^{14}C]-FFA uptake when flow is predominantly non-nutritive significantly correlates ($r=0.987$, $P<0.001$) with the percentage content of slow oxidative fibres.

	Constant Pressure BSA perfusions	
	Control	5-HT
TO hydrolysis ($nmolFFA.h^{-1}.g^{-1}$)	201 ± 35	421 ± 63*
$\dot{V}O_2$ ($\mu mol.g^{-1}.h^{-1}$)	16.2 ± 2.9	6.7 ± 1.8*
PP (mmHg)	84 ± 3	91 ± 8

Table 2. Effect of 5-HT on TO hydrolysis, $\dot{V}O_2$ and PP by the perfused rat hindlimb at constant pressure.

A set of BSA Perfusions were conducted at constant pressure (set at approx. 85 mmHg). The TO substrate was a chylomicron-lipid emulsion (214). TO and oleic acid radioactivity analyses were conducted on perfusate samples taken at intervals of 30 min throughout perfusions of 120 min duration. Average rates were calculated and means ± SE (n=4) for $\dot{V}O_2$ (30 min) and PP (30 min) are shown. *,$P<0.05$ for 5-HT vs. control.

	LPL activity ($nmol.min^{-1}.g^{-1}$)		
	G.Red	G.White	Plantaris
Vehicle	198±52	110±40	150±60
5-HT	180±30	90±30	70±5

Table 3. LPL activity in muscle homogenates after BSA-perfusion with vehicle or 5-HT.

To assess whether 5-HT activated LPL during perfusion and therefore had a direct effect on the rate of TG hydrolysis, perfusions were conducted in which vehicle or 5-HT was infused for 20 min. Muscles were then excised, homogenized and assayed for LPL activity using the technique of G. Bengtsson-Olivecrona and T. Olivecrona (18). No difference was seen in the activity of muscle LPL after perfusion with 5-HT. Values are means ± SE (n=4-5).

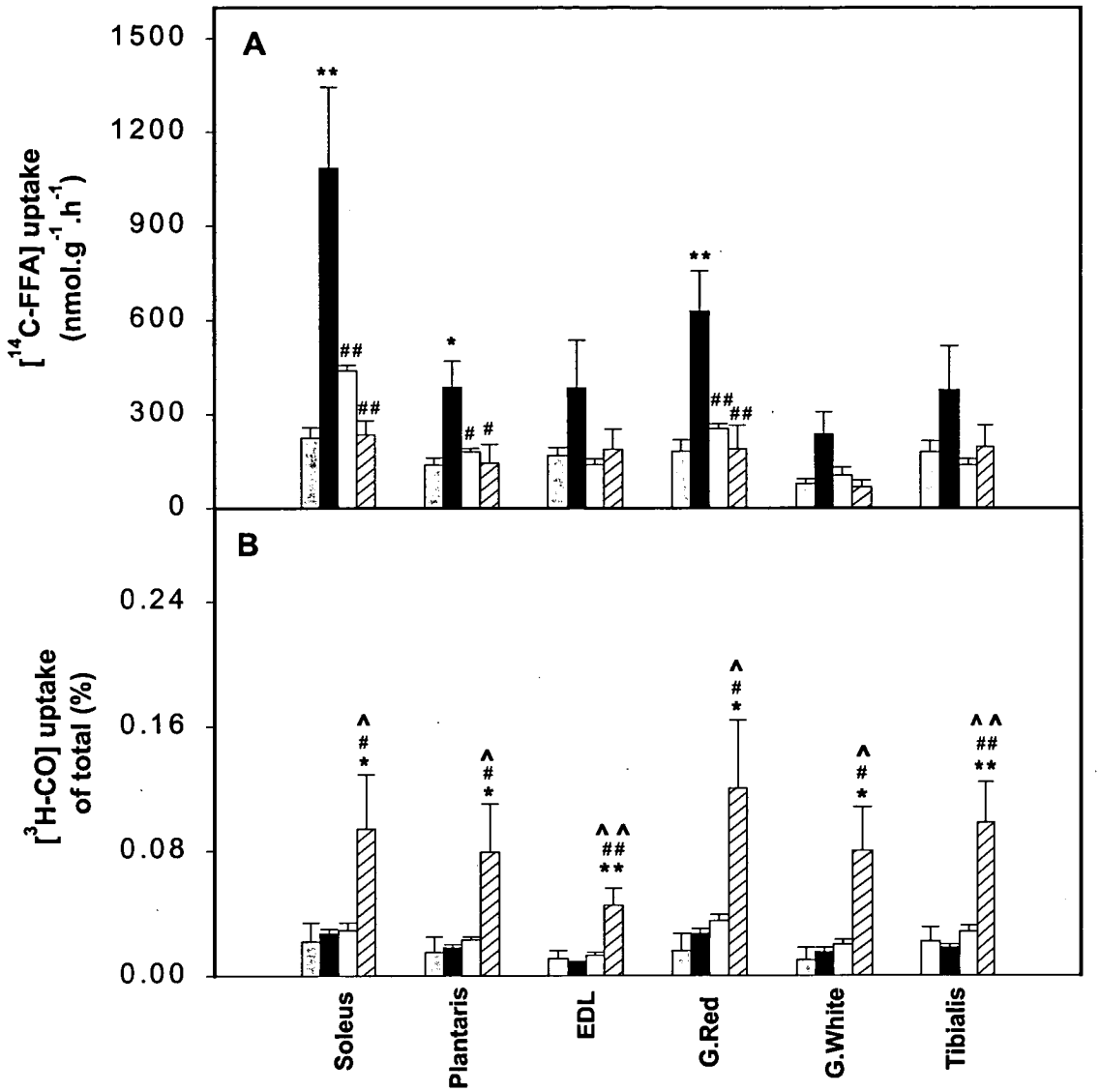

Figure 3. Uptake of [^{14}C]-oleic acid and [^{3}H]-cholesteryl oleate ([^{3}H]-CO) into hindlimb muscles in constant flow Ficoll®-perfused rat hindlimb using a chylomicron lipid emulsion (CLE) and heat-inactivated rat serum (HIRS) as a source of apolipoprotein CII. The effects of 5-HT (0.5-1 μM, 5-HT, black bar), 5-HT and CCh (0.5-1 μM 5-HT + 100 μM CCh, white bar) and vasopressin (0.5 nM, hatched bar) were measured for each CLE type and compared to perfusions with no additions (control, grey bar). CLE contained either or [^{14}C]-triolein ([^{14}C]-TO (panel A)) or [^{3}H]-CO (panel B). The values in panel B are the percentage of total circulating CO that is taken up by each muscle. Values are means ± SE (n=4-7). Significance from 'no additions', from '5-HT' perfusions or from '5-HT+CCh' perfusions, are shown by '*',' #' and '^' respectively, where one symbol denotes $P<0.05$, two symbols, $P\leq0.01$; and three symbols, $P\leq0.001$.

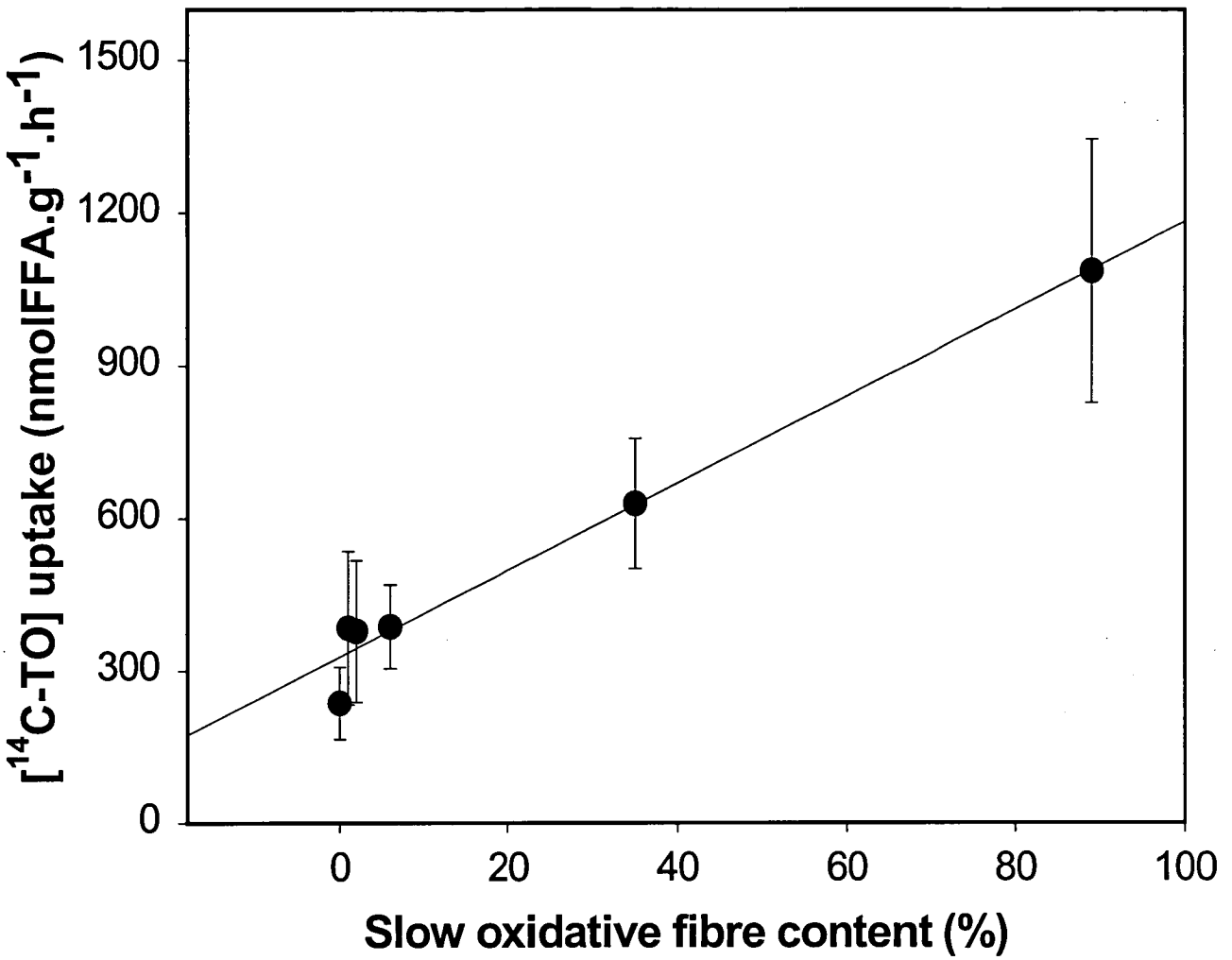

Figure 4. Uptake of FFA from a synthetic chylomicron emulsion using the mean values for uptake with 0.5-1 μM 5-HT for each hindlimb muscle and their corresponding percentage content of slow oxidative fibres. The linear regression produces an $r^2 = 0.975$ ($P<0.001$). The percentage content of slow oxidative fibres was taken from reports by Ariano *et al.* (5) and Armstrong and Laughlin (6). Means are values ± SE (n=5-7).

4.4 Discussion

The importance of SM in total circulating lipid clearance is often underestimated, and all previous reports have neglected the effect of flow partitioning on TG clearance in muscle, due to the presence of nutritive and non-nutritive routes. Here we report that the hydrolysis of TO was markedly increased in the perfused rat hindlimb when a high proportion of CT flow occurred. In contrast, increasing the proportion of nutritive flow (vasopressin infusion) had no effect on TO hydrolysis. The reason for this is not clear, however the results indicate that the hydrolytic enzyme (presumably LPL) is not located exclusively in the non-nutritive vessels.

Recruitment of CT flow for these experiments was induced by the addition of 5-HT, a representative Type B vasoconstrictor, which has previously been reported to decrease oxygen uptake, lactate output, glucose uptake (211) (212) and tension development of aerobically contracting muscle (64). All of these changes are characteristic of Type B vasoconstriction (46) and are representative of decreased nutrient delivery to muscle, and decreased muscle metabolism secondary to increasing the proportion of non-nutritive or CT flow within muscle (48).

When CT flow was increased by addition of the vasoconstrictor, 5-HT, there was a marked increase in TG hydrolysis (indicated by [^{14}C]-FFA uptake) in the soleus, plantaris and G.Red muscles. Uptake of [^{14}C]-FFA greatly exceeded that of the CO with 5-HT. This implies that uptake due to endocytosis of the chylomicron (causing TO radioactivity to be found in the muscle without any detectable amounts of hydrolysis) or of the chylomicron remnant (where all of the [^{14}C]-oleic acid or [^{14}C]-TO in the muscle is due to hydrolysis) could not account for the observed increase. It is important to note that the reported increase in TG hydrolysis occurred without any stimulation of LPL activity by 5-HT. This indicates that the TG hydrolysis due to 5-HT is likely to be the result of a vascular effect whereby the exposure of TG to TG hydrolytic activity, presumably LPL is increased. From this, it would also seem likely that the distribution

of TG hydrolytic activity is greater along the non-nutritive or CT circuit that nourish interlacing adipocytes than along the nutritive route supplying muscle cells.

Evidence that the vessels of non-nutritive flow are those of the CT associated with muscle has been supported by direct visualisation, during various pharmacological intervention (95) (181). The increased TG hydrolytic activity associated with flow through this region implies access to LPL associated with an active population of interfibrillar adipocytes. This population may correspond to the interfasicular fat cells responsible for the marbling effect of meat. The amount of muscle marbling is reported to be highly variable (269), which may contribute to the large error bars for the 5-HT data. In addition, the amount of muscle marbling can be used as a marker for red oxidative (type 1) muscle fibres (301). From the present study the uptake of [^{14}C]-FFA from TG hydrolysis correlated with the percentage of slow oxidative fibres when flow was predominantly non-nutritive (i.e. with 5-HT, Fig. 4). Thus increases in CT blood flow proposed to occur with age, hypertension and diabetes (48) (181) (242) may therefore allow increased fat deposition and perimysial marbling within the muscle.

Reports of fat cells being nourished by CT vessels have been implied from anatomical studies by Erikson and Myrhage (72) and Lindbom and Arfors (156). In addition, Camps *et al.* (35) reported diffuse LPL mRNA levels in the CT of SM. The location of adipocytes in this region would be consistent with the findings herein of increased TG hydrolysis where flow is significantly redirected through these vessels. From this it follows that the non-nutritive vessels supply the CT and the closely associated adipocytes.

It therefore appears likely that the vascular system plays a significant role in partitioning lipid and carbohydrate between muscle and CT fat cells. This type of fuel partitioning is likely to be under the control of the local release of vasomodulators. Whereas predominantly nutritive flow (such as in exercise) allows delivery of glucose and FFA to muscle cells, non-nutritive flow to CT adipocytes could promote either TG hydrolysis or the deposition of FFA to form adipocyte TG. The presence of insulin and glucose in this latter circuit is likely to further nourish and stimulate adipocyte TG enlargement by providing glycolytically-derived glycerol phosphate. Since the two vascular networks are in parallel, FFA and glycerol hydrolysed from TG by the LPL

situated along the non-nutritive circuit must first enter the venous circulation and redistribute throughout the body before it is presented to the myocytes. This implies a mechanism evolved for the storage of excess fat rather than for use by neighbouring myocytes. van der Vusse (283) has suggested muscle CT fat cells may be an important store of TG.

Many reports on muscle TG hydrolytic activity do not discern between myocytes, CT and fat cells. Any measure of such activity, including LPL from a whole muscle sample will contain all of these components. If the TG hydrolytic activity described in this study is of non-nutritive origin then data from whole muscle samples will be more dramatically effected than has previously been recognised (67). Therefore assays of muscle homogenate that are significantly contaminated by CT adipocytes may overestimate muscle TG hydrolytic activity, including that of LPL. Similarly no discrimination is made between the two flow regions possible in SM. A combination of these factors poses further difficulty when interpreting the data of any muscle preparation that receives nutrient by the vascular route.

Until recently little has been reported on the presence of perimysial adipose tissue (which we have given the acronym 'PAT') or 'marbling' in humans. The most comprehensive studies to date are carried out for the meat industry, where marbling affects the tenderness and palatability of a cut of steak. In cattle intramuscular adipose tissue occurs mainly at perimysial sites however a small amount is deposited in the endomysium (182) (301). The amount of muscle marbling is higher in muscles with type 1 fibres (301) where intramuscular deposition is a combination of increased hyperplasia and hypertrophy (cell number and size respectively (174)). Perimysial adipocytes are arranged in discrete compartments (approximately 100 μm in diameter in cattle), each surrounded by newly synthesized CT, and supplied by blood vessels (182) (174). With 5-HT, flow appears to be redistributed through tissue where there is higher fatty acid extraction but decreased metabolic capacity. The blood vessels supplying perimysial adipocytes (174) are therefore strong candidates for the 'non-nutritive' network. Continual flow through these vessels will increase fatty acid uptake to these adipocytes and accelerate rates of marbling.

Gondret *et al.* (88) have proposed that the deposition of PAT may be a result of increased lipogenic enzymes, acetyl CoA carboxylase (rate-limiting step in FFA synthesis) and malic enzyme and glucose-6-phosphate dehydrogenase. Despite only small active levels of these enzymes being present in SM (AT and liver are the main lipogenic tissues), their sudden increase in later life in rabbit correlates to the accelerated rate of muscle marbling. Mourot and Kouba (169) found increases in malic enzyme to be the dominant factor in PAT accretion. Increases in TG synthesis are likely to be due to a combination of increased fatty acid synthesis and possibly increased uptake from the blood. TG are synthesised from the successive esterification of fattyacylCoA units (pre-synthesised or from the circulation) to a glycerol-3-phosphate backbone (derived from ATP-dependent phosphorylation of glycerol or reduction of dihydroxyacetone phosphate). Only small amounts of glycerol kinase are found in AT therefore most of the glycerol-3-phosphate produced is thought to be from glycolytic intermediates. Adipose glycerol kinase is however active in certain obese individuals where glycerol formed from lipolysis is re-esterified (40). Therefore, uptake of glycerol and fatty acids from blood will increase TG synthesis, particularly in certain forms of obesity. Insulin has been shown to increase AT LPL and decrease or not change the levels and activity of SM LPL (55). The addition of insulin will further stimulate LPL in the non-nutritive adipocytes.

Previously ultrasound was used to detect increases in PAT (218). Ultrasound has been now superceded by the better resolution capability of computed tomography, where lipid is recorded as a negative attenuation. Using this technique, Sipila and Suominen reported an increase in muscle attenuation (decreased levels of PAT) in elderly male and female athletes (255). In addition, perimysial fat accretion was found to break up the collagen network between the fibre bundles (182) resulting in a reduction in muscle work capacity. While an increase in muscle density is recorded with training, the opposite appears to be true for obesity. Reduction in muscle density has been correlated with age and body weight (137) (254) (236). Negative attenuation of the mid-thigh is also inversely related to insulin sensitivity (254) (93). Despite these correlations computed tomography is, however, unable to distinguish between fat located within the muscle fibres (intramyocellular) and fat located between the muscle fibres (PAT).

Indeed, many studies (including muscle biopsy) may actually be measuring a combination of both TG stores.

Newer methods using ^{1}H NMR spectroscopy are able to distinguish the two TG compartments in human muscle (245) (28) (195) (269). TG methylene proton signals occurring at 1.4 and 1.6 p.p.m. and are thought to represent TG inside the muscle fibres and TG in AT between the fibres respectively. At present it is unclear why the TG in these two compartments resonate at different frequencies, but is likely to be due to their different spatial arrangement/orientation in each cell type. This may include association of the TG with different structures (for example perilipin in AT) or location of the intramyocellular lipid in a more polar environment (270). Alternatively intramyocellular TG is contained in a spherical droplet unlike the tubular accumulation of PAT (28). These methods have increased in popularity (and are preferred over muscle dissection and painful needle biopsy) due to non-invasive measurements of live subjects.

Intramyocellular TG content has been positively correlated with insulin resistance (reviewed in (91)) despite our reported decrease in capillary blood flow. However it remains uncertain whether increased myocyte TG is a result of or a cause of insulin resistance. Most reports would suggest that an increase in intramyocellular TG is a major cause of insulin resistance (144) (195) (197). Studies on the off-spring of type II diabetics which have a high risk factor for the disease revealed an elevated intramyocellular TG accumulation in the soleus (195). How tissue TG modulates insulin secretion and action is unknown. While the deposition if intramyocellular TG is increased preceding or during the early stages of insulin resistance, the deposition of PAT appears to be later on in life (301) (174) perhaps when muscle insulin resistance has been established. Therefore measurement of PAT content by proton magnetic resonance spectroscopy in the off-spring of Type 2 diabetic parents is similar to the offspring of healthy adults (123). However, acceleration of perimysial adipocyte accretion in the muscle of humans over 60 years old (both an increased size and number) was accompanied by obvious changes in vessel structure (242).

In conclusion, TG hydrolysis was enhanced in the perfused rat hindlimb by the addition of the model vasoconstrictor 5-HT. 5-HT had no direct effect on LPL activity and thus alterations in TG hydrolysis are likely to be due to the ability of 5-HT to alter

flow patterns within muscle. Increases in non-nutritive flow (possibly with hypertension and insulin resistance) may therefore enhance perimysial, endomysial and tendon fat deposition, leading to increases in muscle adiposity. This is more likely to occur later in life and result in changes that are detrimental for muscle function.

CHAPTER 5

5 Effect of predominantly nutritive and non-nutritive flow patterns on amino acid uptake and release by the perfused rat hindlimb.

5.1 Introduction

Chapter 3 of this thesis examined insulin-mediated glucose and palmitic acid uptake by the perfused rat hindlimb with the infusion of an agent (5-HT) that increased the ratio of non-nutritive to nutritive flow. This resulted in the decreased uptake of these metabolites. Long-term reductions in capillary flow may therefore contribute to elevated circulating levels of FFA and glucose. While lipid and carbohydrate fulfill the majority of SM fuel requirements, they are also able to utilize amino acids. As with glucose, amino acids are soluble in water (and plasma). Solutions of radiolabeled and cold amino acids can thus be infused into the vasculature of the hindlimb. Non-metabolizable amino acids such as α amino isobutyric acid (AIB) and α methyl amino isobutyric acid (methAIB) are often used (29). Here we have examined the uptake of the amino acid, α amino isobutyric acid (AIB) by the perfused rat hindlimb. Despite the high affinity of AIB for the muscle system A transporter, the uptake of this derivative in the perfused rat hindlimb is very low when compared to other amino acids such as alanine (120). This non-metabolizable amino acid derivative is, however, advantageous for distinctly studying uptake of AIB only, as it is not incorporated into protein, and provided intracellular levels remain low, it is not re-released into the perfusate.

In addition, we have determined the release of an indicator of SM myofibrillar (actin and myosin) degradation, 3-methyl histidine (3-MH) as well as net release of histidine. Almost 90% of 3-MH released from the body originates from SM (295). The anabolic effect of insulin involves both increased amino acid uptake and decreased amino acid release from muscle (29). As a result, the intracellular amino-acid pool is elevated. While insulin has been shown to attenuate total protein breakdown (tyrosine release (228) (166)), myofibrillar protein breakdown (3-MH release) is unaltered in the

perfused rat hindlimb (228) (130). In these experiments, however, we have altered the proportion of capillary/nutritive flow in the perfused rat hindlimb by the addition of certain vasoconstrictors with or without insulin. Altering the delivery of insulin under these conditions may affect 3-MH or histidine release or AIB uptake.

5.2 Materials and Methods

5.2.1 Perfusion buffer

Bovine RBC were washed in Krebs buffer which is gassed with 95% air:5% CO_2. RBC were filtered through muslin and packed cells were added to 1.27 times 4% BSA/Krebs buffer (Chapter 2 section 2.2.2), 228 µl/l heparin, 2.54 mM $CaCl_2$, 8.3 mM glucose and 1.32 g/l pyruvic acid. Throughout the perfusion, the RBC buffer was continuously gassed with 95% air:5% CO_2, both into the medium and through the artificial lung of the apparatus.

5.2.2 Perfusion protocol

The left hindlimbs of 180-200 g male Hooded Wistar rats were perfused with bovine RBC in a Krebs buffer at 4 ml/min and 37°C. Surgery was performed as described in Chapter 2 section 2.2.4, and the perfusion apparatus used is shown in Fig.2 Chapter 2. The Clark-type oxygen electrode was calibrated using 100% oxygen and 100% nitrogen, and measured dissolved oxygen in the perfusate only.

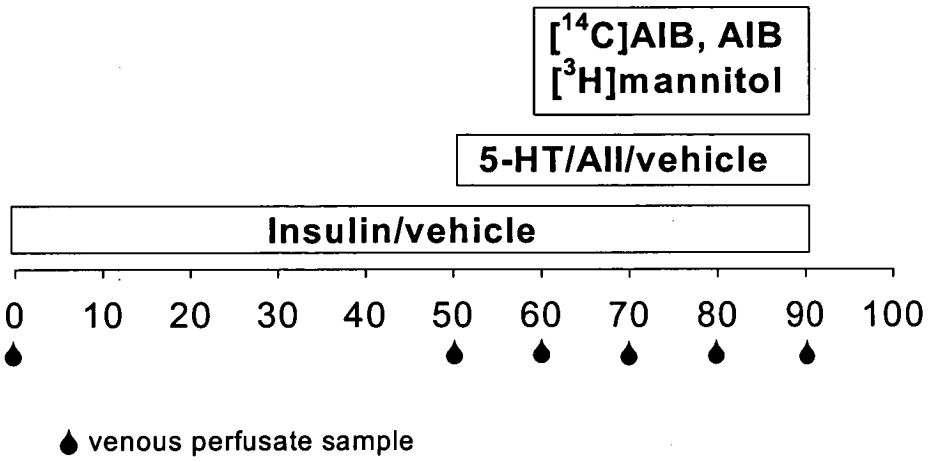

Figure 1. Perfusion protocol for the determination of AIB uptake by the perfused rat hindlimb.

The hindlimbs were perfused according to the protocol shown above (Fig. 1). After a 40 min equilibration period, 50 mM AIB was infused with 400 Ci [^{14}C] AIB and 40 Ci [^{3}H] mannitol for 30 min at a dilution of 1/100 (final concentration 0.5 mM AIB). Perfusions assessing the uptake with insulin used 18 mU/ml of insulin (Ins, Humulin, Eli Lilly) added as a bolus to the perfusion buffer. In some perfusions, either 1 μM 5-HT (5-HT) or 50 nM AII (AII) were infused 5 min prior to AIB infusion. AIB was infused for the remainder of the experiment (30 min). Venous samples were taken during basal conditions and 10, 20 and 30 minutes after AIB infusion.

5.2.3 Radioactivity of hindlimb muscles

Immediately after perfusion, the hindlimb muscles were removed and digested according to Chapter 2 section 2.4 for determination of radioactivity.

5.2.4 Radioactivity of plasma samples

Venous samples were immediately centrifuged to remove RBC and 100 µl of plasma was added to 6 ml of Amersham Biodegradable Counting Scintillant for determination of radioactivity. Samples were counted for a dual-label ([^{3}H] and [^{14}C]).

5.2.5 3-Methyl histidine release

Derivatization of primary amines with fluorescamine (4-phenylspiro[furan-2(3H), 1'-phthalan]-3,3'-dione) produces fluorescent fluorophors (Fig. 2). Un-reacted fluorescamine however, is rapidly destroyed by contact with water (282). Fluorescamine and all hydrolysis products are non-fluorescent (282), allowing easy detection of derivatized amino acids. In this chapter a modification of methods by Wasnner *et al.* (296) and Nakamura and Pisano (175) were used. Arterial and venous perfusate samples (taken 10 mins after the beginning of AIB infusion (70 min)) were derivatized with fluorescamine, and the 3-MH and histidine fluorophors were detected by C_{18} reverse-phase HPLC with an in-line fluorimeter.

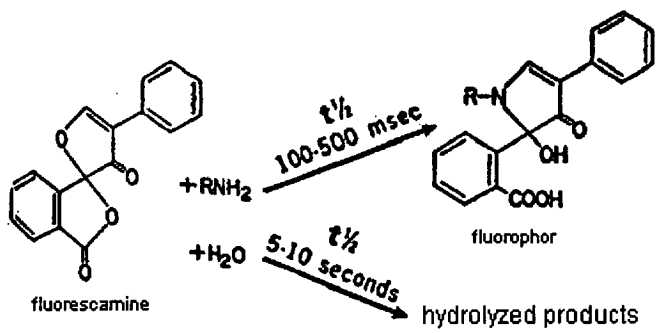

Figure 2. Derivatization of primary amines with fluorescamine (modified from (282)).

Perchloric acid (2 M) was added to all perfusion samples to remove protein. Samples were then neutralized with 2.5 M K_2CO_3. Perfusate samples (50 µl) were added to 200 µl 0.2 M boric acid buffer (pH 9) containing 10 µM L-histidinol (Sigma) as an internal standard, and mixed before the addition of 250 µl of acetonitrile and fluorescamine (0.2 mg/ml, Sigma). The derivatization was performed at room temperature for 5 min in the dark. HCl (250 µl of 2M) was added and samples were then incubated at 80°C for 1 hour. After cooling to room temperature, samples were adjusted to pH 6.5 using 150 µl of 2.5 M K_2CO_3. Samples (100 µl) were then separated on a C_{18} reverse-phase HPLC column, and run using a gradient of 10 mM sodium phosphate buffer in 20-40% acetonitrile (pH 7.5), as the mobile phase. Samples were run at 1.5 ml/min and 3-MH, histidine and histidinol had retention times of approximately 10, 11 and 20 mins respectively. Peaks were detected using a WinDaq data acquisition program attached to an in-line fluorimeter (excitation wavelength of 365 nm and an emission wavelength of 460 nm, sensitivity 100). Standards of 3-MH (Sigma) and L-histidine (Sigma) were conducted regularly to check the consistency of derivatization and separation.

The area under the fluorescent curve for each standard concentration was determined (volts.s) and plotted against the standard concentration. The equations generated from the standard curves for 3-MH and histidine were used to calculate the concentration of these amino acids in the arterial and venous samples. The difference in venous and arterial concentration was used to calculate the release of the respective amino acids by the perfused hindlimb, using the equation:

$$\text{Rate} = \Delta\text{3-MH or histidine (nmol/ml)} \times \text{flow rate (ml/min)} \times 60 / \text{muscle weight (g)} = \text{nmol/g/hr}$$

5.2.6 Statistics

To determine statistically significant differences, one or two way analysis of variance was used (ANOVA). Significance was recognised at $P<0.05$. One, two or three

symbols were used to denote values of $P<0.05$, $P\leq0.01$ and $P\leq0.001$ respectively. Symbols used were '*' (to show significance from control), '+' (to show significance from Ins), '#' (to show significance from 5-HT), '&' (to show significance from AII) and '$' (to show significance from AII+ Ins).

5.3 Results

Due to the variability in basal oxygen tension (resulting from different batches of RBC) all differences are reported in terms of "change in oxygen consumption". The dissolved venous oxygen content and perfusion pressure (PP) of all experiments are shown in Figure 3 (panels A and B respectively). The maximal vasoconstrictor effects occurred at the beginning of constrictor infusion (10 min before AIB infusion). Venous dissolved oxygen content significantly increased by 5.8 ± 0.9 mmHg ($P<0.001$) during maximal stimulation with 5-HT, indicating decreased uptake by the hindlimb. Similarly, PP was significantly increased by 56.9 ± 11 mmHg ($P<0.001$). With the addition of 18 mU/ml (108 nM) Ins to the buffer, 5-HT increased venous dissolved oxygen (by 6.4 ± 1.3 mmHg, $P<0.001$) and PP (by 66.9 ± 15 mmHg, $P<0.001$) by a similar amount. Ins infusion did not significantly alter dissolved oxygen content or PP from control perfusions. Infusion of 50 nM AII significantly decreased venous oxygen content (indicative of increased oxygen uptake, and increased capillary flow) by 11.5 ± 1.5 mmHg during maximal stimulation ($P<0.001$). This was accompanied by an increased PP of 41.4 ± 6.3 mmHg ($P<0.01$). Co-infusion of Ins with AII, however, significantly reduced the vasoactive effect of AII (venous oxygen decreased by 6.5 ± 1.4 mmHg ($P<0.001$ vs control and $P=0.003$ vs AII), and PP increased by 18.3 ± 4.4 mmHg (not significant from control)).

The uptake of AIB by the individual hindlimb muscles with all treatments is shown in Figure 4, panel A. Ins significantly increased AIB uptake into all muscles. When averaging the uptake across all muscles tested (Figure 4, panel B) Ins increased the uptake by approximately 2 times, from 434 ± 59 to 940 ± 87 nmol/30min/g ($P=<0.001$). 5-HT infusion tended to decrease the uptake, however this was not significant ($P=0.075$). The infusion of 5-HT with Ins significantly decreased the uptake

of AIB compared to Ins infusion alone, in three of the six muscle tested (EDL, G.White and tibialis). This reduction in AIB uptake was significant for the average of the muscles tested (from 940 ± 87 to 658 ± 20 nmol/30min/g (P=<0.05)). The infusion of AII did not significantly increase AIB uptake by the hindlimb. The co-infusion of Ins with AII did not further increase AIB uptake above the uptake by ins stimulation alone.

Very little difference was recorded between extracellular space and W.Wt. to D.Wt. ratio of the hindlimb muscles, with any of the treatments used (figures 5 and 6 respectively).

3-MH release from the tissues is an indicator of myofibrillar protein degradation. These values are shown in Figure 7. AII infusion (50 nM) significantly increased the 3-MH release from the hindlimb compared to all other groups (P<0.001 for all groups vs AII), including AII + Ins (from 10.2 ± 0.7 to 3.9 ± 0.2 nmol/g/h). Ins alone did not significantly decrease 3-MH release compared to control perfusions. 5-HT infusion (1 μM) did not alter 3-MH release from control perfusions.

Histidine release from the perfused rat hindlimb is shown in Fig.8. Histidine release was significantly inhibited by the infusion of 18 mU/ml Ins (from 121 ± 15 to 55 ± 20 nmol/g/h, P<0.05). As with the 3-MH, histidine release was significantly increased by the infusion of AII compared to all other groups, including AII+Ins (from 99 ± 12 to 203 ± 17 nmol/g/h, P<0.001). 5-HT infusion (1 μM) did not alter L-histidine release from control perfusions, however 5-HT+Ins significantly decreased histidine release compared to 5-HT infusion alone (from 128 ± 23 to 9.1 ± 5.8 nmol/g/h, P<0.01).

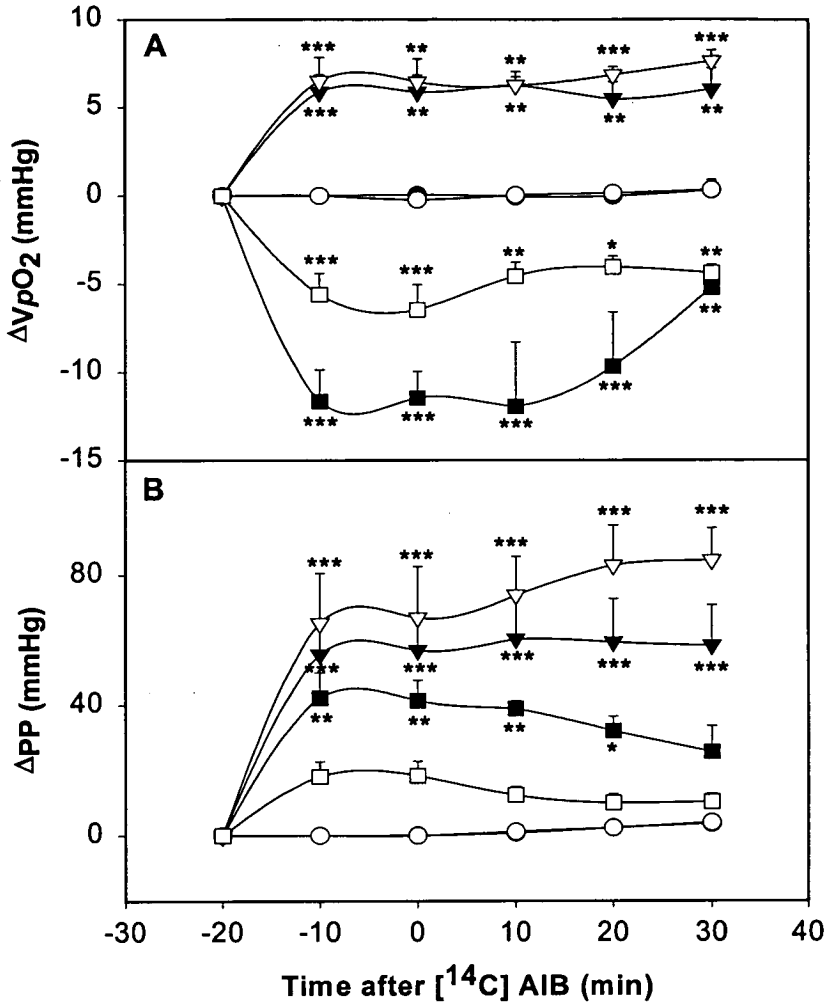

Figure 3. Change in oxygen partial pressure (VpO_2, Panel A) and perfusion pressure (PP, Panel B) in the rat hindlimb perfused with bovine RBC and BSA/Krebs buffer at 4 ml/min, 37°C and either Ins (18mU/ml), 5-HT (1 μM), AII (50 nM) or a combination of these agents. Insulin was added from the beginning of the experiment, while all vasoconstrictors were added 10 minutes before AIB infusion. At 0 min, [^{14}C] AIB were infused in all experiments for the remaining 30 min. Symbols are ○, control; ●, Ins; ■, AII; □, AII+Ins; ▼, 5-HT; ▽, 5-HT+Ins. Significant differences from control experiments are denoted by *, ** or *** to show $P<0.05$, $P\leq0.01$ and $P\leq0.001$ respectively. Values are means ± S.E., n=5-6. Due to the differences between all group, only comparisons to control perfusions were made.

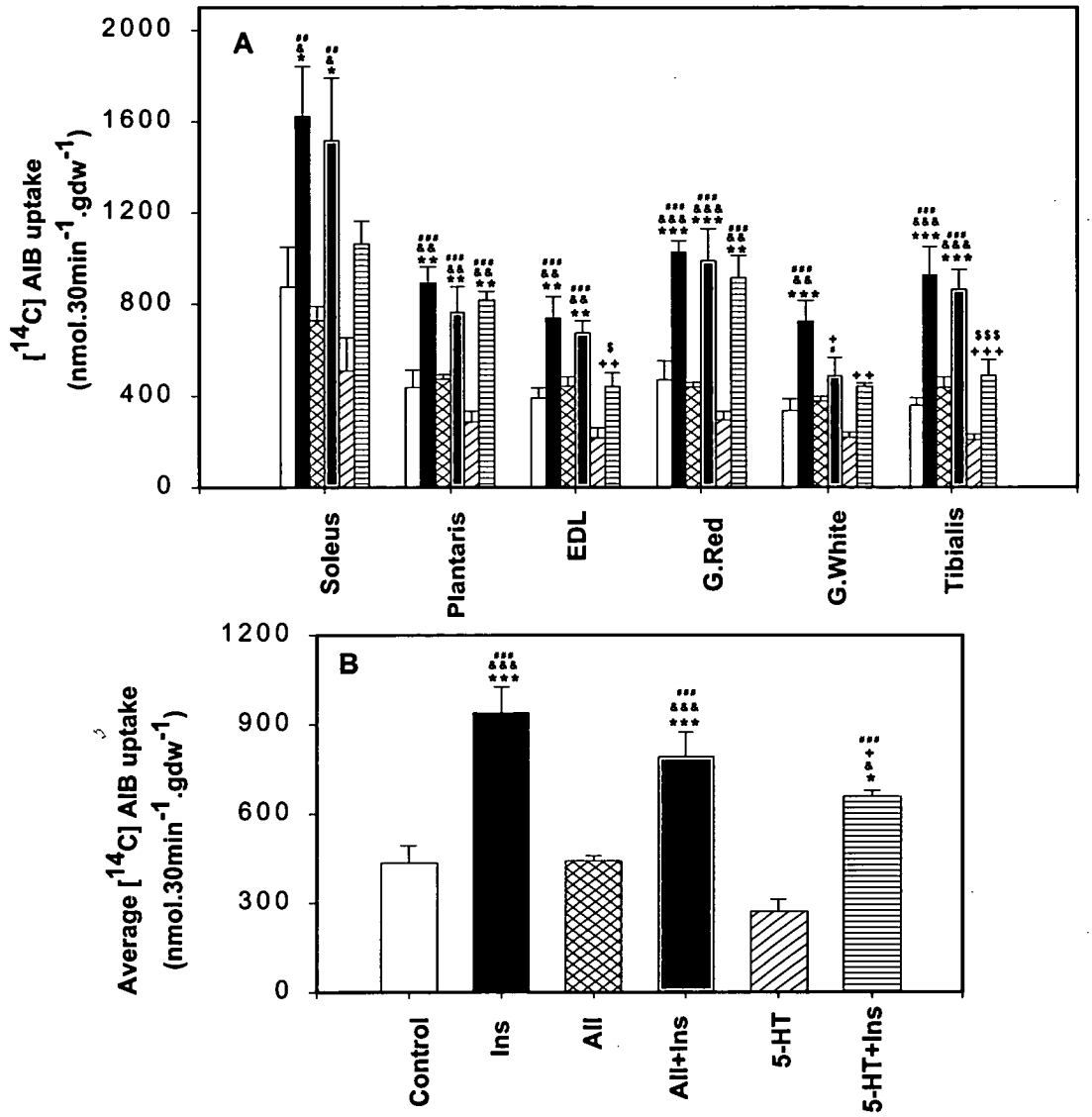

Figure 4. The uptake of [^{14}C] AIB by the rat hindlimb perfused with bovine RBC and BSA/Krebs buffer at 4 ml/min, 37°C and either Ins (18 mU/ml), 5-HT (1 μM), AII (50 nM) or a combination of these agents. Insulin was added from the beginning of the experiment, while all vasoconstrictors were added at 10 min before AIB infusion. At 0 min, [^{14}C] AIB infused in all experiments for the remaining 30 min. The uptake into the individual muscles is shown in Panel A, and the average uptake for those muscles tested, is shown in Panel B. Bars are control (white), Ins (black), AII (cross hatched), AII+Ins (grey), 5-HT (right hatched) and 5-HT+Ins (horizontal stripe). Significant differences are denoted by one, two or three symbols to show $P<0.05$, $P\leq0.01$ and $P\leq0.001$ respectively. Significant differences are denoted by '*', '+', '&', and '$' to show significance from control, Ins, AII and AII+Ins respectively. Values are means ± S.E., n=5-6, for muscles after 30 minutes of AIB infusion.

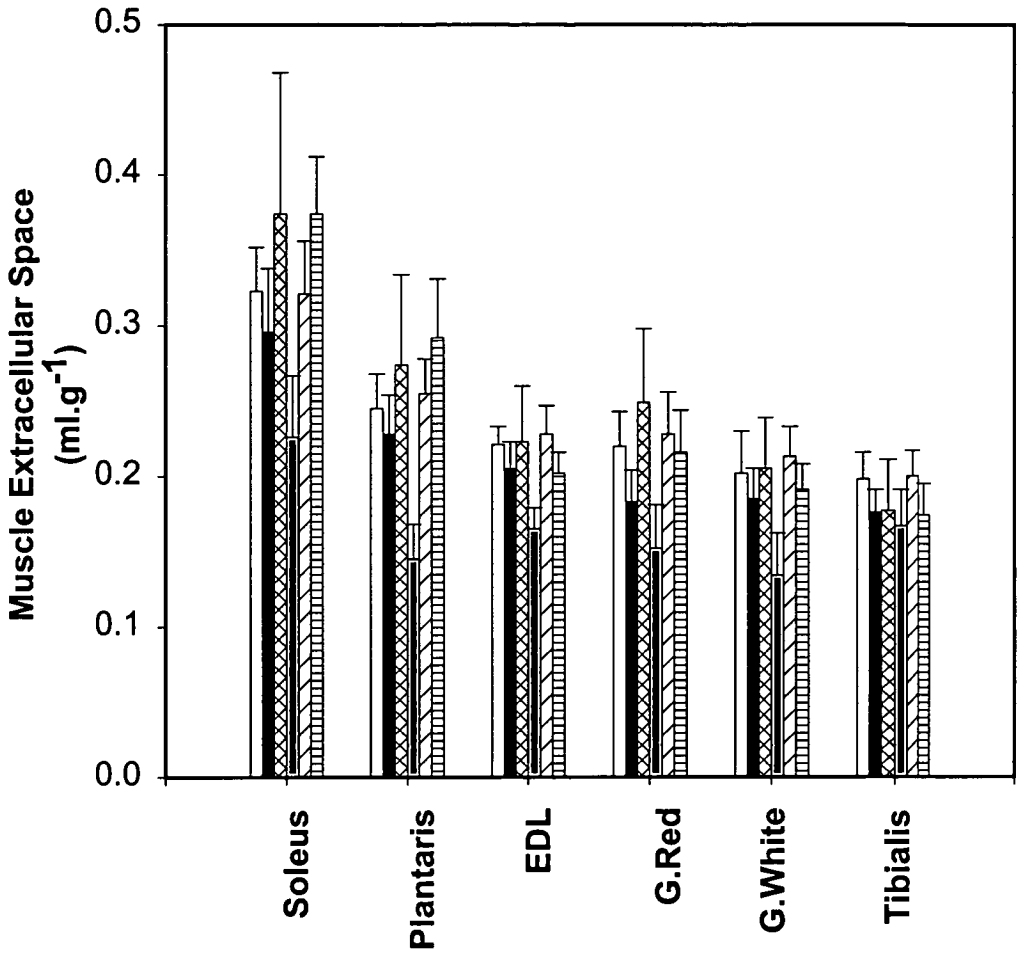

Figure 5 Muscle extracellular space in the rat hindlimb perfused with bovine RBC and BSA/Krebs buffer at 4 ml/min, 37°C and either Ins (18 mU/ml), 5-HT (1 μM), AII (50 nM) or a combination of these agents. Insulin was added from the beginning of the experiment, while all vasoconstrictors were added at 10 min before AIB infusion. At 0 min, [^{14}C] AIB and [^{3}H] mannitol were infused in all experiments for the remaining 30 min. Bars are control (white), Ins (black), AII (cross hatched), AII+Ins (grey), 5-HT (right hatched) and 5-HT+Ins (horizontal stripe). Values are means ± S.E., n=5-6, for muscles dissected after 30 mins of AIB infusion.

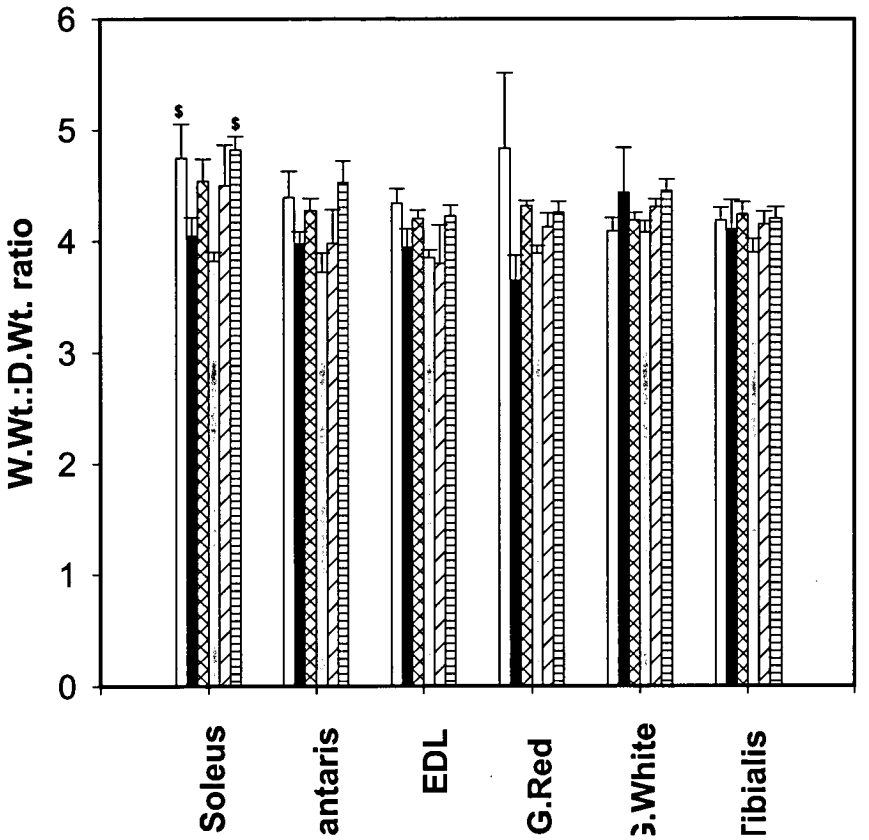

Figure 6 Muscle W.Wt:D.Wt. ratio in the rat hindlimb perfused with bovine RBC and BSA/Krebs buffer at 4 ml/min, 37°C and either Ins (18 mU/ml), 5-HT (1 μM), AII (50 nM) or a combination of these agents. Ins was added from the beginning of the experiment, while all vasoconstrictors were added 10 min before AIB infusion. At 0 min, [^{14}C] AIB was infused in all experiments for the remaining 30 min. Bars are control (white), Ins (black), AII (cross hatched), AII+Ins (grey), 5-HT (right hatched) and 5-HT+Ins (horizontal stripe). Significant differences from AII+Ins are denoted by '$' ($P$<0.05). Values are means ± S.E., n=5-6, for muscles dissected 30 minutes after AIB infusion.

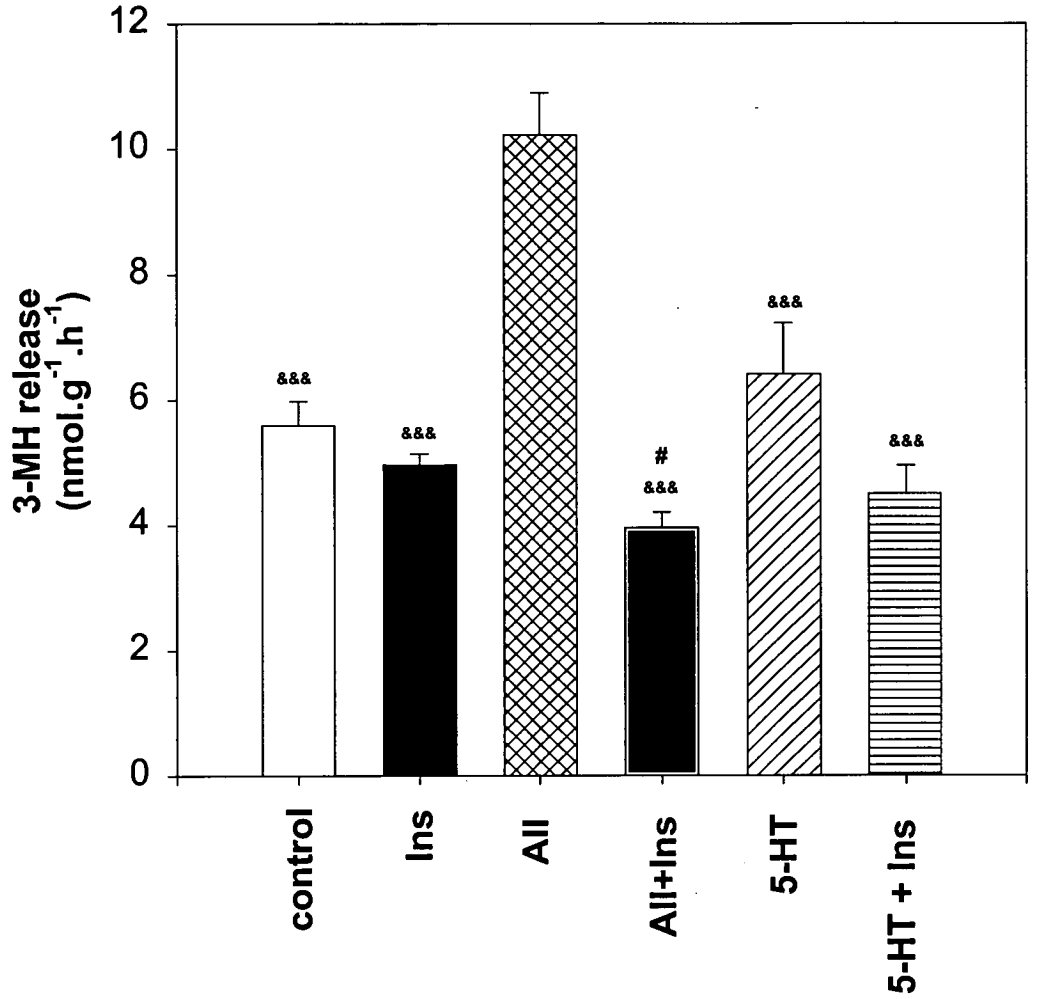

Figure 7 3-methyl histidine release by the rat hindlimb perfused with bovine RBC and BSA/Krebs buffer at 4 ml/min, 37°C and either Ins (18 mU/ml), 5-HT (1 μM), AII (50 nM) or a combination of these agents. Insulin was added from the beginning of the experiment, while all vasoconstrictors were added 10 min before AIB infusion. At 0 min, [^{14}C] AIB was infused in all experiments for the remaining 30 min. Bars are control (white), Ins (black), AII (cross hatched), AII+Ins (grey), 5-HT (right hatched) and 5-HT+Ins (horizontal stripe). Significant differences are denoted by one, two or three symbols to show $P<0.05$, $P\leq0.01$ and $P\leq0.001$ respectively. Significant differences are denoted by '&', and '#' to show significance from AII and 5-HT respectively. Values are means ± S.E., n=5-6, using venous samples taken 10 min after the beginning of AIB infusion.

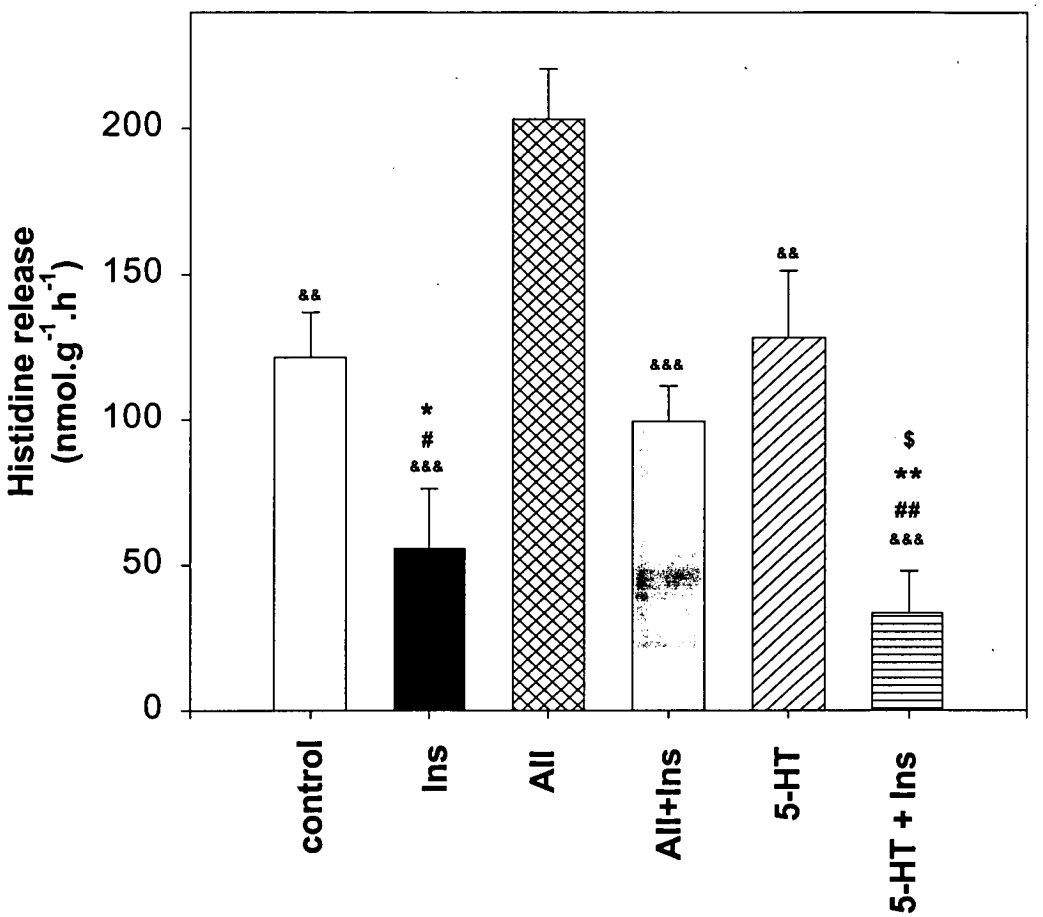

Figure 8 Muscle histidine release by the rat hindlimb perfused with bovine RBC and BSA/Krebs buffer at 4 ml/min, 37°C and either Ins (18 mU/ml), 5-HT (1 μM), AII (50 nM) or a combination of these agents. Insulin was added from the beginning of the experiment, while all vasoconstrictors were added 10 min before AIB infusion. At 0 min, [^{14}C] AIB was infused in all experiments for the remaining 30 min. Bars are control (white), Ins (black), AII (cross hatched), AII+Ins (grey), 5-HT (right hatched) and 5-HT+Ins (horizontal stripe). Significant differences are denoted by '*', '&', '$', and '#' to show significance from control, AII, AII+Ins and 5-HT respectively. Values are means ± S.E., n=5-6, using venous samples taken 10 min after the beginning of AIB infusion.

5.4 Discussion

This chapter demonstrated that the uptake of AIB, and the access to products of protein breakdown, are altered by the addition of vasoconstrictors (5-HT and AII) that have previously been shown to modify the ratio of muscle nutritive and non-nutritive flow in the perfused rat hindlimb (211) (212) (180) (53).

Insulin significantly increased [^{14}C] AIB uptake into all hindlimb muscles, probably due to insulin's stimulatory effect on the System A transporter. Insulin has been shown to increase the uptake of methAIB into incubated soleus muscle (277), and in cultured L6 muscle cells 100 nM insulin increased AIB uptake by greater than 50% (165). In the perfused rat hindlimb, in this study, insulin (108 nM) increased AIB uptake by a similar amount.

AIB uptake was not further increased from control perfusions by capillary recruitment (AII infusion). Angiotensin, however, has been shown to cause significant protein breakdown (33), thus, the net movement of certain amino acids out of the muscle by the System A transporter may inhibit the uptake of AIB, despite an increase in capillary perfusion, causing no net effect on AIB uptake. There was a marked dilatory effect of insulin against AII, that was absent during insulin or 5-HT+Ins infusions. This resulted in a small increase in oxygen consumption, despite no net pressure effect compared to control perfusions. Thus, the effect of AII (with insulin) on AIB uptake would be less than expected if the oxygen consumption reached the same level as with AII alone. However as insulin is also present, the effect of insulin to increase amino acid uptake would oppose that of AII to increase amino acid release. Due to the net uptake of AIB in these experiments, insulin appears to have a stronger effect than AII on protein metabolism.

5-HT tended to decrease the uptake of AIB into all muscles, however this was not significant. 5-HT infusion reduced insulin-mediated AIB uptake in four of the six muscles tested, and significantly decreased AIB uptake across the whole hindlimb when compared to insulin infusion alone. This implies that the infusion of the constrictor, 5-

HT (shown in Chapter 3 to reduce IMGU), is likely to reduce the uptake of all amino acids by the muscle, contributing to muscle protein wasting.

In addition, 3-MH and histidine release from muscle were also influenced by the infusion of AII, 5-HT, insulin or a combination of these agents. 3-MH is an indicator of myofibrillar protein (myosin and actin) breakdown. 3-MH is formed through a post-translational methylation of histidine residues of actin and myosin (reviewed in (306)). It is often monitored in preference to tyrosine or phenylalanine (indicators of total muscle protein degradation) which are not metabolized or produced by SM, but can be resynthesized into muscle proteins (306). Moreover, to measure these amino acids, protein synthesis inhibitors such as cyclohexamide must be added to the perfusate. 3-MH measurement is therefore preferable as it is not re-utilized for protein synthesis.

As shown by others (228) (130), in this study insulin did not decrease muscle 3-MH release compared to control perfusions, however histidine release was significantly reduced. Histidine accounts for 2% of the total amino acids released by the perfused rat hindlimb (reviewed in (90)). Reduced histidine release with insulin has also been shown by Meek *et al.* (166). Thus, from this study it appears that insulin inhibits the breakdown of certain cellular proteins, however not actin and myosin.

AII infusion (capillary recruitment) increased the release of both 3-MH and histidine, which is likely to be due to either a reduction in muscle protein degradation, or a build-up of these amino acids in the previously-unperfused capillaries. While increased 3-MH release with AII may be a phenomenon of washout from newly recruited vascular space, this was found to be unlikely, as a combination of insulin with AII did not increase the release of 3-MH. While it is likely that the reduction in pressure with insulin and AII, may cause some reduction in muscle amino acid efflux, Brink *et al.* (33) have shown that AII has significant effects on muscle protein breakdown and wasting, and as is evident from this study, on both myofibrillar and other cell proteins. It would therefore be of interest to determine the effects of other vasoconstrictors that do not influence amino acid metabolism directly but alter the proportion of nutritive and non-nutritive flow.

5-HT infusion alone had no effect on the release of either amino acid. Since non-nutritive (connective tissue) flow is likely to have reduced muscle capillary perfusion,

along with a reduction blood access to muscle amino acid transporters, then it would be expected that 5-HT would decrease the efflux of histidine and 3-MH. The release of these amino acids however remained unaltered with 5-HT infusion, suggesting 5-HT may also have some metabolic effect to increase muscle protein degradation. A combination of 5-HT and insulin significantly reduced the release of histidine compared to all other perfusion types except insulin alone, however had no effect on 3-MH release. This re-enforces the idea that insulin has no effect on the breakdown of myofibrillar proteins.

It has been shown that amino acids are able to exert control over muscle protein synthesis and amino acid balance (158) (268) (277). Others have shown that branched chain amino acids decrease the rate of protein breakdown. Kadowaki *et al.* (130) measured 3-MH release from the rat hindlimb perfused with RBC containing either insulin or amino acids. Neither had any effect on 3-MH release. Similarly, the inclusion of 0.5 mM AIB in these perfusions is not likely to affect this process, as is not metabolized by the myocyte. The RBC-based perfusion medium, however, contained small amounts of 3-methyl histidine and histidine (probably from the RBC). It is therefore conceivable that there was some uptake of these amino acids by the perfused muscle. From these experiments however there was clearly a net release of these amino acids into the perfusate.

SM holds the largest pool of protein in the body (reviewed in (306)). The conservation of body protein is under complex control and is dependent on the degree of fasting and the age and fat depots of the rat (89). Older rats have been shown to have higher levels of protein synthesis and less proteolysis than younger rats (89). In incubated soleus and epitrochlearis muscles from obese Zucker rats, basal AIB uptake was reduced compared to their lean counterparts (80), which may be a reflection of down-regulation of the system A transporter, due to chronic non-nutritive flow.

These results show that 5-HT and AII are able to alter amino acid uptake and release by perfused muscle, which appears to be a combination of metabolic effects and alterations in the ratio of nutritive and non-nutritive flow. AII clearly stimulates muscle protein degradation and 5-HT may have similar effects. Insulin appears to inhibit the

breakdown of histidine-containing proteins, but not myofibrillar proteins. With regard to amino acid transport into the myocytes, the uptake of AIB was stimulated by insulin. However, increasing the proportion of muscle non-nutritive flow (with 5-HT infusion) reduced insulin-mediated AIB uptake (which is probably indicative of general amino acid uptake) by skeletal myocytes. Thus, non-nutritive flow may contribute to muscle wasting.

CHAPTER 6

6 Substrate effects on hormone action: Lipid infusion impairs insulin-mediated capillary recruitment (nutritive flow) and muscle glucose uptake *in vivo.*

6.1 Introduction

SM accounts for approximately 80% of the insulin-mediated glucose uptake after a meal (58) and becomes resistant to insulin in Type 2 diabetes (59), hypertension (129), obesity (57) and severe forms of stress (193). However, the mechanisms by which muscle insulin resistance develops are not fully understood. One factor that may be central is lipid availability. For example, insulin sensitivity in humans is reduced in obesity (57) and especially when individuals possess an abnormally high proportion of abdominal fat (38). In addition, lipid infusion in humans (25) (293), and in rats (140) gives rise to insulin resistance in muscle. Furthermore, genetically obese Zucker rats have elevated plasma levels of free fatty acids and show marked muscle insulin resistance (19) as do rats fed high fat diets (267) (264); although the type of fatty acid appears rather critical as oils of fish origin are protective against the effects of animal fat diets (265).

Explanations to account for the link between lipid availability and muscle insulin resistance have until recently focused on the Randle glucose-fatty acid cycle (206) in which fatty acid metabolites collectively contribute to the inhibition of oxidative and non-oxidative glucose metabolism. Recently, there has been a number of studies (119) (246) (97) suggesting that fatty acids or their metabolites inhibit insulin signaling at points preceding activation of glycogen synthase or glucose transport.

Insulin *in vivo* has haemodynamic effects additional to its well-described direct metabolic action on muscle. Although the precise role of the haemodynamic effects are

unknown, it is possible that they contribute to the overall metabolic response by enhancing access for both insulin and glucose to muscle (14) (303) (209). There appear to be two components to insulin's haemodynamic actions, one involving an increase in bulk flow and another involving capillary recruitment. A number of laboratories have reported an effect of insulin to increase bulk blood flow to muscles (14) (125) (154) (78) (84) (54) (222) and that this effect is impaired in states of insulin resistance (14) and when lipid is infused in otherwise normally responsive subjects (262). However, the role of the increase in total blood flow mediated by insulin is controversial. There have been claims that insulin-mediated changes in total blood flow relate poorly to muscle glucose uptake under several circumstances, including insulin dose and time course (303). In addition, there have been studies where total flow changes persist when glucose uptake is inhibited (244). Also, most vasodilators that augment total blood flow to the limbs do not enhance insulin action nor do they overcome insulin resistance (177) (178) (150).

Because of techniques unique to our laboratories, we have been the first to report a direct effect of insulin to increase capillary recruitment (or nutritive flow) within SM of anaesthetized rats (209) and the forearm of humans (50). Insulin-mediated capillary recruitment appears to be independent of changes in bulk blood flow to the limb in both rats and humans, particularly if physiologic levels of insulin are used (287). Measurement of capillary exposure (or nutritive flow) in anaesthetized rats was assessed using 1-MX metabolism. Hind limb metabolism of this infused substrate targeted for capillary endothelial xanthine oxidase was shown to increase in the presence of insulin (209). In addition, if α-methyl 5-HT (α-met5HT), an agent that prevented capillary recruitment in the hind limb was administered (210), or if TNFα was infused (305), the ability of insulin to increase either total blood flow or capillary recruitment in the hind limb was markedly impaired and insulin-mediated glucose uptake was blocked by 50-60%.

Since there appears to be a link between insulin-mediated capillary recruitment and insulin-mediated glucose uptake in muscle, it was considered important to explore a model of insulin resistance where insulin-mediated muscle glucose uptake is impaired. Thus the aim of these experiments was to assess whether fatty acid-induced muscle

insulin resistance was accompanied by impaired capillary recruitment at physiologic insulin.

6.2 Methods

6.2.1 Surgery

Details were essentially as described previously. In brief, 250 g rats were anaesthetized using Nembutal (50 $mg.kg^{-1}$ body weight) and had polyethylene cannulas (PE-50, Intramedic®) surgically implanted into the carotid artery, for arterial sampling and measurement of blood pressure (pressure transducer Transpac IV, Abbott Critical Systems) and into both jugular veins for continuous administration of anaesthetic and other intravenous infusions. A tracheotomy tube was inserted, and the animal was allowed to spontaneously breathe room air throughout the course of the experiment. Small incisions (1.5 cm) were made in the skin overlaying the femoral vessels of both legs, and the femoral artery was separated from the femoral vein and saphenous nerve. The epigastric vessels were then ligated, and an ultrasonic flow probe (Transonic Systems, VB series 0.5 mm) was positioned around the femoral artery of the right leg just distal to the rectus abdominis muscle. The cavity in the leg surrounding the flow probe was filled with lubricating jelly (H-R, Mohawk Medical Supply, Utica, NY) to provide acoustic coupling to the probe. The probe was then connected to the flow meter (Model T106 ultrasonic volume flow meter, Transonic Systems). This was in turn interfaced with an IBM compatible PC computer which acquired the data (at a sampling frequency of 100 Hz) for femoral blood flow, heart rate, and blood pressure using WINDAQ data acquisition software (DATAQ instruments). The surgical procedure generally lasted approximately 30 min and then the animals were maintained under anesthesia for the duration of the experiment using a continual infusion of Nembutal (0.6 $mg.min^{-1}.kg^{-1}$) via the left jugular cannula. The femoral vein of the left leg was used for venous sampling, using an insulin syringe with an attached 29G needle (Becton Dickinson). A duplicate venous sample was taken only on completion of the experiment (360 min) to prevent alteration of the blood flow from the hindlimb due to sampling, and

to minimize the effects of blood loss. The body temperature was maintained using a water-jacketed platform and a heating lamp positioned above the rat.

6.2.2 Experimental Procedures

A 60 min equilibration period was allowed after surgery so leg blood flow and blood pressure could become stable and constant. Rats were then allocated into either of three protocols A, B, or C (Fig.1). Protocol A involved 6h infusion of saline with a 2h euglycemic clamp (Humulin R, Eli Lilly & Co., Indianapolis, $3mU.min^{-1}.kg^{-1}$) commenced 4h into the saline infusion (Ins). Protocol B (Lip) involved an initial bolus dose of heparin (10 units) before a 6h infusion of 10% Intralipid ™ / heparin ($33units.ml^{-1}$) at 20 $\mu l.min^{-1}$ with a 2h saline infusion commenced 4h into the lipid infusion. Protocol C (Lip + Ins) was identical to Protocol B except that a 2h euglycemic clamp replaced the 2h saline. Volumes were matched between all three protocols (209) (210) (305). As in previous similar studies and since 1-MX (Sigma Aldrich Inc) clearance was very rapid, it was necessary to partially inhibit the activity of xanthine oxidase, particularly in non-muscle tissues. To do this, an injection of a specific xanthine oxidase inhibitor, allopurinol (71) (10 $\mu mole.kg^{-1}$) was administered as a bolus dose 5 minutes prior to commencing the 1-MX infusion (0.5 $mg.min^{-1}.kg^{-1}$) (Fig. 1). This allowed constant arterial concentrations of 1-MX to be maintained throughout the experiment.

As shown in Fig. 1, a 50 μCi bolus of 2-deoxy-D-[2,6-^{3}H]glucose (2-DG) (specific activity = 44.0 $Ci.mmol^{-1}$, Amersham Life Science) in saline was administered 45 min before completion of the experiment. Plasma samples (20 μl) were collected at 5, 10, 15, 30 and 45 minutes to determine plasma clearance of the radioactivity and for the calculation of R'g. At the conclusion of the experiment, the soleus, plantaris, EDL, G.Red and white and tibialis muscles were removed, clamp frozen in liquid nitrogen and stored at -20°C until assayed for [^{3}H]2-DG uptake.

The total blood volume withdrawn from the animals before the final arterial and venous samples did not exceed 1.5 ml and was easily compensated by the volume of fluid infused.

All other procedures were as described previously (305), including analytical methods for glucose, 1-MX, allopurinol and oxypurinol assays. Free fatty acids were assayed using a NEFA C Colorimetric Kit (Wako).

6.2.3 2-DG uptake assay

The frozen muscles were ground under liquid nitrogen and homogenised using an Ultra Turrax™. Free and phosphorylated [^{3}H]2-DG were separated by ion exchange chromatography using an anion exchange resin (AG1-X8) (145) (126). Biodegradable Counting Scintillant-BCA, (Amersham, USA) was added to each radioactive sample and radioactivity determined using a scintillation counter (Beckman LS3801, USA). From this measurement and a knowledge of plasma glucose and the time course of plasma 2-DG disappearance, R'g, which reflects glucose uptake into the muscle, was calculated as previously described by others (145) (126) and is expressed as $\mu g.min^{-1}.g^{-1}$wet weight of muscle (126).

6.2.4 Data analysis

All data are expressed as means ± SE. Mean femoral blood flow, mean heart rate and mean arterial blood pressure were calculated from 5 second sub-samples of the data, representing approximately 500 flow and pressure measurements every 15 minutes. Vascular resistance in the hind leg was calculated as mean arterial blood pressure in millimetres of mercury divided by femoral blood flow in $ml.min^{-1}$ and expressed as resistance units (RUs). Glucose uptake in the hind leg was calculated from arterio-venous glucose difference and multiplied by femoral blood flow and expressed as $\mu mol.min^{-1}$. The 1-MX disappearance was calculated from arterio-venous plasma 1-MX difference and multiplied by femoral blood flow (corrected for the volume accessible to 1-MX, 0.871, determined from plasma concentrations obtained after additions of standard 1-MX to whole rat blood) and expressed as $nmoles.min^{-1}$.

6.2.5 Statistical analysis

In order to ascertain differences between treatment groups at the end of the experiments (i.e. hindleg glucose uptake, R'g, and 1-MX metabolism) one way analysis of variance was used. Statistical differences between treatment groups for repeated measures throughout the 6 hours (i.e. blood pressure, heart rate, femoral blood flow, vascular resistance, blood glucose and GIR) were determined using two way repeated measures analysis of variance. All comparisons were made using the Student-Newman-Keuls method. The correlation between 1-MX disappearance and hindleg glucose uptake was determined by linear regression. All tests were performed using the SigmaStat™ statistical program (Jandel Software Corp.). Significance was determined by *P* values less than 0.05. One, two or three symbols were used to denote *P* values of <0.05, ≤ 0.01, ≤ 0.001 respectively. The symbols used were '*' (to show significance from Ins treated group) and '†' (to show significance from Lip + Ins treated group).

6.3 Results

6.3.1 Haemodynamic effects

Figure 2 shows the arterial blood pressure (BP), heart rate (HR), femoral arterial blood flow (FBF) and hind leg vascular resistance (VR) for the three different protocols of saline for 6h with Ins over the last 2h (Ins), Intralipid ™/heparin for 6h and Ins over the last 2h (Lip + Ins), and Intralipid ™/heparin for 6h and saline replacing Ins over the last 2h (Lip). Although there was a trend for FBF of Lip + Ins treated rats to be less than Ins treated rats at the closing stages of the clamp (340-360 min), this was not significant. There was no significant difference between Ins, Lip or Lip + Ins treated rats for any of the other three parameters BP, HR, or VR.

6.3.2 Glucose metabolism

Blood glucose levels for the three Ins, Lip and Lip + Ins treated groups are shown in Fig.3. Blood glucose was allowed to set its own level during the first four

hours (0-240 min), and in general this remained constant at approximately 5 mM. However, there was some variability for Intralipid ™ /heparin treated rats and for one group (Lip) there was a small transient fall at 120 min which then recovered, so that at 240 min all three groups were similar. In addition, there was a rise in the blood glucose level in the Lip treated rats at the 360 min time point; which was significantly higher than both Ins and Lip + Ins treated groups. The inset shows glucose infusion rate (GIR) to maintain euglycemia for Ins and Lip + Ins treated groups. For Ins treated group the GIR increased from zero to 9.0 ± 0.3 at 250 min (10 min), then to 11.9 ± 0.6 $mg.kg^{-1}.min^{-1}$ at 360 min (120 min), while that for Ins + Lip group decreased from approx. 9.0 at 250 min to 1.5± 0.6 $mg.kg^{-1}.min^{-1}$ at 360 min. The differences in GIRs to maintain euglycemia became significant as early as 20 min after commencement of the Ins infusion.

Measurements for arterial plasma free fatty acids were taken immediately prior to the commencement of the 2 hour Ins clamp. Four hour infusion of 10% Intralipid ™ /heparin significantly increased arterial plasma free fatty acids to 3.9 ± 0.6 mM ($P<0.001$) in Lip + Ins treated animals and to 5.3 ± 0.6 mM in Lip treated animals ($P<0.001$) compared to animals receiving no lipid infusion (0.3 ± 0.1 mM). There was no significant difference between the free fatty acid levels in the two groups receiving Intralipid ™ /heparin.

Hind leg glucose uptake values for Ins, Lip + Ins, and Lip groups are shown in Fig. 4. Infusion of Intralipid ™ /heparin alone (Lip) for 6h did not affect HGU and the value determined at the end of the experiment was similar to saline (basal) values previously reported at the end of 2h (305). However, the combination of Intralipid ™ /heparin for 4h prior to, and during the 2h clamp significantly reduced the stimulatory effect of Ins from a net of 0.45± to 0.25 $\mu mol.min^{-1}$; an inhibition of 44%.

6.3.3 [^{3}H] 2-DG uptake

[^{3}H]2-DG was administered for the final 45 min of each experiment. Figure 5A shows uptake values for soleus, plantaris, EDL, G.Red and white, as well as tibialis

muscles removed at the completion of the experiment Values for soleus and plantaris muscles were 7.9 ± 0.7 and 4.9± 0.5μg.min^{-1}.g^{-1}, respectively, following infusion of Intralipid ™ /heparin alone (Lip) for 6h. Ins infusion alone (Ins) increased the values for R'g in soleus (3.2 fold), plantaris (2.4 fold), EDL (2 fold) and G.Red (2.4 fold) when compared to Lip treated animals (Fig. 5). Notwithstanding the presence of the lipid in the control situation which may have influenced the rate of basal 2-DG uptake, the magnitude of stimulation by Ins at 3mU.min^{-1}.kg^{-1} was less than previously reported for the higher dose of 10mU.min^{-1}.kg^{-1} of 6.5 fold for soleus and 7.8 fold for plantaris muscles (305). Intralipid ™ /heparin (Lip + Ins) infusion markedly inhibited the stimulatory effect of Ins in three of the six muscles (soleus, plantaris and G.Red). In addition, Figure 5B shows that Lip + Ins significantly inhibited R'g for the combined muscles (aggregated on proportional weight) from a net stimulatory effect by Ins of 6.4 to 2.0 μg.min^{-1}.g^{-1}. This represents an inhibition of 69%.

6.3.4 1-MX metabolism

No significant difference was found between the experimental groups in arterial plasma concentrations of 1-MX (Fig. 6A) or oxypurinol (3.5± 0.5 μM, Ins; 4.0 ± 1.2 μM, Ins + Lip; 4.0 ± 0.7 μM; Lip), the metabolite of allopurinol and inhibitor of xanthine oxidase.

Ins infusion alone (Ins) significantly increased hind leg 1-MX metabolism relative to Lip group (P<0.01) (Fig. 6C). However, the increase in 1-MX metabolism with Ins was inhibited with Intralipid ™ /heparin infusion (P<0.05).

When individual data for hind leg glucose uptake were plotted against corresponding values for 1-MX disappearance and analyzed by linear regression a positive correlation was noted (Fig. 7A; r = 0.6, P = 0.014). There was no correlation between hind leg glucose uptake and FBF (Fig. 7C), nor between FBF and 1-MX metabolism (Fig. 7B).

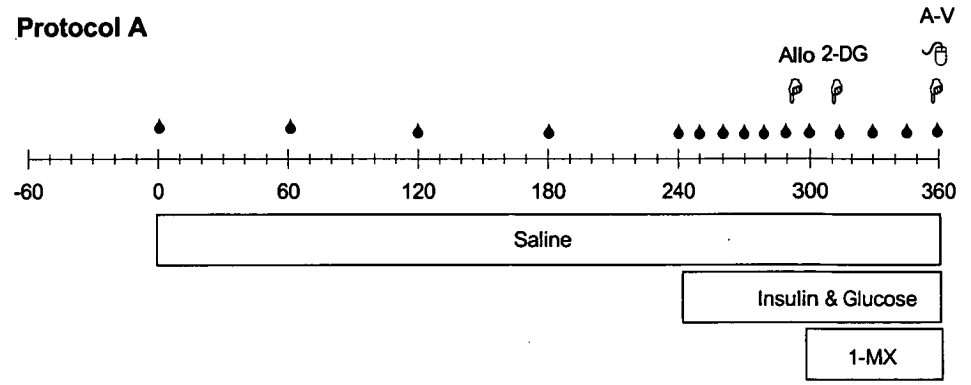
Protocol A
A-V
Allo 2-DG
-60
0
60
120
180
240
300
360
Saline
Insulin & Glucose
1-MX

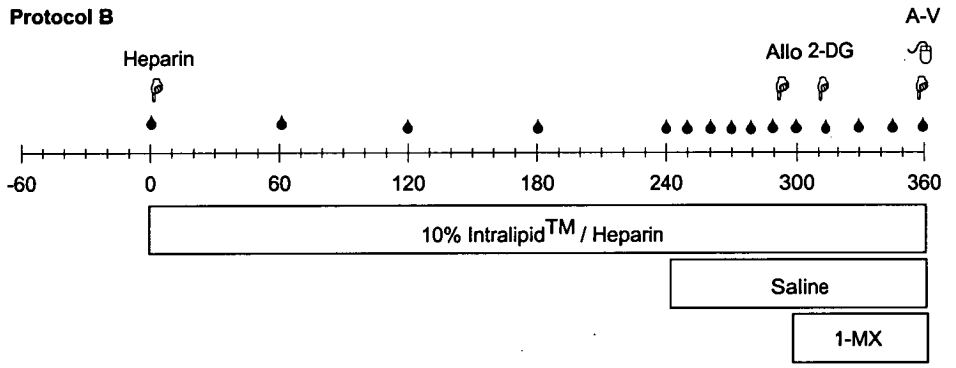
Protocol B
A-V
Heparin
Allo 2-DG
-60
0
60
120
180
240
300
360
10% Intralipid™ / Heparin
Saline
1-MX

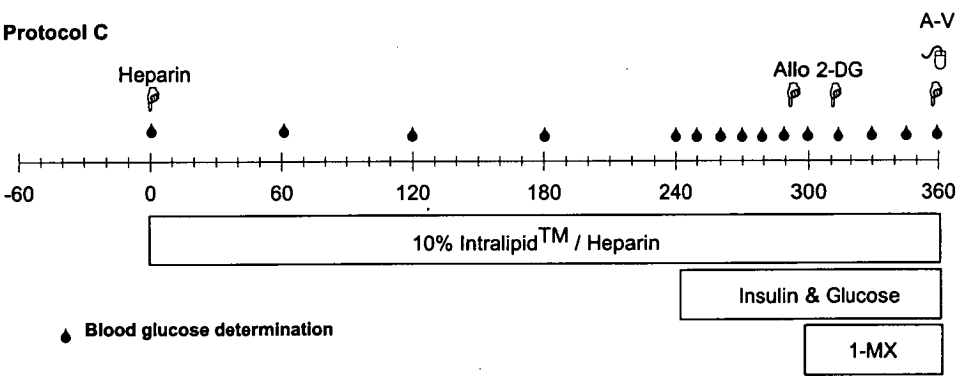
Protocol C
A-V
Heparin
Allo 2-DG
-60
0
60
120
180
240
300
360
10% Intralipid™ / Heparin
Insulin & Glucose
1-MX
Blood glucose determination

Figure 1. Study design. In two (protocols A and C) the euglycemic-hyperinsulinaemic ($3mu.min^{-1}.kg^{-1}$) clamp was commenced 4h after the start of saline (protocol A, Ins) or Intralipid ™/ heparin (protocol C, Lip + Ins) infusion. During protocol B (Lip) saline replaced Ins at 4h. Duplicate arterial and femoral venous plasma samples were collected at 360 min, as indicated by , for HPLC analysis and plasma glucose determinations. Heparin, allopurinol and [^{3}H]2-DG were injected as indicated by at 0, 295 and 315 min, respectively. Arterial samples were also taken for monitoring plasma [^{3}H]2-DG radioactivity at 5, 10, 15, 30 and 45 after injection (not shown). Arterial samples for glucose determinations are indicated by . Venous infusions are indicated by the bars.

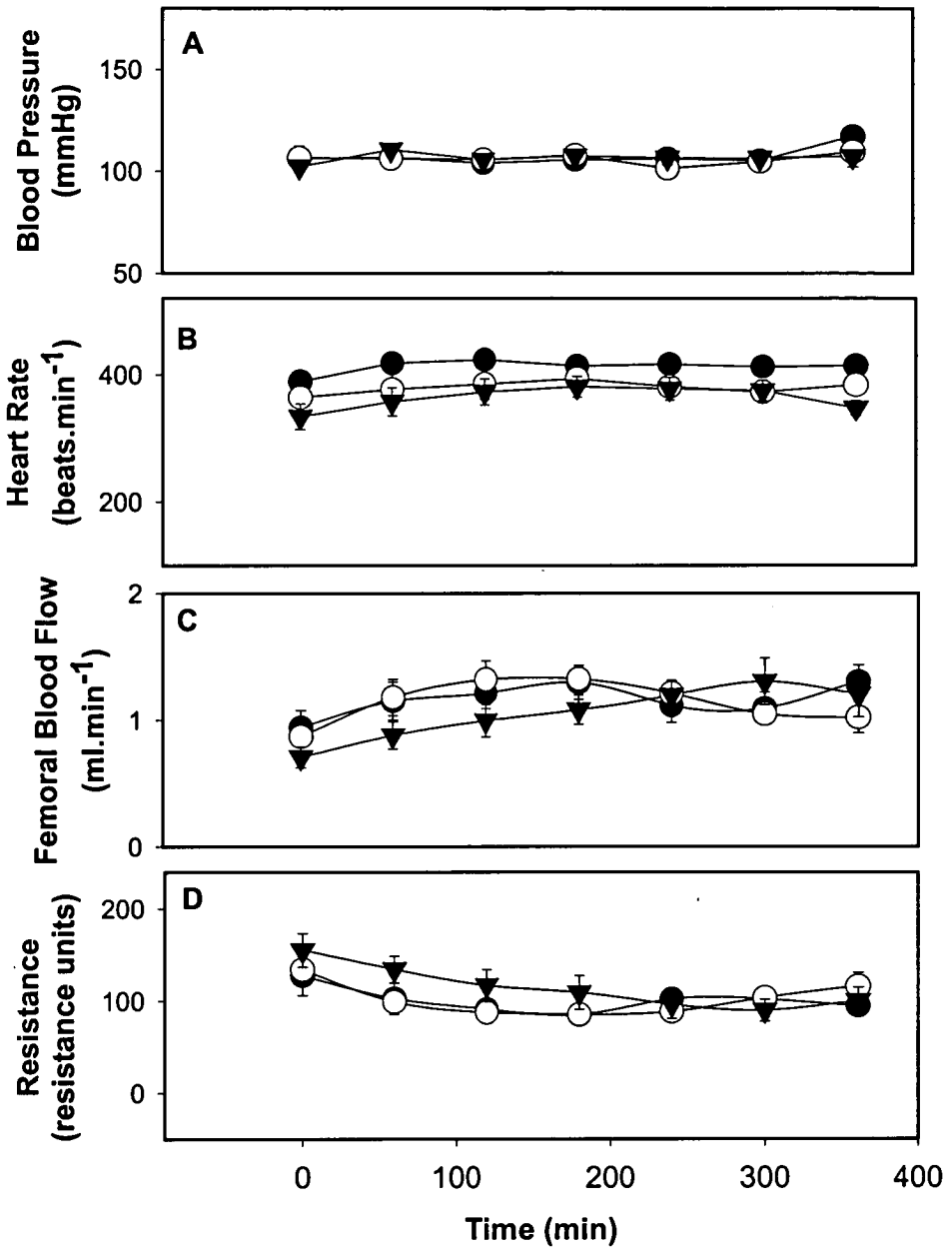

Figure. 2. Mean arterial blood pressure, heart rate, femoral blood flow, and hind leg vascular resistance throughout the experiments. Data were collected from 5-s subsamples as indicated in the text. Mean values are shown at each hour. Symbols: ●, Ins; ○, Lip + Ins; ▼, Lip.

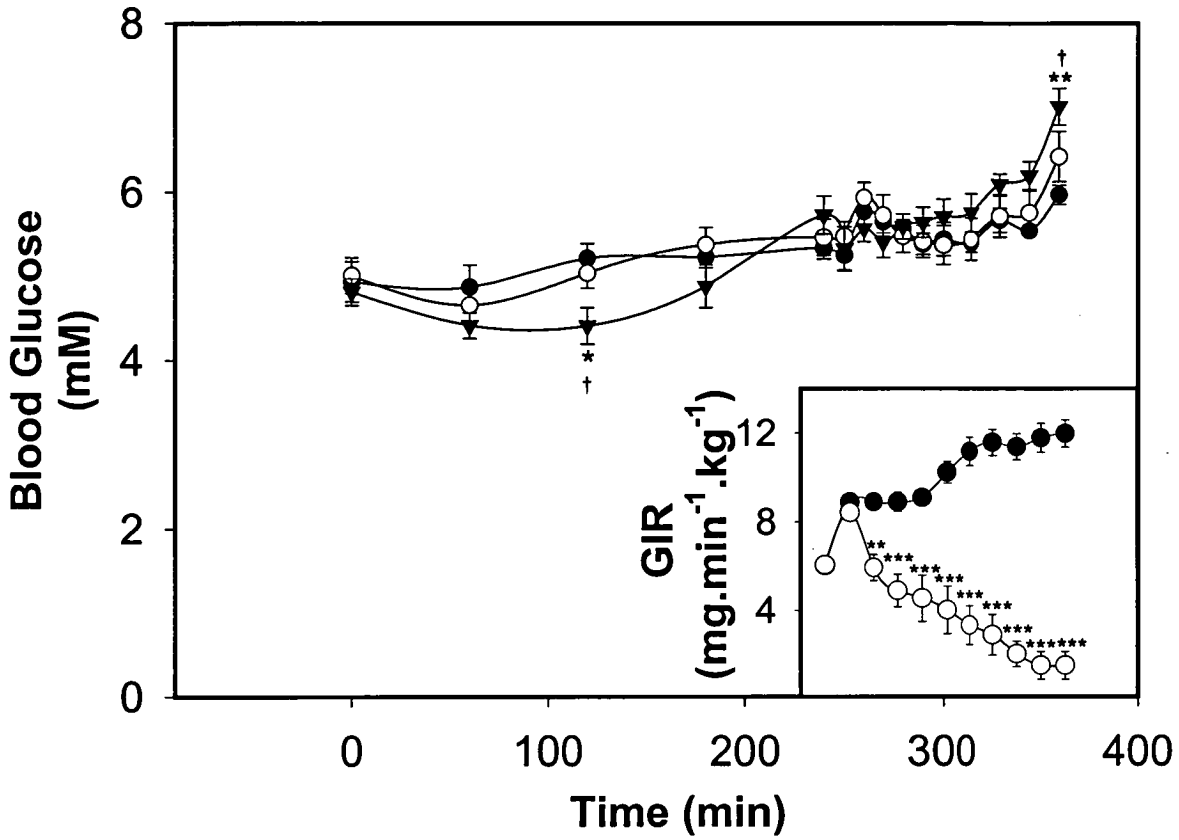

Figure 3. Arterial blood glucose and glucose infusion rate (GIR) for Ins (●), Lip + Ins (○) and Lip (▼). Values are means ± SE. Significant differences from Ins are indicated by *,P <0.05 ;**, $P \leq 0.01$; ***, $P \leq 0.001$ and from Lip + Ins by †, P<0.05.

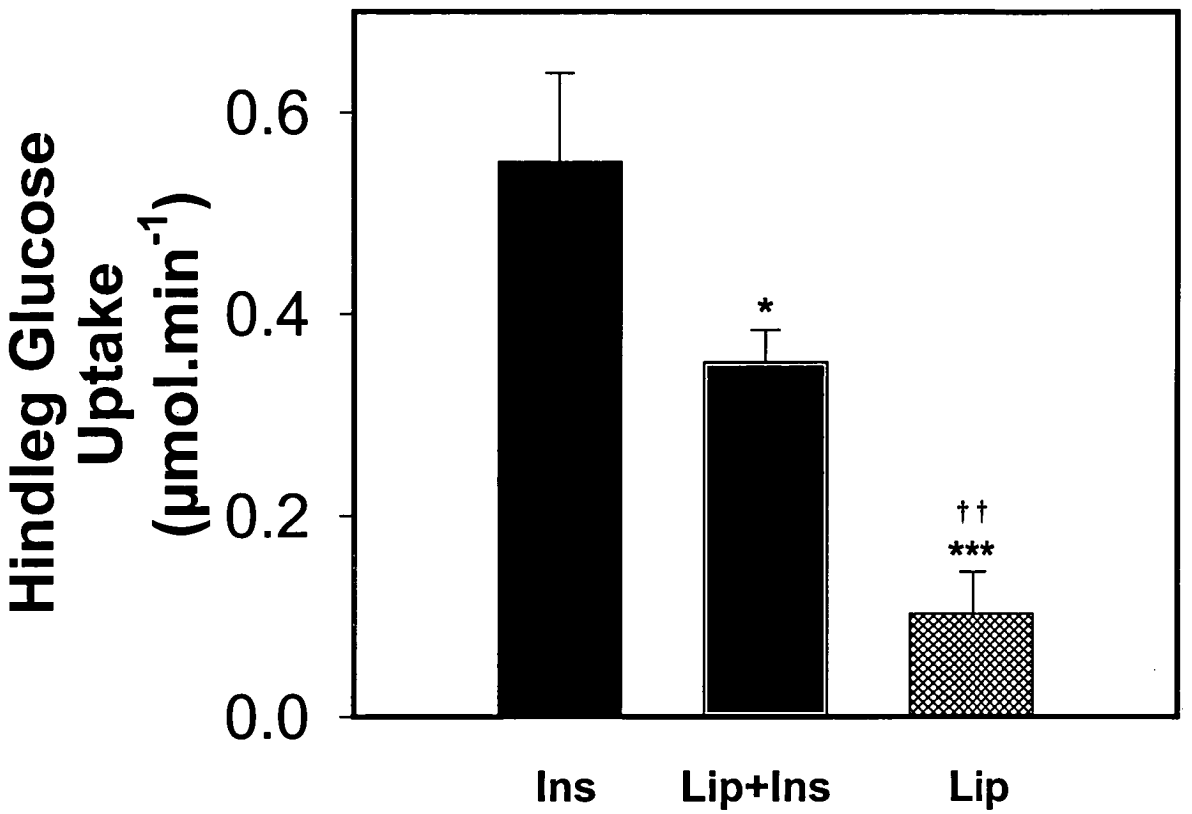

Figure. 4. Hind leg glucose uptake for Ins, Lip + Ins, and Lip . Values are means ± SE. Significant differences from Ins are indicated by *,P <0.05; ***, $P \leq 0.001$ and from Lip + Ins by ††, $P \leq 0.01$.

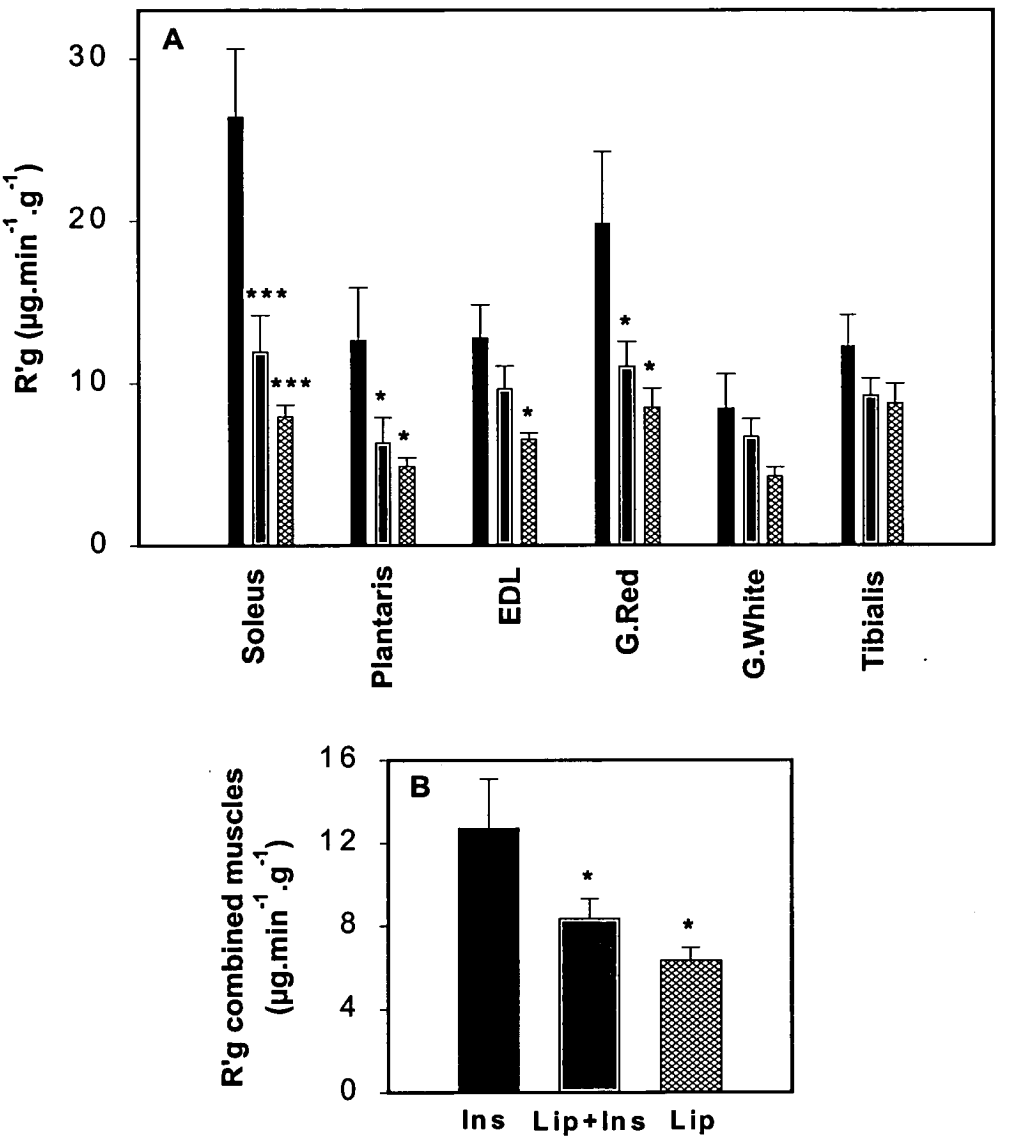

Figure. 5. [^{3}H]2-DG uptake values for individual muscles (A) and for the combination of the six muscles adjusted for differences in weight (B). Conditions were Ins, Lip + Ins, and Lip. Values are means ± SE. Significant differences from Ins are indicated by *,P <0.05; and ***, $P \leq 0.001$.

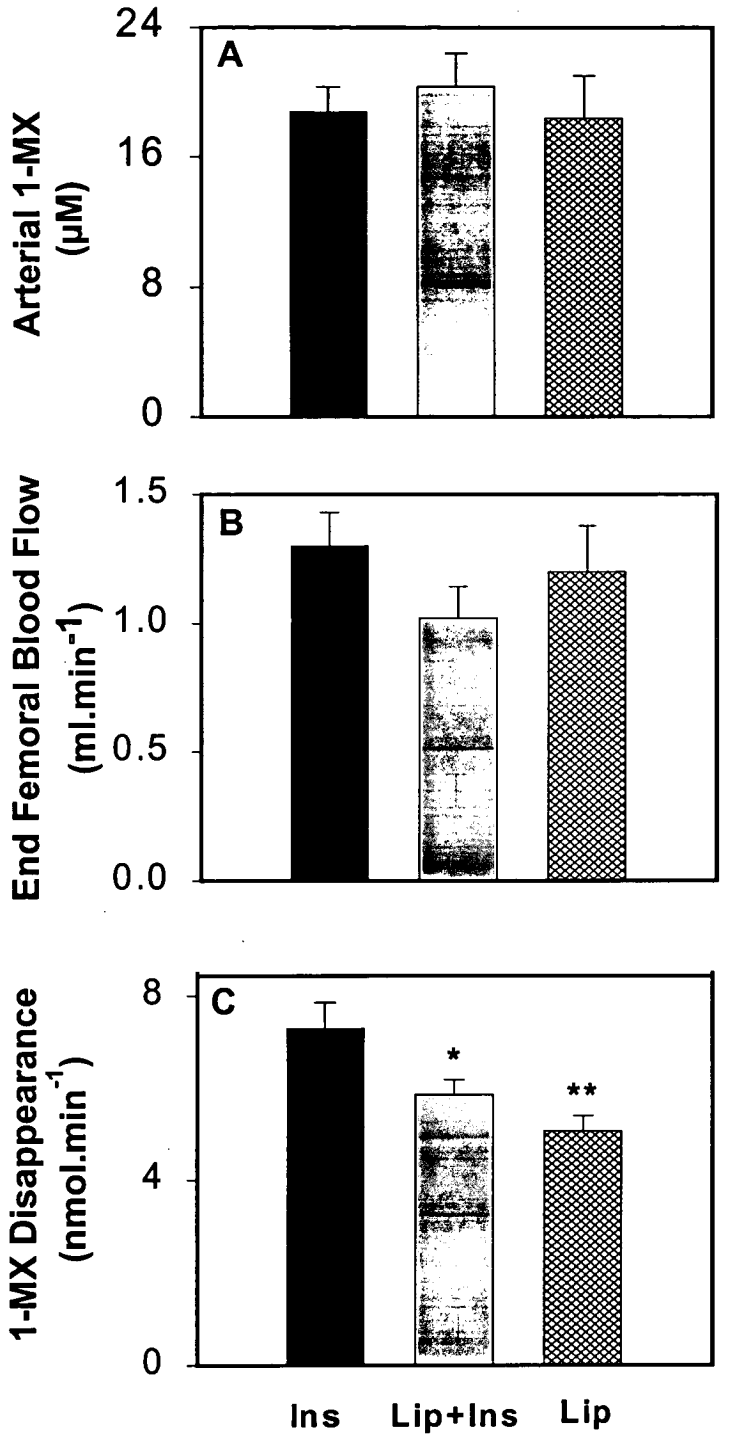

Figure. 6. Arterial 1-MX (A), end arterial femoral blood flow (B) and hind leg 1-MX disappearance (C) values of Ins, Lip + Ins, and Lip groups. Values are means ± SE. Significant differences from Ins are indicated by *, $P < 0.05$; and **, $P \leq 0.01$.

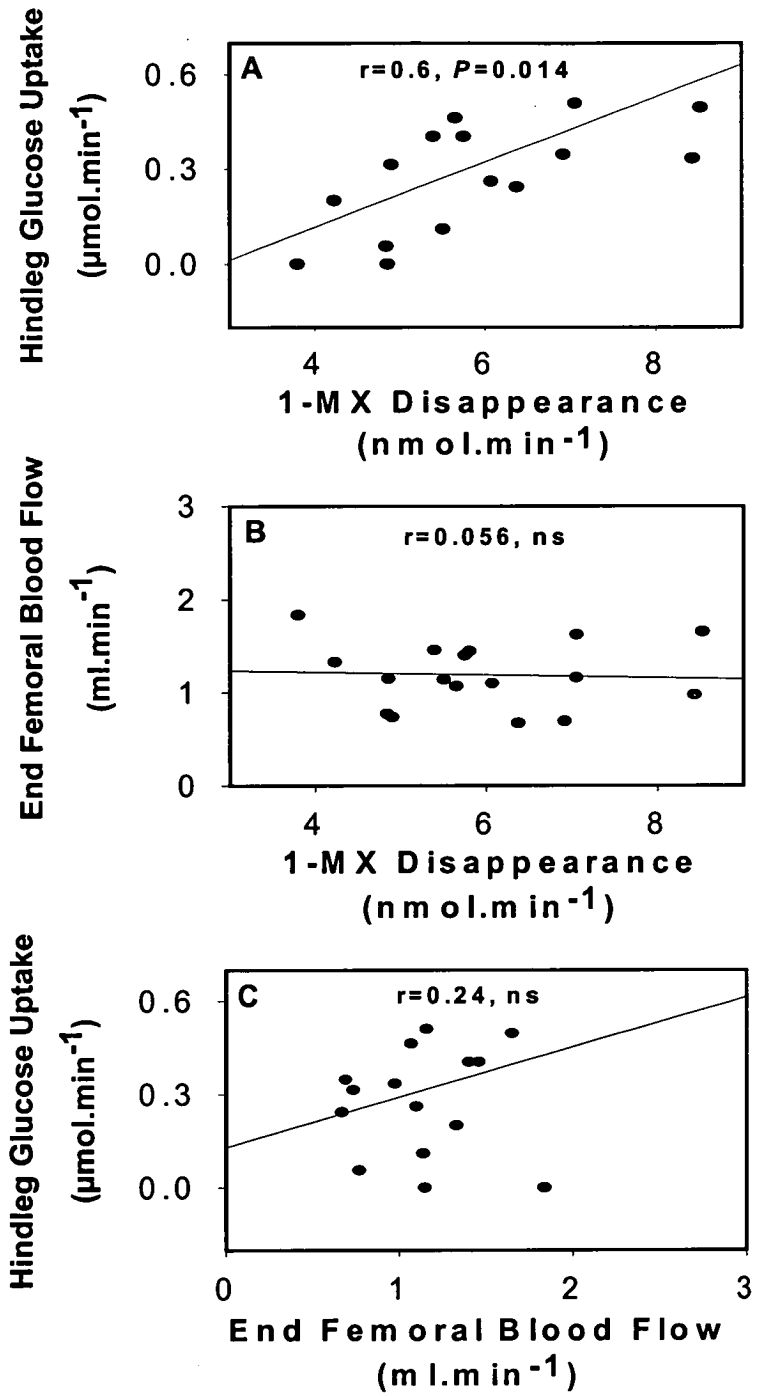

Figure 7. Relationships between hind leg glucose uptake and 1-MX disappearance (A), End femoral arterial blood flow and 1-MX disappearance (B) and hind leg glucose uptake and end femoral arterial blood flow (C). Individual values for n = 15 rats are shown.

6.4 Discussion

The main finding emerging from this study was that Intralipid ™/heparin caused a marked decrease in insulin-mediated capillary recruitment in muscle. This was evident as an inhibition of 65% of the insulin-mediated metabolism of infused 1-MX and occurred in conjunction with insulin resistance at the whole body level characterized by diminished GIR and an equally marked reduction in insulin-mediated metabolic changes in the hind leg. These included an inhibition of 45% of the insulin-mediated glucose uptake by the hind leg, and an inhibition of 69% of the insulin-mediated uptake of 2-DG by muscles of the lower leg. The reductions in insulin-mediated changes occurred at physiologic insulin levels (287) and a total exposure to Intralipid ™/heparin for 6h that included 2h during the hyperinsulinaemic euglycemic clamp. This impairment of insulin-mediated capillary recruitment by Intralipid/heparin is the second haemodynamic defect of insulin to be reported as impaired bulk leg blood flow in humans (261) treated with Intralipid ™/heparin has been described.

A second finding to emerge from this study was the positive correlation between hind leg glucose uptake and 1-MX metabolism (Fig. 7A). This contrasted with hind leg glucose uptake and femoral arterial blood flow, where there was no significant correlation. The absence of a correlation between leg glucose uptake and FBF resulted from the absence of a difference for FBF between any of the three treatment protocols, Ins, Lip or Lip + Ins. This was despite individual animal differences for hind leg glucose uptake and 1-MX metabolism.

The present study represents yet another where we have documented a close relationship between glucose uptake and capillary recruitment under hyperinsulinaemic euglycemic clamp conditions. Previously this has been described for α-methyl 5-HT (210). Other studies with TNFα (305), and exercise-trained rats (213) also show parallel adjustments between insulin-mediated hind leg glucose uptake and capillary recruitment. A recurring correlation between insulin-mediated glucose uptake and insulin-mediated capillary recruitment, implies but does not necessarily prove causality. In one of the prior studies, we reported a marked inhibition of insulin-mediated glucose

uptake when insulin-mediated capillary recruitment was blocked pharmacologically by a peripherally acting serotonergic agonist, α-methyl 5-HT (210). This intervention was based on experiments using the isolated pump-perfused rat hind leg where the vasoconstrictors, α-methyl 5-HT or 5-HT were found to redirect flow from nutritive to the non-nutritive route (179). Indirect evidence that serotonergic agonist-mediated insulin resistance did not result from a direct effect on muscle glucose uptake and metabolism was obtained using isolated incubated muscle preparations (211) where the vascular distribution of insulin and glucose is not involved. In that preparation, 5-HT had no effect on insulin-mediated glucose uptake (211). Thus, it would appear likely that insulin-mediated glucose uptake becomes partly inhibited by denying access for insulin and glucose to regions of the muscles of the perfused hind leg or the hind leg *in vivo*. Similarly, an increase in nutritive blood flow whether mediated in perfused muscle by vasoconstrictors (48), or *in vivo* by insulin (209), leads to increased muscle glucose uptake. However, even if insulin-mediated capillary recruitment contributes in part to the increase in muscle glucose uptake by this hormone *in vivo* by acting to enhance access for itself and glucose, no information emerges from the present or previous studies (209) (210) (305) as to mechanism. Given that an increase in bulk blood flow is not involved, increased capillary (nutritive) flow must then result from a redistribution of flow from the non-nutritive route. That being so, a net vasodilatation of sites controlling entry of blood to the nutritive route mediated by insulin is likely. We know that insulin-mediated capillary recruitment is NO-dependent (289) and there are a number of possible mechanisms to account for the effect. Firstly, insulin may act at insulin receptors on endothelial cells to produce NO, which in turn permeates adjacent vascular smooth muscle cells to lower the vascular tone of pre-capillary sphincters. In favor of this mechanism is that this process is NO-dependent and is thus consistent with our preliminary data (289), that eNOS knock-out mice are insulin resistant (66) and there are data that TNFα interrupts insulin signaling to eNOS in this cell type (139); against, is the fact that to do so insulin must access the sites that it is going to dilate. This requires that some flow is occurring before insulin arrives at these sites. Also against this possibility is the preliminary report that vascular endothelial insulin receptor knock-out mice are not insulin resistant (286). Secondly, insulin may act at insulin

receptors on the vascular smooth muscle cells (131) to cause vasorelaxation. This mechanism would also be NO-dependent (289), but free of endothelial cell involvement in signaling. However, accessing is also a key issue as it is for a direct endothelial effect. The mechanism has some attraction as TNFα is known to inhibit insulin signaling in vascular smooth muscle cells, although to date this has been restricted to the ERK1/2 activation step (85). Thirdly, insulin may act at insulin receptors on SM to activate glucose transport and metabolism to produce a metabolite (e.g. adenosine) that permeates adjacent tissue to react with appropriate receptors on endothelial and/or vascular smooth muscle cells to result in vasorelaxation. Such a mechanism would resemble that occurring in exercise where vasodilatory metabolite(s) are released by working muscle to facilitate local blood flow. This mechanism would not necessarily be NO-dependent, but would be inhibited by agents that inhibit muscle glucose metabolism. A variant of this third mechanism is where a form of NOS is activated in SM independently of glucose metabolism. NO could then permeate neighboring tissue as above. The terminal half of this mechanism (82) might be simulated by AMPK activation with AICAR addition. Regardless, all mechanisms will be sensitive to inhibitors of insulin signaling.

From the present study it is clear that elevated plasma free fatty acids resulting from the infusion of Intralipid ™/heparin has led to an inhibition of insulin-mediated capillary recruitment and glucose uptake in muscle. The question now arises as to how this has occurred. Until recently, the focus has been on the metabolic effects of the fatty acids on muscle glucose metabolism. In 1963 Randle *et al.* (206) proposed the notion of competition between glucose and free fatty acids as oxidative fuel sources in muscle (glucose-fatty acid hypothesis). Despite a number of studies (74) (77) (153) examining the effect of fatty acids on SM glucose metabolism, it is still controversial whether insulin resistance in diabetes and obesity result from increased plasma fatty acids. A number of sites in glucose metabolism have been reported to be inhibited by fatty acids and it is generally agreed that raising free fatty acids increases fatty acid oxidation at the expense of carbohydrate oxidation. Sites in glucose metabolism include inhibition of hexokinase by long-chain acyl CoA (275), which by reducing glucose 6-phosphate concentrations could lead to the inhibition of glycogen synthesis and glycolysis.

However, this may not be the explanation as plasma free fatty acid concentrations of approx. 0.75 mM in humans, give rise to an increase in intramuscular glucose 6-phosphate concentrations (26). There have been independent reports that glycolysis (128) and glycogen synthesis (41) are inhibited. Some have found inhibitory effects on glucose uptake (274) (75) but most did not (20) (300) (30) (21). A complication in identifying the precise site(s) is that the effects of fatty acids on insulin-stimulated glucose metabolism are time-dependent (27) (227). Roden *et al.* (227) claim that the key event is glucose transport. Non-invasive NMR of stable isotope-enriched fuels in the muscle of healthy humans showed that the reduction in glycogen synthesis by elevated plasma free fatty acids was preceded by a fall of muscle glucose 6-phosphate concentrations starting at approximately 1.5h (162). However, This could not be explained by changes in the amount of insulin-regulatable glucose transporter protein in either oxidative or glycolytic muscle. In view of this, recent studies have focused on insulin signaling. A particularly valuable approach has been to assess signaling in muscle *in vivo*. With this approach, Griffin *et al.* (97) reported a decrease in IRS-1 associated PI3-Kinase activity, and a blunting in insulin-stimulated IRS-1 phosphorylation. Since this was accompanied by a marked increase in protein kinase C θ activity, Griffin *et al.* (97) propose that activation of PKC θ is responsible for the decrease in insulin signaling, glucose transport and dependent metabolism including glycolysis, glucose oxidation and glycogen metabolism.

If capillary recruitment is a consequence of glucose metabolism and mediated by a generated product, then impairment of glucose metabolism by fatty acids acting via PKC θ would be expected to curtail the component of 1-MX metabolism increased by insulin. However, if we assume insulin signaling mechanisms are similar in most tissues, then impairment of insulin signaling in vascular tissue by any of the mechanisms discussed above could also inhibit insulin-mediated capillary recruitment. On balance, existing data would favor the latter direct mechanism to affect vascular tissue. There is some data that helps this argument. Thus Lind *et al.* (155) have demonstrated impairment in endothelial function by free fatty acids in human forearm in terms of a reduced response to local intra-arterial methacholine relative to nitroprusside. In addition, Steinberg *et al.* (261) have shown that free fatty acid elevation impairs insulin-

mediated vasodilatation and NO production in the legs of insulin-sensitive subjects undergoing euglycemic-hyperinsulinaemic ($40mU.m^{-2}.min^{-1}$) clamps.

In conclusion, elevation of plasma free fatty acid levels for 6h during a hyperinsulinaemic-euglycemic clamp at physiologic insulin, leads to whole body insulin resistance with impaired insulin-mediated muscle glucose uptake and capillary recruitment. We propose that the fatty acids induce an impairment of insulin signaling in vascular tissue. The reduction of insulin-mediated muscle glucose uptake may in part be due to reduced access for insulin and glucose.

CHAPTER 7

7 General discussion

7.1 Summary of thesis results

This thesis primarily investigated the interplay between hormone and substrate to influence muscle fuel uptake, by altering regional muscle blood flow. A key approach involved the uptake of metabolites by perfused rat SM when a high non-nutritive to nutritive ratio was maintained pharmacologically. During hyperinsulinaemia and a high non-nutritive to nutritive ratio, the uptake of palmitic acid, α amino isobutyric acid (AIB) and glucose were reduced. This paralleled reduced oxygen uptake and lactate efflux previously reported by this laboratory (46) (211). The reduced uptake is likely to be a combination of reduced insulin and substrate access to the muscle cells, thus creating an acute state of haemodynamic insulin resistance. Chronic effects of non-nutritive flow may therefore contribute to the elevation of these fuels in the plasma. Moreover, the reduction in uptake of fuels by myocytes (if maintained for extended periods) may alter muscle oxidative capacity and long-term insulin sensitivity. In contrast, the hydrolysis of chylomicron-TG was increased with predominantly non-nutritive flow. This was attributed to an increased exposure of the chylomicrons to lipolytic enzymes (probably LPL) located in non-nutritive vessels adjacent to CT adipocytes. Continual nourishment of non-nutritive adipocytes may lead to fat accretion between the muscle fibres. A further effect studied concerned the influence of FFA on glucose uptake by muscle, and on muscle's action to augment this process by increasing access for itself and glucose *in vivo*. Thus, the latter part of this thesis showed elevated FFA to attenuate the vasodilatory action of insulin on capillary recruitment. Elevated FFA may therefore augment non-nutritive flow and the associated adverse metabolic effects. This inability of insulin in the presence of fatty acids to shift flow from the non-nutritive vessels may be an innate protective mechanism by the muscle to prevent excess

FFA uptake into the myocytes. FFA may therefore indirectly modulate capillary flow, thus exerting some control over fuel partitioning in SM.

7.2 Implications of this work

Combined results from chapters 3 and 5 showed that the infusion of 5-HT with insulin reduced muscle uptake of glucose, fatty acids and amino acids. As this was common to all fuels tested (with the exception of chylomicron TG), it appears that this drug causes a defect in bulk clearance, which is most likely due to changes in muscle blood flow distribution and capillary recruitment. The high proportion of non-nutritive/nutritive flow stimulated by 5-HT may adversely affect fuel partitioning within the muscle. It is likely in a healthy human there is considerable oscillation between blood flow in the nutritive and non-nutritive networks. For example, during rest, flow is likely to predominantly partition into the non-nutritive network in parallel with a reduced metabolic requirement. However during periods of exercise, flow to the nutritive capillaries increases. Low physical activity and fat rich diets may impinge sufficiently to create a state where the magnitude of these oscillations is reduced and flow predominantly occupies the non-nutritive vessels. This will result in less uptake and release of metabolites from the muscle and may produce adverse metabolic effects, including acute haemodynamic insulin resistance, and in the longer term phenotypic characteristics of chronic insulin resistance.

Chronic insulin resistance is associated with reduced oxidative capacity of muscle, which may be a reflection of chronic non-nutritive flow (as above). Obese and diabetic muscle have been shown by others to have reduced oxidative enzyme activity (succinate dehydrogenase) and increased glycolytic capacity (α-glycerol-phosphate dehydrogenase) despite no significant difference in muscle fibre type (110). Such results suggest that the impairment in oxidative metabolism chronologically precedes the change of fibre type (which has previously been suggested as the cause of insulin resistance. Hernandez *et al.* (112) showed that in SM biopsies of hypertensive men there was a significant decrease in beta-hydroxy-acyl-CoA dehydrogenase, citrate synthase and hexokinase, but no change in muscle TG or FFA, suggesting reduced oxidation and

reduced FFA uptake. Reduced oxidative enzymes in SM has also been positively correlated with insulin resistance (22). In some animal models the relationship is less clear. For example, Pujol *et al.* (204) reported increased activity of citrate synthase and beta-hydroxy-acyl-CoA dehydrogenase in SM of obese Zucker rats, while Ide *et al.*, (121) showed that the SM of obese Zucker rats had reduced ability to oxidize palmitic acid.

Chapter 4 of this thesis reported that increased non-nutritive or CT flow at the expense of muscle capillary (or nutritive) flow using the model vasoconstrictor 5-HT (5-HT), increases chylomicron TG hydrolysis in muscles with predominantly slow-oxidative fibres. Therefore vessels diverting flow away from muscle capillaries with 5-HT (and reducing oxygen uptake) are probably accessing a highly active perimysial adipose tissue (PAT). Since the perimysium is the major site of intramuscular fat accretion in red muscles (182) the vessels running through the perimysium are likely to be those of the non-nutritive network. Therefore SM blood flow has the potential to deliver unesterified fatty acids to the muscle for oxidation, or to the adjacent CT for storage. As shown by Rattigan *et al.* (209), when non-nutritive flow predominates to create an acute state of insulin resistance, there is a breakdown of control over this partitioning whereby insulin is unable to recruit muscle capillary flow. Therefore it would be expected that excess glucose and lipid would be delivered to the muscle CT. The presence of insulin in this circuit would stimulate glucose uptake into PAT and provide the glycerol-3-phosphate backbone needed for subsequent TG synthesis. By this mechanism, insulin should further stimulate fatty acid uptake and storage into non-nutritive adipocytes of red muscles. Altering the access of lipoprotein-TG to LPL enables fuel partitioning between the SM fibres and the adipocytes interlaced between them. Healthy muscle may contain small amounts of PAT between the muscle fibre bundles. With insulin resistance however, continual deposition may force the fibres apart, or fat cells may enlarge in conjunction with fibre atrophy as a consequence of reduced muscular activity. PAT probably evolved as a storage depot for excess TG adjacent to the myocytes. Adipocyte accretion within SM is therefore more likely to be the result rather than the cause of insulin resistance. Whether these cells contribute to insulin resistance once it has been established remains to be determined. The release of

factors such as TNF α, leptin and adipocyte related protein (ACRP) from PAT may contribute to the general systemic (paracrine?) signals that affect metabolism and insulin sensitivity in SM.

Excess TNFα secretion clearly has adverse effects on insulin action (305). It is primarily secreted by adipocytes to regulate size of fat cells (reviewed in (205)), but has recently also been shown to be produced by SM (183). A number of reports have shown that TNFα release is increased with insulin resistance (191) (183). Excessive PAT may contribute to this increased TNFα production with insulin resistance. Reports on the action of TNFα to inhibit IMGU by SM however have been conflicting. While Del Aguila *et al.* (60) reported that TNFα decreases IMGU by muscle cells in culture, Storz *et al.* (266) showed no decrease in IMGU by cultured differentiated muscle cells despite significant reductions in early events in the insulin-signaling cascade (i.e. reduced tyrosine phosphorylation of IR and IRS1 and PI3-Kinase). However, in these experiments it is possible that the activity of GLUT1 had increased to compensate for the reduced GLUT4 activity. Nolte *et al.* (184) however saw no decrease in the phosphorylation of the insulin receptor, IRS-1 and the association of PI3-Kinase (thus no decrease in IMGU) in isolated SM acutely pretreated with very high levels of TNFα for extended periods (e.g. up to 8 hrs) before insulin stimulation. However, TNFα may exclusively interrupt insulin-signaling to produce NO in endothelial cells *in vivo* (139), in which case, effects of TNFα in *in vitro* preparations may not be expected.

Leptin is another paracrine signaling molecule secreted from fat cells which has been shown to have beneficial effects on SM fatty acid uptake and metabolism (259) in addition to its well documented action on the central nervous system (reviewed in (216)). Leptin receptors are situated in SM, and leptin promotes lipolysis and lipid metabolism, thus decreasing SM TG (151). Yaspelkis III *et al.* (302) showed that leptin administration to rats fed a high fat diet ameliorated the decrease in IMGU by SM, by increasing GLUT4 translocation to the plasma membrane. Excessive release of leptin in humans (87), from large fat deposits (possibly including PAT) can cause leptin resistance contributing to both decreased FFA oxidation by muscle (259) and increased appetite (reviewed in (216)).

Recently another signaling molecule released exclusively from adipocytes, adipocyte related protein (ACRP or AdipQ), was discovered. Fruebis *et al.* (81) produced a recombinant form of ACRP that was found to increase both SM fatty acid uptake and oxidation. It also decreased plasma glucose by an unknown mechanism. The release of ACRP has been shown to be reduced in obesity (117). Excess PAT may contribute to this phenomenon, resulting in decreased FFA uptake.

Chapter 6 of this thesis showed that the infusion of Intralipid^{TM} and heparin during a euglycaemic/hyperinsulinaemic clamp in rats prevented insulin-mediated capillary recruitment. It will be of considerable interest to determine if the signal for insulin-induced capillary recruitment originates from the muscle, endothelial cell, or smooth muscle, and where FFA interfere with this signal. Some evidence comes from experiments by Baron and coworkers involving FFA-impaired endothelial dependent vasodilatation (as measured by total leg blood flow (262)). NO production was attenuated (261), but no evidence could be found for NOS inactivation within isolated aorta (251). If endothelial cells lining SM blood vessels react in a similar manner to isolated aorta, then it is of interest to determine how FFA act to indirectly inhibit eNOS. One possibility is that elevated FFA induce a signaling molecule that interferes with eNOS. Alternatively, FFA may inhibit the release of a molecule that normally acts on the endothelium for NO production, which is released directly or indirectly from SM glucose metabolism. Alternatively, FFA may inhibit insulin signaling in the myocytes, endothelium or both. As discussed in chapter 6, FFA have been shown by others to inhibit events earlier in the insulin signaling cascade such as at PKC theta (97) or phosphorylation of the insulin receptor, IRS-1 and PKB/Akt (266).

There seems little doubt that FFA therefore interfere with endothelial dependent vasodilatation (262) (261). Whether FFA interfere with capillary recruitment during exercise by the same mechanism is unknown, and unlikely. Insulin-mediated capillary recruitment is generally thought to be endothelial NO dependent (289), however with exercise-induced dilation this remains contentious. In exercise, NO may be released by the muscle, as discussed earlier. Acute exercise increases NOS (e and nNOS) in SM

myocytes (225). Regardless, elevated FFA do not attenuate exercise increases in blood flow (187) as they do with insulin (261).

7.3 Future considerations

Reduced nutritive capillary flow with insulin resistance will reduce oxygen, insulin glucose, amino acid and lipid availability to the muscle fibres and contribute to a decline in metabolic capacity. This thesis underscores the importance of regional muscle blood flow in fuel partitioning and insulin sensitivity, which can be manipulated through diet, exercise or possible pharmacological agents.

Determining the cellular mechanism for capillary recruitment will help to develop drugs to increase muscle metabolism and insulin sensitivity. Insulin is initially detected by the extracellular domain of the insulin receptor that is located on both the endothelial plasmamembrane and the sarcolemma. This causes a conformational change that stimulates autophosphorylation of certain residues on the intracellular domain of the insulin receptor, then attracting and causing phosphorylation of the downstream IRS1. This allows association of IRS1 with PI3-Kinase to activate PKB/Akt. PKB/Akt is now thought to be involved with both GLUT4 translocation (reviewed in (114) (133)) and NOS activation (62) through divergent pathways. In SM this would provide a direct coupling of metabolism to dilation. If we are able to determine where FFA interfere with this signal we may be able to initiate mechanisms to prevent it. Moreover, the administration of drugs that enhance signalling effects at an early point in insulin signaling (i.e. before PKB/Akt) are likely to be beneficial. Alternatively, substances that increased SM glucose metabolism may also enhance capillary recruitment, particularly if the dilatory signal emanates from skeletal muscle.

Controlling dietary intake may be beneficial in the prevention and treatment of insulin resistance. In addition to their protective effects against muscle insulin resistance (263), n-3 polyunsaturated fats have been shown to have beneficial affects on blood flow (23). In addition, cod protein extracts have recently been shown to enhance IMGU in cultured muscle cells and isolated muscles (152). This effect could be simulated by

the addition of the same mixture of amino acids (152). A mixed cocktail of amino acids has also been shown to have positive effects on muscle blood flow (159).

The most beneficial treatment for NIDDM is exercise. Exercise has been shown to have positive effects on IMGU by muscles, and reductions in TG in fat depots. Exercise also has positive effects on eNOS (225). Unlike visceral fat, PAT has been shown to be very resistant to stimuli such as exercise. For example, regular walking does not reduce the amount of fat infiltrating SM (255). For many people however drugs targeted at enhancing capillary recruitment will need to be administered during periods of low activity because the same individuals who are insulin resistant are also almost always obese, and either unable to exercise or non-compliant.

One potential substance that may be beneficial in improving nutritive flow is tetrahydrobiopterin (BH4). BH4 is a cofactor for NOS dimerization and is synthesised from guanosine triphosphate (reviewed in (173)). Intravenous administration of BH4 significantly increased myocardial blood flow, as assessed by positron emission tomography in healthy volunteers (294). Recently BH4 has also been shown to improve arginine uptake into rat cardiomyocytes, probably through upregulation of arginine transporters (247). It has also been shown that BH4 is released from endothelial cells, and it is likely to diffuse to underlying smooth muscle as a cofactor for NOS in this tissue (reviewed in (243)). Importantly, BH4 incubation improved endothelial dependent vasodilator in aortic strips of fructose fed rats, suggesting a deficiency in these rats (252). Moreover, administration of a pteridine derivative (6-methyl-5,6,7,8 tetrahydrobiopterin) abolished endothelial dysfunction in aortic rings of streptozotocin diabetic rats (198).

Vitamin C treatment of cultured human umbilical vein endothelial cells increased the activity of eNOS without increasing the expression of this enzyme. The increased activity was thought to be due to augmented levels of BH4 (8). This effect was also seen with the administration of the BH4 precursor sepiapterin but not another scavenger of superoxide anions, Mn (III) tetra kis (4-benzoic acid) porphyrin chloride (8), and it was concluded that vitamin C increased the delivery of BH4 to eNOS independently of its antioxidant effect. Another beneficial effect of vitamin C is the antioxidant property of scavenging free radicals, which drastically reduce the half-life of

NO (271). Vitamin C improved endothelial dysfunction in the forearm of type II diabetics (276).

Oxidative stress is associated with a reduction in PKB/Akt and GLUT4. This effect can be prevented by the administration of lipoic acid, which induces marked dilator responses with insulin in diabetic aorta. Lipoic acid also stimulates PKB/Akt and glucose transport in 3T3-L1 adipocytes by reducing oxidative stress (235), and stimulates PI3-Kinase and PKB/Akt and glucose uptake in L6 myotubes (143).

Statins (HMGCoA reductase inhibitors) also have the ability to increase eNOS independently of their effect to lower cholesterol. Two week administration of mevastatin increased coronary blood flow by 30% (reviewed in (3)).

S-acyl cysteine sulfoxide (SACS) isolated from garlic was shown to be beneficial in alloxan diabetic rats (7). Inducible NOS (iNOS) is upregulated as an inflammatory response by TNFα but is shown to be down-regulated by SACS, while SACS activated eNOS and suppressed hydroxyl radical production (141). Another substance isolated from garlic, Alliosan, has also been shown to be beneficial in augmenting the skin microcirculation of healthy volunteers (as assessed by Laser-Doppler fluxometry) (299).

The effects of these substances on capillary recruitment (and dissociation of total flow effects) may be assessed using currently established methods in our laboratory or the laboratory of our collaborators in the USA. The metabolism of the capillary endothelial enzyme, xanthine oxidase, can be assessed by the metabolism of 1-MX as used in this thesis. Alternatively, contrast enhanced ultrasound could be employed, where circulating albumin microbubbles depict areas of capillary blood flow.

While increased FFA may produce some reduction in total flow, it is likely that capillary recruitment is also affected. Insulin effects on capillary recruitment *in vivo* occur after 30 minutes of infusion (287). If insulin was acting directly on the endothelial cell, myocyte or vascular smooth muscle to produce vasodilatation then we may expect recruitment earlier on. Ultimately this can be tested by infusion of a substance that interfere with the translocation of GLUT4. By disrupting a signal further downstream in the cascade from PKB/Akt (which has effects on NOS), the effects may be separated, as

vasodilatation may remain, but metabolism may not. If neither occurs, then it is likely that the metabolism caused the vasodilatation. Recently it has been shown that the protease inhibitors (indinavir, ritonavir and amprenavir) significantly reduce IMGU by directly inactivating GLUT4 (171). Indinavir inhibited insulin-mediated GLUT4 transport to the plasmamembrane and glucose uptake of incubated rat muscles, however did not decrease insulin stimulation of PI3-Kinase activity or PKB/Akt phosphorylation (185). However, Caron *et al.* (39) incubated differentiated 3T3-F442A cells with Indinavir and found reduced insulin binding to the insulin receptor, and reduced MAP Kinase activity, but no reduction in IRS-1 phosphorylation. The effect of these substances however needs to be determined on capillary recruitment *in vivo.*

7.4 Summary of conclusions

In vivo, the elevated FFA associated with insulin resistance will prevent capillary recruitment with insulin, probably by interfering with endothelial cell insulin signaling. Flow will therefore favorably partition into the non-nutritive (likely to be perimysial) vessels and affect the uptake of blood-borne nutrients. Due to the denial of insulin and glucose to the myocytes, non-nutritive flow will induce a state of muscle insulin-resistance for glucose. The uptake of fatty acids and amino acids will be similarly affected. Hydrolytic activity for circulating chylomicron TG, however, could be expected to be more active in the non-nutritive vessels of the red muscles, thereby elevating FFA levels. Moreover, the elevated FFA (from increased TG hydrolysis, and decreased muscle uptake) will magnify the high non-nutritive to nutritive muscle blood flow. FFA may thus be indirect mediators for non-nutritive flow, a mechanism preventing their excessive FFA uptake by SM. Ultimately, continual elevation of fatty acids will increase non-nutritive flow and contribute to the inability of muscle to take up amino acids, fatty acids and glucose in the presence of insulin, and accelerate adipocyte accretion (human marbling) associated with muscle fibres. Finally, an important case for the future will be determining the role of PAT in contributing to the production of both endocrine and other signaling factors in SM.

Reference List

1. Abbink-Zandbergen, E. J., G. Vervoort, C. J. Tack, J. A. Lutterman, N. C. Schaper, and P. Smits. The role of adenosine in insulin-induced vasodilation. *J Cardiovasc.Pharmacol.* 34: 374-380, 1999.

2. Ahmed, A., D. L. Maxwell, P. M. Taylor, and M. J. Rennie. Glutamine transport in human skeletal muscle. *Am J Physiol* 264: E993-1000, 1993.

3. Amin-Hanjani, S., N. E. Stagliano, M. Yamada, P. L. Huang, J. K. Liao, and M. A. Moskowitz. Mevastatin, an HMG-CoA reductase inhibitor, reduces stroke damage and upregulates endothelial nitric oxide synthase in mice. *Stroke* 32: 980-986, 2001.

4. Anderson, E. A., R. P. Hoffman, T. W. Balon, C. A. Sinkey, and A. L. Mark. Hyperinsulinemia produces both sympathetic neural activation and vasodilation in normal humans. *J Clin.Invest* 87: 2246-2252, 1991.

5. Ariano, M. A., R. B. Armstrong, and V. R. Edgerton. Hindlimb muscle fiber populations of five mammals. *J.Histochem.Cytochem.* 21: 51-55, 1973.

6. Armstrong, R. B. and M. H. Laughlin. Muscle function during locomotion in mammals. In Gilles, R., ed. Circulation, Respiration, and Metabolism. Springer-Verlag Berlin. 1985, 56-63.

7. Augusti, K. T. and C. G. Sheela. Antiperoxide effect of S-allyl cysteine sulfoxide, an insulin secretagogue, in diabetic rats. *Experientia* 52: 115-120, 1996.

8. Baker, T. A., S. Milstien, and Z. S. Katusic. Effect of vitamin C on the availability of tetrahydrobiopterin in human endothelial cells. *J Cardiovasc.Pharmacol.* 37: 333-338, 2001.

9. Ballard, S. T., M. A. Hill, and G. A. Meininger. Effect of vasodilation and vasoconstriction on microvascular pressures in skeletal muscle. *Microcirc.Endothelium Lymphatics* 7: 109-131, 1991.

10. Banz, W. J., M. A. Abel, and M. B. Zemel. Insulin regulation of vascular smooth muscle glucose transport in insulin-sensitive and resistant rats. *Horm.Metab Res* 28: 271-275, 1996.

11. Barlow, T. E., A. L. Haigh, and D. N. Walder. A search for arteriovenous anastomoses in skeletal muscle. *Proc.Physiol.Soc.* 80P-81P, 1958.

12. Barlow, T. E., A. L. Haigh, and D. N. Walder. Evidence for two vascular pathways in skeletal muscle. *Clin Sci* 20: 367-385, 1961.

13. Barnard, R. J. and J. F. Youngren. Regulation of glucose transport in skeletal muscle. *FASEB J* 6: 3238-3244, 1992.

14. Baron, A. D. Hemodynamic actions of insulin. *Am J Physiol* 267: E187-E202, 1994.

15. Baron, A. D. and M. G. Clark. Role of blood flow in the regulation of muscle glucose uptake. *Annu.Rev.Nutr.* 17: 487-499, 1997.

16. Baron, A. D., H. Steinberg, G. Brechtel, and A. Johnson. Skeletal muscle blood flow independently modulates insulin-mediated glucose uptake. *Am J Physiol* 266: E248-E253, 1994.

17. Bell, D. M., T. E. Johns, and L. M. Lopez. Endothelial dysfunction: implications for therapy of cardiovascular diseases. *Ann.Pharmacother.* 32: 459-470, 1998.

18. Bengtsson-Olivecrona, G. and T. Olivecrona. Assay of lipoprotein lipase and hepatic lipase. In Converse, C. A. and E. R. Skinner, eds. Lipoprotein analysis, a practical approach. New York, Oxford University Press. 1992, 169-185.

19. Bergeron, R., S. F. Previs, G. W. Cline, P. Perret, R. R. Russell, III, L. H. Young, and G. I. Shulman. Effect of 5-aminoimidazole-4-carboxamide-1-beta-D-ribofuranoside infusion on in vivo glucose and lipid metabolism in lean and obese Zucker rats. *Diabetes* 50: 1076-1082, 2001.

20. Bevilacqua, S., R. Bonadonna, G. Buzzigoli, C. Boni, D. Ciociaro, F. Maccari, M. A. Giorico, and E. Ferrannini. Acute elevation of free fatty acid levels leads to hepatic insulin resistance in obese subjects. *Metabolism* 36: 502-506, 1987.

21. Bevilacqua, S., G. Buzzigoli, R. Bonadonna, L. S. Brandi, M. Oleggini, C. Boni, M. Geloni, and E. Ferrannini. Operation of Randle's cycle in patients with NIDDM. *Diabetes* 39: 383-389, 1990.

22. Blaak, E. E., A. J. Wagenmakers, J. F. Glatz, B. H. Wolffenbuttel, G. J. Kemerink, C. J. Langenberg, G. A. Heidendal, and W. H. Saris. Plasma FFA utilization and fatty acid-binding protein content are diminished in type 2 diabetic muscle. *Am J Physiol Endocrinol.Metab* 279: E146-E154, 2000.

23. Black, S. C., S. Katz, and J. H. McNeill. Influence of omega-3 fatty acid treatment on cardiac phospholipid composition and coronary flow of streptozocin-diabetic rats. *Metabolism* 42: 320-326, 1993.

24. Blumberg, A. L., S. E. Denny, G. R. Marshall, and P. Needleman. Blood vessels-hormone interactions: Angiotensin, bradykinin, and prostaglandins. *Am.J.Physiol.* 232: H305-H310, 1977.

25. Boden, G. and X. Chen. Effects of fat on glucose uptake and utilization in patients with non-insulin-dependent diabetes. *J Clin Invest* 96: 1261-1268, 1995.

26. Boden, G., X. Chen, J. Ruiz, J. V. White, and L. Rossetti. Mechanisms of fatty acid-induced inhibition of glucose uptake. *J Clin.Invest* 93: 2438-2446, 1994.

27. Boden, G., F. Jadali, J. White, Y. Liang, M. Mozzoli, X. Chen, E. Coleman, and C. Smith. Effects of fat on insulin-stimulated carbohydrate metabolism in normal men. *J Clin.Invest* 88: 960-966, 1991.

28. Boesch, C., J. Slotboom, H. Hoppeler, and R. Kreis. In vivo determination of intra-myocellular lipids in human muscle by means of localized 1H-MR-spectroscopy. *Magn Reson.Med.* 37: 484-493, 1997.

29. Bonadonna, R. C., M. P. Saccomani, C. Cobelli, and R. A. DeFronzo. Effect of insulin on system A amino acid transport in human skeletal muscle. *J Clin Invest* 91: 514-521, 1993.

30. Bonadonna, R. C., K. Zych, C. Boni, E. Ferrannini, and R. A. DeFronzo. Time dependence of the interaction between lipid and glucose in humans. *Am J Physiol* 257: E49-E56, 1989.

31. Bonen, A., J. J. Luiken, S. Liu, D. J. Dyck, B. Kiens, S. Kristiansen, L. P. Turcotte, G. J. van der Vusse, and J. F. Glatz. Palmitate transport and fatty acid transporters in red and white muscles. *Am J Physiol* 275: E471-E478, 1998.

32. Borgstrom, P., L. Lindbom, K. E. Arfors, and M. Intaglietta. Beta-adrenergic control of resistance in individual vessels in rabbit tenuissimus muscle. *Am J Physiol* 254: H631-H635, 1988.

33. Brink, M., S. R. Price, J. Chrast, J. L. Bailey, A. Anwar, W. E. Mitch, and P. Delafontaine. Angiotensin II induces skeletal muscle wasting through enhanced protein degradation and down-regulates autocrine insulin-like growth factor I. *Endocrinology* 142: 1489-1496, 2001.

34. Burant, C. F. Insulin Sensitization. In Lockwood, D. H. and T. G. Heffner, eds. Obesity:Pathology and Therapy. New York, Springer-Verlag. 2000, 369-400.

35. Camps, L., M. Reina, M. Llobera, S. Vilaro, and T. Olivecrona. Lipoprotein lipase: cellular origin and functional distribution. *Am J Physiol* 258: C673-C681, 1990.

36. Carayannopoulos, M. O., M. M. Chi, Y. Cui, J. M. Pingsterhaus, R. A. McKnight, M. Mueckler, S. U. Devaskar, and K. H. Moley. GLUT8 is a glucose transporter responsible for insulin-stimulated glucose uptake in the blastocyst. *Proc.Natl.Acad.Sci.U.S.A* 97: 7313-7318, 2000.

37. Cardillo, C., S. S. Nambi, C. M. Kilcoyne, W. K. Choucair, A. Katz, M. J. Quon, and J. A. Panza. Insulin stimulates both endothelin and nitric oxide activity in the human forearm. *Circulation* 100: 820-825, 1999.

38. Carey, D. G., A. B. Jenkins, L. V. Campbell, J. Freund, and D. J. Chisholm. Abdominal fat and insulin resistance in normal and overweight women: Direct measurements reveal a strong relationship in subjects at both low and high risk of NIDDM. *Diabetes* 45: 633-638, 1996.

39. Caron, M., M. Auclair, C. Vigouroux, M. Glorian, C. Forest, and J. Capeau. The HIV protease inhibitor indinavir impairs sterol regulatory element-binding protein-1 intranuclear localization,

inhibits preadipocyte differentiation, and induces insulin resistance. *Diabetes* 50: 1378-1388, 2001.

40. Chakrabarty, K., J. W. Tauber, B. Sigel, C. T. Bombeck, and H. Jeffay. Glycerokinase activity in human adipose tissue as related to obesity. *Int.J Obes.* 8: 609-622, 1984.

41. Chalkley, S. M., M. Hettiarachchi, D. J. Chisholm, and E. W. Kraegen. Five-hour fatty acid elevation increases muscle lipids and impairs glycogen synthesis in the rat. *Metabolism* 47: 1121-1126, 1998.

42. Christensen, H. N., M. Liang, and E. G. Archer. A distinct Na+-requiring transport system for alanine, serine, cysteine, and similar amino acids. *J Biol.Chem.* 242: 5237-5246, 1967.

43. Christensen, H. N., D. L. Oxender, M. Liang, and K. A. Vatz. The use of N-methylation to direct route of mediated transport of amino acids. *J Biol.Chem.* 240: 3609-3616, 1965.

44. Clark, A. D., E. J. Barrett, S. Rattigan, M. G. Wallis, and M. G. Clark. Insulin stimulates laser Doppler signal by rat muscle in vivo, consistent with nutritive flow recruitment. *Clin.Sci.(Colch.)* 100: 283-290, 2001.

45. Clark, A. D., J. M. Youd, S. Rattigan, E. J. Barrett, and M. G. Clark. Heterogeneity of laser Doppler flowmetry in perfused muscle indicative of nutritive and nonnutritive flow. *Am J Physiol Heart Circ.Physiol* 280: H1324-H1333, 2001.

46. Clark, M. G., E. Q. Colquhoun, S. Rattigan, K. A. Dora, T. P. D. Eldershaw, J. L. Hall, and Y. Jiming. Vascular and endocrine control of muscle metabolism. *Am.J.Physiol.* 268: E797-E812, 1995.

47. Clark, M. G., J. M. Newman, and A. D. Clark. Microvascular regulation of muscle metabolism. *Curr.Opin.Clin.Nutr.Metab Care* 1: 205-210, 1998.

48. Clark, M. G., S. Rattigan, K. A. Dora, J. M. Newman, J. T. Steen, K. A. Miller, and M. A. Vincent. Vascular and metabolic regulation of muscle. In Kinney, J. M. and H. N. Tucker, eds. Physiology, stress, and malnutrition: functional correlates, nutritional intervention. New York, Lippincott-Raven publishers. 1997, 325-346.

49. Cleland, S. J., J. R. Petrie, S. Ueda, H. L. Elliott, and J. M. Connell. Insulin-mediated vasodilation and glucose uptake are functionally linked in humans. *Hypertension* 33: 554-558, 1999.

50. Coggins, M. P., Fasy, E., Lindner, J., Jahn, L., Kaul, S., and Barrett, E. J. Physiologic hyperinsulinemia increases skeletal muscle microvascular blood volume in healthy humans. Diabetes 48, Supplement 1, A220. 1999.
Ref Type: Abstract

51. Colberg, S. R., J. A. Simoneau, F. L. Thaete, and D. E. Kelley. Skeletal muscle utilization of free fatty acids in women with visceral obesity. *J Clin.Invest* 95: 1846-1853, 1995.

52. Collins, D. M., W. T. McCullough, and M. L. Ellsworth. Conducted vascular responses: communication across the capillary bed. *Microvasc.Res.* 56: 43-53, 1998.

53. Colquhoun, E. Q., M. Hettiarachchi, J. M. Ye, E. A. Richter, A. J. Hniat, S. Rattigan, and M. G. Clark. Vasopressin and angiotensin II stimulate oxygen uptake in the perfused rat hindlimb. *Life Sci.* 43: 1747-1754, 1988.

54. Creager, M. A., C. S. Liang, and J. D. Coffman. Beta adrenergic-mediated vasodilator response to insulin in the human forearm. *J.Pharmacol.Exp.Ther.* 235: 709-714, 1985.

55. Cryer, A. Tissue lipoprotein lipase activity and its action in lipoprotein metabolism. *Int.J Biochem.* 13: 525-541, 1981.

56. Cynober, L. A. Understanding the pathological mechanisms underlying protein breakdown for new therapeutic strategies. *Nutrition* 11: 398, 1995.

57. DeFronzo, R. A. Insulin secretion, insulin resistance, and obesity. *Int.J Obes.* 6 Suppl 1: 73-82, 1982.

58. DeFronzo, R. A. Lilly lecture 1987. The triumvirate: beta-cell, muscle, liver. A collusion responsible for NIDDM. *Diabetes* 37: 667-687, 1988.

59. DeFronzo, R. A., R. C. Bonadonna, and E. Ferrannini. Pathogenesis of NIDDM. A balanced overview. *Diabetes Care* 15: 318-368, 1992.

60. del Aguila, L. F., K. P. Claffey, and J. P. Kirwan. TNF-alpha impairs insulin signaling and insulin stimulation of glucose uptake in C2C12 muscle cells. *Am J Physiol* 276: E849-E855, 1999.

61. Dela, F. and B. Stallknecht. No role of interstitial adenosine in insulin-mediated vasodilation. *Acta Physiol Scand.* 167: 37-42, 1999.

62. Dimmeler, S., I. Fleming, B. Fisslthaler, C. Hermann, R. Busse, and A. M. Zeiher. Activation of nitric oxide synthase in endothelial cells by Akt-dependent phosphorylation. *Nature* 399: 601-605, 1999.

63. Dora, K. A., E. Q. Colquhoun, M. Hettiarachchi, S. Rattigan, and M. G. Clark. The apparent absence of serotonin-mediated vascular thermogenesis in perfused rat hindlimb may result from vascular shunting. *Life Sci.* 48: 1555-1564, 1991.

64. Dora, K. A., S. Rattigan, E. Q. Colquhoun, and M. G. Clark. Aerobic muscle contraction impaired by serotonin-mediated vasoconstriction. *J Appl.Physiol* 77: 277-284, 1994.

65. Duan, C. and W. W. Winder. Control of malonyl-CoA by glucose and insulin in perfused skeletal muscle. *J Appl.Physiol* 74: 2543-2547, 1993.

66. Duplain, H., R. Burcelin, C. Sartori, S. Cook, M. Egli, M. Lepori, P. Vollenweider, T. Pedrazzini, P. Nicod, B. Thorens, and U. Scherrer. Insulin resistance, hyperlipidemia, and hypertension in mice lacking endothelial nitric oxide synthase. *Circulation* 104: 342-345, 2001.

67. Eaton, P. and D. Steinberg. Effects of medium fatty acid concentration, epinephrine, and glucose on palmitate-1-C14 oxidation and incorporation into neutral lipids by skeletal muscle *in vitro*. *J.Lipid Res.* 2: 376-382, 1961.

68. Eckel, R. H. Lipoprotein lipase. A multifunctional enzyme relevant to common metabolic diseases. *N.Engl.J Med* 320: 1060-1068, 1989.

69. Ellis, B. A., A. Poynten, A. J. Lowy, S. M. Furler, D. J. Chisholm, E. W. Kraegen, and G. J. Cooney. Long-chain acyl-CoA esters as indicators of lipid metabolism and insulin sensitivity in rat and human muscle. *Am J Physiol Endocrinol.Metab* 279: E554-E560, 2000.

70. Ellsworth, M. L. and R. N. Pittman. Arterioles supply oxygen to capillaries by diffusion as well as by convection. *Am J Physiol* 258: H1240-H1243, 1990.

71. Emmerson, B. T., R. B. Gordon, M. Cross, and D. B. Thomson. Plasma oxipurinol concentrations during allopurinol therapy. *Br.J.Rheumatol.* 26: 445-449, 1987.

72. Eriksson, E. and R. Myrhage. Microvascular dimensions and blood flow in skeletal muscle. *Acta Physiol.Scand.* 86: 211-222, 1972.

73. Falholt, K., I. Jensen, J. S. Lindkaer, H. Mortensen, A. Volund, L. G. Heding, P. P. Noerskov, and W. Falholt. Carbohydrate and lipid metabolism of skeletal muscle in type 2 diabetic patients. *Diabet.Med.* 5: 27-31, 1988.

74. Felber, J. P., E. Ferrannini, A. Golay, H. U. Meyer, D. Theibaud, B. Curchod, E. Maeder, E. Jequier, and R. A. DeFronzo. Role of lipid oxidation in pathogenesis of insulin resistance of obesity and type II diabetes. *Diabetes* 36: 1341-1350, 1987.

75. Felley, C. P., E. M. Felley, G. D. van Melle, P. Frascarolo, E. Jequier, and J. P. Felber. Impairment of glucose disposal by infusion of triglycerides in humans: role of glycemia. *Am J Physiol* 256: E747-E752, 1989.

76. Fenn, W. O. The effect of anaerobiosis and other factors on the oxygen consumption of irritable and non-irritable muscles. *Am.J.Physiol* 93: 124-137, 1930.

77. Ferrannini, E., E. J. Barrett, and S. Bevilacqua. Effect of fatty acids on glucose production and utilization in man. *J.Clin.Invest.* 72: 1737-1747, 1983.

78. Fisher, B. M., G. Gillen, H. J. Dargie, G. C. Inglis, and B. M. Frier. The effects of insulin-induced hypoglycaemia on cardiovascular function in normal man: studies using radionuclide ventriculography. *Diabetologia* 30: 841-845, 1987.

79. Foster, L. J. and A. Klip. Mechanism and regulation of GLUT-4 vesicle fusion in muscle and fat cells. *Am J Physiol Cell Physiol* 279: C877-C890, 2000.

80. Friedman, J. E., P. W. Lemon, and J. A. Finkelstein. Effect of exercise and obesity on skeletal muscle amino acid uptake. *J Appl.Physiol* 69: 1347-1352, 1990.

81. Fruebis, J., T. S. Tsao, S. Javorschi, D. Ebbets-Reed, M. R. Erickson, F. T. Yen, B. E. Bihain, and H. F. Lodish. Proteolytic cleavage product of 30-kDa adipocyte complement-related protein increases fatty acid oxidation in muscle and causes weight loss in mice. *Proc.Natl.Acad.Sci U.S.A* 98: 2005-2010, 2001.

82. Fryer, L. G., E. Hajduch, F. Rencurel, I. P. Salt, H. S. Hundal, D. G. Hardie, and D. Carling. Activation of glucose transport by AMP-activated protein kinase via stimulation of nitric oxide synthase. *Diabetes* 49: 1978-1985, 2000.

83. Fugmann, A., L. Lind, P. E. Andersson, J. Millgard, A. Hanni, C. Berne, and H. Lithell. The effect of euglucaemic hyperinsulinaemia on forearm blood flow and glucose uptake in the human forearm. *Acta Diabetol.* 35: 203-206, 1998.

84. Gelfand, R. A. and E. J. Barrett. Effects of physiologic hyperinsulinemia on skeletal muscle protein synthesis and breakdown in man. *J.Clin.Invest* 80: 1-6, 1987.

85. Goetze, S., U. Kintscher, H. Kawano, Y. Kawano, S. Wakino, E. Fleck, W. A. Hsueh, and R. E. Law. Tumor necrosis factor alpha inhibits insulin-induced mitogenic signaling in vascular smooth muscle cells. *J.Biol.Chem.* 275: 18279-18283, 2000.

86. Goldman, D. and A. S. Popel. A computational study of the effect of capillary network anastomoses and tortuosity on oxygen transport. *J.Theor.Biol.* 206: 181-194, 2000.

87. Gomez, J. M., A. Molina, M. Fernandez-Castaner, and J. Soler. Leptin in type 2 diabetic or myotonic dystrophic women. *Horm.Metab Res* 33: 246-249, 2001.

88. Gondret, F., J. Mourot, and M. Bonneau. Developmental changes in lipogenic enzymes in muscle compared to liver and extramuscular adipose tissues in the rabbit (Oryctolagus cuniculus). *Comp Biochem.Physiol B Biochem.Mol.Biol.* 117: 259-265, 1997.

89. Goodman, M. N., P. R. Larsen, M. M. Kaplan, T. T. Aoki, V. R. Young, and N. B. Ruderman. Starvation in the rat. II. Effect of age and obesity on protein sparing and fuel metabolism. *Am J Physiol* 239: E277-E286, 1980.

90. Goodman, M. N. and N. B. Ruderman. Influence of muscle use on amino acid metabolism. *Exerc.Sport Sci.Rev.* 10: 1-26, 1982.

91. Goodpaster, B. H. and D. E. Kelley. Role of muscle in triglyceride metabolism. *Curr.Opin.Lipidol.* 9: 231-236, 1998.

92. Goodpaster, B. H., F. L. Thaete, and D. E. Kelley. Thigh adipose tissue distribution is associated with insulin resistance in obesity and in type 2 diabetes mellitus. *Am J Clin.Nutr.* 71: 885-892, 2000.

93. Goodpaster, B. H., F. L. Thaete, J. A. Simoneau, and D. E. Kelley. Subcutaneous abdominal fat and thigh muscle composition predict insulin sensitivity independently of visceral fat. *Diabetes* 46: 1579-1585, 1997.

94. Goodpaster, B. H., R. Theriault, S. C. Watkins, and D. E. Kelley. Intramuscular lipid content is increased in obesity and decreased by weight loss. *Metabolism* 49: 467-472, 2000.

95. Grant, R. T. and H. P. Wright. Anatomical basis for non-nutritive circulation in skeletal muscle exemplified by blood vessels of rat biceps femoris tendon. *J Anat.* 106: 125-133, 1970.

96. Greene E.C. Anatomy of the rat. U.S.A., Hafner Publishing Co. 1968.

97. Griffin, M. E., M. J. Marcucci, G. W. Cline, K. Bell, N. Barucci, D. Lee, L. J. Goodyear, E. W. Kraegen, M. F. White, and G. I. Shulman. Free fatty acid-induced insulin resistance is associated with activation of protein kinase C theta and alterations in the insulin signaling cascade. *Diabetes* 48: 1270-1274, 1999.

98. Griffiths, C. D., T. P. Eldershaw, D. P. Geraghty, J. L. Hall, and E. Q. Colquhoun. Capsaicin-induced biphasic oxygen uptake in rat muscle: antagonism by capsazepine and ruthenium red provides further evidence for peripheral vanilloid receptor subtypes (VN1/VN2). *Life Sci.* 59: 105-117, 1996.

99. Groop, L. C., C. Saloranta, M. Shank, R. C. Bonadonna, E. Ferrannini, and R. A. DeFronzo. The role of free fatty acid metabolism in the pathogenesis of insulin resistance in obesity and non insulin-dependent diabetes mellitus. *J Clin Endocrinol.Metab* 72: 96-107, 1991.

100. Grubb, B. and J. F. Snarr. Effect of flow rate and glucose concentration on glucose uptake rate by the rat limb. *Proc.Soc.Exp.Biol.Med.* 154: 33-36, 1977.

101. Guo, Z. and M. D. Jensen. Blood glycerol is an important precursor for intramuscular triacylglycerol synthesis. *J Biol.Chem.* 274: 23702-23706, 1999.

102. Hall, J. L., J. M. Ye, M. G. Clark, and E. Q. Colquhoun. Sympathetic stimulation elicits increased or decreased VO2 in the perfused rat hindlimb via alpha 1-adrenoceptors. *Am J Physiol* 272: H2146-H2153, 1997.

103. Hamilton, J. A., R. A. Johnson, B. Corkey, and F. Kamp. Fatty acid transport: the diffusion mechanism in model and biological membranes. *J Mol.Neurosci.* 16: 99-108, 2001.

104. Hamilton, J. A. and F. Kamp. How are free fatty acids transported in membranes? Is it by proteins or by free diffusion through the lipids? *Diabetes* 48: 2255-2269, 1999.

105. Hammer, L. W., A. L. Ligon, and R. L. Hester. ATP-mediated release of arachidonic acid metabolites from venular endothelium causes arteriolar dilation. *Am J Physiol Heart Circ.Physiol* 280: H2616-H2622, 2001.

106. Hammersen, F. The terminal vascular bed in skeletal muscle with special regard to the problem of shunts. In Crone, C. and N. A. Lassen, eds. Capillary Permeability. The Transfer of Molecules and Ions Between Capillary Blood and Tissue". Munksgaard Copenhagen. 1970, 351-371.

107. Hardie, D. G., J. Corton, Y. P. Ching, S. P. Davies, and S. Hawley. Regulation of lipid metabolism by the AMP-activated protein kinase. *Biochem.Soc.Trans.* 25: 1229-1231, 1997.

108. Harrison, D. K., S. Birkenhake, S. K. Knauf, and M. Kessler. Local oxygen supply and blood flow regulation in contracting muscle in dogs and rabbits. *J Physiol* 422: 227-243, 1990.

109. Havel, R. J. Lipid transport function of lipoproteins in blood plasma. *Am J Physiol* 253: E1-E5, 1987.

110. He, J., S. Watkins, and D. E. Kelley. Skeletal muscle lipid content and oxidative enzyme activity in relation to muscle fiber type in type 2 diabetes and obesity. *Diabetes* 50: 817-823, 2001.

111. Helge, J. W., A. D. Kriketos, and L. H. Storlien. Insulin sensitivity, muscle fibre types, and membrane lipids. *Adv.Exp.Med.Biol.* 441: 129-138, 1998.

112. Hernandez, N., S. H. Torres, O. Vera, J. B. De Sanctis, and E. Flores. Muscle fiber composition and capillarization in relation to metabolic alterations in hypertensive men. *J Med.* 32: 67-82, 2001.

113. Holling, H. E. Observations on the oxygen content of venous blood from the arm vein and on the oxygen consumption of resting human muscle. *Clin Sci* 4: 103, 1940.

114. Holman, G. D. and M. Kasuga. From receptor to transporter: insulin signalling to glucose transport. *Diabetologia* 40: 991-1003, 1997.

115. Holman, G. D. and M. Kasuga. From receptor to transporter: insulin signalling to glucose transport. *Diabetologia* 40: 991-1003, 1997.

116. Hsu, R. and T. W. Secomb. A Green's function method for analysis of oxygen delivery to tissue by microvascular networks. *Math.Biosci.* 96: 61-78, 1989.

117. Hu, E., P. Liang, and B. M. Spiegelman. AdipoQ is a novel adipose-specific gene dysregulated in obesity. *J Biol.Chem.* 271: 10697-10703, 1996.

118. Huang, A., D. Sun, C. J. Smith, J. A. Connetta, E. G. Shesely, A. Koller, and G. Kaley. In eNOS knockout mice skeletal muscle arteriolar dilation to acetylcholine is mediated by EDHF. *Am J Physiol Heart Circ.Physiol* 278: H762-H768, 2000.

119. Hubert, P., C. Bruneau-Wack, G. Cremel, Y. Marchand-Brustel, and C. Staedel. Lipid-induced insulin resistance in cultured hepatoma cells is associated with a decreased insulin receptor tyrosine kinase activity. *Cell Regul.* 2: 65-72, 1991.

120. Hundal, H. S., M. J. Rennie, and P. W. Watt. Characteristics of acidic, basic and neutral amino acid transport in the perfused rat hindlimb. *J.Physiol.(Lond.)* 408: 93-114, 1989.

121. Ide, T., T. Nakazawa, T. Mochizuki, and K. Murakami. Tissue-specific actions of antidiabetic thiazolidinediones on the reduced fatty acid oxidation in skeletal muscle and liver of Zucker diabetic fatty rats. *Metabolism* 49: 521-525, 2000.

122. Ikeda, T., H. Terasawa, M. Ishimura, H. Ochi, I. Noguchi, K. Fujiyama, T. Hoshino, Y. Tanaka, and H. Mashiba. Inhibitory effect of fatty acids on glucose and insulin uptake in the perfused rat hindquarter. *Biochem.Med.Metab Biol.* 52: 97-100, 1994.

123. Jacob, S., J. Machann, K. Rett, K. Brechtel, A. Volk, W. Renn, E. Maerker, S. Matthaei, F. Schick, C. D. Claussen, and H. U. Haring. Association of increased intramyocellular lipid content with insulin resistance in lean nondiabetic offspring of type 2 diabetic subjects. *Diabetes* 48: 1113-1119, 1999.

124. Jamerson, K. A., S. D. Nesbitt, J. V. Amerena, E. Grant, and S. Julius. Angiotensin mediates forearm glucose uptake by hemodynamic rather than direct effects. *Hypertension* 27: 854-858, 1996.

125. James, D. E., K. M. Burleigh, L. H. Storlien, S. P. Bennett, and E. W. Kraegen. Heterogeneity of insulin action in muscle: influence of blood flow. *Am.J.Physiol.* 251: E422-E430, 1986.

126. James, D. E., A. B. Jenkins, and E. W. Kraegen. Heterogeneity of insulin action in individual muscles in vivo: euglycemic clamp studies in rats. *Am.J.Physiol.* 248: E567-E574, 1985.

127. Janssen, I., S. B. Heymsfield, Z. M. Wang, and R. Ross. Skeletal muscle mass and distribution in 468 men and women aged 18-88 yr. *J Appl.Physiol* 89: 81-88, 2000.

128. Jucker, B. M., A. J. Rennings, G. W. Cline, and G. I. Shulman. 13C and 31P NMR studies on the effects of increased plasma free fatty acids on intramuscular glucose metabolism in the awake rat. *J Biol.Chem.* 272: 10464-10473, 1997.

129. Julius, S. Insulin, insulin resistance, and blood pressure elevation. *Arch.Int.Med.* 153: 290-291, 1993.

130. Kadowaki, M., T. Nagasawa, T. Hirata, T. Noguchi, and H. Naito. Effects of insulin, amino acids and fasting on myofibrillar protein degradation in perfused hindquarters of rats. *J Nutr.Sci Vitaminol.(Tokyo.)* 31: 431-440, 1985.

131. Kahn, A. M., C. L. Seidel, J. C. Allen, R. G. O'Neil, H. Shelat, and T. Song. Insulin reduces contraction and intracellular calcium concentration in vascular smooth muscle. *Hypertension* 22: 735-742, 1993.

132. Kelley, D. E., B. Goodpaster, R. R. Wing, and J. A. Simoneau. Skeletal muscle fatty acid metabolism in association with insulin resistance, obesity, and weight loss. *Am J Physiol* 277: E1130-E1141, 1999.

133. Kelley, D. E. and L. J. Mandarino. Fuel selection in human skeletal muscle in insulin resistance: a reexamination. *Diabetes* 49: 677-683, 2000.

134. Kelley, D. E., M. A. Mintun, S. C. Watkins, J. A. Simoneau, F. Jadali, A. Fredrickson, J. Beattie, and R. Theriault. The effect of non-insulin-dependent diabetes mellitus and obesity on glucose transport and phosphorylation in skeletal muscle. *J Clin.Invest* 97: 2705-2713, 1996.

135. Kelley, D. E., M. Mokan, J. A. Simoneau, and L. J. Mandarino. Interaction between glucose and free fatty acid metabolism in human skeletal muscle. *J Clin.Invest* 92: 91-98, 1993.

136. Kelley, D. E., J. P. Reilly, T. Veneman, and L. J. Mandarino. Effects of insulin on skeletal muscle glucose storage, oxidation, and glycolysis in humans. *Am J Physiol* 258: E923-E929, 1990.

137. Kelley, D. E., B. S. Slasky, and J. Janosky. Skeletal muscle density: effects of obesity and non-insulin-dependent diabetes mellitus. *Am J Clin.Nutr.* 54: 509-515, 1991.

138. Kern, M., E. B. Tapscott, R. D. Snider, and G. L. Dohm. Differences in glucose transport rates between perfused and in vitro incubated muscles. *Horm.Metab Res* 22: 366-368, 1990.

139. Kim, F., B. Gallis, and M. A. Corson. TNF-alpha inhibits flow and insulin signaling leading to NO production in aortic endothelial cells. *Am J Physiol Cell Physiol* 280: C1057-C1065, 2001.

140. Kim, J. K., J. K. Wi, and J. H. Youn. Plasma free fatty acids decrease insulin-stimulated skeletal muscle glucose uptake by suppressing glycolysis in conscious rats. *Diabetes* 45: 446-453, 1996.

141. Kim, K. M., S. B. Chun, M. S. Koo, W. J. Choi, T. W. Kim, Y. G. Kwon, H. T. Chung, T. R. Billiar, and Y. M. Kim. Differential regulation of NO availability from macrophages and endothelial cells by the garlic component S-allyl cysteine. *Free Radic.Biol.Med.* 30: 747-756, 2001.

142. Koller, A., G. Dornyei, and G. Kaley. Flow-induced responses in skeletal muscle venules: modulation by nitric oxide and prostaglandins. *Am.J.Physiol* 275: H831-H836, 1998.

143. Konrad, D., R. Somwar, G. Sweeney, K. Yaworsky, M. Hayashi, T. Ramlal, and A. Klip. The antihyperglycemic drug alpha-lipoic acid stimulates glucose uptake via both GLUT4 translocation and GLUT4 activation: potential role of p38 mitogen-activated protein kinase in GLUT4 activation. *Diabetes* 50: 1464-1471, 2001.

144. Koyama, K., G. Chen, Y. Lee, and R. H. Unger. Tissue triglycerides, insulin resistance, and insulin production: implications for hyperinsulinemia of obesity. *Am J Physiol* 273: E708-E713, 1997.

145. Kraegen, E. W., D. E. James, A. B. Jenkins, and D. J. Chisholm. Dose-response curves for in vivo insulin sensitivity in individual tissues in rats. *Am.J.Physiol.* 248: E353-E362, 1985.

146. Krogh, A. The number and distribution of capillaries in muscles with calculations of the oxygen pressure head necessary for supplying the tissue. *J.Physiol.(Lond.)* 52: 409-415, 1919.

147. Krogh, A. The supply of oxygen to the tissues and the regulation of the capillary circulation. *J.Physiol.(Lond.)* 52: 457-474, 1919.

148. Laakso, M., S. V. Edelman, G. Brechtel, and A. D. Baron. Decreased effect of insulin to stimulate skeletal muscle blood flow in obese man. A novel mechanism for insulin resistance. *J Clin.Invest* 85: 1844-1852, 1990.

149. Laakso, M., S. V. Edelman, G. Brechtel, and A. D. Baron. Impaired insulin-mediated skeletal muscle blood flow in patients with NIDDM. *Diabetes* 41: 1076-1083, 1992.

150. Laine, H., H. Yki-Jarvinen, O. Kirvela, T. Tolvanen, M. Raitakari, O. Solin, M. Haaparanta, J. Knuuti, and P. Nuutila. Insulin resistance of glucose uptake in skeletal muscle cannot be ameliorated by enhancing endothelium-dependent blood flow in obesity. *J.Clin.Invest.* 101: 1156-1162, 1998.

151. Lau, R., W. D. Blinn, A. Bonen, and D. J. Dyck. Stimulatory effects of leptin and muscle contraction on fatty acid metabolism are not additive. *Am J Physiol Endocrinol.Metab* 281: E122-E129, 2001.

152. Lavigne, C., F. Tremblay, G. Asselin, H. Jacques, and A. Marette. Prevention of skeletal muscle insulin resistance by dietary cod protein in high fat-fed rats. *Am J Physiol Endocrinol.Metab* 281: E62-E71, 2001.

153. Lee, K. U., H. K. Lee, C. S. Koh, and H. K. Min. Artificial induction of intravascular lipolysis by lipid-heparin infusion leads to insulin resistance in man. *Diabetologia* 31: 285-290, 1988.

154. Liang, C., J. U. Doherty, R. Faillace, K. Maekawa, S. Arnold, H. Gavras, and W. B. J. Hood. Insulin infusion in conscious dogs. Effects on systemic and coronary hemodynamics, regional blood flows, and plasma catecholamines. *J.Clin.Invest.* 69: 1321-1336, 1982.

155. Lind, L., A. Fugmann, S. Branth, B. Vessby, J. Millgard, C. Berne, and H. Lithell. The impairment in endothelial function induced by non-esterified fatty acids can be reversed by insulin. *Clin.Sci.(Colch.)* 99: 169-174, 2000.

156. Lindbom, L. and K. E. Arfors. Non-homogeneous blood flow distribution in the rabbit tenuissimus muscle Differential control of total blood flow and capillary perfusion. *Acta Physiol.Scand.* 122: 225-233, 1984.

157. Linder, C., S. S. Chernick, T. R. Fleck, and R. O. Scow. Lipoprotein lipase and uptake of chylomicron triglyceride by skeletal muscle of rats. *Am J Physiol* 231: 860-864, 1976.

158. Long, W., L. Saffer, L. Wei, and E. J. Barrett. Amino acids regulate skeletal muscle PHAS-I and p70 S6-kinase phosphorylation independently of insulin. *Am J Physiol Endocrinol.Metab* 279: E301-E306, 2000.

159. Lundholm, K., K. Bennegard, H. Zachrisson, F. Lundgren, E. Eden, and A. C. Moller-Loswick. Transport kinetics of amino acids across the resting human leg. *J Clin.Invest* 80: 763-771, 1987.

160. Lundman, P., M. Eriksson, K. Schenck-Gustafsson, F. Karpe, and P. Tornvall. Transient triglyceridemia decreases vascular reactivity in young, healthy men without risk factors for coronary heart disease. *Circulation* 96: 3266-3268, 1997.

161. Mackie, B. G., G. A. Dudley, H. Kaciuba-Uscilko, and R. L. Terjung. Uptake of chylomicron triglycerides by contracting skeletal muscle in rats. *J Appl.Physiol* 49: 851-855, 1980.

162. Magnan, C., M. Gilbert, and B. B. Kahn. Chronic free fatty acid infusion in rats results in insulin resistance but no alteration in insulin-responsive glucose transporter levels in skeletal muscle. *Lipids* 31: 1141-1149, 1996.

163. Marshall, J. M. Adenosine and muscle vasodilatation in acute systemic hypoxia. *Acta Physiol Scand.* 168: 561-573, 2000.

164. McDermott, J. C., A. Hutber, M. H. Tan, and A. Bonen. The use of a cell-free perfusate in the perfused rat hindquarter: methodological concerns. *Can.J Physiol Pharmacol.* 67: 1450-1454, 1989.

165. McDowell, H. E., P. A. Eyers, and H. S. Hundal. Regulation of System A amino acid transport in L6 rat skeletal muscle cells by insulin, chemical and hyperthermic stress. *FEBS Lett.* 441: 15-19, 1998.

166. Meek, S. E., M. Persson, G. C. Ford, and K. S. Nair. Differential regulation of amino acid exchange and protein dynamics across splanchnic and skeletal muscle beds by insulin in healthy human subjects. *Diabetes* 47: 1824-1835, 1998.

167. Michel, C. C. and F. E. Curry. Microvascular permeability. *Physiol Rev.* 79: 703-761, 1999.

168. Mitchell, D., J. Yu, and K. Tyml. Comparable effects of arteriolar and capillary stimuli on blood flow in rat skeletal muscle. *Microvasc.Res* 53: 22-32, 1997.

169. Mourot, J. and M. Kouba. Development of intra- and intermuscular adipose tissue in growing large white and Meishan pigs. *Reprod.Nutr.Dev.* 39: 125-132, 1999.

170. Muoio, D. M., G. L. Dohm, E. B. Tapscott, and R. A. Coleman. Leptin opposes insulin's effects on fatty acid partitioning in muscles isolated from obese ob/ob mice. *Am J Physiol* 276: E913-E921, 1999.

171. Murata, H., P. W. Hruz, and M. Mueckler. The mechanism of insulin resistance caused by HIV protease inhibitor therapy. *J Biol.Chem.* 275: 20251-20254, 2000.

172. Murrant, C. L. and I. H. Sarelius. Coupling of muscle metabolism and muscle blood flow in capillary units during contraction. *Acta Physiol Scand.* 168: 531-541, 2000.

173. Nagatsu, T. and H. Ichinose. Regulation of pteridine-requiring enzymes by the cofactor tetrahydrobiopterin. *Mol.Neurobiol.* 19: 79-96, 1999.

174. Nakajima, I., T. Yamaguchi, K. Ozutsumi, and H. Aso. Adipose tissue extracellular matrix: newly organized by adipocytes during differentiation. *Differentiation* 63: 193-200, 1998.

175. Nakamura, H. and J. J. Pisano. Fluorescamine derivatives of Histidine, Histamine, and Certain related Imidazoles: Using Fluorescence after Heating in Acid. *Arch Biochem.Biophys.* 177: 334-335, 1976.

176. Narimiya, M., T. Ohashi, T. Kubokura, M. Kaburagi, Y. Someya, and Y. Ikeda. Can plasma glucose and nonesterified fatty acid be regulators of glucose utilization in skeletal muscle? *Endocr.J* 41: 197-206, 1994.

177. Natali, A., R. Bonadonna, D. Santoro, A. Q. Galvan, S. Baldi, S. Frascerra, C. Palombo, S. Ghione, and E. Ferrannini. Insulin resistance and vasodilation in essential hypertension. Studies with adenosine. *J Clin.Invest* 94: 1570-1576, 1994.

178. Natali, A., G. A. Quinones, N. Pecori, G. Sanna, E. Toschi, and E. Ferrannini. Vasodilation with sodium nitroprusside does not improve insulin action in essential hypertension. *Hypertension* 31: 632-636, 1998.

179. Newman, J. M. and M. G. Clark. Stimulation and inhibition of resting muscle thermogenesis by vasoconstrictors in perfused rat hind limb [In Process Citation]. *Can.J Physiol Pharmacol.* 76: 867-872, 1998.

180. Newman, J. M., K. A. Dora, S. Rattigan, S. J. Edwards, E. Q. Colquhoun, and M. G. Clark. Norepinephrine and serotonin vasoconstriction in rat hindlimb control different vascular flow routes. *Am J Physiol* 270: E689-E699, 1996.

181. Newman, J. M. B., J. T. Steen, and M. G. Clark. Vessels supplying septa and tendons as functional shunts in perfused rat hindlimb. *Microvasc.Res.* 54: 49-57, 1997.

182. Nishimura, T., A. Hattori, and K. Takahashi. Structural changes in intramuscular connective tissue during the fattening of Japanese black cattle: effect of marbling on beef tenderization. *J Anim Sci.* 77: 93-104, 1999.

183. Noguchi, Y., T. Yoshikawa, D. Marat, C. Doi, T. Makino, K. Fukuzawa, A. Tsuburaya, S. Satoh, T. Ito, and S. Mitsuse. Insulin resistance in cancer patients is associated with enhanced tumor necrosis factor-alpha expression in skeletal muscle. *Biochem.Biophys.Res Commun.* 253: 887-892, 1998.

184. Nolte, L. A., P. A. Hansen, M. M. Chen, J. M. Schluter, E. A. Gulve, and J. O. Holloszy. Short-term exposure to tumor necrosis factor-alpha does not affect insulin-stimulated glucose uptake in skeletal muscle. *Diabetes* 47: 721-726, 1998.

185. Nolte, L. A., K. E. Yarasheski, K. Kawanaka, J. Fisher, N. Le, and J. O. Holloszy. The HIV protease inhibitor indinavir decreases insulin- and contraction-stimulated glucose transport in skeletal muscle. *Diabetes* 50: 1397-1401, 2001.

186. Nuutila, P., M. Raitakari, H. Laine, O. Kirvela, T. Takala, T. Utriainen, S. Makimattila, O. P. Pitkanen, U. Ruotsalainen, H. Iida, J. Knuuti, and H. Yki-Jarvinen. Role of blood flow in regulating insulin-stimulated glucose uptake in humans. Studies using bradykinin, [15O]water, and [18F]fluoro-deoxy-glucose and positron emission tomography. *J Clin.Invest* 97: 1741-1747, 1996.

187. Odland, L. M., G. J. Heigenhauser, D. Wong, M. G. Hollidge-Horvat, and L. L. Spriet. Effects of increased fat availability on fat-carbohydrate interaction during prolonged exercise in men. *Am J Physiol* 274: R894-R902, 1998.

188. Ohashi T, Narimiya, M., Kubokura, T., and Kaburaki M, Someya Y Tajima N Ikeda Y Isogai Y. The effects of insulin and glucose on the utilization of non-esterified fatty acid in the resting rat skeletal muscle. Nippon Naibunpi Gakkai Zasshi: abstract only 71(2), 173-178. 20-3-1995.

189. Okada, T., Y. Kawano, T. Sakakibara, O. Hazeki, and M. Ui. Essential role of phosphatidylinositol 3-kinase in insulin-induced glucose transport and antilipolysis in rat adipocytes. Studies with a selective inhibitor wortmannin. *J Biol.Chem.* 269: 3568-3573, 1994.

190. Orena, S. J., A. J. Torchia, and R. S. Garofalo. Inhibition of glycogen-synthase kinase 3 stimulates glycogen synthase and glucose transport by distinct mechanisms in 3T3-L1 adipocytes. *J Biol.Chem.* 275: 15765-15772, 2000.

191. Paolisso, G., M. R. Rizzo, G. Mazziotti, M. R. Tagliamonte, A. Gambardella, M. Rotondi, C. Carella, D. Giugliano, M. Varricchio, and F. D'Onofrio. Advancing age and insulin resistance: role of plasma tumor necrosis factor-alpha. *Am J Physiol* 275: E294-E299, 1998.

192. Pappenheimer, J. R. Vasoconstrictor nerves and oxygen consumption in the isolated perfused hindlimb muscles of the dog. *J.Physiol.* 99: 182-200, 1941.

193. Paternostro, G., P. G. Camici, A. A. Lammerstma, N. Marinho, R. R. Baliga, J. S. Kooner, G. K. Radda, and E. Ferrannini. Cardiac and skeletal muscle insulin resistance in patients with coronary heart disease - A study with positron emission tomography. *J.Clin.Invest.* 98: 2094-2099, 1996.

194. Patti, M. E. Nutrient modulation of cellular insulin action. *Ann.N.Y.Acad.Sci.* 892:187-203.: 187-203, 1999.

195. Perseghin, G., P. Scifo, F. De Cobelli, E. Pagliato, A. Battezzati, C. Arcelloni, A. Vanzulli, G. Testolin, G. Pozza, A. Del Maschio, and L. Luzi. Intramyocellular triglyceride content is a determinant of in vivo insulin resistance in humans: a 1H-13C nuclear magnetic resonance spectroscopy assessment in offspring of type 2 diabetic parents. *Diabetes* 48: 1600-1606, 1999.

196. Peyrollier, K., E. Hajduch, A. S. Blair, R. Hyde, and H. S. Hundal. L-leucine availability regulates phosphatidylinositol 3-kinase, p70 S6 kinase and glycogen synthase kinase-3 activity in L6 muscle cells: evidence for the involvement of the mammalian target of rapamycin (mTOR) pathway in the L-leucine-induced up-regulation of system A amino acid transport. *Biochem.J* 350 Pt 2:361-8.: 361-368, 2000.

197. Phillips, D. I., S. Caddy, V. Ilic, B. A. Fielding, K. N. Frayn, A. C. Borthwick, and R. Taylor. Intramuscular triglyceride and muscle insulin sensitivity: evidence for a relationship in nondiabetic subjects. *Metabolism* 45: 947-950, 1996.

198. Pieper, G. M. Acute amelioration of diabetic endothelial dysfunction with a derivative of the nitric oxide synthase cofactor, tetrahydrobiopterin. *J Cardiovasc.Pharmacol.* 29: 8-15, 1997.

199. Piiper, J. and S. Rosell. Attempt to demonstrate large arteriovenous shunts in skeletal muscle during stimulation of sympathetic vasodilator nerves. *Acta Physiol Scand* 53: 214-217, 1961.

200. Pitkanen, O. P., H. Laine, J. Kemppainen, E. Eronen, A. Alanen, M. Raitakari, O. Kirvela, U. Ruotsalainen, J. Knuuti, V. A. Koivisto, and P. Nuutila. Sodium nitroprusside increases human skeletal muscle blood flow, but does not change flow distribution or glucose uptake. *J.Physiol* 521 Pt 3: 729-737, 1999.

201. Pitkanen, O. P., H. Laine, J. Kemppainen, E. Eronen, A. Alanen, M. Raitakari, O. Kirvela, U. Ruotsalainen, J. Knuuti, V. A. Koivisto, and P. Nuutila. Sodium nitroprusside increases human skeletal muscle blood flow, but does not change flow distribution or glucose uptake. *J Physiol* 521 Pt 3: 729-737, 1999.

202. Pollare, T., B. Vessby, and H. Lithell. Lipoprotein lipase activity in skeletal muscle is related to insulin sensitivity. *Arterioscler.Thromb.* 11: 1192-1203, 1991.

203. Potter, R. F. and A. C. Groom. Capillary diameter and geometry in cardiac and skeletal muscle studied by means of corrosion casts. *Microvasc.Res* 25: 68-84, 1983.

204. Pujol, A., L. Lefaucheur, P. Ecolan, L. Picon, and L. Penicaud. Fiber type composition and enzyme activities of muscles in two models of obese rats. *Comp Biochem.Physiol B* 106: 269-272, 1993.

205. Qi, C. and P. H. Pekala. Tumor necrosis factor-alpha-induced insulin resistance in adipocytes. *Proc.Soc.Exp.Biol.Med.* 223: 128-135, 2000.

206. Randle, P. J., C. N. Hales, P. B. Garland, and E. A. Newsholme. The glucose fatty-acid cycle. Its role in insulin sensitivity and the metabolic disturbances of diabetes mellitus. *The Lancet* 785-789, 1963.

207. Rao, G. A., M. F. Sorrels, and R. Reiser. Production and preferential utilization of dihydroxyacetone phosphate for glyceride synthesis in the presence of glycerol 3-phosphate. *Biochem.Biophys.Res Commun.* 44: 1279-1284, 1971.

208. Rattigan, S., G. J. Appleby, K. A. Miller, J. T. Steen, K. A. Dora, E. Q. Colquhoun, and M. G. Clark. Serotonin inhibition of 1-methylxanthine metabolism parallels its vasoconstrictor activity and inhibition of oxygen uptake in perfused rat hindlimb. *Acta Physiol Scand.* 161: 161-169, 1997.

209. Rattigan, S., M. G. Clark, and E. J. Barrett. Hemodynamic actions of insulin in rat skeletal muscle: evidence for capillary recruitment. *Diabetes* 46: 1381-1388, 1997.

210. Rattigan, S., M. G. Clark, and E. J. Barrett. Acute vasoconstriction-induced insulin resistance in rat muscle in vivo. *Diabetes* 48: 564-569, 1999.

211. Rattigan, S., K. A. Dora, E. Q. Colquhoun, and M. G. Clark. Serotonin-mediated acute insulin resistance in the perfused rat hindlimb but not in incubated muscle: a role for the vascular system. *Life Sci.* 53: 1545-1555, 1993.

212. Rattigan, S., K. A. Dora, A. C. Tong, and M. G. Clark. Perfused skeletal muscle contraction and metabolism improved by angiotensin II-mediated vasoconstriction. *Am J Physiol* 271: E96-103, 1996.

213. Rattigan, S., M. G. Wallis, J. M. Youd, and M. G. Clark. Exercise training improves insulin-mediated capillary recruitment in association with glucose uptake in rat hind limb. *Diabetes* submitted: 2001.

214. Redgrave, T. G. and M. J. Callow. The effect of insulin deficiency on the metabolism of lipid emulsion models of triacylglycerol-rich lipoproteins in rats. *Metabolism* 39: 1-10, 1990.

215. Redgrave, T. G., R. C. Maranhao, A. M. Tercyak, E. C. Lincoln, and H. Brunengraber. Uptake of artificial model remnant lipoprotein emulsions by the perfused rat liver. *Lipids* 23: 101-105, 1988.

216. Reidy, S. P. and J. Weber. Leptin: an essential regulator of lipid metabolism. *Comp Biochem.Physiol A Mol.Integr.Physiol* 125: 285-298, 2000.

217. Reimer, F., G. Loffler, G. Hennig, and O. H. Wieland. The influence of insulin on glucose and fatty acid metabolism in the isolated perfused rat hind quarter. *Hoppe Seylers.Z.Physiol Chem.* 356: 1055-1066, 1975.

218. Reimers, K., C. D. Reimers, S. Wagner, I. Paetzke, and D. E. Pongratz. Skeletal muscle sonography: a correlative study of echogenicity and morphology. *J Ultrasound Med.* 12: 73-77, 1993.

219. Renkin, E. M. Effects of blood flow on diffusion kinetics in isolated, perfused hindlegs of cats: A double circulation hypothesis. *Am.J.Physiol.* 183: 125-136, 1955.

220. Rennie, M. J. and J. O. Holloszy. Inhibition of glucose uptake and glycogenolysis by availability of oleate in well-oxygenated perfused skeletal muscle. *Biochem.J* 168: 161-170, 1977.

221. Rennie, M. J., S. E. Khogali, S. Y. Low, H. E. McDowell, H. S. Hundal, A. Ahmed, and P. M. Taylor. Amino acid transport in heart and skeletal muscle and the functional consequences. *Biochem.Soc.Trans.* 24: 869-873, 1996.

222. Richter, E. A., K. J. Mikines, H. Galbo, and B. Kiens. Effect of exercise on insulin action in human skeletal muscle. *J.Appl.Physiol.* 66: 876-885, 1989.

223. Richter, E. A., N. B. Ruderman, H. Gavras, E. R. Belur, and H. Galbo. Muscle glycogenolysis during exercise: dual control by epinephrine and contractions. *Am.J.Physiol.* 242: E25-E32, 1982.

224. Rigalleau, V., C. Binnert, K. Minehira, N. Stefanoni, P. Schneiter, E. Henchoz, O. Matzinger, C. Cayeux, E. Jequier, and L. Tappy. In normal men, free fatty acids reduce peripheral but not splanchnic glucose uptake. *Diabetes* 50: 727-732, 2001.

225. Roberts, C. K., R. J. Barnard, A. Jasman, and T. W. Balon. Acute exercise increases nitric oxide synthase activity in skeletal muscle. *Am J Physiol* 277: E390-E394, 1999.

226. Roden, M., M. Krssak, H. Stingl, S. Gruber, A. Hofer, C. Furnsinn, E. Moser, and W. Waldhausl. Rapid impairment of skeletal muscle glucose transport/phosphorylation by free fatty acids in humans. *Diabetes* 48: 358-364, 1999.

227. Roden, M., T. B. Price, G. Perseghin, K. F. Petersen, D. L. Rothman, G. W. Cline, and G. I. Shulman. Mechanism of free fatty acid-induced insulin resistance in humans. *J Clin.Invest* 97: 2859-2865, 1996.

228. Rodnick, K. J., G. M. Reaven, S. Azhar, M. N. Goodman, and C. E. Mondon. Effects of insulin on carbohydrate and protein metabolism in voluntary running rats. *Am J Physiol* 259: E706-E714, 1990.

229. Ross, B. D. Perfusion techniques in biochemisty: a laboratory manual. Oxford, Clarendon Press. 1972.

230. Rotta, A. and J. N. Stannard. Studies on the oxygen debt of frog tissues. *Am.J.Physiol* 127: 281-289, 1939.

231. Roy, D., M. Perreault, and A. Marette. Insulin stimulation of glucose uptake in skeletal muscles and adipose tissues in vivo is NO dependent. *Am.J.Physiol* 274: E692-E699, 1998.

232. Ruderman, N. B., M. N. Goodman, M. Berger, and S. Hagg. Effect of starvation on muscle glucose metabolism: studies with the isolated perfused rat hindquarter. *Fed.Proc.* 36: 171-176, 1977.

233. Ruderman, N. B., C. R. Houghton, and R. Hems. Evaluation of the isolated perfused rat hindquarter for the study of muscle metabolism. *Biochem.J* 124: 639-651, 1971.

234. Ruderman, N. B., A. K. Saha, D. Vavvas, and L. A. Witters. Malonyl-CoA, fuel sensing, and insulin resistance. *Am J Physiol* 276: E1-E18, 1999.

235. Rudich, A., A. Tirosh, R. Potashnik, M. Khamaisi, and N. Bashan. Lipoic acid protects against oxidative stress induced impairment in insulin stimulation of protein kinase B and glucose transport in 3T3-L1 adipocytes. *Diabetologia* 42: 949-957, 1999.

236. Ryan, A. S. and B. J. Nicklas. Age-related changes in fat deposition in mid-thigh muscle in women: relationships with metabolic cardiovascular disease risk factors. *Int.J Obes.Relat Metab Disord.* 23: 126-132, 1999.

237. Ryder, J. W., A. V. Chibalin, and J. R. Zierath. Intracellular mechanisms underlying increases in glucose uptake in response to insulin or exercise in skeletal muscle. *Acta Physiol Scand.* 171: 249-257, 2001.

238. Saha, A. K., T. G. Kurowski, J. R. Colca, and N. B. Ruderman. Lipid abnormalities in tissues of the KKAy mouse: effects of pioglitazone on malonyl-CoA and diacylglycerol. *Am J Physiol* 267: E95-101, 1994.

239. Saleh, J., A. D. Sniderman, and K. Cianflone. Regulation of Plasma fatty acid metabolism. *Clin.Chim.Acta* 286: 163-180, 1999.

240. Sarabi, M., L. Lind, J. Millgard, A. Hanni, A. Hagg, C. Berne, and H. Lithell. Local vasodilatation with metacholine, but not with nitroprusside, increases forearm glucose uptake. *Physiol Res.* 48: 291-295, 1999.

241. Sarelius, I. H., K. D. Cohen, and C. L. Murrant. Role for capillaries in coupling blood flow with metabolism. *Clin.Exp.Pharmacol.Physiol* 27: 826-829, 2000.

242. Sato, I., M. Sunohara, H. Takahashi, M. Kumagai, and T. Sato. Distributions of adipocyte, blood vessel, and muscle fiber in human lateral petrygoid muscle during ageing. *Okajimas Folia Anat.Jpn.* 76: 101-105, 1999.

243. Schaffner, A., N. Blau, M. Schneemann, J. Steurer, C. J. Edgell, and G. Schoedon. Tetrahydrobiopterin as another EDRF in man. *Biochem.Biophys.Res Commun.* 205: 516-523, 1994.

244. Scherrer, U., D. Randin, P. Vollenweider, L. Vollenweider, and P. Nicod. Nitric oxide release accounts for insulin's vascular effects in humans. *J Clin.Invest* 94: 2511-2515, 1994.

245. Schick, F., B. Eismann, W. I. Jung, H. Bongers, M. Bunse, and O. Lutz. Comparison of localized proton NMR signals of skeletal muscle and fat tissue in vivo: two lipid compartments in muscle tissue. *Magn Reson.Med.* 29: 158-167, 1993.

246. Schmitz-Peiffer, C., D. L. Craig, and T. J. Biden. Ceramide generation is sufficient to account for the inhibition of the insulin-stimulated PKB pathway in C2C12 skeletal muscle cells pretreated with palmitate. *J Biol.Chem.* 274: 24202-24210, 1999.

247. Schwartz, I. F., D. Schwartz, Y. Wollman, T. Chernichowski, M. Blum, Y. Levo, and A. Iaina. Tetrahydrobiopterin augments arginine transport in rat cardiac myocytes through modulation of CAT-2 mRNA. *J Lab Clin Med.* 137: 356-362, 2001.

248. Segal, S. S. Dynamics of microvascular control in skeletal muscle. In Saltin, B., R. Boushel, N. Secher, and J. H. Mitchell, eds. Exercise and Circulation in Health and Disease. Champaign, Human Kinetics. 2000, 141-153.

249. Segal, S. S. Integration of blood flow control to skeletal muscle: key role of feed arteries. *Acta Physiol Scand.* 168: 511-518, 2000.

250. Segal, S. S., S. E. Brett, and W. C. Sessa. Codistribution of NOS and caveolin throughout peripheral vasculature and skeletal muscle of hamsters. *Am.J.Physiol* 277: H1167-H1177, 1999.

251. Shankar R.R., Yong-Gang W., Baron, A., and Shankar S.S. Elevation of free fatty acids does inhibit nitric oxide synthase. The European Association for the Study of Diabetes.Abstract volume of the 36th Annual Meeting. A166. 2001.

252. Shinozaki, K., A. Kashiwagi, Y. Nishio, T. Okamura, Y. Yoshida, M. Masada, N. Toda, and R. Kikkawa. Abnormal biopterin metabolism is a major cause of impaired endothelium-dependent relaxation through nitric oxide/O2- imbalance in insulin-resistant rat aorta. *Diabetes* 48: 2437-2445, 1999.

253. Sidossis, L. S. and R. R. Wolfe. Glucose and insulin-induced inhibition of fatty acid oxidation: the glucose-fatty acid cycle reversed. *Am J Physiol* 270: E733-E738, 1996.

254. Simoneau, J. A., S. R. Colberg, F. L. Thaete, and D. E. Kelley. Skeletal muscle glycolytic and oxidative enzyme capacities are determinants of insulin sensitivity and muscle composition in obese women. *FASEB J* 9: 273-278, 1995.

255. Sipila, S. and H. Suominen. Knee extension strength and walking speed in relation to quadriceps muscle composition and training in elderly women. *Clin.Physiol* 14: 433-442, 1994.

256. Sleeman, M. W., N. P. Donegan, R. Heller-Harrison, W. S. Lane, and M. P. Czech. Association of acyl-CoA synthetase-1 with GLUT4-containing vesicles. *J Biol.Chem.* 273: 3132-3135, 1998.

257. Spence, R. J., B. J. Rhodes, and H. N. Wagner. Regulaiton of arteriovenous anastomotic and capillary blood flow in the dog leg. *Am J Physiol* 222: 326-332, 1972.

258. Stansberry, K. B., M. A. Hill, S. A. Shapiro, P. M. McNitt, B. A. Bhatt, and A. I. Vinik. Impairment of peripheral blood flow responses in diabetes resembles an enhanced aging effect. *Diabetes Care* 20: 1711-1716, 1997.

259. Steinberg, G. R. and D. J. Dyck. Development of leptin resistance in rat soleus muscle in response to high-fat diets. *Am J Physiol Endocrinol.Metab* 279: E1374-E1382, 2000.

260. Steinberg, H. O., G. Brechtel, A. Johnson, N. Fineberg, and A. D. Baron. Insulin-mediated skeletal muscle vasodilation is nitric oxide dependent. A novel action of insulin to increase nitric oxide release. *J Clin.Invest* 94: 1172-1179, 1994.

261. Steinberg, H. O., G. Paradisi, G. Hook, K. Crowder, J. Cronin, and A. D. Baron. Free fatty acid elevation impairs insulin-mediated vasodilation and nitric oxide production. *Diabetes* 49: 1231-1238, 2000.

262. Steinberg, H. O., M. Tarshoby, R. Monestel, G. Hook, J. Cronin, A. Johnson, B. Bayazeed, and A. D. Baron. Elevated circulating free fatty acid levels impair endothelium-dependent vasodilation. *J Clin.Invest* 100: 1230-1239, 1997.

263. Storlien, L. H., J. A. Higgins, T. C. Thomas, M. A. Brown, H. Q. Wang, X. F. Huang, and P. L. Else. Diet composition and insulin action in animal models. *Br.J Nutr.* 83 Suppl 1: S85-S90, 2000.

264. Storlien, L. H., D. E. James, K. M. Burleigh, D. J. Chisholm, and E. W. Kraegen. Fat feeding causes widespread in vivo insulin resistance, decreased energy expenditure, and obesity in rats. *Am J Physiol* 251: E576-E583, 1986.

265. Storlien, L. H., E. W. Kraegen, D. J. Chisholm, G. L. Ford, D. G. Bruce, and W. S. Pascoe. Fish oil prevents insulin resistance induced by high-fat feeding in rats. *Science* 237: 885-888, 1987.

266. Storz, P., H. Doppler, A. Wernig, K. Pfizenmaier, and G. Muller. Cross-talk mechanisms in the development of insulin resistance of skeletal muscle cells palmitate rather than tumour necrosis factor inhibits insulin-dependent protein kinase B (PKB)/Akt stimulation and glucose uptake. *Eur.J Biochem.* 266: 17-25, 1999.

267. Susini, C. and M. Lavau. In-vitro and in-vivo responsiveness of muscle and adipose tissue to insulin in rats rendered obese by a high-fat diet. *Diabetes* 27: 114-120, 1978.

268. Svanberg, E., A. C. Moller-Loswick, D. E. Matthews, U. Korner, M. Andersson, and K. Lundholm. The role of glucose, long-chain triglycerides and amino acids for promotion of amino acid balance across peripheral tissues in man. *Clin Physiol* 19: 311-320, 1999.

269. Szczepaniak, L. S., E. E. Babcock, F. Schick, R. L. Dobbins, A. Garg, D. K. Burns, J. D. McGarry, and D. T. Stein. Measurement of intracellular triglyceride stores by H spectroscopy: validation in vivo. *Am J Physiol* 276: E977-E989, 1999.

270. Szczepaniak, L. S., E. E. Babcock, F. Schick, R. L. Dobbins, A. Garg, D. K. Burns, J. D. McGarry, and D. T. Stein. Measurement of intracellular triglyceride stores by H spectroscopy: validation in vivo. *Am J Physiol* 276: E977-E989, 1999.

271. Taddei, S., A. Virdis, L. Ghiadoni, A. Magagna, and A. Salvetti. Vitamin C improves endothelium-dependent vasodilation by restoring nitric oxide activity in essential hypertension. *Circulation* 97: 2222-2229, 1998.

272. Tan, M. H., T. Sata, and R. J. Havel. The significance of lipoprotein lipase in rat skeletal muscles. *J Lipid Res* 18: 363-370, 1977.

273. Terjung, R. L. and D. A. Hood. The role of amino acids as a fuel for contractile activity in skeletal muscle. In Benzi, G., ed. Advances in Myochemistry Vol. 2. John Libbey Eurotext Ltd. 1989, 251-261.

274. Thiebaud, D., R. A. DeFronzo, E. Jacot, A. Golay, K. Acheson, E. Maeder, E. Jequier, and J. P. Felber. Effect of long chain triglyceride infusion on glucose metabolism in man. *Metabolism* 31: 1128-1136, 1982.

275. Thompson, A. L. and G. J. Cooney. Acyl-CoA inhibition of hexokinase in rat and human skeletal muscle is a potential mechanism of lipid-induced insulin resistance. *Diabetes* 49: 1761-1765, 2000.

276. Ting, H. H., F. K. Timimi, K. S. Boles, S. J. Creager, P. Ganz, and M. A. Creager. Vitamin C improves endothelium-dependent vasodilation in patients with non-insulin-dependent diabetes mellitus. *J Clin Invest* 97: 22-28, 1996.

277. Tovar, A. R., J. K. Tews, N. Torres, and A. E. Harper. Neutral amino acid transport into rat skeletal muscle: competition, adaptive regulation, and effects of insulin. *Metabolism* 40: 410-419, 1991.

278. Turcotte, L. P., B. Kiens, and E. A. Richter. Saturation kinetics of palmitate uptake in perfused skeletal muscle. *FEBS Lett.* 279: 327-329, 1991.

279. Turcotte, L. P., C. Petry, B. Kiens, and E. A. Richter. Contraction-induced increase in Vmax of palmitate uptake and oxidation in perfused skeletal muscle. *J.Appl.Physiol.* 84: 1788-1794, 1998.

280. Turcotte, L. P., J. R. Swenberger, T. M. Zavitz, and A. J. Yee. Increased fatty acid uptake and altered fatty acid metabolism in insulin-resistant muscle of obese Zucker rats. *Diabetes* 50: 1389-1396, 2001.

281. Turpeinen, A. K., T. O. Takala, P. Nuutila, T. Axelin, M. Luotolahti, M. Haaparanta, J. Bergman, H. Hamalainen, H. Iida, M. Maki, M. I. Uusitupa, and J. Knuuti. Impaired free fatty acid uptake in skeletal muscle but not in myocardium in patients with impaired glucose tolerance: studies with PET and 14(R,S)-[18F]fluoro-6-thia-heptadecanoic acid. *Diabetes* 48: 1245-1250, 1999.

282. Undenfriend, S., S. Stein, P. Bohlen, W. Dairman, W. Leimgruber, and M. Weigle. Fluorescamine: A reagent for assay of amino acids, peptides, and primary amines in the picomole range. *Science* 178: 871-872, 1972.

283. van der Vusse, G. J. Lipid metabolism in muscle. In Rowell, L. B. and J. T. Shepherd, eds. Handbook of physiology. New York, Amercian Physiological Society, Oxford Press. 1996, 952-994.

284. van Veen, S. and P. C. Chang. Prostaglandins and nitric oxide mediate insulin-induced vasodilation in the human forearm. *Cardiovasc.Res.* 34: 223-229, 1997.

285. Vicent, D, Ilany, J, Neruse, K, Yanagisawa, M, and Kahn, C. R. Insulin receptor in endothelial cells is not required for glucose homeostasis. The European Association for the Study of

Diabetes.Abstract volume of the 36th Annual Meeting. A33. 2000.

Ref Type: Abstract

286. Vincent, D., J. Ilany, M. Yanagisawa, and C. R. Kahn. Insulin receptor in endothelial cells is not required for glucose homeostasis. *Diabetologia* 43: 2000.

287. Vincent, M. A., Dawson, D, Clark, A. D., Lindner, J. R., and Barrett, E. J. Physiologic hyperinsulinaemia recruits capillaries in skeletal muscle *in vivo* independent of changes in total muscle blood flow. Diabetes Abstract Book.61st Scientific Sessions. A334. 2001.

Ref Type: Abstract

288. Vincent, M. A., S. Rattigan, and M. G. Clark. Microsphere infusion reverses vasoconstrictor-mediated change in hindlimb oxygen uptake and energy status. *Acta Physiol Scand.* 164: 61-69, 1998.

289. Vincent, M. A., Rattigan, S., Clark, M. G., and Barrett, E. J. Inhibition of nitric oxide synthase prevents insulin-mediated capillary recruitment and glucose uptake in skeletal muscle in vivo. Diabetes Abstract Book.61st Scientific Sessions. A334. 2001.

Ref Type: Abstract

290. Vollenweider, P., L. Tappy, D. Randin, P. Schneiter, E. Jequier, P. Nicod, and U. Scherrer. Differential effects of hyperinsulinemia and carbohydrate metabolism on sympathetic nerve activity and muscle blood flow in humans. *J Clin.Invest* 92: 147-154, 1993.

291. von Euler, U. S. The peripheral stimulatory action of adrenaline on cellular metabolism. Influence of the antagonist ergotamine. Article translated from French. *C.R.Soc.Biol.* 108: 246-249, 1931.

292. Wagenmakers, A. J. Muscle amino acid metabolism at rest and during exercise: role in human physiology and metabolism. *Exerc.Sport Sci Rev.* 26: 287-314, 1998.

293. Walker, M., G. R. Fulcher, C. F. Sum, H. Orskov, and K. G. Alberti. Effect of glycemia and nonesterified fatty acids on forearm glucose uptake in normal humans. *Am J Physiol* 261: E304-E311, 1991.

294. Walter, R., P. A. Kaufmann, A. Buck, T. Berthold, C. Wyss, G. K. von Schulthess, A. Schaffner, and G. Schoedon. Tetrahydrobiopterin increases myocardial blood flow in healthy volunteers: a double-blind, placebo-controlled study. *Swiss.Med.Wkly.* 131: 91-94, 2001.

295. Wassner, S. J. and J. B. Li. N tau-methylhistidine release: contributions of rat skeletal muscle, GI tract, and skin. *Am J Physiol* 243: E293-E297, 1982.

296. Wassner, S. J., J. L. Schlitzer, and J. B. Li. A rapid, sensitive method for the determination of 3-methylhistidine levels in urine and plasma using high-pressure liquid chromatography. *Anal.Biochem.* 104: 284-289, 1980.

297. Watford, M. Functional glycerol kinase activity and the possibility of a major role for glyceroneogenesis in mammalian skeletal muscle. *Nutr.Rev.* 58: 145-148, 2000.

298. Wilmoth, F. R., P. D. Harris, and F. N. Miller. Differential serotonin responses in the skeletal muscle microcirculation. *Life Sci.* 34: 1135-1141, 1984.

299. Wohlrab, J., D. Wohlrab, and W. C. Marsch. Acute effect of a dried ethanol-water extract of garlic on the microhaemovascular system of the skin. *Arzneimittelforschung.* 50: 606-612, 2000.

300. Wolfe, B. M., S. Klein, E. J. Peters, B. F. Schmidt, and R. R. Wolfe. Effect of elevated free fatty acids on glucose oxidation in normal humans. *Metabolism* 37: 323-329, 1988.

301. Wood, J. D., M. Enser, A. V. Fisher, G. R. Nute, R. I. Richardson, and P. R. Sheard. Manipulating meat quality and composition. *Proc.Nutr Soc.* 58: 363-370, 1999.

302. Yaspelkis, B. B., III, J. R. Davis, M. Saberi, T. L. Smith, R. Jazayeri, M. Singh, V. Fernandez, B. Trevino, N. Chinookoswong, J. Wang, Z. Q. Shi, and N. Levin. Leptin administration improves skeletal muscle insulin responsiveness in diet-induced insulin-resistant rats. *Am J Physiol Endocrinol.Metab* 280: E130-E142, 2001.

303. Yki-Jarvinen, H. and T. Utriainen. Insulin-induced vasodilatation: physiology or pharmacology? *Diabetologia* 41: 369-379, 1998.

304. Youd, J. M., J. M. Newman, M. G. Clark, G. J. Appleby, S. Rattigan, A. C. Tong, and M. A. Vincent. Increased metabolism of infused 1-methylxanthine by working muscle. *Acta Physiol Scand.* 166: 301-308, 1999.

305. Youd, J. M., S. Rattigan, and M. G. Clark. Acute impairment of insulin-mediated capillary recruitment and glucose uptake in rat skeletal muscle in vivo by TNF-alpha. *Diabetes* 49: 1904-1909, 2000.

306. Young, V. R. and H. N. Munro. Ntau-methylhistidine (3-methylhistidine) and muscle protein turnover: an overview. *Fed.Proc.* 37: 2291-2300, 1978.

307. Zeng, G., F. H. Nystrom, L. V. Ravichandran, L. N. Cong, M. Kirby, H. Mostowski, and M. J. Quon. Roles for insulin receptor, PI3-kinase, and Akt in insulin-signaling pathways related to production of nitric oxide in human vascular endothelial cells. *Circulation* 101: 1539-1545, 2000.

308. Zierler, K. Whole body glucose metabolism. *Am J Physiol* 276: E409-E426, 1999.

309. Zorzano, A., T. W. Balon, M. N. Goodman, and N. B. Ruderman. Additive effects of prior exercise and insulin on glucose and AIB uptake by rat muscle. *Am J Physiol* 251: E21-E26, 1986.

310. Zorzano, A., T. W. Balon, J. A. Jakubowski, M. N. Goodman, D. Deykin, and N. B. Ruderman. Effects of insulin and prior exercise on prostaglandin release from perfused rat muscle. *Biochem.J.* 240: 437-443, 1986.

311. Zweifach, B. W. and D. B. Metz. Selective distribution of blood through the terminal vascular bed of mesenteric structures and skeletal muscle. *Angiology* 6: 282-289, 1955.

Increased chylomicron triglyceride hydrolysis by connective tissue flow in perfused rat hindlimb: implications for lipid storage

L. H. Clerk, M. E. Smith, S. Rattigan, and M. G. Clark[1]

Division of Biochemistry, Medical School, University of Tasmania, Hobart, Australia 7001

Abstract **Skeletal muscle has two circulatory routes, nutritive (in contact with muscle) and non-nutritive (part of which is located in the connective tissue), and the balance of flow between the two is controlled by neural input and circulating vasomodulators. The purpose of this study was to assess muscle triglyceride hydrolysis given that the two circuits may have a differing vascular distribution of hydrolytic activity. The isolated rat hindlimb was perfused with 6% Ficoll® and a radiolabeled chylomicron–lipid emulsion containing apolipoprotein C-II. Serotonin (0.5–1 μM), a model vasoconstrictor previously shown to preferentially increase connective tissue flow, inhibited hindlimb oxygen uptake (from 16.7 ± 0.6 to 10.2 ± 1.0, mean ± SE, n = 7 ($P < 0.001$)) and stimulated [^{14}C]-labeled fatty acid uptake into muscles (from 184 ± 28 to 602 ± 132, mean ± SE, n = 7 ($P = 0.009$)). These effects were reversed by the vasodilator carbamyl choline. Vasopressin resulted in increased oxygen consumption but no change in triglyceride hydrolysis. Cholesteryl oleate uptake (an indicator of endocytosis of the chylomicron or remnant particle) was unaltered by serotonin. It is concluded that chylomicron triglyceride hydrolysis is enhanced by vasoconstrictors that increase connective tissue flow in the perfused rat hindlimb. Increased hydrolysis appears to be primarily due to an increased access of triglyceride to hydrolytic enzymes, presumably lipoprotein lipase associated with the fat cells commonly observed interlaced amongst bundles of muscle fibers.**—Clerk, L. H., M. E. Smith, S. Rattigan, and M. G. Clark. **Increased chylomicron triglyceride hydrolysis by connective tissue flow in perfused rat hindlimb: implications for lipid storage.** *J. Lipid Res.* **2000.** 41: **329–335.**

Supplementary key words lipoprotein lipase • nutritive flow • non-nutritive flow • oxygen consumption • perfusion pressure

The uptake of lipoprotein triglycerides (TG) into target tissues requires initial hydrolysis and this is thought to be facilitated by the enzyme lipoprotein lipase (LPL). LPL is attached to the vascular endothelium by proteoglycans which allow protrusion of the enzyme into the vascular lumen. Here it acts to hydrolyze TG from circulating TG-rich lipoproteins (chylomicrons and very low density lipoproteins) into free fatty acids (FFA) and glycerol. The resulting FFA are taken up by tissues capable of lipid oxidation (e.g., muscle) or storage (e.g., adipose tissue, muscle) (1, 2).

The hydrolysis of TG to FFA and glycerol has been found to be proportional to the active amount of LPL in the vasculature (3) and ultimately may depend on whether circulating TG has access to the active form of LPL or other hydrolytic enzymes. In skeletal muscle an important determinant of muscle metabolism is substrate supply to the myocytes and is controlled by the proportioning of flow between two distinct vascular circuits (4, 5). The first is termed nutritive and describes flow predominantly to the muscle cells. Blood flowing through the second circuit, termed non-nutritive, almost certainly passes through vessels of the connective tissue associated with the muscle (6). Flow through this route results in the physical isolation of nutrients and hormones (including oxygen, glucose, TG, and insulin) from the myocytes (7). As a result there is limited opportunity for muscle nutrient uptake. As TG hydrolysis is dependent upon its exposure to hydrolytic enzymes, it follows that the total hydrolysis of TG entering the muscle will be greater when the predominance of flow is through the circuit in which the majority of the hydrolytic activity is distributed. To date there have been no studies describing the location of skeletal muscle TG hydrolytic activity including LPL, and its relative distribution in muscle nutritive capillaries or in connective tissue vessels (non-nutritive for muscle) (6).

The concept of a dual vascular system in skeletal muscle was proposed as early as the 1940s. Experiments done by Pappenheimer (8) showed that norepinephrine administration to the gastrocnemius muscle of dogs resulted in an increase in oxygen consumption while stimulation of vaso-

---

Abbreviations: 5-HT, serotonin; apoC-II, apolipoprotein C-II; CO, cholesteryl oleate; LPL, lipoprotein lipase; HIRS, heat-inactivated rat serum; $\dot{V}O_2$, oxygen consumption; PP, perfusion pressure; CLE, chylomicron lipid emulsion; TO, triolein; FFA, free fatty acid (unesterified); TG, triglyceride; BSA, bovine serum albumin; HEPES, N-[2-hydroxyethyl]piperazine-N′ [2-ethanesulfonic acid]; CCh, carbamyl choline.

[1] To whom correspondence should be addressed.

choice. Thus 5-HT (Sigma) was added as a bolus into the buffer reservoir of the appropriate perfusions to give a final concentration of 0.5–1 μM (to achieve a peak perfusion pressure of approximately 100 mm Hg above basal). After discarding the first 30 ml of perfusate (of the 130 ml perfusion medium containing CLE) the remaining 100 ml was recirculated through the hindlimb for 1 h. Samples (2.5 ml) were withdrawn from the venous line every 15 min.

In some experiments the vasodilator CCh was infused at a final concentration of 100 μM to reverse the effects of 5-HT on PP and $\dot{V}O_2$. CCh infusion commenced before buffer was recirculated. This was designed to allow the PP and $\dot{V}O_2$ to return to near-basal states before TG recirculation and prevent perfusion under predominantly non-nutritive conditions. Infusion was continued for a further 12.5 min after recirculation.

The type A vasoconstrictor vasopressin was added as a bolus dose (0.5 nM) to the reservoir of some perfusions to investigate the effects of increased $\dot{V}O_2$ and PP on chylomicron TG hydrolysis.

Triglyceride hydrolysis

Perfusate samples (1 ml) from perfusions using [^{14}C]TO were added to 4 ml methanol–chloroform 2:1 in 10-ml glass tubes with screw caps. The tubes were vortexed (3 × 30 s) and maintained at room temperature (22°C) before centrifuging at 2500 *g* for 10 min. The entire lower layer was removed with a glass pipette into a 5-ml test tube and evaporated to dryness in a water bath at 40°C under a stream of nitrogen. The residue was reconstituted into 100 μl of the chloroform–methanol mixture and 15 μl was immediately applied to a Merck silica gel 60 F_{254} aluminium sheet (Merck). Standards (10 μl of 10 mg/ml) of TO, CO, and oleic acid were also applied as spots. The plates were run using a mixture of n-heptane–diethyl ether–glacial acetic acid 80:20:1. Plates were visualized in an iodine tank and TO and oleic acid spots were scraped into separate plastic tubes and counted with 4 ml of Amersham Biodegradable Counting Scintillant. Recovery of counts after thin-layer chromatography was periodically checked by comparing the total radioactivity scraped from one lane of the silica plate (a lane was designated for each perfusate sample) with the known amount of radioactivity of the corresponding perfusate sample before solvent extraction. The recovery was between 90 and 110%.

Muscle radioactivity uptake

After perfusion, the soleus, plantaris, gastrocnemius white and red, tibialis and extensor digitorum longus muscles of the perfused hindlimb were removed. Within the context of this study it is important to note that interfibrillar connective tissue adipocytes are contained within each muscle. Excised muscles were freeze-dried overnight to obtain dry weight and later re-hydrated with 1 ml of water and 1 ml of Soluene® (tissue solubiliser; Packard). When digestion was complete, 100 μl of acetic acid was added together with 14 ml of Amersham Biodegradable Counting Scintillant.

Statistical analysis

The statistical significance of differences between groups of data was assessed by unpaired, two-tailed Student's *t*-test. Significant differences were recognized at $P < 0.05$.

RESULTS

Clearance of chylomicron TG by perfused muscle has not previously been studied and it was therefore necessary to conduct a number of preliminary experiments to determine an optimal procedure. The commonly used albumin-containing perfusion medium was not entirely satisfactory as FFA released by LPL were subsequently bound by the albumin and little was taken up by the hindlimb. A second difficulty encountered was the high contamination of serum albumin by lipases. Thus lipase substrates such as *p*-nitrophenyl palmitate were rapidly hydrolyzed (data not shown) causing basal rates of hydrolysis to be largely attributable to these contaminants when using albumin-containing perfusion medium. Accordingly, we chose to use Ficoll®-containing perfusion medium. With this medium there was no hydrolysis due to the perfusion medium alone and the uptake of released FFA occurred so that muscle-specific uptake could be compared at the completion of each perfusion.

Figure 1 shows the time course for the effects of 0.5–1 μmol 5-HT, 0.5-1 μM 5-HT with 100 μM CCh or 0.5 nM vasopressin on changes in $\dot{V}O_2$ and PP in the constant flow, Ficoll® perfused rat hindlimb. Changes in $\dot{V}O_2$ and PP both reached a maximum at 15 min and then declined as the vasoconstrictors were metabolized by the hindlimb during the recirculating perfusion. However, changes in $\dot{V}O_2$ and PP were significantly different ($P < 0.05$) from controls at all time points for 5-HT and vasopressin. The

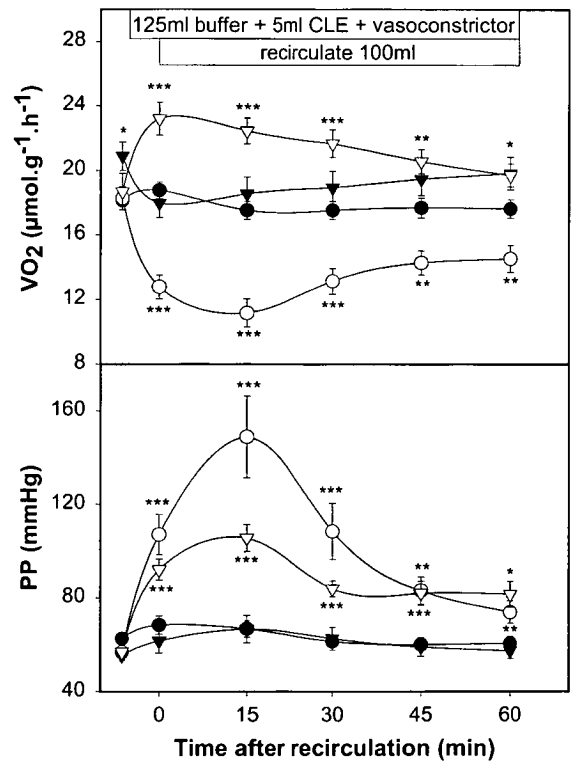

Fig. 1. Time course for the effects of serotonin (5-HT), 5-HT with carbamyl choline (CCh), and vasopressin on oxygen consumption ($\dot{V}O_2$) and perfusion pressure (PP) in the constant flow Ficoll®-perfused rat hindlimb. All perfusions were conducted at constant flow (8 ml/min) using a recirculating mode (total buffer volume = 100 ml). Basal values are at t = −6.25 min. Additions at −6.25 min were vehicle (●), 0.5–1 μM 5-HT (○), 0.5–1 μM 5-HT + 100 μM CCh (▼) or 0.5 nM vasopressin (▽). Values are means ± SE. ** $P < 0.01$; *** $P < 0.001$ for treatment vs. vehicle (n = 10–12).

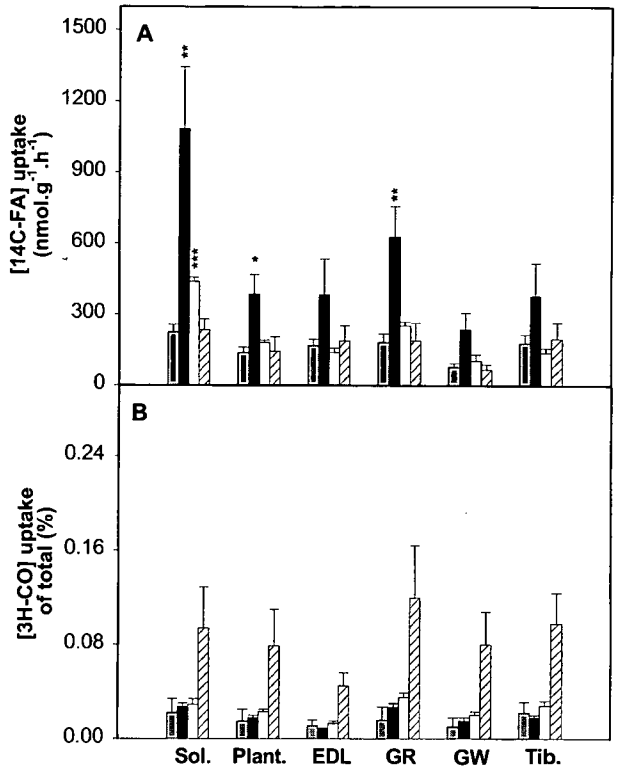

Fig. 2. Uptake of [^{14}C]oleic acid and [^{3}H]cholesteryl oleate ([^{3}H]CO) into hindlimb muscles in constant flow Ficoll®-perfused rat hindlimb using a chylomicron lipid emulsion (CLE) and heat-inactivated rat serum (HIRS) as a source of apolipoprotein CII. Hindlimb muscles dissected include the soleus (Sol.), plantaris (Plant.), extensor digitorum longus (EDL), gastrocnemius red (GR), gastrocnemius white (GW) and tibialis (Tib.). The effects of serotonin (0.5–1 μM, 5-HT, black bar), 5-HT and carbamyl choline (0.5–1 μM 5-HT + 100 μM CCh, white bar) and vasopressin (0.5 nM, hatched bar) were measured for each CLE type and compared to perfusions with no additions (control, grey bar). CLE contained either [^{14}C]triolein ([^{14}C]TO (panel A)) or [^{3}H]CO (panel B). The values in panel B are the percentage of total circulating CO that is taken up by each muscle. Values are means ± SE (n = 4–7) * $P < 0.05$; ** $P < 0.01$; *** $P < 0.001$ for treatment versus vehicle.

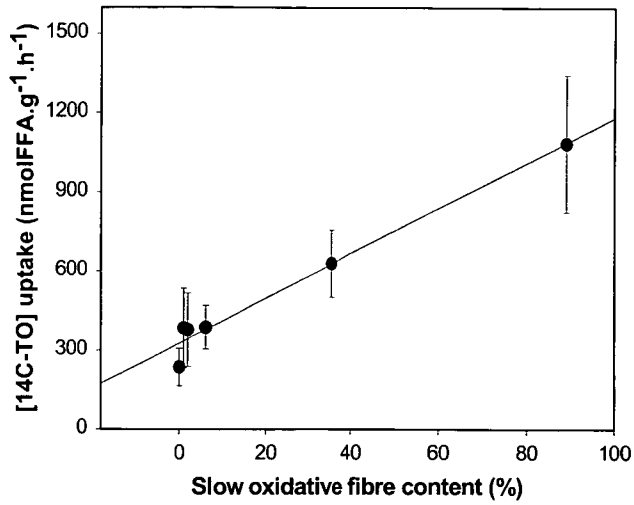

Fig. 3. Uptake of FFA from a synthetic chylomicron emulsion using the mean values for uptake with 0.5–1 μM serotonin (5-HT) for each hindlimb muscle and their corresponding percentage content of slow oxidative fibers. The linear regression produces an $r^2 = 0.975$ ($P < 0.001$). The percentage content of slow oxidative fibres was taken from reports by Ariano, Armstrong, and Edgerton (31) and Armstrong and Laughlin (32).

micron must remain in the perfusate. In fact, the perfusate FFA levels with vasopressin are significantly higher than the control value (Table 1).

Figure 3 is a plot of the percentage content of slow oxidative fibers against the uptake of [^{14}C]FA in a hindlimb preconstricted with 5-HT for each muscle. [^{14}C]FA uptake when flow is predominantly non-nutritive significantly correlates ($r = 0.987$, $P < 0.001$) with the percentage content of slow oxidative fibers.

DISCUSSION

The importance of skeletal muscle in total circulating lipid clearance is often underestimated, and all previous reports have neglected the effect of flow partitioning on TG clearance in muscle, due to the presence of nutritive and non-nutritive routes. Here we report that the hydrolysis of TO was markedly increased in the perfused rat hindlimb when a high proportion of connective tissue flow occurred. Recruitment of connective tissue flow for these experiments was induced by the addition of 5-HT, a representative type B vasoconstrictor, which has previously been reported to decrease oxygen uptake, lactate output, insulin-mediated glucose uptake (21, 22), and tension development of aerobically contracting muscle (23). All of these changes are characteristic of type B vasoconstriction (7) and are representative of decreased nutrient delivery to muscle, and decreased muscle metabolism secondary to increasing the proportion of non-nutritive or connective tissue flow within muscle (5).

When connective tissue flow was increased by addition of the vasoconstrictor, 5-HT, there was a marked increase in TG hydrolysis (indicated by [^{14}C]FA uptake) in the soleus, plantaris and gastrocnemius red muscles. Uptake of [^{14}C]FA greatly exceeded that of the CO with serotonin. This implies that uptake due to endocytosis of the chylomicron (causing TO radioactivity to be found in the muscle without any detectable amounts of hydrolysis) or of the chylomicron remnant (where all of the [^{14}C] oleic acid or [^{14}C]TO in the muscle is due to hydrolysis) could not account for the observed increase. It is important to note that the reported increase in TG hydrolysis occurred without any stimulation of LPL activity by 5-HT. This indicates that the TG hydrolysis due to 5-HT is likely to be the result of a vascular effect whereby the exposure of TG to TG hydrolytic activity, presumably LPL, is increased. From this, it would also seem likely that the distribution of TG hydrolytic activity is greater along the non-nutritive or connective tissue circuit that nourishes interlacing adipocytes than along the nutritive route supplying muscle cells.

Evidence that the vessels of non-nutritive flow are those

15. Redgrave, T. G., and M. J. Callow. 1990. The effect of insulin deficiency on the metabolism of lipid emulsion models of triacylglycerol-rich lipoproteins in rats. *Metabolism.* **39:** 1–10.
16. Bengtsson-Olivecrona, G., and T. Olivecrona. 1992. Assay of lipoprotein lipase and hepatic lipase. *In* Lipoprotein Analysis, a Practical Approach. C. A. Converse and E. R. Skinner, editors. Oxford University Press, New York. 169–185.
17. Ruderman, N. B., C. R. Houghton, and R. Hems. 1971. Evaluation of the isolated perfused rat hindquarter for the study of muscle metabolism. *Biochem. J.* **124:** 639–651.
18. Colquhoun, E. Q., M. Hettiarachchi, J. M. Ye, E. A. Richter, A. J. Hniat, S. Rattigan, and M. G. Clark. 1988. Vasopressin and angiotensin II stimulate oxygen uptake in the perfused rat hindlimb. *Life Sci.* **43:** 1747–1754.
19. Dora, K. A., S. M. Richards, S. Rattigan, E. Q. Colquhoun, and M. G. Clark. 1992. Serotonin and norepinephrine vasoconstriction in rat hindlimb have different oxygen requirements. *Am. J. Physiol.* **262:** H698–H703.
20. Dora, K. A., E. Q. Colquhoun, M. Hettiarachchi, S. Rattigan, and M. G. Clark. 1991. The apparent absence of serotonin-mediated vascular thermogenesis in perfused rat hindlimb may result from vascular shunting. *Life Sci.* **48:** 1555–1564.
21. Rattigan, S., K. A. Dora, E. Q. Colquhoun, and M. G. Clark. 1993. Serotonin-mediated acute insulin resistance in the perfused rat hindlimb but not in incubated muscle: a role for the vascular system. *Life Sci.* **53:** 1545–1555.
22. Rattigan, S., K. A. Dora, A. C. Tong, and M. G. Clark. 1996. Perfused skeletal muscle contraction and metabolism improved by angiotensin II-mediated vasoconstriction. *Am. J. Physiol.* **271:** E96–103.
23. Dora, K. A., S. Rattigan, E. Q. Colquhoun, and M. G. Clark. 1994. Aerobic muscle contraction impaired by serotonin-mediated vasoconstriction. *J. Appl. Physiol.* **77:** 277–284.
24. Grant, R. T., and H. P. Wright. 1970. Anatomical basis for nonnutritive circulation in skeletal muscle exemplified by blood vessels of rat biceps femoris tendon. *J. Anat.* **106:** 125–133.
25. Szczepaniak, L. S., E. E. Babcock, F. Schick, R. L. Dobbins, A. Garg, D. K. Burns, J. D. McGarry, and D. T. Stein. 1999. Measurement of intracellular triglyceride stores by H spectroscopy: validation in vivo. *Am. J. Physiol.* **276:** E977–E989.
26. Wood, J. D., M. Enser, A. V. Fisher, G. R. Nute, R. I. Richardson, and P. R. Sheard. 1999. Manipulating meat quality and composition. *Proc. Nutr. Soc.* **58:** 363–370.
27. Eriksson, E., and R. Myrhage. 1972. Microvascular dimensions and blood flow in skeletal muscle. *Acta Physiol. Scand.* **86:** 211–222.
28. Camps, L., M. Reina, M. Llobera, S. Vilaro, and T. Olivecrona. 1990. Lipoprotein lipase: cellular origin and functional distribution. *Am. J. Physiol.* **258:** C673–C681.
29. van der Vusse, G. J. 1996. Lipid metabolism in muscle. *In* Handbook of Physiology. L. B. Rowell and J. T. Shepherd, editors. American Physiological Society, Oxford Press, New York. 952–994.
30. Eaton, P., and D. Steinberg. 1961. Effects of medium fatty acid concentration, epinephrine, and glucose on palmitate-1-C14 oxidation and incorporation into neutral lipids by skeletal muscle in vitro. *J. Lipid Res.* **2:** 376–382.
31. Ariano, M. A., R. B. Armstrong, and V. R. Edgerton. 1973. Hindlimb muscle fiber populations of five mammals. *J. Histochem. Cytochem.* **21:** 51–55.
32. Armstrong, R. B., and M. H. Laughlin. 1985. Muscle function during locomotion in mammals. *In* Circulation, Respiration, and Metabolism. R. Gilles, editor. Springer-Verlag Berlin. 56–63.

Acta Physiol Scand 2000, **168**, 519–530

Nutritive and non-nutritive blood flow: rest and exercise

M.G. CLARK, S. RATTIGAN, L.H. CLERK, M.A. VINCENT, A.D.H. CLARK, J.M. YOUD and J.M.B. NEWMAN

Division of Biochemistry, Medical School, University of Tasmania, Hobart, Australia

ABSTRACT

There is growing evidence to support the notion of two vascular routes within, or closely associated with skeletal muscle. One route is in intimate contact with muscle cells (hence is known as 'nutritive') and the other functions as a vascular shunt (and has had the interesting misnomer of 'non-nutritive'). Recent findings suggest that the 'non-nutritive' route may, in part, be those vessels in closely associated (interlacing?) connective tissue that nourishes attached fat cells, and may form the basis of 'marbling' of muscle in obesity. In addition, embolism studies using various size microspheres indicate that the 'non-nutritive' vessels are likely to be capillaries fed by terminal arterioles that branch from the same transverse arterioles as those supplying terminal arterioles of the muscle capillaries (i.e. two vascular systems operating in parallel). The proportion of flow distributed between the two routes is tightly regulated and controls muscle metabolism and contraction by regulating hormone and substrate delivery as well as product removal. Because a high proportion of nutritive flow may elevate the set point for basal metabolism, a low proportion of nutritive flow in muscle at rest confers an evolutionary advantage, particularly when food is scarce. In addition, the proportion of flow that is carried by the non-nutritive routes at rest affords a flow reserve that can be switched to the nutritive route to amplify nutrient supply during exercise. Alternatively the non-nutritive route may allow flow to escape when active muscle contraction compresses its nutritive capillaries. Thus rhythmic oscillation of blood flow between the non-nutritive and nutritive networks may aid the muscle pump.

Keywords amplification of nutrient delivery, connective tissue adipocytes, connective tissue flow, microsphere embolism, muscle capillary flow, resting muscle metabolism.

Received 18 November 1999, accepted 9 December 1999

The metabolic needs of the muscle are met by changes in blood flow that are in turn tightly regulated by central neural mechanisms, local reflexes, circulating mediators and locally produced vasoactive substances. The microcirculation of muscle plays a major role in the control of metabolism and it now seems probable that muscle metabolism at rest and during exercise may be controlled by the distribution of blood flow within muscle, albeit between nutritive and non-nutritive routes. The reader is directed to our previous reviews on this topic (Clark *et al.* 1995, 1997, 1998a, b). The aim of this article is to throw some new light on the identity and function of the so-called 'non-nutritive' vascular route of skeletal muscle at rest and during exercise.

Concept of nutritive and non-nutritive flow routes in muscle

The concept of two vascular routes, one nutritive and the other 'non-nutritive' in muscle presents serious implications for some commonly held theories. For example, because the two routes operate in parallel, changes in the proportion of flow distributed between the two routes as mediated by adrenaline or other vasoactive substances, inevitably results in arteriovenous extraction fractions that differ although the total blood flow does not change. Indeed it has been observations of this kind that have given rise to the concept of two routes. Thus, these have involved studies where total blood flow into muscle did not correlate with (a) metabolic or heat transfer responses or (b) the clearance of intramuscular injected or infused radioactive substances. We have recently reviewed the earlier literature (Clark *et al.* 1998b) and the reader is referred therein for references.

The key observations that impact on our present interpretations are those of Zweifach & Metz (1955), Barlow *et al.* (1958, 1961), Grant & Wright (1970), Lindbom & Arfors (1984, 1985) and Borgstrom *et al.* (1988). Barlow *et al.* (1961) simultaneously recorded clearance of radioactive ions (either ^{24}Na, ^{42}K or ^{131}I)

Correspondence: Prof. Michael G. Clark, Division of Biochemistry, University of Tasmania, GPO Box 252-58, Hobart 7001 TAS, Australia.

is. Indeed they have shown that the vascular arrangement of the tenuissimus muscle exists as a basic unit in hind leg musculature generally. Moreover, vascular connections between the muscle tissue proper and adjacent connective tissue septa have also been reported as a feature in several muscles of different species [e.g. rat (Eriksson & Myrhage 1972, Grant & Wright 1970), cat (Myrhage & Eriksson 1980) and monkey (Hammersen 1970)]. Importantly, these same connective tissue vessels have been variously associated with the interlacing fat cell deposits, and thus may be nutritive for connective tissue and the associated adipocytes although they are clearly 'non-nutritive' for muscle. As both connective tissue and adipocytes would have considerably lower metabolic activity than muscle, the overall oxygen extraction and lactate production would very likely fall when flow is switched from the nutritive capillaries of muscle to these connective tissue vessels.

RECENT EVIDENCE FOR NON-NUTRITIVE ROUTES IN MUSCLE

The mechanically pumped constant flow perfused rat hindlimb has proved to be a useful *in vitro* model system to investigate haemodynamic effects on skeletal muscle. It has provided important new information concerning the regulation of flow within muscle. In particular, we now know that vasoactive agents can control skeletal muscle metabolism and performance by their effects on the vasculature (Clark *et al.* 1995, 1997). Thus, our studies have shown that vasoconstrictors, which increase the perfusion pressure in the constant-flow perfused rat hindlimb, can be categorized into two types depending on their metabolic actions in the hindlimb. One type A results in an increase in oxygen consumption (Colquhoun *et al.* 1988), lactate (Hettiarachchi *et al.* 1992), glycerol (Clark *et al.* 1994), urate (Clark *et al.* 1990) and uracil (Clark *et al.* 1990) efflux. These type A vasoconstrictors include α_1-adrenergic agonists, angiotensins, vasopressin, vanilloids and low-frequency (< 2Hz) sympathetic nerve stimulation (Hall *et al.* 1997). Angiotensin II, one of the type A vasoconstrictors, was found to increase aerobic tension development, contraction-mediated oxygen uptake and 2-deoxyglucose uptake by plantaris and gastrocnemius red and white muscles during electrical tetanic stimulation of the hindlimb (Rattigan *et al.* 1996). Type B vasoconstrictors which can produce identical pressure to type A result in decreased oxygen consumption (Dora *et al.* 1991), lactate (Hettiarachchi *et al.* 1992), glycerol (Clark *et al.* 1995), urate and uracil efflux (Clark *et al.* 1995). These vasoconstrictors include serotonin (5-HT), high-dose noradrenaline, high-frequency (>5 Hz) sympathetic nerve stimulation and high-dose vanilloids (Clark *et al.* 1995) and act opposite to type A to decrease insulin-mediated glucose uptake (Rattigan *et al.* 1993, 1995), aerobic tension development and contraction-mediated oxygen uptake (Dora *et al.* 1994). All effects of both types of vasoconstrictors occur while total flow is held constant and are caused by their vascular actions and not owing to direct actions on the skeletal muscle as all of the effects could be reversed by vasodilators (Colquhoun *et al.* 1988, 1990, Hettiarachchi *et al.* 1992, Rattigan *et al.* 1993), regardless of the mechanism of action of the vasodilators. In addition, none of the vasoconstrictors had any effect upon contractility or insulin-mediated glucose uptake of isolated incubated muscles where supply of nutrients was by diffusion and not dependent upon the vasculature (Dora *et al.* 1994, Rattigan *et al.* 1993, 1995). It is also important to note that the sites responsible for types A and B vasoconstriction could be distinguished by their metabolic requirements for constriction. Thus removal of extracellular calcium or inhibition of oxidative metabolism (cyanide, azide or by anoxic perfusion) prevented type A but not type B vasoconstriction (Dora *et al.* 1992, Clark *et al.* 1994).

The controversial nature of the non-nutritive route

A major stumbling block in the acceptance of non-nutritive flow in skeletal muscle has been the anatomical identity of a discrete route associated with muscle that essentially denies nutrient exchange but is capable of high flow. The first stage in shedding some light on their location came from the use of flow measurement using fluorescent microspheres. The aim was to assess whether flow redistributed between muscles of differing fibre composition, or between muscle and non-muscle tissue when vasoconstrictors such as noradrenaline or serotonin acted to vasoconstrict in the constant-flow perfused rat hindlimb and stimulate or inhibit metabolism, respectively. Thus microspheres of 15 μm were infused under conditions of steady-state with or without noradrenaline or serotonin. Muscles, including soleus, plantaris, gastrocnemius red, gastrocnemius white, tibialis, extensor digitorum longus, remaining calf muscles, vastus, remaining thigh and trunk muscle, as well as bone, skin and subcutaneous white adipose tissue of the perfused leg were dissected free. In addition, tissues were collected from unperfused regions to check for leakage. For each sample, wet weight and microsphere content were determined. The results of Fig. 2 show that when compared with control (vehicle), neither noradrenaline nor serotonin infusion altered microsphere recovery in muscle, spine, skin, white adipose tissue or tissues of the lower abdomen. Of the muscles, only two, soleus and tibialis, showed a significant change and this was a decrease

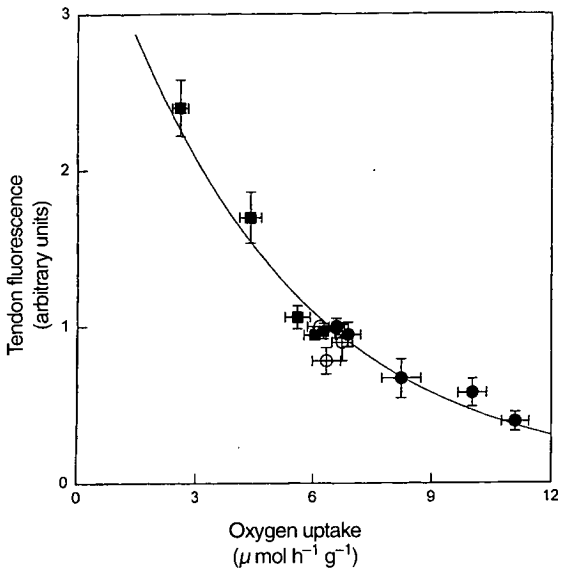

Figure 3 Plot of tendon vessel flow as a function of oxygen uptake modified by vasoconstrictor addition. Experiments were conducted using the isolated constant-flow perfused rat hindlimb where oxygen uptake, an indicator of relative nutritive flow in this preparation, was altered systematically by addition of various doses of either noradrenaline (●), serotonin (■) or vehicle (○). Tendon vessel flow was determined from fluorescence signal strength of infused fluorescein isothiocyanate-labelled dextran (M_r 150 000) over the tibial tendon region of the biceps femoris muscle. Data are from Newman *et al.* (1997).

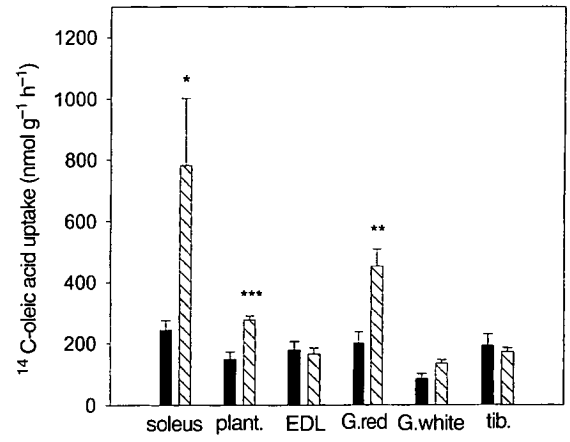

Figure 4 Effects of serotonin (0.5–1 μM) on the uptake of oleate from triolein-containing chylomicron emulsions into muscles of the perfused rat hindlimb. Hindlimb muscles dissected were soleus, plantaris (plant.), extensor digitorum longus (EDL), gastrocnemius red (G. red), gastrocnemius white (G. white) and tibialis (tib.). Data are from Clerk *et al.* (1999) and show effects of no addition (■) or serotonin (▨); significant differences are marked by *. These effects were not the result of increased pinocytotic uptake by 5-HT (data not shown).

micron emulsion. Quite unexpectedly we found that clearance was increased under conditions of predominantly non-nutritive flow (Clerk *et al.* 1999) (Fig. 4), indicating that lipoprotein lipase was more concentrated in the non-nutritive than the nutritive route. As lipoprotein lipase is synthesized in fat and muscle cells and secreted into neighbouring capillaries and adipose tissue contains more activity of lipoprotein lipase than muscle, the higher clearance of triglyceride during non-nutritive flow would suggest an active presence of adipocytes on this route. Indeed adipocytes have been reported on connective tissue vessels in muscle, particularly on the vessels that pass through the perimysium and epimysium (Myrhage & Eriksson 1980). Figure 5 shows such an arrangement where adipocytes can be seen attached to the connective tissue vessels on the superoanterior border of the rat biceps femoris muscle. It is also apparent from this picture that blood is supplied to both muscle and adipocytes by a common vessel (i.e. two systems are operating in parallel).

As foreshadowed earlier, it would now seem likely that the so-called 'non-nutritive' vessels of muscle are connective tissue vessels that are closely associated with each muscle and which can be viewed as separate entities on relatively exposed thin tendons such as the tibial tendon of the rat biceps femoris (Grant & Wright 1970). In addition, it is likely that these vessels are interspersed between fibre bundles and constitute loci where fat accretion can take place to possibly give rise to the 'marbling' of meat. There are sufficient available data to suggest that these vessels are high capacitance and low resistance and therefore capable of carrying high flow when muscle is at rest. Finally, although they may be larger than the nutritive capillaries nourishing muscle cells, these connective tissue adipocyte vessels do not allow the passage of 15-μm microspheres [i.e. when non-nutritive flow is high (Rattigan *et al.* 1997a)].

Figure 5 Photomicroscopy of blood vessels of the superoanterior border of the rat biceps femoris muscle showing connective tissue adipocytes adjacent to the muscle. Blood is supplied to both muscle and adipocytes by a common vessel.

involving a selective increase in muscle nutritive flow consistent with our observations using the constant-flow perfused rat hindlimb. The vasodilator, isoproterenol would appear to have selectively increased flow to the non-nutritive pathway at the expense of nutritive flow. In our experience (Colquhoun *et al.* 1990) isoproterenol opposes type A vasoconstrictor effects in the constant-flow perfused hindlimb by relaxing constricted sites in the vasculature that are reducing flow to non-nutritive routes. As already indicated above microspheres probably do not allow the discrimination between nutritive and non-nutritive routes of muscle and we know that agents such as serotonin do not alter the distribution of 15-μm microspheres, yet have a marked inhibitory effect on oxygen uptake and metabolism generally (Rattigan *et al.* 1997a).

From our point of view the study of Kuznetsova *et al.* (1998) suggested that LDF measured nutritive flow in muscle. Accordingly, we have recently conducted a series of studies aimed at comparing muscle LDF signal during various states of nutritive flow in the constant-flow blood perfused rat hindlimb. In this work a single LDF probe was positioned over the mid region of the exposed biceps femoris. The LDF signal strength was found to directly relate to the extent of oxygen consumption when total flow was constant (Clark *et al.* 1999). Thus type A vasoconstrictors that increased metabolism in this preparation increased the LDF signal. Conversely, type B vasoconstrictors that decreased metabolism, also decreased LDF signal (Clark *et al.* 1999). These findings, although welcome in terms of paving the way for nutritive flow measurement in humans, raise a major question concerning the anatomical location of the non-nutritive vessels and their relative invisibility to LDF detection when probes are placed over the muscle body. Initial consideration might suggest the data to be entirely consistent with the notion that the type B vasoconstrictors have acted to redirect flow from capillaries within muscle (and therefore the region of LDF measurement) to vessels outside the region in connective tissue. However, other possibilities cannot be ignored. For example, from LDF signal measurements (which are non-vectorial) made on blood cell-perfused isolated polymer tubes of single pass and triple pass (zigzag) configurations, each with identical flow rates, it was found that the LDF signal strengths were low and high, respectively (Clark *et al.* 1999). This might imply that decreases in LDF signal caused by the type B vasoconstrictors in perfused muscle result from switching of flow from long zigzag capillaries that pass several times under the detector and give a high LDF signal, to short capillaries that pass fewer times under the detector and give a low LDF signal. Type A vasoconstrictors would have the reverse effect and with this model of the microvasculature, only the length and therefore surface area available for nutrient exchange would distinguish nutritive from non-nutritive route. At the moment we favour a model consistent with the observations of Myrhage & Eriksson (1980) where the connective tissue vessels that operate in parallel to the muscle capillary networks and are visible on the distal edge of flat muscles such as the tenuissimus, are internalized to run between the fibres in the cylindrical bulk muscles.

Size-dependent effects of microsphere embolism: clues to the nature of nutritive and non-nutritive routes

As indicated above, vasoconstriction of the constant-flow perfused rat hindlimb can either increase or decrease skeletal muscle metabolism possibly owing to flow redistribution through nutritive or non-nutritive flow routes, respectively. In a recent unpublished study, we have used microspheres of different size and number to assess whether specific occlusion of either flow route was possible, as well as to determine the largest average diameter at which flow can be redistributed from one to the other route by microsphere embolism. Microspheres of 5.4, 11.8, 23.4 or 93.6 μm, with one size allocated for each series of experiments, were injected and their effects on flow recruitment and metabolism assessed. Injections were conducted during angiotensin II (high nutritive: non-nutritive flow) or serotonin (low nutritive: non-nutritive flow), or under control conditions and the effects on oxygen uptake, perfusion pressure and venous flow rate monitored. The effects were very much dependent on the size of the microspheres. Thus, the inhibitory effects of serotonin on oxygen uptake were partly reversed by 5.4 or 11.8 μm microspheres but not by the larger sizes (23.4 and 93.6 μm). Similarly, only the smaller sizes (5.4 and 11.8 μm) increased oxygen uptake during vehicle infusion. The stimulatory effect of angiotensin II on oxygen uptake was reversed by all four sizes of microspheres. Most importantly, the particular number of microspheres used in these experiments did not significantly affect the venous flow rate. The larger size microspheres of 23.4 and 93.6 μm were inhibitory during serotonin, angiotensin II and vehicle infusions with increased perfusion pressure. Interestingly, the number of the smaller microspheres required to reverse the inhibitory effects of serotonin differed. Thus 1.5×10^7 of the 5.4 μm were equivalent to 3.0×10^6 of 11.8 μm in recovering $\approx$1.6 μmol h^{-1} g^{-1} of oxygen uptake previously inhibited by serotonin. Taken together, it would appear likely that the 5.4 and 11.8 μm but not the 23.4 and 93.6 μm microspheres were capable of occluding the flow route recruited by a specific vasoconstrictor and re-diverting this flow through the opposite flow route. The size-dependent

There are two schools of thought concerning the origin of the oxygen deficit. Traditionally, it was thought to be the result of a delay in skeletal muscle blood flow and thus oxygen delivery to skeletal muscle. Recently, this view has been challenged (Grassi *et al.* 1996, Sahlin *et al.* 1988) and attributed to a lag in mitochondrial metabolism owing to poor substrate supply to the mitochondria. Two experimental approaches support this latter notion. In one, administration of dichloracetate, an activator of the pyruvate dehydrogenase complex, resulted in increased acetyl group availability and attenuation of creatine phosphate breakdown and lactate accumulation in human skeletal muscle during exercise (Timmons *et al.* 1998). In the second, increased fatty acid availability and enhanced muscle oxidative capacity (following a period of short-term training) were shown to attenuate creatine phosphate degradation, glycogenolysis and lactate accumulation during exercise (Chesley *et al.* 1996, Dyck *et al.* 1996). However, at this point of time it is unknown whether dichloracetate could affect microvascular flow, particularly the proportion of nutritive/non-nutritive flow within skeletal muscle. There are indications that a period of short-term training or prior muscle contractions (Matsuhisa *et al.* 1998) could very well increase the proportion of nutritive flow and could account for the observations (Chesley *et al.* 1996, Dyck *et al.* 1996) that creatine phosphate degradation, glycogenolysis and lactate accumulation were attenuated.

Our view is that the presence of a secondary (non-nutritive) route or shunt within muscle affords a distinct advantage in terms of amplification for nutrient delivery during exercise. This is over and above the proportionate increase in total blood flow to muscle. The extent of the amplification depends on the ratio of nutritive/non-nutritive flow for resting muscle, which is unknown at present. Best estimates are based on the data of Lindbom & Arfors (1984) for the tenuissimus muscle receiving an approximate arterial oxygen tension of 70 mmHg and suggest that the ratio nutritive/non-nutritive could be as low as 30/70, although the authors (Lindbom & Arfors 1984) claim a more conservative position of 80/20. There is also indirect data from hydrogen clearance measurements (Harrison *et al.* 1990) that nutritive/non-nutritive flow is low (i.e. 16% of total flow).

It is claimed that at rest not all muscle capillaries are perfused (Harrison *et al.* 1990) and thus even with no change in non-nutritive flow the ratio nutritive/non-nutritive could have the potential to increase when total flow to muscle is increased in exercise. However, at a maximum exercise rate it is likely that flow in nutritive pathways becomes maximal and that flow in non-nutritive pathways becomes minimal. Harrison *et al.* (1990) were perhaps the first to recognize that the non-nutritive pathway provides a flow reserve to be recruited during muscular contractions. Thus, if the ratio of nutritive/non-nutritive flow at rest is 0.3 then the combination of increased sympathetic nervous system vasoconstrictor activity, a 3-fold increase in total blood flow to muscle and the release of metabolic vasodilators is an increase of 9.5-fold for blood flow to muscle nutritive vessels (Clark *et al.* 1998b). Excessive (high frequency; >6 Hz) sympathetic vasoconstrictor activity is thought to increase non-nutritive flow at the expense of nutritive flow (Hall *et al.* 1997). In addition, vasoconstrictors of this nature decrease aerobic muscle contractility (Dora *et al.* 1994) and thus excessive sympathetic vasoconstrictor activity in combination with exercise would lead to a decrease in nutritive blood flow and a probable decline in performance. Furthermore, the sites of vasoconstriction that have this deleterious effect are not affected by metabolic vasodilators (Dora *et al.* 1994).

Until precise figures are available for oxygen uptake by individual muscles at rest and during exercise the relationship between blood flow and oxygen uptake ($\dot{V}O_2$) for muscles of different fibre type cannot be

Table 1 Oxygen/flow ratios for muscle at rest and during exercise

	Isolated dog gastrocnemius			Perfused rat hindlimb *in vitro*			
		Exercise					
	Rest	4.46	6.69	Rest	Rest + AII	Exercise	Exercise + AII
$\dot{Q}_v$ (mL · min^{-1} · 100 g^{-1})	12.9	39.0	81.0	92.0	92.0	92.0	92.0
$\dot{V}O_2$ (μmol · min^{-1} · 100 g^{-1})	31.2	178.6	535.7	53.6	93.8	102.7	133.9
$\dot{V}O_2/\dot{Q}_v$ (μmol · mL^{-1})	2.4	4.6	6.6	0.58	1.02	1.12	1.46

Modified from Clark *et al.* (1998b). Data are from Cerretelli *et al.* (1984) for isolated autoperfused dog gastrocnemius muscle and from Rattigan *et al.* (1996) for constant-flow blood cell perfused rat hindlimb at 37 °C. For the former (Cerretelli *et al.* 1984) values are given at constant arteriovenous O_2 difference of 4.46 and 6.69 μmol O_2 mL^{-1} blood. In the latter (Rattigan *et al.* 1996), the sciatic nerve was stimulated resulting in much of the calf muscle group (≈20% of the hindlimb muscle mass) being active; addition of the vasoconstrictor, angiotensin (AII) increases $\dot{V}O_2/\dot{Q}_v$ both at rest and during exercise.

metabolism and exercise. In: M. Hargreaves & M. Thompson (eds) *Biochemistry of Exercise X*, pp. 35–46. Human Kinetics, Champaign, IL.

Clark, M.G., Rattigan, S., Newman, J.M. & Eldershaw, T.P. 1998b. Vascular control of nutrient delivery by flow redistribution within muscle: implications for exercise and post-exercise muscle metabolism. *Int J Sports Med* **19,** 391–400.

Clark, M.G., Richards, S.M., Hettiarachchi, M. *et al.* 1990. Release of purine and pyrimidine nucleosides and their catabolites from the perfused rat hindlimb in response to noradrenaline, vasopressin, angiotensin II and sciatic-nerve stimulation. *Biochem J* **266,** 765–770.

Clark, A.D.H., Youd, J.M., Rattigan, S. & Clark, M.G. 1999. Laser Doppler flowmetry detects changes in muscle nutritive flow: a rat model study. *Circulation* submitted.

Clerk, L.H., Smith, M.E., Rattigan, S. & Clark, M.G. 2000. Increased chylomicron triglyceride hydrolysis by connective tissue flow in perfused rat hindlimb. Implications for lipid storage. *J Lipid Res* in press.

Coggins, M., Fasy, E., Lindner, J., Kaul, S. & Barrett, E.J. 1999. Physiologic hyperinsulinemia increases skeletal muscle microvascular blood volume in healthy humans. *Diabetes* **48** (Suppl 1), A220.

Colquhoun, E.Q., Hettiarachchi, M., Ye, J.M., Rattigan, S. & Clark, M.G. 1990. Inhibition by vasodilators of noradrenaline and vasoconstrictor-mediated, but not skeletal muscle contraction-induced oxygen uptake in the perfused rat hindlimb; implications for non-shivering thermogenesis in muscle tissue. *Gen Pharmacol* **21,** 141–148.

Colquhoun, E.Q., Hettiarachchi, M., Ye, J.M. *et al.* 1988. Vasopressin and angiotensin II stimulate oxygen uptake in the perfused rat hindlimb. *Life Sci* **43,** 1747–1754.

Dora, K.A., Colquhoun, E.Q., Hettiarachchi, M., Rattigan, S. & Clark, M.G. 1991. The apparent absence of serotonin-mediated vascular thermogenesis in perfused rat hindlimb may result from vascular shunting. *Life Sci* **48,** 1555–1564.

Dora, K.A., Rattigan, S., Colquhoun, E.Q. & Clark, M.G. 1994. Aerobic muscle contraction impaired by serotonin-mediated vasoconstriction. *J Appl Physiol* **77,** 277–284.

Dora, K.D., Richards, S.M., Rattigan, S., Colquhoun, E.Q. & Clark, M.G. 1992. Serotonin and norepinephrine vasoconstriction in rat hindlimb have different oxygen requirements. *Am J Physiol* **262,** H698–H703.

Dyck, D.J., Peters, S.J., Wendling, P.S., Chesley, A., Hultman, E. & Spriet, L.L. 1996. Regulation of muscle glycogen phosphorylase activity during intense aerobic cycling with elevated FFA. *Am J Physiol* **270,** E116–E125.

Eriksson, E. & Myrhage, R. 1972. Microvascular dimensions and blood flow in skeletal muscle. *Acta Physiol Scand* **86,** 211–222.

Freis, E.D. & Schnapper, H.W. 1958. The effect of a variety of haemodynamic changes on the rapid and slow components of the circulation in the human forearm. *J Clin Invest* **37,** 838–845.

Friedman, J.J. 1966. Total, non-nutritional, and nutritional blood volume in isolated dog hindlimb. *Am J Physiol* **210,** 151–156.

Friedman, J.J. 1968. Single-passage extraction of 86Rb from the circulation of skeletal muscle. *Am J Physiol* **216,** 460–466.

Friedman, J.J. 1971. 86Rb extraction as an indicator of capillary flow. *Circ Res* **28,** I15–I20.

Grant, R.T. & Wright, H.P. 1970. Anatomical basis for non-nutritive circulation in skeletal muscle exemplified by blood vessels of rat biceps femoris tendon. *J Anat* **106,** 125–133.

Grassi, B., Poole, D.C., Richardson, R.S., Knight, D.R., Erickson, B.K. & Wagner, P.D. 1996. Muscle O_2 uptake kinetics in humans: implications for metabolic control. *J Appl Physiol* **80,** 988–998.

Hall, J.L., Ye, J.M., Clark, M.G. & Colquhoun, E.Q. 1997. Sympathetic stimulation elicits increased or decreased VO_2 in the perfused rat hindlimb via alpha 1-adrenoceptors. *Am J Physiol* **272,** H2146–H2153.

Hammersen, F. 1970. The terminal vascular bed in skeletal muscle with special regard to the problem of shunts. In: C. Crone & N.A. Lassen (eds) *Capillary Permeability. The Transfer of Molecules and Ions Between Capillary Blood and Tissue*, pp. 351–371. Munksgaard, Copenhagen.

Harrison, D.K., Birkenhake, S., Knauf, S.K. & Kessler, M. 1990. Local oxygen supply and blood flow regulation in contracting muscle in dogs and rabbits. *J Physiol* **422,** 227–243.

Hellsten, Y., Frandsen, U., Orthenblad, N., Sjodin, B. & Richter, E.A. 1997. Xanthine oxidase in human skeletal muscle following eccentric exercise: a role in inflammation. *J Physiol (Lond)* **498,** 239–248.

Hettiarachchi, M., Parsons, K.M., Richards, S.M., Dora, K.M., Rattigan, S., Colquhoun, E.Q. & Clark, M.G. 1992. Vasoconstrictor-mediated release of lactate from the perfused rat hindlimb. *J Appl Physiol* **73,** 2544–2551.

Hudlicka, O. 1969. Resting and post contraction blood flow in slow and fast muscles of the chick during development. *Microvasc Res* **1,** 390–402.

Hudlicka, O. 1973. Basic mechanisms regulating muscle blood flow. In: Anonymous (ed.) *Muscle Blood Flow: Its Relation to Muscle Metabolism and Function*, pp. 29–54. Swets & Zeitlinger, Amersterdam.

Jarasch, E.D., Bruder, G. & Heid, H.W. 1986. Significance xanthine oxidase capillary endothelial cells. *Acta Physiol Scand (Suppl)* **548,** 39–46.

Joyner, M.J. & Wieling, W. 1997. Sympathetic nerves continue to regulate blood flow in exercising muscles [comment]. *J Physiol (Lond)* **505,** 549.

Kjellmer, I., Lindbjerg, I., Prerovsky, I. & Tonnesen, H. 1967. The relation between blood flow in an isolated muscle measured with the Xe133 clearance and a direct recording technique. *Acta Physiol Scand* **69,** 69–78.

Kuznetsova, L.V., Tomasek, N., Sigurdsson, G.H., Banic, A., Erni, D. & Wheatley, A.M. 1998. Dissociation between volume blood flow and laser-Doppler signal from rat muscle during changes in vascular tone. *Am J Physiol* **274,** H1248–H1254.

Lindbom, L. & Arfors, K.E. 1984. Non-homogeneous blood flow distribution in the rabbit tenuissimus muscle Differential control of total blood flow and capillary perfusion. *Acta Physiol Scand* **122,** 225–233.

were essentially capillary-like. This and the inability to account for physiological data (Pappenheimer 1941, Walder 1953, 1955, Barlow et al. 1958) provided the impetus for a search for vessels that would fulfill the role as a non-nutritive route in muscle. Zweifach & Metz (1955) were probably the first to realize that these non-nutritive vessels may be outside the capillary bed of the muscle fibrils. In 1955 these authors described "preferential capillary channels at the edge of the spino-trapezius muscle of the rat". Barlow and colleagues (1959, 1961) added to this notion by concluding that the secondary non-nutritive route was located in the septa and tendons. Their findings, along with others that preceded them, were based on clearance kinetics of $^{24}Na^{+}$ administered either intravenously or intramuscularly. In 1970 Grant & Wright noted that blood vessels in the tibial tendon of the biceps femoris muscle could be readily viewed and also claimed them to be the non-nutritive vessels of skeletal muscle (Grant & Wright 1970). These vessels were dilated by acetylcholine or histamine and constricted by noradrenaline or adrenaline, but did not respond to changes in body temperature and were thus unlikely to be involved in thermoregulation.

As yet, there have been no attempts to integrate metabolic data with anatomical studies. This is surprising as the intravital microscopy studies of the rabbit tenuissimus muscle by Lindbom, Arfors and their colleagues (Lindbom & Arfors 1984, 1985, Borgstrom et al. 1988) would appear to provide key information that could explain much of the metabolic data obtained by us and others with the perfused rat hindlimb preparation. Most importantly, the microvasculature of the tenuissimus muscle shows two vascular compartments that could very well provide an anatomical basis for the notion of nutritive and non-nutritive routes in muscle.

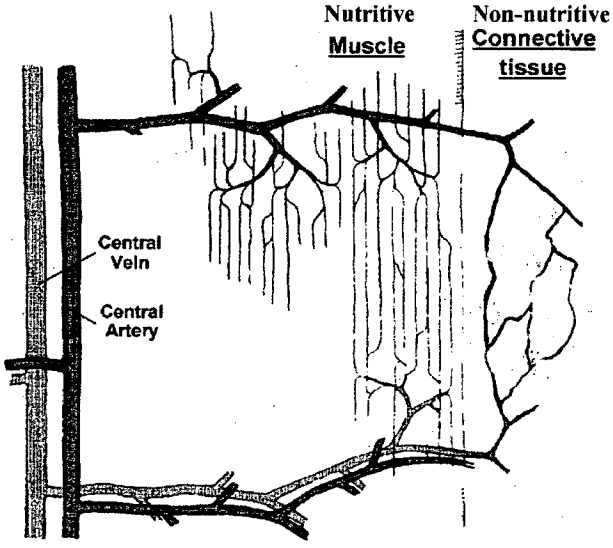

Fig. 1. This illustration is adapted from Borgstrom et al. (1988) and shows a transverse arteriole of the rabbit tenuissimus muscle supplying both capillaries in muscle tissue and adjacent connective tissue.

The tenuissimus muscle is a muscle that is accessible and transparent, thereby allowing both the detailed illustration and study of changes that affect flow in each of the two routes. Although this muscle may be considered by some as atypical in being relatively flat, the vascular arrangement of the tenuissimus muscle is proposed to exist as a basic unit in all hind leg muscles (Myrhage & Eriksson 1980). The vasculature of the rabbit tenuissimus muscle is shown in Fig. 1. Transverse arterioles supply both capillaries in muscle tissue proper and adjacent connective tissue. Using intravital microscopy, Lindbom, Arfors and their colleagues measured microvascular blood flow at two points on several transverse arterioles in the tenuissimus muscle of anesthetized rabbits (positions A and B, Fig. 1) while studying the influence of environmental (muscle bathing solution) oxygen tension as well as perfusion pressure, isoproterenol, epinephrine, functional hyperemia (exercise induced) and reactive hyperemia (Table 1). Under resting conditions the proportion of total flow passing into the connective tissue was approximately 44%. This dramatically increased to 91% if the bathing oxygen concentration was increased to 20 kPa even though total muscle flow dropped by 46%. Topically applied isoproterenol, a β-adrenergic agonist and potent vasodilator, also markedly increased the proportion of connective tissue flow. Thus, despite total flow increasing from 0.73 to 2.65 $nl \cdot s^{-1}$, an increase of 263%, most of this flow (97%) was carried by the connective tissue vessels. It is important to note that this particular result emphasizes the potential capacity of the connective tissue route for flow, as under the conditions of isoproterenol-mediated vasodilation the connective tissue vessels carry 3.5-fold the total basal flow rate. Exercise induced functional hyperemia increased muscle capillary flow at the expense of connective tissue flow. Thus, capillary flow increased from 56% to 76% of total flow with a corresponding decrease in connective tissue flow from 44% to 24%. Lowering of the perfusion pressure also tended to favor muscle capillary flow at the expense of connective tissue flow. In contrast, neither epinephrine, nor reactive hyperemia (in response to occlusion) altered the proportion of connective tissue to muscle flow, even though total flow was decreased and increased, respectively.

Reciprocal control of flow between connective tissue and muscle

Our studies using the constant-flow perfused rat hindlimb were initially intended to investigate the ef-

Control of hindlimb metabolism from a redistribution of flow between muscle and connective tissue

Several recent studies, particularly from our own laboratory, suggest that the perfused rat hindlimb is a two compartment model and that changes in metabolism mediated by vasomodulators result from a redistribution of flow between these two compartments. There is also strong evidence to suggest that the second compartment of muscle is that of connective tissue. Table 2 summarizes the data and shows that type A vasoconstrictors that act to increase metabolism of the hindlimb overall decrease the flow volume in tendon vessels, which can be viewed in an area essentially free of capillaries.

Measurements were made in the constant flow perfused rat hindlimb using 6 min pulse infusions of fluorescein isothiocyanate (FITC)-labeled dextran (Mr 150 000) while positioning a fluorescence sensor over exposed vessels of the tibialis tendon of the biceps femoris (Newman et al. 1997), the same vessels claimed by Grant & Wright to be representative of the non-nutritive route of muscle (Grant & Wright 1970). Readings were taken during vehicle infusion and again under constant infusion of a type A (noradrenaline), or type B (serotonin) vasoconstrictor (Newman et al. 1997). The intensity of the signal at steady state was inversely related to VO_2, the surrogate indicator of muscle nutritive flow. In addition, photomicroscopy of the vessels following injection of India ink clearly showed that the change in signal was due to the relative filling of the vessels. To our knowledge, this was the first report of vasoconstrictors selectively directing flow to, or away from tendon vessels (Newman et al. 1997). Interestingly, Grant & Wright in their anatomical study of these vessels, noted that they were about twice the diameter of muscle nutritive capillaries (Grant & Wright 1970). According to Poiseulle's Law ($Q=kPr^4/l$, where Q= flow; k=constant; P=pressure; r=radius; and l= length of vessel), at the same vessel length and perfusion pressure, these functional shunts could be capable of carrying 16 times the flow of a typical muscle capillary. Applying this reasoning, the potential ratio of flow rates was approx. 1:12 for norepinephrine:serotonin. These calculations combined with the fact that the vessels in question are located in a tissue of low metabolic activity makes the hypothesis of a significant non-nutritive flow pathway through tendon highly plausible.

Table 2. Effects of type A and B vasoconstrictors on perfused rat hindlimb characteristics likely to result from the redistribution of flow between skeletal muscle capillaries and connective tissue vessels of tendon and septa

	Type A	Type B	Ref.
Metabolism (including VO_2, J_{Lac}, J_{Gly} etc.)	↑	↓	a
Parameter			
Tendon vessel volume	↓	↑	b
Vascular volume perfused	↑	↓	c
Arterial cast (30 μm acrylate)			
Weight		↓	c
Volume	↑	↓	c
Passage of microspheres (11.8 μm)	1.1±0.1	2.2±0.2	c
Microsphere embolism (11.8 μm)	–	+	d
1-Methylxanthine metabolism	↑	↓	e
Chylomicron triglyceride hydrolysis	↓	↑	f

Abbreviations: VO_2, oxygen uptake; J_{Lac}, lactate efflux, J_{Gly}, glycerol efflux. For microsphere embolism "–" and "+" indicate inhibition and stimulation of metabolism, respectively. Values for the passage of microspheres are percent of total injected, which in each case was 2×10^6. Refs: a, Clark et al. 1995; b, Newman et al. 1997; c, Newman et al. 1996; d, Vincent et al. 1998; e, Rattigan et al. 1997; f, Clerk et al. 2000.

Another approach (Table 2) was the assessment of perfused vascular volume. In these experiments, again using the perfused rat hindlimb at constant total flow, the effects of each vasoconstrictor were compared in terms of vascular entrapment of fluorescein-labeled dextran (Fx) (Newman et al. 1996). Fx was infused at a constant rate and during this infusion norepinephrine was also infused (if a new vascular region was being recruited then this would fill with Fx). Subsequently, infusion of the Fx was halted and a few minutes allowed for the material remaining to wash out. A second infusion of norepinephrine succeeded in releasing the previously entrapped Fx. By varying the time between each infusion of norepinephrine it was possible to deduce that approximately 31% of the pre-norepinephrine vascular volume had been recruited. Although there was no evidence that norepinephrine had acted to derecruit a previously perfused vascular volume, recruitment of an additional vascular volume under conditions of constant total flow must have been at the expense of flow elsewhere (presumably from the non-nutritive connective tissue route). For serotonin, a type B vasoconstrictor that inhibits metabolism, a new space was not recruited, but rather, vasoconstriction by this agonist resulted in the closing off of a space. Presumably the de-recruited space represented a portion of the previously perfused muscle nutritive route. Again, since the total flow was kept constant, this would mean that flow has been directed to the non-nutritive route, consistent with the observed increase in tendon vessel volume induced by serotonin and discussed previously.

The third piece of evidence in support of vasoconstrictor-mediated redistribution of flow between skeletal muscle capillaries and connective tissue vessels comes from a comparison of the extent of arterial vascular tree filling for control (vehicle only), norepinephrine and serotonin (Newman et al. 1996). For these experiments, corrosion casts were made using 30 μm spheres of methyl methacrylate. Whereas nor-

nutritive flow could be made, so it is unknown whether this changed.

We have proposed elsewhere (Clark et al. 1998) that the presence of a secondary (non-nutritive) route or shunt within muscle affords a distinct advantage in terms of amplification for nutrient delivery during exercise. This is over and above the proportionate increase in total blood flow to the muscle. The extent of amplification depends on the ratio of nutritive/non-nutritive flow for resting muscle, which is unknown at present but could be as low as 16% of total (Harrison et al. 1990). We would argue that if this were the case then vasoconstriction from increased sympathetic outflow during exercise could act to switch blood flow from the non-nutritive to the nutritive route, thereby amplifying nutrient delivery. Depending on the extent of vasoconstriction and the proportion of nutritive/non-nutritive flow at rest, the amplification could approach 5-fold. Data from Takemiya and colleagues (Takemiya et al. 1982) reported that tendon/muscle blood flow ratio of rabbit hindlimbs was greater than 2:1 and implications from a later paper from the same group (Takemiya & Maeda 1988) showing that infused noradrenaline preferentially decreased tendon blood flow, adds support to the notion that increased sympathetic outflow in exercise may well act to redirect blood flow from tendon to muscle.

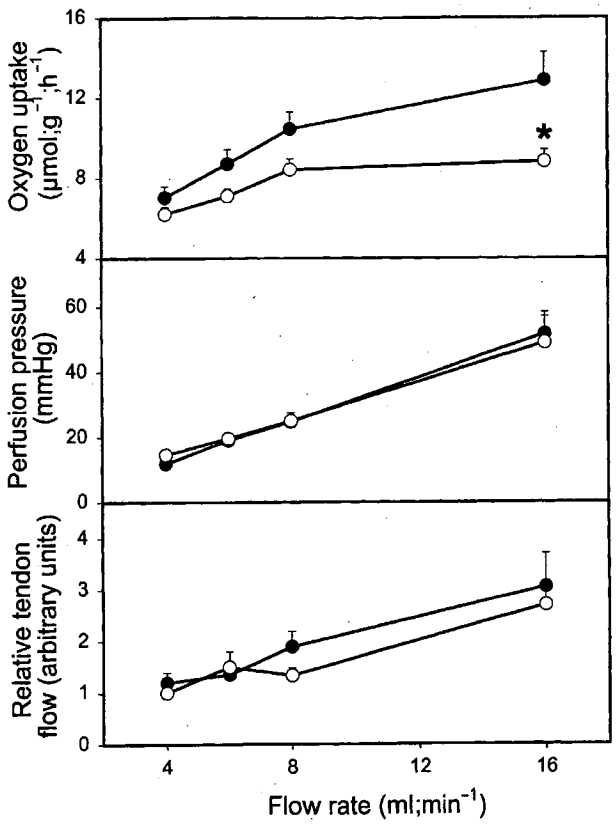

Fig. 2. Effect of flow rate on oxygen uptake, perfusion pressure and relative tendon flow in the pump perfused rat hindlimb. Animals were housed in cages with or without access to a 1 m circumference running wheel. Exercise-trained rats ran a minimum of 10 km per week. Technical detail can be found elsewhere (Newman et al. 1997). Significant difference between trained (○) and untrained (●) indicated by asterisk ($P<0.05$). Values are means±SEM for $n=7$ in each group.

The editors of Gray's Anatomy regard the non-nutritive route as a route through which the blood passes when the flow in the endomysial capillary bed is impeded, e.g. during contraction (Gray's Anatomy 1973). Thus, rhythmic oscillation of blood flow between the non-nutritive and nutritive routes may aid the muscle pump. If this were so, then this would rule out the afore-mentioned possibility for flow amplification. However, evidence from Lindbom (1986) from studies on the rabbit tenuissimus muscle and from Takemiya & Maeda (1988) would suggest that during exercise flow is proportionately increased to the muscle capillaries in preference to the connective tissue or tendons. This may mean that there is an active recruitment of flow from non-nutritive to nutritive route.

Unfortunately, most attempts to measure tendon vessel flow during exercise have not compared it to muscle blood flow and have invariably chosen to measure tendon vessel flow in the midportion or peritendinous area. Thus, direct comparisons with data from the rabbit tenuissimus muscle above and direct assessment of our amplification proposal cannot be made. However, it is interesting to note that from the few studies conducted, exercise was found to both decrease (Astrom & Westlin 1994) and increase (Langberg et al. 1998, 1999) tendon blood flow. Differences may relate to methodology, as Astrom & Westlin (1994) used laser Doppler flowmetry and Langberg et al. (1998, 1999) used clearance of injected ^{133}Xe. There are also findings from rabbits where tendon blood flow was found to increase in exercise (Landi et al. 1983). In addition, a study by Bulow and Tondevold (1982) using radioactive 15 μm microspheres in dogs showed that exercise increased Achilles tendon blood flow aproximately 3-fold. However, blood flow to muscle was likely to have increased much more than this, and so there is still the possibility of blood flow being recruited to muscle at the expense of connective tissue and tendon. Further experiments are clearly required to resolve this, avoiding the possibility that tendon vessel flow in exercise is not restricted due to mechanical effects.

Effects of physical training on intrinsic resistance and capacitance of tendon vessels

As indicated above, we have developed a technique for monitoring tendon vessel flow/volume during rat hindlimb perfusion when total flow is held constant

vascular shunting. Life Sci 1991: 48: 1555–64.
Dora KA, Rattigan S, Colquhoun EQ, Clark MG. Aerobic muscle contraction impaired by serotonin-mediated vasoconstriction. J Appl Physiol 1994: 77: 277–84.
Dora KD, Richards SM, Rattigan S, Colquhoun EQ, Clark MG. Serotonin and norepinephrine vasoconstriction in rat hindlimb have different oxygen requirements. Am J Physiol 1992: 262: H698–703.
Grant RT, Wright HP. Anatomical basis for non-nutritive circulation in skeletal muscle exemplified by blood vessels of rat biceps femoris tendon. J Anat 1970: 106: 125–33.
Gray's Anatomy, 35th edn. London: Longman, 1973.
Hall JL, Ye JM, Clark MG, Colquhoun EQ. Sympathetic stimulation elicits increased or decreased VO_2 in the perfused rat hindlimb via alpha 1-adrenoceptors. Am J Physiol 1997: 272: H2146–53.
Hammersen F. The terminal vascular bed in skeletal muscle with special regard to the problem of shunts. In: Crone C, Lassen NA, eds. Capillary permeability. The transfer of molecules and ions between capillary blood and tissue. Copenhagen: Munksgaard, 1970: 351–71.
Harrison DK, Birkenhake S, Knauf SK, Kessler M. Local oxygen supply and blood flow regulation in contracting muscle in dogs and rabbits. J Physiol 1990: 422: 227–43.
Hellsten-Westing Y. Immunohistochemical localization of xanthine oxidase in human cardiac and skeletal muscle. Histochemistry 1993: 100: 215–22.
Hellsten Y, Frandsen U, Orthenblad N, Sjodin B, Richter EA. Xanthine oxidase in human skeletal muscle following excentric exercise: a role in inflammation. J Physiol (Lond) 1997: 498: 239–48.
Hettiarachchi M, Parsons KM, Richards SM, Dora KM, Rattigan S, Colquhoun EQ, et al. Vasoconstrictor-mediated release of lactate from the perfused rat hindlimb. J Appl Physiol 1992: 73: 2544–51.
Jarasch ED, Bruder G, Heid HW. Significance of xanthine oxidase in capillary endothelial cells. Acta Physiol Scand 1986: 124 (Suppl. 548): 39–46.
Kannus P, Jozsa L, Natri A, Jarvinen M. Effects of training, immobilization and remobilization on tendons. Scand J Med Sci Sports 1997: 7: 67–71.
Kraus BL, Kirker-Head CA, Kraus KH, Jakowski RM, Steckel RR. Vascular supply of the tendon of the equine deep digital flexor muscle within the digital sheath. Vet Surg 1995: 24: 102–11.
Landi A, Elves M, Piaggi W. The blood flow of rabbits' tendons. Variation with age, activity and hypoxia. Acta Orthop Scand 1983: 54: 832–5.
Langberg H, Bulow J, Kjaer M. Blood flow in the peritendinous space of the human Achilles tendon during exercise. Acta Physiol Scand 1998: 163: 149–53.
Langberg H, Bulow J, Kjaer M. Standardized intermittent static exercise increases peritendinous blood flow in human leg. Clin Physiol 1999: 19: 89–93.
Lindbom L. Distribution patterns of blood flow in the rabbit tenuissimus muscle in response to brief ischemia and muscle contraction. Microvasc Res 1986: 31: 143–56.
Lindbom L, Arfors KE. Non-homogeneous blood flow distribution in the rabbit tenuissimus muscle. Differential control of total blood flow and capillary perfusion. Acta Physiol Scand 1984: 122: 225–33.
Lindbom L, Arfors KE. Mechanism and site of control for variation in the number of perfused capillaries in skeletal muscle. Int J Microcirc Exp 1985: 4: 19–30.
Myrhage R, Eriksson E. Vascular arrangements in hindlimb muscles of the cat. J Anat 1980: 131: 1–17.
Newman JM, Dora KA, Rattigan S, Edwards SJ, Colquhoun EQ, Clark MG. Norepinephrine and serotonin vasoconstriction in rat hindlimb control different vascular flow routes. Am J Physiol 1996: 270: E689–99.
Newman JM, Steen JT, Clark MG. Vessels supplying septa and tendons as functional shunts in perfused rat hindlimb. Microvasc Res 1997: 54: 49–57.
Nishimura T, Hattori A, Takahashi K. Structural changes in intramuscular connective tissue during the fattening of Japanese black cattle: effect of marbling on beef tenderization. J Anim Sci 1999: 77: 93–104.
O'Brien M. Structure and metabolism of tendons. Scand J Med Sci Sports 1997: 7: 55–61.
Pappenheimer JR. Vasoconstrictor nerves and oxygen consumption in the isolated perfused hindlimb muscles of the dog. J Physiol 1941: 99: 182–200.
Piiper J, Rosell S. Attempt to demonstrate large arteriovenous shunts in skeletal muscle during stimulation of sympathetic vasodilator nerves. Acta Physiol Scand 1961: 53: 214–7.
Rattigan S, Appleby GJ, Miller KA, Steen JT, Dora KA, Colquhoun EQ, et al. Serotonin inhibition of 1-methylxanthine metabolism parallels its vasoconstrictor activity and inhibition of oxygen uptake in perfused rat hindlimb. Acta Physiol Scand 1997: 161: 161–9.
Rattigan S, Dora KA, Colquhoun EQ, Clark MG. Serotonin-mediated acute insulin resistance in the perfused rat hindlimb but not in incubated muscle: a role for the vascular system. Life Sci 1993: 53: 1545–55.
Rattigan S, Dora KA, Colquhoun EQ, Clark MG. Inhibition of insulin-mediated glucose uptake in rat hindlimb by an alpha-adrenergic vascular effect. Am J Physiol 1995: 268: E305–11.
Rattigan S, Dora KA, Tong AC, Clark MG. Perfused skeletal muscle contraction and metabolism improved by angiotensin II-mediated vasoconstriction. Am J Physiol 1996: 271: E96–103.
Sakamoto Y. Histological features of endomysium, perimysium and epimysium in rat lateral pterygoid muscle. J Morphol 1996: 227: 113–9.
Takemiya T, Hashiba Y, Hashizume K, Kao SC, Tanaka Y. Simultaneous measurements of muscle and tendon blood flow by hydrogen gas clearance method at rest and exercise of rabbit hindlimbs. J Phys Fitness Jpn 1982: 31: 41–50.
Takemiya T, Maeda J. The functional characteristics of tendon blood circulation in the rabbit hindlimbs. Jpn J Physiol 1988: 38: 361–74.
Vincent MA, Rattigan S, Clark MG. Microsphere infusion reverses vasoconstrictor-mediated change in hindlimb oxygen uptake and energy status. Acta Physiol Scand 1998: 164: 61–9.
Walder DN. The local clearance of radioactive sodium from muscle in normal subjects and those with peripheral vascular disease. Clin Sci 1953: 12: 153–67.
Walder DN. The relationship between blood flow, capillary surface area and sodium clearance in muscle. Clin Sci 1955: 14: 303–15.
Youd JM, Newman JMB, Clark MG, Appleby GJ, Rattigan S, Tong ACY, et al. Increased metabolism of infused 1-methylxanthine by working muscle. Acta Physiol Scand 1999: 166: 301–8.
Zweifach BW, Metz DB. Selective distribution of blood through the terminal vascular bed of mesenteric structures and skeletal muscle. Angiology 1955: 6: 282–9.